This is to certify that the
dissertation entitled

SPECTROSCOPIC AND CHEMICAL CHARACTERIZATION OF
BIOMASS

presented by

LIZBETH LAUREANO-PEREZ

has been accepted towards fulfillment
of the requirements for the

Doctoral degree in Chemical Engineering

Bruce T. Dale

Major Professor's Signature

June 10, 2005

Date

SPECTROSCOPIC AND CHEMICAL CHARACTERIZATION OF BIOMASS

By

Lizbeth Laureano-Pérez

A DISSERTATION

Submitted to
Michigan State University
In partial fulfillment of the requirements
For the degree of

DOCTOR OF PHILOSOPHY

Department of Chemical Engineering and Materials Science

2005

ABSTRACT

SPECTROSCOPIC AND CHEMICAL CHARACTERIZATION OF BIOMASS

By

Lizbeth Laureano-Pérez

Spectroscopic characterization of both untreated and treated material is being performed in order to determine changes in the biomass and the effects of pretreatment on crystallinity, lignin content, selected chemical bonds and depolymerization of hemicellulose and lignin. The methods used are X-Ray diffraction for determination of cellulose crystallinity (CrI); diffuse reflectance Fourier transform infrared (DRIFT) for changes in C-C and C-O bonds; and fluorescence to determine lignin content. Changes in spectral characteristics and crystallinity are statistically correlated with enzymatic hydrolysis results to identify and better understand the fundamental features of biomass that govern its enzymatic conversion to monomeric sugars. Raman spectroscopy was also used to create a statistical model that relates the spectral characteristics of poplar to its enzymatic hydrolysis results. DRIFT can be used to compare various pretreatments and their effect on the biomass along with their parameters. The PCR model gives not only better correlation, but also better prediction for initial rate and 72-hr conversion for poplar samples. On the other hand, MLR gives a better correlation and prediction for the AFEX pretreated corn stover. This difference in model applicability is due to the nature of the samples. The models for 72-hr conversion give a better correlation and prediction than the initial rate models indicating that factors, other than lignin, biomass crystallinity and acetyl content, affect enzymatic hydrolysis. The pretreated corn stover MLR model

indicates that the factor that most affects the initial rate is the aldehyde content or the bonds between the lignin and hemicellulose. However, for the 72 hr conversion the model indicates that lignin is the primary factor affecting hydrolysis. The PCR model indicates that both initial rate and 72-hr conversion is more affected by O-H content.

DEDICATION

Dedicated to my mom, Lourdes Perez, who continually encourages and supports me and whose personal sacrifices helped me to succeed in my endeavors. To my best friends, Alexei J. Lozada-Ruiz and Ayrin A. Peñaloza Arroyo, whose love, support, and encouragement were indispensable in the achievement of my goals.

ACKNOWLEDGEMENTS

I would like to thank Dr. Bruce Dale, for excellent guidance, encouragement, understanding and support throughout my project. The best advisor anyone can have.

I am very grateful for the advice of my guidance committee members: Dr. R. M. Worden, Dr. Dennis Miller and Dr. Merlin Bruening. In addition, I would like to thank Dr. Mariam Sticklen for let me use her laboratory and equipment.

I am very thankful to Dr. Hasan Alizadeh, and Dr. Farzaneh Teymouri for their suggestions, comments and technical assistance.

I am very grateful to Dr. Barbara O'Kelly and Linda Leon for their help in financial and emotional support. Furthermore, I must thank the Chemical Engineering and Crop and Soil Sciences office staff for all of their help.

Last but not least, I would like to thank all my colleagues and collaborators at Auburn University, Dartmouth University, Purdue University, NREL and Texas A&M University.

TABLE OF CONTENTS

Page

List of Figures xi

List of Tables xiii

Chapter 1: Introduction 1

Chapter 2: Literature Review 5
- 2.1 Bioethanol 5
- 2.2 Cell Wall 6
  - 2.2.1 Cellulose 7
  - 2.2.2 Hemicellulose 9
  - 2.2.3 Lignin 10
- 2.3 Pretreatments 13
  - 2.3.1 Ammonia Fiber Explosion (AFEX) 14
  - 2.3.2 Ammonia Recycle Percolation (ARP) 14
  - 2.3.3 Uncatalyzed Explosion/ Dilute Acid 15
  - 2.3.4 Controlled pH 16
  - 2.3.5 Lime 16
- 2.4 Pretreatment Effectiveness 17
- 2.5 Enzymatic Hydrolysis Hindrance 17
  - 2.5.1 Cellulose Crystallinity 19
  - 2.5.2 Lignin Content 19
  - 2.5.3 Changes in C-O, C-H bonds and deacetylation 20
- 2.6 Analytical Analyses 21
  - 2.6.1 X-Ray Diffraction 21
  - 2.6.2 Fluorescence 22
  - 2.6.3 Diffuse Reflectance FT-IR(DRIFT) 23
  - 2.6.4 Raman 24
- 2.7 Statistical Analysis 25
  - 2.7.1 Multilinear Regression 26
  - 2.7.2 Principal Component Regression 28

Chapter 3: Effect of pretreatment on corn stover as measured by DRIFT 33
- 3.1 Background 33
- 3.2 Materials and Methods 37
  - 3.2.1 Materials 37
  - 3.2.2 Experimental Equipment and Procedures 39

3.2.2.1 AFEX Treatment 39
3.2.2.2 ARP Treatment 42
3.2.2.3 Uncatalyzed Explosion/
Dilute Acid Treatment 42
3.2.2.4 Controlled pH Pretreatment 43
3.2.2.5 Lime Pretreatment 44
3.2.3 Analytical Methods 44
3.2.3.1 Diffuse Reflectance FT-IR(DRIFT) 44
3.2.3.2 Enzymatic Hydrolysis 45
3.2.3.3 Simultaneous Saccharification
and Fermentation (SSF) 46
3.2.3.4 Acid Hydrolysis 46
3.3 Results and Discussion 47
3.4 Conclusions 63

Chapter 4: Statistical correlation of spectroscopic analysis
and enzymatic hydrolysis of corn stover 65
4.1 Background 65
4.2 Materials and Methods 69
4.2.1 Materials 69
4.2.2 Experimental Equipment and Procedures 69
4.2.3 Analytical Methods 69
4.2.3.1 Fluorescence 70
4.2.3.2 Diffuse Reflectance FT-IR(DRIFT) 70
4.2.3.3 X-Ray Diffraction 70
4.2.3.4 Enzymatic Hydrolysis 70
4.2.3.5 Simultaneous Saccharification
and Fermentation (SSF) 70
4.2.3.6 Acid Hydrolysis 70
4.2.4 Statistical Analysis 70
4.3 Results and Discussion 73
4.4 Conclusions 87

Chapter 5: Statistical correlation of spectroscopic analysis and
hydrolysis of poplar samples 89
5.1Background 89
5.2 Materials and Methods 92
5.2.1 Materials 92
5.2.2 Analytical Methods 92
5.2.2.1 Fluorescence 92
5.2.2.2 Diffuse Reflectance FT-IR(DRIFT) 92
5.2.2.3 X-Ray Diffraction 92
5.2.2.4 Raman Spectroscopy 92
5.2.2.5 Enzymatic Hydrolysis 92
5.2.3 Statistical Analysis 93

5.3 Results and Discussion... 93
5.4 Conclusions 114

Chapter 6: Conclusions and Recommendations 116

Appendices 119
Appendix 1: Ammonia MSDS 120
Appendix 2: Safety Requirements and Equipment 125
Appendix 3: DRIFT Results (Raw Data) 126
Appendix 4: Corn Stover Characterization Raw Data 138
Appendix 5: Poplar Characterization Raw Data 168

Bibliography 211

LIST OF TABLES

Page

Table 3.1: Corn stover main peaks in DRIFT spectra 37

Table 3.2. Composition of the corn stover 38

Table 3.3: Changes in DRIFT results from changes in AFEX temperature 51

Table 3.4: Changes in DRIFT results from changes in ammonia loading 53

Table 3.5: Changes in DRIFT results from corn stover moisture content 56

Table 3.6: Changes in DRIFT results from AFEX pretreatment time 58

Table 3.7: Changes in DRIFT results from the different Pretreatments 63

Table 4.1: AFEX Crystallinity Index 74

Table 4.2: Different Pretreatment Crystallinity Indices 75

Table 4.3: Prediction using MLR model for corn stover 81

Table 4.4: Corn stover MLR data for hypothesis testing 82

Table 4.5: Correlation using various spectroscopic techniques 83

Table 4.6: Prediction using PCR model for corn stover 86

Table 4.7: Corn stover PCR data for hypothesis testing 87

Table 5.1: Poplar crystallinity index 97

Table 5.2: ANOVA correlations obtained using various Techniques for MLR 103

Table 5.3: Correlations obtained using various techniques for PCR 106

Table 5.4: Predictions using MLR model for poplar 110

Table 5.5: Predictions using PCR model for poplar 112

Table 5.6: Poplar MLR and PCR data for hypothesis testing 113

Table A4.1: Crystallinity Index for AFEX pretreated corn stover 138

Table A4.2: Crystallinity Index for pretreated corn stover 140

Table A4.3: MLR model coefficients for corn stover using all spectroscopic data 141

Table A4.4: PCR model coefficients for corn stover using DRIFT data...... 142

Table A4.5: MLR Raw data for AFEX treated corn stover Unscrambler modeling 143

Table A4.6: MLR Raw data for pretreated corn stover Unscrambler modeling 144

Table A5.1: Crystallinity Index for TAMU poplar samples 168

Table A5.2: MLR model coefficients for poplar using Raman, DRIFT and XRD data 173

Table A5.3: PCR model coefficients for poplar using DRIFT data 174

Table A5.4: MLR Raw Data for poplar Unscrambler Modeling 175

LIST OF FIGURES

Page

Figure 2.1: A three-dimensional molecular model of a cell wall 8

Figure 2.2: Cellulose microfibril 9

Figure 2.3: Most common lignin monomers 11

Figure 2.4: Bonds in lignin 12

Figure 2.5: Enzymatic hydrolysis scheme 18

Figure 2.6: Matrix **R** plotted in column space with the first eigenvector 30

Figure 3.1: AFEX equipment setup 41

Figure 3.2: DRIFT spectrum of potassium nitrate 48

Figure 3.3: DRIFT reproducibility 49

Figure 3.4: Effect of AFEX pretreatment temperature on the DRIFT spectra of corn stover 51

Figure 3.5: Effect of ammonia loading on DRIFT spectra of corn stover 53

Figure 3.6: Effect of moisture content of corn stover on the DRIFT spectra 55

Figure 3.7: Effect of pretreatment time on the DRIFT spectra of corn stover 57

Figure3.8: Effect of ARP in biomass as determined by DRIFT 59

Figure 3.9: Effect of dilute acid pretreatment on DRIFT results 60

Figure 3.10: Effect of controlled pH pretreatment on the DRIFT Results 61

Figure 3.11: Effect of various pretreatments on corn stover as determined by DRIFT 62

Figure 4.1: Fluorescence results for the different pretreatments 76

Figure 4.2: Initial Rate MLR Model using a) DRIFT data only and; b) all the data 78

Figure 4.3: MLR model for the 72 hrs glucan conversion using a) DRIFT data only and; b) all the data 79

Figure 4.4: PCR model for initial rate using only DRIFT data 84

Figure 4.5: PCR model for glucan conversion at 72 hrs using only DRIFT data 84

Figure 5.1: Effect of acetyl content on DRIFT spectra 94

Figure 5.2: Effect of lignin content on the DRIFT spectra of Poplar 95

Figure 5.3: Effect of crystallinity on the DRIFT spectra 96

Figure 5.4: Effect of acetyl content on fluorescence results 98

Figure 5.5: Effect of lignin content on fluorescence results 99

Figure 5.6: Effect of crystallinity on the fluorescent results 99

Figure 5.7: Effect of acetyl content on the Raman spectra 100

Figure 5.8: Effect of lignin on the Raman spectra 101

Figure 5.9: Effect of crystallinity on the Raman spectra 102

Figure 5.10: MLR model for the initial rate using DRIFT, Raman and XRD 104

Figure 5.11: MLR model for the 72 hr conversion using DRIFT, Raman and XRD 105

Figure 5.12: PCR model for initial rate using DRIFT data 107

Figure 5.13: PCR model for the 72 hr conversion using DRIFT data only 108

Figure A3.1: AFEX DRIFT results (20%, 0.7:1, 60-90C) 126

Figure A3.2: AFEX DRIFT results (20%, 1.3:1, 60-90C) 127

Figure A3.3: AFEX DRIFT results (40%, 0.5:1, 60-90C) 128

Figure A3.4: AFEX DRIFT results (40%, 1:1, 60-90C) 129

Figure A3.5: AFEX DRIFT results (40%, 1:3, 70-90C) 130

Figure A3.6: AFEX DRIFT results (60%, 0.5:1, 70-90C) 131

Figure A3.7: AFEX DRIFT results (60%, 0.7:1, 60-90C) 132

Figure A3.8: AFEX DRIFT results (60%, 1.3:1, 60-90C) 133

Figure A3.9: AFEX DRIFT results (80%, 1:1, 90C, 5-15 min) 134

Figure A3.10: AFEX DRIFT results (80%, 1:1, 100C, 5-15 min) 135

Figure A3.11: NREL samples DRIFT results 136

Figure A3.12: Lime treated sample DRIFT results 137

Figure A4.1: AFEX fluorescence results (20%, 0.7:1, 60-90C) 145

Figure A4.2: AFEX fluorescence results (20%, 1.3:1, 60-90C) 146

Figure A4.3: AFEX fluorescence results (40%, 0.5:1, 60-90C) 147

Figure A4.4: AFEX fluorescence results (40%, 1:1, 60-90C) 148

Figure A4.5: AFEX fluorescence results (40%, 1.3:1, 60-90C) 149

Figure A4.6: AFEX fluorescence results (60%, 0.5:1, 60-90C) 150

Figure A4.7: AFEX fluorescence results (60%, 0.7:1, 60-90C) 151

Figure A4.8: AFEX fluorescence results (60%, 1:1, 60-90C) 152

Figure A4.9: AFEX fluorescence results (60%, 1.3:1, 60-90C) 153

Figure A4.10: AFEX fluorescence results (80%, 1:1, 90C, 5-15min) 154

Figure A4.11: AFEX fluorescence results (80%, 1:1, 100C, 5-15min) 155

Figure A4.12: AFEX fluorescence results (60%, 1:1, 110C, 5-15min) 156

Figure A4.13: ARP fluorescence results 157

Figure A4.14: Controlled pH fluorescence results 158

Figure A4.15: Dilute acid fluorescence results 159

Figure A4.16: NREL samples fluorescence results 160

Figure A4.17: Lime treated samples fluorescence results 161

Figure A4.18: PCR initial rate model using fluorescence data 162

Figure A4.19: PCR 72-hr model using fluorescence data 162

Figure A4.20: PCR initial rate model using XRD data 163

Figure A4.21: PCR 72-hr model using XRD data 163

Figure A4.22: PCR initial rate model using DRIFT and fluorescence data 164

Figure A4.23: PCR 72-hr model using DRIFT and fluorescence data 164

Figure A4.24: PCR initial rate model using DRIFT and XRD data 165

Figure A4.25: PCR 72-hr model using DRIFT and XRD data 165

Figure A4.26: PCR initial rate model using fluorescence and XRD data 166

Figure A4.27: PCR 72-hr model using fluorescence and XRD data 166

Figure A4.28: PCR initial rate model using DRIFT, fluorescence and XRD data 167

Figure A4.29: PCR 72-hr model using DRIFT, fluorescence and XRD data 167

Figure A5.1: MLR initial rate model using DRIFT data 187

Figure A5.2: MLR 72-hr model using DRIFT data 187

Figure A5.3: MLR initial rate model using Raman data 188

Figure A5.4: MLR 72-hr model using Raman data 188

Figure A5.5: MLR initial rate model using DRIFT and Raman data 189

Figure A5.6: MLR 72-hr model using DRIFT and Raman data 189

Figure A5.7: MLR initial rate model using DRIFT and XRD data 190

Figure A5.8: MLR 72-hr model using DRIFT and XRD data 190

Figure A5.9: MLR initial rate model using DRIFT and fluorescence data 191

Figure A5.10: MLR 72-hr model using DRIFT and fluorescence data 191

Figure A5.11: MLR initial rate model using Raman and XRD data 192

Figure A5.12: MLR 72-hr model using Raman and XRD data 192

Figure A5.13: MLR initial rate model using Raman and fluorescence data 193

Figure A5.14: MLR 72-hr model using Raman and fluorescence data 193

Figure A5.15: MLR initial rate model using DRIFT, Raman and fluorescence data 194

Figure A5.16: MLR 72-hr model using DRIFT, Raman and fluorescence data 194

Figure A5.17: MLR initial rate model using XRD, Raman and fluorescence data 195

Figure A5.18: MLR 72-hr model using XRD, Raman and fluorescence data 195

Figure A5.19: MLR initial rate model using DRIFT, XRD, Raman and fluorescence data 196

Figure A5.20: MLR 72-hr model using DRIFT, XRD, Raman and fluorescence data 196

Figure A5.21: PCR initial rate model using Raman data 197

Figure A5.22: PCR 72-hr model using Raman data 197

Figure A5.23: PCR initial rate model using XRD data 198

Figure A5.24: PCR 72-hr model using XRD data 198

Figure A5.25: PCR initial rate model using fluorescence data 199

Figure A5.26: PCR 72-hr model using fluorescence data 199

Figure A5.27: PCR initial rate model using Raman and DRIFT data 200

Figure A5.28: PCR 72-hr model using Raman and DRIFT data 200

Figure A5.29: PCR initial rate model using XRD and DRIFT data 201

Figure A5.30: PCR 72-hr model using XRD and DRIFT data 201

Figure A5.31: PCR initial rate model using DRIFT and fluorescence data 202

Figure A5.32: PCR 72-hr model using DRIFT and fluorescence data 202

Figure A5.33: PCR initial rate model using Raman and XRD data 203

Figure A5.34: PCR 72-hr model using Raman and XRD data 203

Figure A5.35: PCR initial rate model using Raman and fluorescence data 204

Figure A5.36: PCR 72-hr model using Raman and fluorescence data 204

Figure A5.37: PCR initial rate model using XRD and fluorescence data 205

Figure A5.38: PCR 72-hr model using XRD and fluorescence data 205

Figure A5.39: PCR initial rate model using DRIFT, XRD and Raman data 206

Figure A5.40: PCR 72-hr model using DRIFT, XRD and Raman data 206

Figure A5.41: PCR initial model using DRIFT, fluorescence and Raman data 207

Figure A5.42: PCR 72-hr using DRIFT, fluorescence and Raman data 207

Figure A5.43: PCR initial rate using XRD, fluorescence and Raman data 208

Figure A5.44: PCR 72-hr using XRD, fluorescence and Raman data 208

Figure A5.45: PCR initial rate model using DRIFT, XRD and fluorescence data 209

Figure A5.46: PCR 72-hr model using DRIFT, XRD and fluorescence data 209

Figure A5.47: PCR initial rate model using DRIFT, Raman, XRD and fluorescence data 210

Figure A5.48: PCR 72-hr model using DRIFT, Raman, XRD and fluorescence data 210

Chapter 1
Introduction

Production of ethanol from lignocellulosic biomass such as corn stover could improve energy security, reduce trade deficits, decrease urban pollution and contribute little, if any to the net atmospheric carbon dioxide accumulation [124]. Biomass can be transformed into liquid transportation fuels that have inherent convenience, cost and efficiency. In this process, pretreatment is necessary (key) to achieve high glucose yields from cellulose in enzyme-catalyzed processes. Pretreatment will break or affect the complex hemicellulose-lignin shield that surrounds cellulose and limits its accessibility to enzymes, making digestibility easier. Pretreatment alters many characteristics of the plant material that impede digestion including: 1) cellulose crystallinity, 2) lignin content, 3) acetyl linkages and 4) the complex hemicellulose-lignin shield that surrounds cellulose in the plant cell wall.

The diverse composition of biomass lends itself to manufacture a variety of products. Cellulose (40-50%) and hemicellulose (25-30%) can be broken down to sugars for fermentation or chemical reaction to a wide range of fuels and chemicals. Lignin (15-20%) can be converted into aromatic compounds or burned to provide heat and electricity to the process. In addition, a significant amount of protein in some biomass can be recovered for food and feed [123].

Pretreatment technology development has been pursued for decades, but lack of fundamental understanding of pretreatment effectiveness has limited technological applications. For example, several studies have tried to explain the roles of lignin content and crystallinity on the hydrolysis rate, along with the effect of acetylation, pore volume and surface area accessibility but contradictory results have emerged. No widely accepted models for predicting the effects of pretreatment on plant materials exist. If we are to unlock the energy and nutrients in lignocellulosic materials for food, feed, fuel and chemical uses, we must better understand the fundamental factors that affect lignocellulose conversion.

Better understanding and application of pretreatment would allow to recycle biomass that otherwise is discarded and will make its transformation to fuel easier allowing a better enzymatic hydrolysis and recovery of sugars for production of useful products, such as ethanol. Pretreatment information will also be useful in the creation of a model for product recovery from biomass. The optimization of biomass conversion will reduce waste and decrease environmental pollution by utilizing discarded material and/or replacing the oil used nowadays for fuel and chemical production

This research involves the spectroscopic characterization of lignocellulose (initially corn residue) prepared using different pretreatments to determine their effectiveness in reducing biomass processing cost by improving hydrolysis. Analytical techniques used are X-Ray Diffraction to determine cellulose crystallinity; Diffuse Reflectance Infra Red (DRIFT) for changes in C-C and C-O bonds; and Fluorescence for the determination of lignin content. Raman spectroscopy is also used in an effort to compare the information obtained with DRIFT and x-ray diffraction and/or complement it.

Pretreatment of lignocellulosic biomass is necessary to obtain high sugar yields by enzyme catalysis. However, the fundamental characteristics of biomass that limit its enzymatic conversion are not clearly understood. A better fundamental understanding of these factors would help improve pretreatment/hydrolysis systems. Toward this end of improved fundamental understanding, leading biomass pretreatment techniques are being studied in an integrated multi-university research project funded by the U. S. Department of Agriculture's Initiative for Future Agriculture and Food Systems (IFAFS). As part of this joint research effort, Michigan State University (MSU) is using spectroscopy and other methods to characterize corn stover pretreated by a variety of approaches including aqueous ammonia recycle percolation (ARP) performed at Auburn University, uncatalyzed hydrolysis and dilute acid hydrolysis, performed at Dartmouth University. In addition, controlled pH treatment was performed by Purdue University, lime preteatment was done at Texas A&M University and ammonia fiber explosion (AFEX) was performed at MSU. The overall objective of the IFAFS research is to develop comparative information on five different pretreatment operations, (e.g AFEX) for production of sugars from hemicellulose and cellulose fractions of biomass for fermentation or chemical reaction to a wide range of commodity products.

The current research objectives are:

- ✓ Apply AFEX pretreatment to corn stover and determine optimum conditions based on sugar and ethanol yields.
- ✓ Monitor recovery, reactions and fate of lignin, hemicellulose, cellulose and protein for each pretreatment by X-Ray Diffraction, DRIFT and Fluorescence analysis.
- ✓ Develop accurate material balances for the AFEX process.
- ✓ Hydrolyze AFEX pretreated solids and evaluate their fermentability.

- ✓ Compare performance of the different pretreatment systems by X-Ray Diffraction, DRIFT and Fluorescence results.
- ✓ Develop a statistical model that would predict the ethanol/sugar yield based on changes in the chemical structure, lignin content and crystallinity of the biomass.
- ✓ Study the biomass structure information provided by Raman Spectroscopy as compared to X-Ray Diffraction and DRIFT for poplar.

Chapter 2
Literature Review

2.1 Bioethanol

Biomass is defined as all non-fossil organic materials that have an intrinsic chemical energy content. It includes all water- and land-based vegetation and trees, or virgin biomass, and all waste biomass such as; municipal solid waste, municipal bio-solid (sewage) and animal waste (manure), forestry and agricultural residues, and certain types of industrial waste [71]. The conversion of biomass to liquid fuels, such as ethanol, has been the focus of much interest during the 20th century. The process of making alcohol from cellulose, in principle, is relatively simple: after hydrolysis of cellulose to glucose and a subsequent fermentation, the ethanol can be recovered by distillation. Much of the United States' (USA) energy use is derived from petroleum, over half of which is imported, rendering us dependent on resources from unstable regions of the world. An economically feasible biomass conversion technology would reduce crude oil dependence. The attractiveness of bioethanol as a potential substance for replacement of conventional fossil fuel lies in its low carbon dioxide release compared to when fossil fuels are burned. The conversion of lignocellulosic materials to ethanol does not require net energy input from fossil fuels [123]. Lignin, which is a by-product, can be burned to provide the energy required for bioethanol production. The carbon dioxide released during the production and the use of bioethanol can be converted back to biomass in the cultivation of energy crops to provide new raw material for the production [123]. As a result, the contribution of biomass ethanol to the greenhouse gas content of the atmosphere is negligible.

In addition, domestically abundant sources of biomass including agricultural and forestry residues are available for bioethanol production. Biomass feedstocks for energy can be provided by short-rotation intensive-culture plantations of trees or plantations of herbaceous plants such as sugar cane, switch grass and corn stover [51]. The biomass can be converted by acid or enzymatic based approaches. Enzymes are used to break apart or hydrolyze hemicellulose and cellulose chains to form their component sugars. The sugars are fermented to bioethanol by adding yeast, bacteria or other suitable organisms. The ethanol is then recovered and used as fuel. A very detailed study on bioethanol production, possible uses, characteristics and demand is presented elsewhere [123].

2.2 Cell Wall

Plant cell walls directly affect the raw material quality of human and animal food, textiles, wood and paper and may play a role in medicine [17]. Modification of various cell wall constituents is a goal in the food processing, agriculture and biotechnology industries. Successful achievement of this goal depends on understanding the molecular basis for mechanical and structural properties of plant-derived materials. A better understanding of plant structures and the effect pretreatment has on these structures, will help identify of specific variables (e.g. crystallinity, acetyl content, types of bond) that can be used to tune the pretreatment parameters (e.g pretreatment time, moisture content, etc.) to obtain the desired product and/or manipulate the system in such a way as to obtain the optimum yield.

Plants use complex polymers of arabinose, mannose, glucose and xylose to intertwine with, and thus strengthen and stabilize homogeneous polymers of cellulose

[17]. These polymers are mainly in the plant cell wall. Currently, no definitive model of the cell wall exists, particularly one that relates the cell wall composition to its mechanical properties. However, the architectural features of the primary cell wall are the following. The primary cell wall is made of two, sometimes three, structurally independent but interactive networks. The fundamental framework of cellulose and cross-linking glucans lies embedded in a second matrix of pectic polysaccharides. The third independent network consists of the structural proteins or a phenylpropanoid network. Cellulose and pectin networks are largely independent or only interact weakly through hydrogen bonding. Pectin facilitates the realignment of cellulose microfibrils in systems under strain, but hemicellulose interacts much more strongly with cellulose and makes the network more rigid. Plant cell walls and structural tissues are primarily composed of cellulose, a polymer of β(1,4)-linked cellobiose residues, hemicellulose and lignins (Figure 2.1).

2.2.1 Cellulose

Cellulose is the most abundant polysaccharide on earth, accounting for 15% to 30% of the dry mass of all primary cell walls and an even larger percentage of secondary walls [17]. Cellulose in lignocellulosics is composed of crystalline and amorphous components. The amorphous component is digested more easily by enzymes than the crystalline component. The crystalline cellulose exists in the form of microfibrils, which are paracrystalline assemblies of several dozen (1→4) β-D- glucan chains hydrogen-bonded to one another along their length. Each (1→4) β-D- glucan may be several thousands units long but individual chains begin and end at different places within the microfibril to allow the microfibril to reach the length of thousands of micrometers and to contain thousands of individuals glucan chains. The (1→4) β-D- glucan chains are tightly linked by numerous hydrogen bonds, both side-to-side and top-to-bottom in a lattice like manner. The glucan chains in the core of the microfibril have a precise spacing (Figure 2.2). The arrangement of atoms in the unit structure of the microfibril core has been determined by X-Ray Diffraction [108].

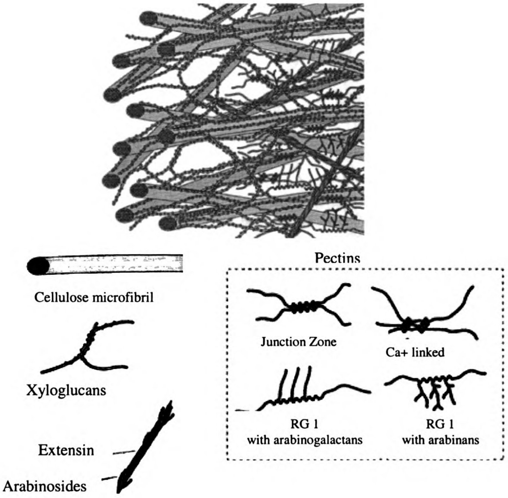

Figure 2.1: A three-dimensional molecular model of a cell wall. Reprinted with permission.

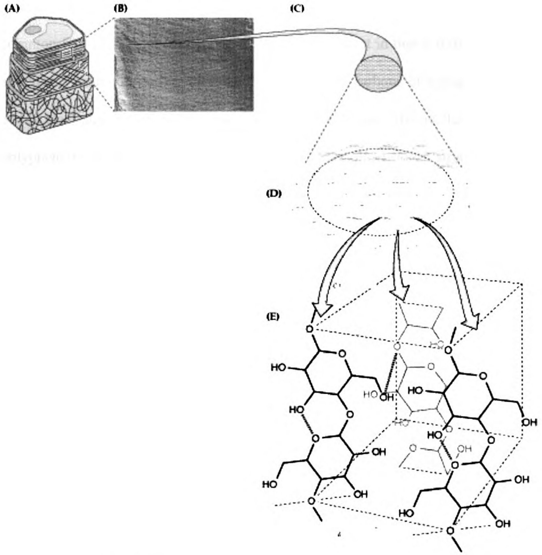

Figure 2.2: Cellulose microfibril. Reprinted with permission from Buchanan, Bob B.. Wilhelm Gruissem and Russell L. Jones. Biochemistry & Molecular Biology of Plants, 3rd edition Courier Companies, Inc., 2001

2.2.2 Hemicellulose

Cross-linking glycans are a class of polysaccharides that can hydrogen-bond to cellulose microfibrils. They may coat microfibrils but are also long enough to span the aldopentoses (arabinose, xylose, galactose), which are in either pyranose or a furanose form. The principal pentose sugar in hemicellulose is β-D-Xylopyranose. The other common five-carbon sugar is arabinose, which is distinct in that it forms a furanose ring structure. Arabinose is usually linked to the 2-and-3 carbons of xylose in arabinoxylan and at the 3-and 6- carbons of galactose in arabinogalactan. Hemicelluloses also link the polyphenolic portion of the plant cell in the three-dimensional structures, known as lignin-carbohydrate complexes [17].

2.2.3 Lignin

The most distinguishing feature of secondary walls is the incorporation of lignins, complex networks of aromatic compounds called phenylpropanoids. After cellulose, lignins are the most abundant organic natural products known and account for as much as 20% to 30% of all vascular plant tissue. Lignins are irregular phenylpropane polymers with different linkages and substitutions on the primary branch [123]. Lignins are thought to be racemic (optically inactive). Practically, no lignin exists in primary walls. The phenylpropanoids, hydroxycinnamoyl alcohol and "monolignols" (p-coumaryl, coniferyl and sinapyl alcohols (Figure 3 [16])) account for most of the lignin networks [17]. Non-woody plants contain lignins that appear to be formed from mixtures of monolignols and hydroxycinnamic acids. The monolignols are linked by way of ester, ether or carbon-carbon bonds. Monolignols form lignin. Lignin is covalently linked to cellulose and xylans in ways that indicate the orientations of polysaccharides may serve as a template for the lignin patterning. A range of cross-linking possibilities exists including hydrogen-bonding, ionic bonding with Ca+ ions, covalent ester linkages, ether linkages and van der Waals interactions (Figure 4 [17]). Lignin-carbohydrate interactions exert a great influence on digestibility of forage crops by animals.

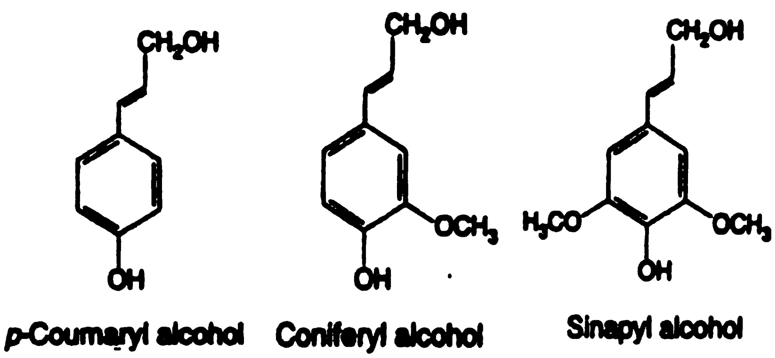

Figure 2.3: Most common lignin monomers

Figu

W;

3rd e

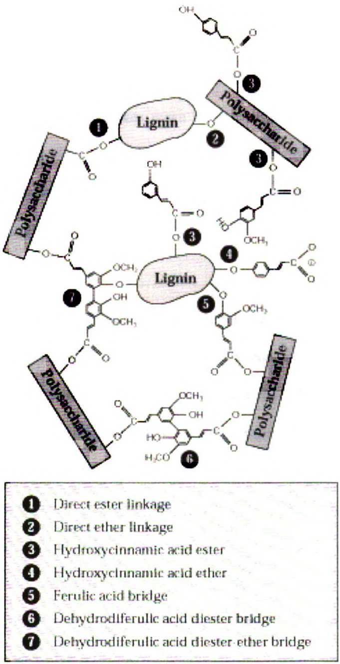

Figure 2.4: Bonds in lignin. Reprinted with permission from Buchanan, Bob B.. Wilhelm Gruissem and Russell L. Jones. <u>Biochemistry & Molecular Biology of Plants</u>, 3rd edition Courier Companies, Inc., 2001

2.3 Pretreatments

Lignocellulosic biomass feedstocks typically contain 55%–75% by dry weight carbohydrates that are polymers of five-and-six carbon sugar units [123]. These carbohydrate polymers must be broken down to their respective low-molecular weight sugar components before microorganisms can complete the conversion to ethanol. Due to the location of the cellulose fraction within the cell wall, enzymatic access is restricted by the lignin and hemicelullose interference. As a result, pretreatment of the biomass is necessary.

Many pretreatments have been studied through the years [23, 57, 58, 125], each one having their advantages and disadvantages. Pretreatments can be categorized as chemical, physical or physicochemical treatments by the effect they have on the biomass. The pretreatments can be acidic, alkaline or neutral. Strong acids can break glycosidic linkages of polysaccharides, freeing the individual monosaccharide components. Some alkaline pretreatments yield highly digestible cellulose and produce liquid streams rich in extracted lignins and polymeric hemicellulose. For industrial applications, a pretreatment must be effective, economical, safe, environmentally friendly and easy to use. This study emphasizes the use of AFEX. A comparison between aqueous ammonia recycle percolation (ARP), uncatalyzed hydrolysis, dilute acid hydrolysis, controlled pH, lime and ammonia fiber explosion (AFEX) is also presented.

2.

pr

ca

bi

us

m

bi

bi

pre

acc

lea

sul

enz

app

2.3

pre

wh

als

2.3.1 Ammonia Fiber Explosion (AFEX)

The ammonia fiber explosion treats lignocellulosic biomass with moderate pressure liquid ammonia, and an explosively release of the pressure [58]. The ammonia can then be recovered and recycled. The small amount of ammonia that remains in the biomass (~1% by weight of the biomass) serves as a nitrogen source for the microbes that use the sugars enzymatically hydrolyzed from the lignocellulose [34]. AFEX uses moderate pressures (up to 280 psi) and moderate temperatures (60-100°C) to treat the biomass.

AFEX is thought to affect both chemical and physical characteristics of the biomass. The chemical effects include cellulose decrystallization, hemicellulose prehydrolysis and lignin alterations. The physical effects include the increase of accessible surface area and decrease in bulk density by disrupting the fiber. AFEX also leaves behind small amounts of ammonia that can serve as a nitrogen source in subsequent fermentations. These effects increase the susceptibility of the biomass to enzymatic hydrolysis. However, AFEX does not change significantly the macroscopic appearance of the substrate.

2.3.2 Ammonia Recycle Percolation (ARP)

In Ammonia Recycle Percolation (ARP) aqueous ammonia is used as a pretreatment reagent in a packed bed flowthrough-type reactor in the recirculation mode where the ammonia is continuously recycled. ARP is a delignification pretreatment that also solubilizes significant amounts of xylan into the pretreatment effluent. The process in

15

re

th

he

p

2.3

ho

ter

and

all

are

sug

oli

Ac

pre

mi

involves treating biomass with an ammonium hydroxide solution at temperatures above 150°C and pressures around 325psi. Most of the delignification and hemicellulose removal occur within 30 minutes of beginning the pretreatment. A detailed description of the experimental setup is presented elsewhere [125].

ARP enhances the enzymatic digestibility of cellulose by removing lignin and hemicelluloses and leaving the remaining solids containing nearly pure celluloses [60]. Physically, ARP increases the pore size and porosity of biomass.

2.3.3 Uncatalyzed Explosion/Dilute Acid

The uncatalyzed explosion is based on heating biomass rapidly with steam, holding the material for a time and rapidly discharging to flash cool the product. The temperature used is about 220°C for a few minutes. This process removes hemicellulose and produces digestible cellulose.

The dilute acid pretreatment uses acidic hot water through a biomass bed, which allows a fairly selective removal of hemicellulose from biomass but the remaining solids are high in lignin [60]. The acid breaks down the hemicellulose to form xylose and other sugars. The hemicellulose or xylan component is converted into arabinose, xylose, plus oligomeric sugar products that constitute 30% or more of the total recovered products. Acid also catalyzes hydrolysis of the cellulose fraction to produce glucose. The pretreatment uses high temperature (140-180°C) and pressures from 50-200 psi for 1-40 minutes and an acid concentration of 0-1.5%, which may cause formation of undesirable su

co

se

Sa

ce

2.

g

m

ot

pr

15

in

ac

2.3

rec

to

loa

sugar degradation products such as furfural and hydroxymethyl furfural, which in turn could be degraded to form tars that might inhibit the hydrolysis.

The main advantage of the dilute acid pretreatment includes the production of a soluble pentose stream that can be physically separated from the particulate residue. Secondly, a substantially increased reaction rate on enzymatic hydrolysis of the residual cellulose portion results presumably due to the acid induced increased fiber porosity [56].

2.3.4 Controlled pH Pretreatment

The controlled pH pretreatment is carried out at a pH between 4 and 7 to result in greater susceptibility of the cellulose to enzymes and also to minimize formation of the monosaccharide degradation products, furfural and hydroxymethyl furfural, which otherwise interfere with subsequent cellulose hydrolysis or ethanol fermentation. The process uses high temperatures (180 to 200°C) and pressures of about 150-250 psi for 5-15 minutes. The run is carried about at 200 g of corn stover per liter of deionized water; in other words a mass ratio of 1:5 solid to liquid.

Physical changes include increase in pore size. There is also an increase in accessible cellulose by decreasing its crystallinity and association with lignin.

2.3.5 Lime

Lime is used as a pretreatment reagent because it is inexpensive, safe and can be recovered with carbonating wash water. The biomass is pretreated with lime and air at 25 to 55°C for 1-5 months. The lime loading is 0.1 g $Ca(OH)_2$ /g biomass and a water loading of 5 to 15 g of H_2O/g biomass.

re

re

en

re

th

2.

su

ac

to

en

att

ex

cel

gl

[12

2.5

lig

cel

of

The treatment effect on biomass is some lignin removal and complete acetate removal. Lime has a selective effect on hemicellulose. The likely mechanism is that lime removes acetate groups from hemicellulose rendering it more accessible to hydrolytic enzymes [23, 25]. This pretreatment produces calcium carbonate that needs to be regenerated in order to recycle the lime, and other product that might be formed during the pretreatment is calcium acetate, which also inhibits the hydrolysis.

2.4 Pretreatment Effectiveness

The effectiveness of a pretreatment is measured by its success in increasing the susceptibility of the biomass to enzymatic hydrolysis. Enzymatic hydrolysis is accomplished by cellulolytic enzymes. A mixture of different enzymes is normally used to obtain efficient hydrolysis of the cellulose. The mixture should contain endoglucanases, exoglucanases, and ß-glucosidases. The endoglucanases randomly attack cellulose chains to produce polysaccharides of shorter chain length, whereas exoglucanases attach to the nonreducing ends of those shorter chains and remove cellobiose molecules. ß-glucosidases act on cellobiose and oligosaccharides to produce glucose for fermentation into ethanol. A scheme of this process is presented in Figure 5 [124]. This research only focuses on cellulases and not in xylanases.

2.5 Enzymatic Hydrolysis Hindrance

Several structural and compositional factors affect the enzymatic digestibility of lignocellulosic materials. The most generally cited factors are cellulose crystallinity, cellulose protection by lignin, accessible surface area, hemicellulose sheathing and degree of hemicellulose acetylation [23]. Analytical methods have been developed through the years to measure these biomass properties in an effort to identify the effect these factors have on the enzymatic hydrolysis.

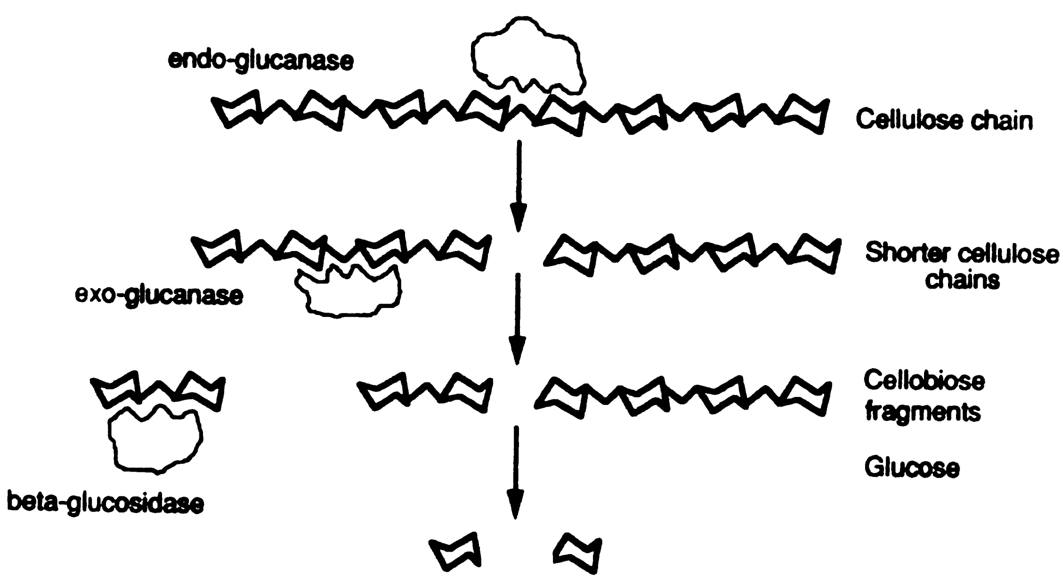

Figure 2.5: Enzymatic hydrolysis scheme

2.5.1 Cellulose Crystallinity

It is well known that cellulose is composed of crystalline and amorphous components [1, 17, 102, 123]. It is also known that the amorphous component is digested more easily than the crystalline component [1]. Hence, anything that will increase the amorphous component in cellulose will also increase the digestibility. Several pretreatments have been used to study the decrystallization of cellulose. Pretreatment of cellulose opens up the cellulose structure and reduces the interaction between glucose chains.

The degree of crystallinity of cellulose is expressed in terms of the crystallinity index (CrI) as defined by Segal et al.[102]. This index is determined by the ratio of the crystalline peak to valley (amorphous region) in the diffractogram based on a monoclinic structure of cellulose.

2.5.2 Lignin Content

Lignin is covalently bonded to polysaccharides in the intact plant cell wall. Relatively little is known about the structure of these lignin-polysaccharides complexes. It is known, however, that the composition is polymeric with a great variety of bonds. The mechanism that explains the protective effect of lignin against polysaccharides hydrolysis remains uncertain although a number of factors; like the degree and type of cross-linkage to polysaccharide, the diversity of structures found in the lignin component and the distribution of phenolic polymers through the cell wall are important [114]. Since cell walls are solubilized by alkali it can be supposed that much of the lignin in those walls is bound through ester linkages. Also, since reducing sugars were found in the low molecular weight fractions from alkaline solubilization, ether linkages of the lignin to the phenolics are suggested [114].

In other studies cellulase inhibition by lignin was reported to be due to lignin-enzyme adsorption [104]. Lignin also reduces fiber digestibility, presumably by interlinkages with carbohydrates. Morrison [87] suggested that the phenolic acids may act as cross-linking agents between lignin and a carbohydrate component consisting of a backbone of β-1,4 linked xylose with 1,3 linked arabinose side chains and a significant amount of b-1,4 linked D-glucose which may have originated from a cellulose-like polymer (probably xyloglucan).

2.5.3 Changes in C-O, C-H bonds and Deacetylation

Pretreatments that have a chemical effect on the biomass may do so by affecting the types of bonds between the lignin-polysaccharides complexes, the hydrogen bonds that keep the molecular chains of cellulose in a highly ordered arrangement (microfibrils) [12] as well as the bonds of the acetyl groups in hemicellulose.

In lignin the monomer units produce a range of highly complex compounds, which may contain some twenty different bond types. Aryl ether linkages, which predominate in the uncondensed part of the molecule, and carbon-carbon bonds contributing to the condensed portion, are the most numerous [114]. The bonds between lignin and carbohydrates are predominantly ester-linked to arabinose side chains of arabinoxylans. Xylans are extensively acetylated. It has been shown that an increase in the degree of deacetylation increases the yield of sugars from enzymatic hydrolysis [75].

2.6 Analytical Analyses

Several analytical techniques have been developed in order to monitor the changes in the biomass cell wall structure and composition and to determine the effect these changes have on the enzymatic hydrolysis. A brief explanation of the different techniques for biomass characterization is presented here. Cellulose crystallinity is measured with X-ray diffraction. The changes in C-H, C-O bonds and acetylation are measured with DRIFT. The amount of lignin in the biomass is measured with fluorescence spectroscopy. Raman spectroscopy is also used as a way to compare and/or complement the data obtained from the other spectroscopic analyses.

2.6.1 X-Ray Diffraction

X-ray diffraction is the use of electromagnetic radiation to determine the interplanar spacings and crystal structure. The pattern of diffraction obtained is directly related to the unit cell size and shape. X-ray diffraction measurements (XRD) of relative crystallinity showed that the crystalline structure of cellulose is affected by pretreatment. Cellulose crystallinity decreases in extent and changes its molecular arrangement to an amorphous form that is highly susceptible to enzymatic hydrolysis.

The crystallinity as defined by Segal et al. was calculated using:

$$\text{Crystallinity Index (CrI)} = \frac{(I_{200} - I_{am}) * 100}{I_{200}} \qquad (2.1)$$

- I_{200} is the intensity of the peak at 22.30°
- I_{am} peak is the intensity of the peak at 18°

The planes were calculated using the equation 2.2 obtained from Cullity and Stock [30] for a monoclinic unit cell.

$$\frac{1}{d^2} = \frac{1}{\sin^2\beta}\left(\frac{h^2}{a^2} + \frac{k^2 \sin^2\beta}{b^2} + \frac{l^2}{c^2} - \frac{hl\cos\beta}{ac}\right) \tag{2.2}$$

Where:

h, k, l = Miller Indices

d = interplanar spacing

l = Copper wavelength (target) = 1.54 A

a, b, c = axial lengths; a = 8.01 A, b = 8.17 A; c = 10.36 A [46]

b = angle between axes a and c ; b = 97.3°

Each spectrum is collected using the θ-2θ method in a Rigaku Rotaflex 200B diffractometer at 45 kV and 100mA with slits size 0.5°,0.5°, 0.3° and 0.45°, respectively. The sample is placed vertically in the slide using double-sided tape to hold it in place and analyzed using the horizontal goneometer.

2.6.2 Fluorescence

The determination of Klason lignin in biomass (the more accurate estimate of plant cell wall lignin reference) is part of two-stage sulfuric acid hydrolysis that is commonly used to determine the neutral sugar components of cell wall polysaccharides [66]. However, lignin behaves as if it contained one single chromophore, which makes it a good candidate for fluorescence analysis [82]. Fluorescence is a form of luminescence in which light is emitted by a molecule following excitation with radiation of a shorter wavelength. Complex conjugated and/or aromatic compounds generally absorb in the ultraviolet range and are fluorescent, since excited states may be stabilized through delocalization over the aromatic system [14]. Fluorescence has been attributed to structures in lignin such as aromatic carbonyl groups; biphenyls, phenylcoumarins and stilbenes, and changes in emission are thought to be due to the formation or destruction of these fluorophores. The intensity of the peaks in the fluorescence spectra is directly related to the lignin concentration in the sample. Fluorescence is a surface technique. It does not penetrate the solid but measures what is present at the surface.

Fluorescence spectra are recorded using a SPEX-3 Fluorolog instrument. Auto emission spectra were obtained at an excitation wavelength of 350 nm with an interval of 0.5 nm. The excitation and emission slits were set at 3 and 5 nm, respectively. The solid sample holder is filled with powdered sample and is held in place with a quartz cover slip. Sample was placed 45 ° from the incident beam. The mode of detection was front face.

2.6.3 Diffuse Reflectance Fourier Transform Infrared (DRIFT)

A molecule absorbs infrared (IR) radiation only when the permanent electric dipole changes during molecular vibration. In IR a more polar bond gives greater peak intensity and nonsymmetric vibrations are stronger. For example, carbonyl groups are strong in IR [107]. IR spectroscopy is a very useful tool for obtaining rapid information about the structure of biomass constituents and chemical changes taking place in biomass due to pretreatments. Diffuse reflectance infrared (DRIFT) has been used to study the differences in the chemical structures of biomass and to estimate the relative amount of lignin and cellulosic polymer [94]. It is a quick, easy, and nondestructive method (the structure of the biomass is maintained as compared to other analyses such as Klason lignin and wet chemistry). In addition, changes in relative proportions of crystalline and amorphous cellulose accompanying chemical treatments are reflected in DRIFT. These results, however, have not been proven to be precise quantitatively but are useful qualitatively.

The DRIFT results presented were obtained in a Nicolet Protégé 460 Magna IR instrument with an auxiliary experiment module for diffuse reflectance. Spectra were obtained using 100 scans of the sample, triangular apodization, a resolution of 16 cm^{-1} and an interval of 1 cm^{-1}. The sample is loaded in the holder and analyzed. The equipment was calibrated using KBr for water and air background. Peaks are identified following Stewart et al [107].

2.6.4 Raman Spectroscopy

Raman is a light scattering process. Raman spectra are obtained by irradiating a sample with a powerful laser source of a visible or infrared monochromatic radiation [105]. In Raman the wavelength of a small fraction of the radiation scattered by certain molecules differs from that of the incident beam and the shifts in wavelength depend upon the chemical structure of the molecules responsible for the scattering. Raman intensity is usually directly proportional to the concentration of the active species. In general, in Raman less polar bonds give greater scattering, for example, C-C double bonds are strong in Raman.

The advantages of this non-destructive technique include small sample requirements, minimal sensitivity toward interference by water, the spectra detail and the conformational and environmental sensitivity [105]. Raman spectra have regions that are useful for functional group detection and fingerprints region that permit the identification of specific compounds. Raman studies are potentially useful sources of information concerning the composition, structure and stability of coordination compounds. A drawback to the use of Raman is the interference by fluorescence of the sample or impurities in the sample.

The Raman analysis is performed with a Hololab Series 1000 from Kaiser Optical Systems, Inc. The sample is analyzed without removing it from a clear plastic bag. The laser probe (Model HFPH-632.8nm) is placed in close contact to the sample and exposed to the laser 10 times for 5 seconds each time and the spectra collected. The bag spectrum is "invisible" to Raman.

2.7 Statistical Analysis

The analysis of the different spectra (DRIFT, XRD, Fluorescence, Raman) for the different samples create an enormous amount of data that must be analyzed and correctly interpreted in order for it to be useful. Multivariate analysis allows the scientist to relate and model different variables simultaneously. In other words, multivariate statistics is a collection of powerful mathematical tools that can be applied to chemical analysis when more than one measurement is acquired for each sample [10].

Multivariate analysis is used for different purposes of which the following are important: (1) Structural simplification, by transforming a set of interdependent variables to dependence, or reducing the dimensionality of a complex (matrix). (2) Classification, whether the objects fall into groups or clusters, or are randomly scattered. (3) Grouping variables, whereas classification is concerned with the grouping of the objects. (4)

Analysis of interdependence, whether a variable is a linear or nonlinear function of the others. (5) Analysis of dependence, one or more variables are singled out to examine their dependence on the others, as in regression analysis. (6) Hypothesis construction and testing [68].

Multivariate calibrations are useful in spectral analyses and can greatly improve the precision and applicability of quantitative spectral analysis [114]. With multivariate calibrations, empirical models are developed that relate the spectral data for multiple samples to the known concentration of the samples. These empirical relationships can then be used in multivariate prediction analyses of spectra of unknown samples to predict their concentrations.

The analysis presented here consists of two parts: calibration and prediction. Analysis begins with the construction of a data matrix (**R**) obtained from the instrument (variables) for a given set of calibration samples. A matrix of concentration values (**C**) using independent methods such as rate of enzymatic hydrolysis is then constructed. The goal of the calibration is to produce a model that relates the data from the instrument to the results by an independent method. The prediction then uses the model to predict the value for an unknown sample.

2.7.1 Multiple Linear Regression (MLR)

The goal of MLR in this study is to find a linear combination of the variables such that the rate of enzymatic hydrolysis value estimated by the model is as close to the experimental value as possible. The criterion of closeness for MLR is defined as minimizing the sum of the squares of the deviations of the predicted values from the true values.

The procedure followed for the coefficient calculation for MLR is presented below. As a way to demonstrate the process let us use a spectral matrix (**R**) and a concentration vector (**c**)

$$\mathbf{R} = \begin{bmatrix} 39 & 29 \\ 18 & 15 \\ 11 & 6 \end{bmatrix}; \qquad \mathbf{c} = \begin{bmatrix} 30 \\ 20 \\ 10 \end{bmatrix}$$

The rows represent the samples and the columns the variables. In matrix **R** columns are spectral data and in the **c** column is the sample concentration as measured by an independent method. The two columns in **R** define a subspace in a row space. To perform MLR, one can plot the **c** in the same row space and project c onto the plane formed by the $\mathbf{r_1}$ and $\mathbf{r_2}$ (columns of **R**). The regression coefficients are in this case.

$$\mathbf{S} = \begin{bmatrix} 0.20 \\ 0.85 \end{bmatrix}$$

From **S** one can estimate **c**;

$$\mathbf{proj\,c} = \begin{bmatrix} 39 & 29 \\ 18 & 15 \\ 11 & 6 \end{bmatrix} \begin{bmatrix} 0.20 \\ 0.85 \end{bmatrix} = \begin{bmatrix} 32.5 \\ 16.4 \\ 7.3 \end{bmatrix}$$

To predict the concentrations of an unknown sample with a given vector (e.g. $\mathbf{r}_{unk}$= [10,5]) one multiplies the vector by **S**

$$\mathbf{c\,pred} = \begin{bmatrix} 10 & 5 \end{bmatrix} \begin{bmatrix} 0.20 \\ 0.85 \end{bmatrix} = 6.25$$

In statistical language MLR is the regression of the columns of **c** onto the space defined by the columns of **R** [110].

an
pa
m
li
n
a
s
2
c
v
s
T
po
co
mo
pa
on
ei
of
wi
of

The MLR is a straightforward matrix algebra, which makes the analysis simple and fast. Since there is direct relationship between the model coefficients and the parameters included in the regression, an easier identification of the factors affecting the model is obtained by simple observation of the absolute value of these coefficients. A limiting factor for this regression is the need for more samples than variables, making it necessary to identify the important parameters to consider in the model in anticipation and eliminating data points that might be considered as noise. This regression utilizes the samples characteristics (parameters) to make the prediction.

2.7.2 Principal Component Regression (PCR)

This model building procedure has two steps. The first step is the determination of the eigenvectors of factors for the matrix **R**; eigenvectors are used to redefine the variables using a smaller number of factors. This approach is used to convert **R** into a score matrix **U** by projecting the **R** matrix onto the space defined by the eigenvectors. The first principal component is the linear combination of the original variables that points in a direction that is more correlated to all the columns in row space. The principal component is also the direction that best describes the variation of the sample. At the moment of factor building PCR ignores the matrix **C**, which is only used in the second part of the model. The second step of the PCR method uses MLR to regress the **C** matrix onto the score matrix as **US=C**, where **S** is a matrix of regression coefficients. The eigenvectors and the matrix of regression coefficients (**S**) form the PCR model. One way of viewing this procedure is that MLR uses all the space described by the columns of **R**, whereas PCR determines the subspace (plane formed in the space formed with the rows of **R** as the axes (row space)) by possibly ignoring some of the eigenvectors.

ca

sp

th

to

Pr

fro

2.6

co

For principal component analysis (PCA), the first step in data analysis is the calculation of the average spectra. This average is then subtracted from the individual spectra, in order to study the deviations of the data (mean-centered). The columns are then scaled, dividing each entry by the variance of the column. This gives equal weight to each column. A mean-centered and scaled matrix **R** is presented below.

$$\mathbf{R} = \begin{bmatrix} 2 & 4 \\ 1 & 2 \\ 0 & 0 \\ -1 & -2 \\ -2 & -4 \end{bmatrix}$$

Principal component analysis is then performed on the covariance matrix $\mathbf{R}^T\mathbf{R}$ formed from the mean centered and scaled matrix. Plotting the matrix in column space (Figure 2.6) gives the data distribution and shows the eigenvalue. In this case the eigenvector covers all the data.

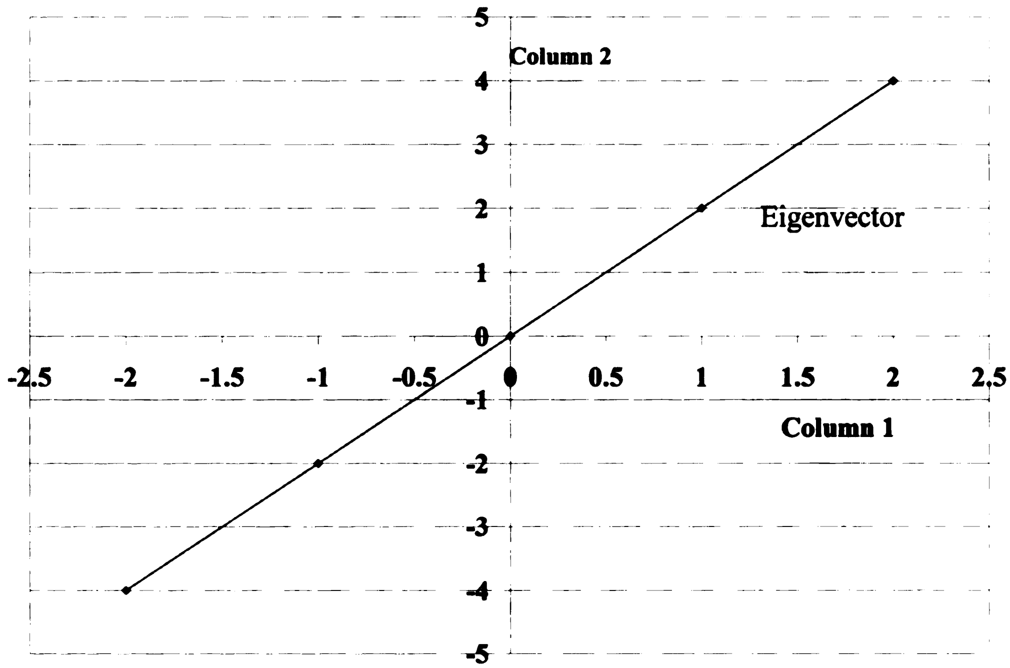

Figure 2.6: Matrix **R** plotted on column space with the first eigenvector

The eigenvector from the figure is $\mathbf{v}^T = [0.447, 0.894]$. The first factor of the principal component can be shown to equal a linear combination.

$$\mathbf{Rv} = \mathbf{u} \qquad (2.3)$$

Where:

R = original matrix response

v = first eigenvector of $\mathbf{R}^T\mathbf{R}$

u = score vector (projection of **R** onto the first eigenvector)

W

the

W

V

-lo

eig

sm

hig

is

R

(U

eig

The

pre

unl

and

When more than one eigenvalue is calculated and use to form an I x J matrix of **U** scores the original variables in **R** can be expressed:

$$\mathbf{R} = \mathbf{U}\mathbf{V}^{\mathbf{T}}(\mathbf{V}\mathbf{V}^{\mathbf{T}})^{-1} \qquad (2.4)$$

Where:

$\mathbf{V}^{\mathbf{T}}(\mathbf{V}\mathbf{V}^{\mathbf{T}})^{-1}$ = generalized inverse of **V**

In PCA notation the elements in $\mathbf{V}^{\mathbf{T}}(\mathbf{V}\mathbf{V}^{\mathbf{T}})^{-1}$ are called principal component "loadings", they range from –1 to +1 and are the cosine of the angles between the eigenvectors and the variable axes. High loadings correspond to high correlation and small loadings (orthogonality) to low correlation.

In more complicated situations, like the one analyzed here, the object can be of higher dimensionality than two, and eigen values are calculated until the sample variation is explained. In the calibration step **R** is re-expressed as a score matrix **U**, by projecting **R** into the eignevectors V:

$$\mathbf{U} = \mathbf{R}\mathbf{V} \qquad (2.5)$$

(**U** is composed of the original data in a new coordinate system described by the eigenvectors) then regressing the **C** matrix as:

$$\mathbf{C} = \mathbf{U}\mathbf{S} \qquad (2.6)$$

The prediction of an unknown sample uses the **V** and **S** derived in the calibration. To predict the concentration of an unknown sample ($\mathbf{C}_{\mathbf{unk}}$) the spectral data matrix of the unknown $\mathbf{R}_{\mathbf{unk}}$ is multiplied by the eigenvector matrix:

$$\mathbf{U}_{\mathbf{unk}} = \mathbf{R}_{\mathbf{unk}}\mathbf{V} \qquad (2.7)$$

and then multiplied by the regression matrix

$$\mathbf{C}_{\mathbf{unk}} = \mathbf{S}\mathbf{R}_{\mathbf{unk}} \qquad (2.8)$$

PCR is a more complex matrix algebra that uses orthogonality of the data to create components that are independent from one another in order to reduce the dimensionality of the data. An advantage of this regression is the fact that due to this processing of the data, all the data available can be used and, the analysis extract the relevant information and removes the noise from the data. This in turn causes a variable reduction and data compression giving a more clear view of the important factors or relation between factors that affects the model. It uses the relationship between the parameters to make the predictions.

3.

he
pl
in
bo
gr
ce
bo

wo
hy
ara
the
the
fib
he
ce
wa

in
cou

Chapter 3
Effect of pretreatment on corn stover as measured by DRIFT

3.1 Background

Corn stover is a crop residue whose major constituents include cellulose, hemicellulose, lignin, protein, and structural inorganics [52]. The hemicellulose in corn plants is a complex network consisting of an acetylated xylan backbone with branches incorporating galactose, arabinose and uronic acids. The lignin in corn stover contains both syringyl and guaiacyl aromatic rings and the side chains are enriched in ester groups. Cellulose is composed of both crystalline and amorphous regions. These cellulose polymers are held tightly together in the microfibril structure by hydrogen bonding

Cellulose is interconnected to the hemicellulose in the plant cell wall while lignin works as glue that keeps the structure together. The hemicellulose, xyloglucan, is hydrogen bonded to the surface of the cellulose microfibrils. The pectic polymers arabinogalactan and rhamngalacturonan interconnect the cellulose microfibrils through the hemicellulose. Lignin is a three dimensional polyphenol and can be visualized filling the space between microfibrils, and also penetrating the spaces between elementary fibrils in noncrystalline regions [48]. Cell wall polymeric lignin is covalently bound to hemicelluloses in the plant cell wall. Ferulic and para-coumaric acids are esterified to cell wall polysaccharides and appear to be the primary means of lignin attachment to cell wall polysaccharides [69].

These substituted cinnamic acids, mainly ferulic and p-coumaric acids, are present in the cell walls in different bonding arrangements and different forms. Ferulic and p-coumaric acid can be linked by ester bonds alone to arabinose residues or arabinoxylans

in
pr
m
as
an
of
si

im
th
fo
p

ce
the
re
re
an
vib
mo
tec
for
spe

in secondary walls and to arabinans and galactans in some primary walls. A high proportion of ferulic acid residues is also linked to secondary walls by ether bonds and may act as ester/ether bridges [6]. In addition 5-5'-dihydrodiferulic acid has been found as a diester bridge between two polysaccharide chains as well as being further joined by an ether link to lignin [88]. Homogeneous and heterogeneous cyclobutane-type dimers of both ferulic and p-coumaric acid have also been identified and may be linked in similar ways.

It is believed that the cross-linkage effect on cell wall digestibility may be more important than concentration of the lignin or phenolic acids. We usually are not aware of these influences when studying normal forage samples because the cross-linkages are formed in conjunction with the deposition of lignin and phenolic acids in the developing plant cell wall [64].

The types of bonds present in the cell wall molecules can be used to identify the cell wall components. Infrared (IR) spectrometry has made the greatest contribution to the knowledge of structures because of its sampling versatility, high resolution and relative freedom from environmental pressure and temperature limitations [112]. Diffuse reflectance Fourier-transform infrared (DRIFT) spectroscopy measures the changes in the amount of bonds present based on the intensity of the stretching, bending or deformation vibrations of the different bonds. DRIFT has been identified as a reliable method for monitoring structural changes in biomass [7,12,14,39,94,107]. The diffuse reflectance technique measures the spectrum, which, when converted into Kubelka-Munk (K-M) format, is proportional to the sample concentration [29]. The diffuse reflection spectroscopic technique was developed to facilitate analysis of materials such as papers and powders in their neat state. When a material is illuminated, some of the radiation penetrates the sample and some is reflected from the surface. The portion that penetrates the sample undergoes scattering at a large number of points in its path. The fraction of this radiation that comes back out of the sample is the diffusely reflected component. This component is theoretically described by Kubelka-Munk model.

The K-M theory relates sample concentration and scattered radiation intensity [42]. The K-M equation is as follows:

$$f(R_\infty) = \frac{(1 - R_\infty)^2}{2R_\infty} = \frac{k}{s} \qquad (3.1)$$

Where R_∞ is the absolute reflectance of the layer, *s* is a scattering coefficient, and *k* is the molar absorption coefficient.

The K-M theory predicts a linear relationship between the molar absorption coefficient, *k*, and the peak value of $f(R_\infty)$ for each band, provided *s* remains constant. Since *s* depends on particle size and range, these parameters should be made as consistent as possible if quantitative data are needed. The K-M equation is only expected to hold for moderately absorbing species at controlled particle size. Therefore the samples analyzed were ground to the same particle size and loaded without pressure in the sample cup. The greatest contribution to $f(R_\infty)$ originates in the first few layers of sample. Area or peak intensity of infrared absorption bands in the spectra can be used as a measure of a functional group concentration in the analyte.

Several peaks have been identified in the DRIFT spectra of corn stover samples, both treated and untreated. Seven main peaks are identified and presented in table 3.1.

E
tc
th
sy
b
b
c
a
he
de
rir
is
fo
cr

m
w
qu
a
Th
qu
inc
star

Each peak can be related to a cell wall component. The peak present at 3400 cm^1 is due to the O-H stretch. The C-H stretch peak is observed around 2900 cm^{-1}. An increase of these peaks signifies an increase in these kinds of bonds, which are more abundant in smaller molecules. Hence, the concentration of these bonds is directly related to breakage of biomass into smaller molecules. The hydrogen bonds in the polymers have been broken down to produce carbohydrates. Another peak can be found around 1720 cm^{-1} related to the ester carbonyl. Such bonds are present in hemicellulose. The aldehyde peak is found at 1640 cm^{-1}. These types of bonds are found in the hemicellulose-lignin complex. A decrease in these peaks will be directly related to delignification and hydrolysis of hemicellulose. The peak at 1595 cm^{-1} is due to aromatic ring stretch that is strongly associated with C-O stretching mode. The peak at 1510 cm^{-1} is due to ring stretch vibration. Both peaks are associated with the monoligols bonds that form lignin such as p-coumaryl, coniferyl alcohol and sinapyl alcohol. The peak at 900 cm^{-1} is due to the antisymmetric, out of phase ring stretch of amorphous cellulose.

Since the plant cell wall is a strongly interrelated matrix of structures rather than merely a complex of isolated fractions the effect that pretreatment has on the cell wall will affect all parts of the cell wall. Spectra in which all peaks vary can not be used for quantification purposes. When quantification of the component concentrations is needed, a reference peak is desired, a peak that does not change from one sample to the other. This peak will provide a reference point on which all the peak changes are based. To quantify precisely the effect that the pretreatment has on the biomass and in an effort to increase the precision of the analytical method an internal standard was selected. This standard, potassium nitrate, was chosen because it has a relatively simple spectrum. The peak in the standard sample that did not interfere with the biomass main peaks was the one chosen. By using this technique the differences in particle size and physical properties would not affect the quantitative results [47, 52, 88].

Table 3.1: Corn stover main peaks in DRIFT spectra

Functional Group	**Absorption (cm^{-1})**
Alcohol O-H stretch	3400
Alkyl C-H stretch	2900
Ester C=O stretch	1720
Aldehyde C=O stretch	1640
Aromatic C-O stretch	1595
Aromatic C=C stretch with C≡C stretch contribution	1510
Ring C=C stretch	900

3.2 Materials and Methods

3.2.1 Materials

The feedstock used by all the collaborating institutions, corn stover, is milled (to pass a 6-mm screen) and dried (about 10% moisture content). Corn stover and its composition were provided by National Renewable Energy Laboratory (NREL) Golden, CO. The composition is presented in Table 3.2.

Table 3.2: Composition of the corn stover

Component	Percentage (based on dry basis)
Glucan	36.1
Xylan	21.4
Arabinan	3.5
Mannan	1.8
Galactan	2.5
Lignin	17.2
Protein	4.0
Acetyl	3.2
Ash	7.1
Uronic Acid (est)	3.6
Non-structural Sugars	1.2
Total	101.6

Auburn University, Dartmouth University, Michigan State University, Purdue University and Texas A&M University pretreated the corn stover with their treatment of expertise (ARP, Steam, AFEX, Controlled pH and Lime, respectively). The biomass is then provided to the other universities to be analyzed. β-glucosidase (Novozymes188, lot number 11K1088) was obtained from Sigma, St Louis, MO. Cellulase enzyme (Spezyme cp) was provided by NREL, CAS 9012-548, activity: 28 FPU/ml; the activity was measured based on NREL standard filter paper unit assay protocol, LAP-006. A Sigma α-cellulose (catalog # C-8002, lot number 11K0246) provided by Auburn University was u

(

p

3

3

I

a

fr

ra

gr

G

30

sta

mi

lic

us

Th

tar

is

pic

used as a standard in the analyses. Anhydrous ammonia was obtained from AGA (Lansing, MI).

The internal standard used was potassium nitrate (Baker,) and ground to the same particle size as the powder samples.

3.2.2 Experimental Equipment and Procedures

3.2.2.1 AFEX Treatment

The AFEX process treats lignocellulosic materials with liquid ammonia under pressure and then the pressure is rapidly released. The moisture of the material treated ranges from 20% to 80 % moisture (dry weight basis). The ammonia to biomass ratio used ranges from 0.5:1 to 1.3:1 (mass:mass) and pressure are generally up to 300 psia. Fifteen grams (15 g) of previously chopped and cleaned corn stover provided by NREL in Golden, CO. is prewetted in order to obtain the desired moisture content, and loaded in a 300 mL stainless steel vessel (PARR Instrument Co., IL). The vessel is topped with stainless steel pellets (approximately 1mm diameter) to occupy the void space and thus minimize transformation of the ammonia from liquid to gas during loading, and then the lid is bolted shut. The predetermined amount of liquid ammonia is delivered to the vessel using precalibrated ammonia cylinders to reach the desired ammonia to biomass ratio. The temperature of the vessel is increased using a 400W PARR heating mantle until the target temperature is obtained. After reaching the target temperature/pressure the reactor is held at these conditions for 5 minutes and then the pressure is suddenly released. A picture of the AFEX experimental apparatus is presented below (Figure 3.1). The

pretreated corn stover is then removed from the vessel and left under a fume hood until the remaining liquid ammonia evaporates (approximately 24 hr). The treated samples are kept in plastic bags at 4°C for further analysis. In AFEX the rapid pressure release literally blows the fiber apart, greatly increasing the surface area available for enzymatic and microbial attack by splitting fiber bundles axially (across the fiber radius). The cellulose swelling or decrystallizing effect of liquid ammonia also distends the unit cell of crystalline cellulose, opening cellulose up for hydrolysis on the molecular level. Essentially complete conversion of plant cellulose and hemicellulose to fermentable sugars is achieved by enzymatic hydrolysis of many AFEX treated materials [37].

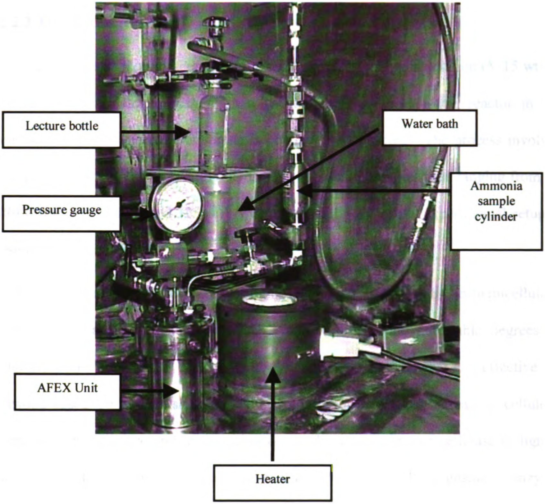

Figure 3.1: AFEX experimental setting

bo

da

sc

ac

Th

loa

Th

3.2

ho

ter

add

low

3.2.2.2 ARP Treatment

In Ammonia Recycle Percolation (ARP), aqueous ammonia solution (5–15 wt.%) is used as a pretreatment reagent in a packed bed flowthrough-type reactor in the recirculation mode where the ammonia is continuously recycled. The process involves treating biomass with an ammonium hydroxide solution at temperatures ranging from 80 –180°C and pressure around 325psi. A detailed description of the experimental setup is presented elsewhere [125].

Aqueous ammonia depolymerizes lignin including breaking lignin-hemicellulose bonds but degrades little cellulose. ARP achieves high and adjustable degrees of delignification for hardwood and agricultural residues but is somewhat less effective for softwood-based pulp mill sludge. Removing lignin helps by increasing cellulose accessibility to cellulase and by reducing nonproductive binding of cellulase to lignin. The digestibility of ARP treated corn stover was 90% with 10 FPU/g-glucan of enzyme loading, far better yields than possible when more enzyme is used with α-cellulose [18]. The challenge for ARP is to reduce liquid loadings to keep energy costs low.

3.2.2.3 Uncatalyzed Explosion/Dilute Acid Treatment

The uncatalyzed explosion is based on heating biomass rapidly with steam, holding the material for a time and rapidly discharging to flash cool the product. The temperature used is about 220°C for a few minutes. Pretreatment performed without addition of dilute acid (i.e. using autohydrolysis) produces hemicellulose sugars yields lower than when dilute acid is added.

In the flowthrough dilute acid pretreatment hot water flows through the biomass bed. Percolation reactors are used because they reduce the treatment time causing fewer sugars to be degraded. Forcing liquid through a packed biomass bed enhances hemicellulose and lignin removal and gives high yields of hemicellulose and cellulose sugars even without acid addition. However, percolation or flowthrough reactor are challenging to implement commercially, and the high amounts of water used result in high-energy requirements for pretreatment and product recovery. This pretreatment uses high temperature (140-180°C) and pressures from 50-200 psi for 1-40 minutes and an acid concentration of 0-1.5%.

The dilute-acid pretreatment (~0.5-1.0% sulfuric) at moderate temperatures (~140-190°C) is effective in removing and recovering most of the hemicellulose as dissolved sugars, and glucose yields from cellulose increase with hemicellulose removal to almost 100% for complete hemicellulose hydrolysis [83]. Lignin is disrupted, increasing cellulose susceptibility to enzymes [124]. Sulfuric acid is cheap, up to 90% hemicellulose yields are achieved, and enzymatic hydrolysis yields of glucose can be over 90% [124]. Nonetheless, dilute acid pretreatment results in costly materials of construction, high pressures, neutralization and conditioning of hydrolyzate prior to biological steps, slow cellulose digestion by enzymes, and non-productive binding of enzymes to lignin [32,39]

3.2.2.4 Controlled pH Pretreatment

The controlled pH pretreatment is carried out at a pH between 4 and 7. The process uses high temperatures (180 to 200°C) and pressures of about 150-250 psi for 5-15 minutes. The run is carried about at 200 g of corn stover per liter of deionized water;

it
h
m
s
3.
a
w
b
b
a
its
3.
Sa
w
ov
si
an
3.
To
si

in other words a mass ratio of 1:5 solid to liquid. The goal is to stop hemicellulose hydrolysis with formation of soluble oligomers and minimize break down to sugar monomers that are subject to subsequent degradation reactions, hurting yields. This system is being applied to release hemicellulose sugars.

3.2.2.5 Lime Pretreatment

Lime is used as a pretreatment reagent. The biomass is pretreated with lime and air at 25 to 55°C for 1-5 months. The lime loading is 0.1 g $Ca(OH)_2$ /g biomass and a water loading of 5 to 15 g of H_2O/g biomass. Lime also removes acetyl groups that have been shown to affect hydrolysis rates. Lignin removal again improves cellulose digestion by enzymes through opening up the structure and reducing non-productive cellulase adsorption. The action of lime is slower than for ammonia or more expensive bases, but its simplicity may make it applicable for pretreatment in piles [25].

3.2.3 Analytical Methods

In order to perform the analytical procedures both the untreated and treated samples must be prepared. The samples treated with ARP, controlled pH and dilute acid were washed before we received them. The wet samples received were dried at 45°C overnight. Once the samples were dry, they were ground using a mortar and pestle and sieved through a 140 –mesh screen with 106μm openings. The fine powder obtained is analyzed by the following techniques.

3.2.3.1 Diffuse Reflectance FT-IR (DRIFT)

The DRIFT results presented are performed in a Nicolet Protégé 460 Magna IR Technology equipment with an auxiliary experiment module for diffuse reflectance. The signal was calibrated using a mirror. Spectra were obtained using 100 scans of the powdered sample diluted with potassium nitrate (1:0.75), triangular apodization, a resolution of 16 cm^{-1} and an interval of 1 cm^{-1}. The compartment was filled with nitrogen to create an inert atmosphere. The sample is loaded in the cup without pressure, the surface smoothed with a spatula and analyzed. The standard was ground to the same size of the sample using a mortar and pestle and was mixed 0.75:1 just before analysis. The equipment was calibrated using KBr for water and air background. Peaks are identified following Stewart *et al* [58,59].

3.2.3.2 Enzymatic Hydrolysis

The digestibility of the treated and untreated corn stover was determined using NREL Laboratory Analytical Procedure (LAP) - 009*. All the samples are hydrolyzed in a pH 4.8 citrate buffer with the desired cellulase enzyme (provided by NREL, CAS 9012-548, activity: 28 FPU/ml) at loadings of (60, 15, and 7.5 FPU/g of glucan) and a β-glucosidase from Sigma (St. Louis, MO) at 40 IU/g of glucan. All the samples are hydrolyzed at 50°C with gentle rotation (75 RPM) for a period of 168 hrs. At predetermined time intervals (0, 3, 6, 24, 48, 72, and 168 hrs), 1 mL of hydrolyzate is taken for sugar analysis. Sugar analysis is performed using a BioRad (Richmond, CA) High Performance Liquid Chromatograph (HPLC) unit equipped with an Aminex carbohydrate analysis column HPX87P and a BioRad Deashing Cartridge guard column. The mobile phase used is degassed HPLC water at a flow rate of 0.6mL/min at 85°C. The injection volume used is 20μL with run time of 20 minutes.

* http://www.ott.doe.gov/biofuels/analytical_methods.html

3.2.3.3 Simultaneous Saccharification and Fermentation (SSF)

SSF experiments were conducted according to NREL standard protocol LAP-008*. Each SSF flask is loaded with 6% w/w glucan, 1% w/v yeast extract, 2% w/v peptone, 0.05 M citrate buffer (pH 4.8), the appropriate amount of cellulase enzyme for 15 FPU/g of glucan and the appropriate amount of *Saccharomyces cerevisiae* D_5A (provided by NREL) inocula (starting O.D. 0.5). The SSF flasks are equipped with water traps to maintain the anaerobic condition and are incubated at 37°C with gentle rotation (130 RPM) for 168 hrs.

At time intervals of 0, 3, 6, 24, 48, 72, 96 and 168 hrs, a 2 mL aliquot is removed aseptically from each flask. The samples are centrifuged; and the supernatants filtered for sugar analysis by HPLC and ethanol analysis on a gas chromatograph (GC). At the last time point, a sample from each SSF flask is streaked on an YPD (yeast-peptone-dextrose) plate to check for any contamination.

The samples taken from fermentation at different time intervals are analyzed for ethanol yield by a GC 17 Shimadzu (Maryland, USA) unit. The injection temperature is 240°C and the detector temperature is 255°C. The carbowax column is first maintained at 80°C for 3 min then ramped up to 125°C in 6 min.

3.2.3.4 Acid Hydrolysis

The lignin content (soluble and insoluble) and carbohydrates in biomass were obtained by following the NREL LAP - 002, 003 and 004* procedure. The treated biomass was passed through a 40-mesh sieve. Both pretreated and untreated corn stover along with the high purity sugars and the method verification standard are loaded in a test tube to be hydrolyzed. Sulfuric acid (H_2SO_4) at a concentration of 72% is added. The samples are hydrolyzed for exactly two hours and then diluted with water to obtain a final concentration of 4% H_2SO_4. The diluted samples are autoclaved for 1hr at 121°C.

Once the samples reach room temperature they are vacuum filtered using a filtering crucible. The supernatant is neutralized with calcium carbonate and filtered for sugar analysis by HPLC. In addition, the supernatant is diluted and its absorbance obtained at λ=205nm using a Perkin Elmer Lambda 3A UV/VIS Spectrophotometer. The solids left in the crucible are dried at 105°C, then weighed and burned at 575°C to determine the amount of insoluble lignin and ash in the sample, respectively.

3.3 Results and Discussion

The standard selected was potassium nitrate (KNO_3). The selection was based on its low toxicity and no reaction with the biomass samples and/or any element of biomass pretreatment (i.e. acid, ammonia, etc). Another aspect to consider was the alteration of the biomass spectra. This was modified by the dilution ratio. The final dilution (1g of sample: 0.75 g of potassium nitrate) was selected because an increase in KNO_3 would offset the biomass signal and vice versa. Figure 3.2 shows the DRIFT spectrum of KNO_3. When analyzing this spectrum and comparing the standard peaks to the important peaks found in biomass (Table 3.1) it was found that the KNO_3 peak at 2400 cm^{-1} does not interfere with the key biomass peaks. The spectra of the pretreated and untreated samples were normalized to this peak.

Figure 3.3 depicts the reproducibility of DRIFT analysis. The sample mixed with the standard was divided in three parts. One part was loaded, analyzed by DRIFT and spectrum recorded. The same procedure was repeated with the other two parts. The spectra of the parts were recorded and are presented in figure 3.3. DRIFT shows a good reproducibility with ±12, ±13 and ±9 % difference in the aldehyde, C-H and lignin peaks intensity, respectively. The whole spectra have a standard deviation (s) of 0.187.

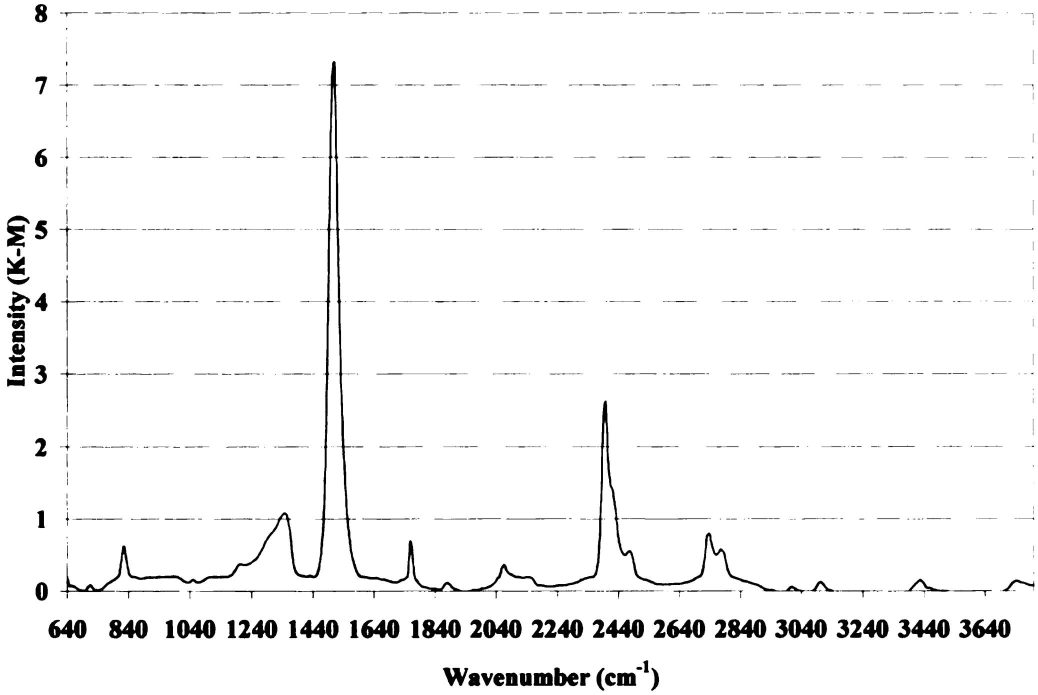

Figure 3.2: DRIFT spectrum of potassium nitrate

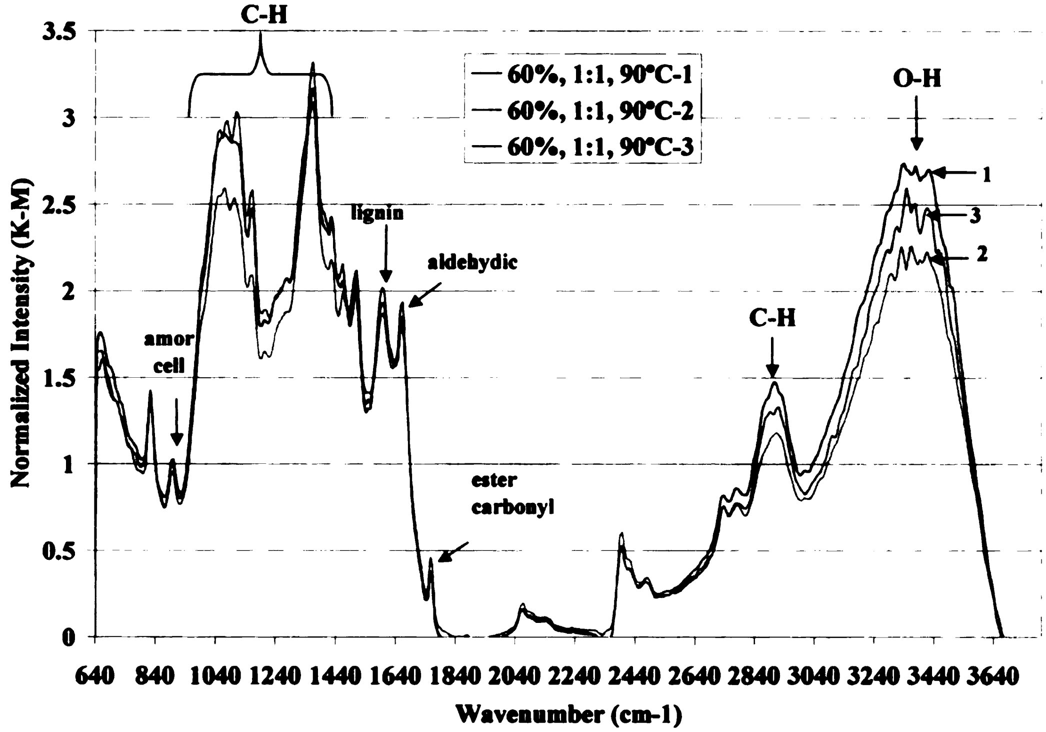

Figure 3.3: DRIFT reproducibility

The analysis of the changes in the peak intensities was performed taking into consideration the variation of the DRIFT technique. Figure 3.4 shows the effect of the AFEX treatment temperature on the corn stover DRIFT spectrum. As seen in the plot the treatment at 60°C, as compared to the untreated sample, shows a decrease in ester carbonyl, C-H and O-H peaks, while there is an increase in the aldehydic peak. In addition, there is negligible change in the lignin and amorphous cellulose peaks. These results imply hydrolysis of the hemicellulose.

When the pretreatment temperature is increased to 70°C it can be seen, as compared to 60°C, that C-H, O-H and aldehydic peaks are increased. On the other hand, ester carbonyl, lignin and amorphous cellulose peaks show negligible changes. In this case increased temperature improve the breakage into smaller molecules. When compared to the untreated sample, the 70°C treatment shows a decrease in ester carbonyl, lignin and amorphous cellulose and an increase in the aldehyde peak, indicating some delignification and hydrolysis of hemicellulose.

A pretreatment temperature of 80°C, as compared to 70°C, shows an increase in amorphous cellulose, and O-H peaks. This implies that an increase in temperature affects positively the breakage into smaller molecules and decrystallization. When compared with the untreated sample, the 80°C treatment shows an increase in aldehydic and O-H bonds and a decrease in ester carbonyl indicating depolymerization and hydrolysis of the hemicellulose.

The pretreatment temperature of 90°C, as compared to 80°C, shows a decrease in amorphous cellulose, aldehyde, ester carbonyl and O-H peaks. However, when compared to the untreated sample it shows a decrease in amorphous cellulose, lignin, ester carbonyl and O-H peaks, implying delignification and hydrolysis of hemicellulose.

Table 3.3 is a summary of the comparative changes in DRIFT results between the different pretreatment temperatures and the untreated corn stover. The enzymatic hydrolysis data indicate that the sample treated at 90°C has the highest glucan conversion. According to this result a decrease in depolymerization of corn stover macromolecules is observed by the decrease in the C-H and O-H peaks intensity. However, it seems that with an increase in temperature two factors have influence in the glucan conversion. These two factors are the hydrolysis of the hemicellulose and delignification of corn stover. In other words, certain degree of depolymerization of cellulose, hemicellulose and lignin, is enough to improve conversion, beyond, which further depolymerization is not effective. Apparently, other factors, perhaps surface area or pore size distribution are affected enough by the 90°C treatment vs. 80°C to more than compensate for the less favorable trends in these peak intensities.

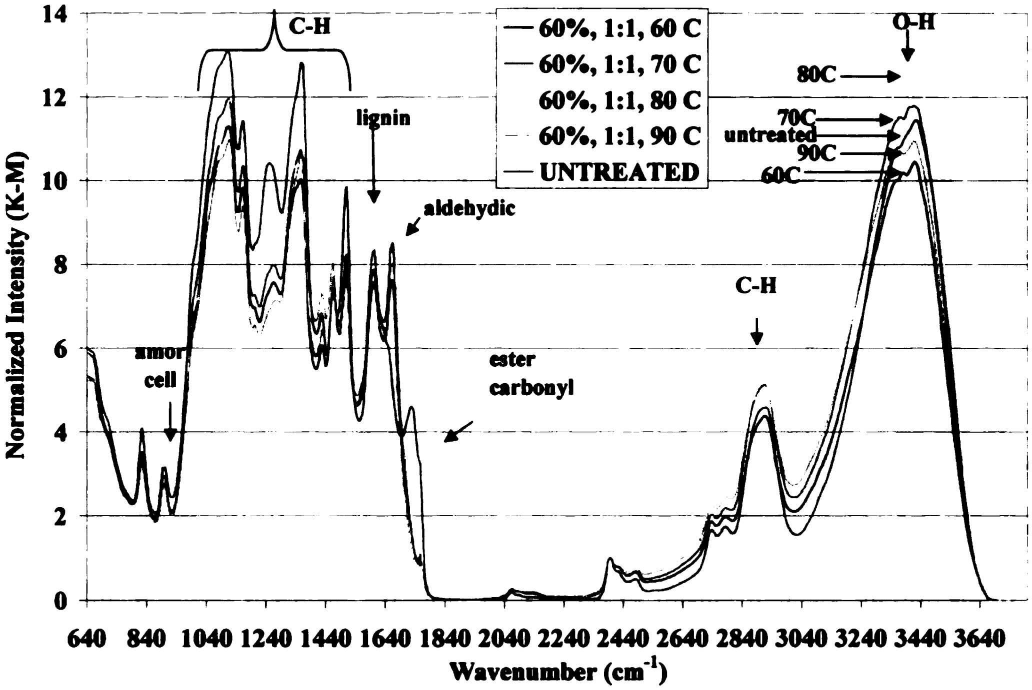

Figure 3.4: Effect of AFEX pretreatment temperature on the DRIFT spectra of corn stover

Table 3.3: Changes in DRIFT results from changes in AFEX temperature

Predominant Peaks	60°C Compared to untreated	70°C Compared to untreated	70°C Compared to 60°C	80°C Compared to untreated	80°C Compared to 70°C	90°C Compared to untreated	90°C Compared to 80°C
amorphous cellulose	0	-	0	0	+	-	-
lignin	0	-	0	0	0	-	0
aldehyde	+	+	+	+	0	+	-
ester carbonyl	-	-	0	-	0	-	-
C-H	-	0	+	0	0	0	0
O-H	-	0	+	+	+	-	-

Legend: + : increase
- : decrease
0 : no change

Figure 3.5 depicts the effect of ammonia loading during the AFEX pretreatment of corn stover on the DRIFT spectra. When compared to untreated corn stover, a loading of 0.5 g of ammonia per g of dry biomass (0.5:1) causes a decrease in amorphous cellulose, ester carbonyl, C-H and O-H peaks at the same time that it shows an increase in the aldehyde peak. This amount of ammonia in the AFEX pretreatment causes some hydrolysis of the hemicellulose, but does not affect much the breakage into smaller molecules, delignification and decrystallization of the biomass. Using more ammonia (0.7:1) decreases the amorphous cellulose and O-H peaks and has negligible effect on the lignin, aldehyde, ester carbonyl, and C-H peaks.

The use of a higher amount of ammonia (1:1), when compared to 0.7:1, gives an increase in amorphous cellulose, aldehyde C-H and O-H peaks. In addition the spectrum shows a decrease in the ester carbonyl peak. These results indicate hydrolysis of the hemicellulose accompanied by some breakage into smaller molecules and some decrystallization. An additional increase in ammonia loading (1.3:1) decreases aldehyde, C-H and O-H peaks. By enzymatic hydrolysis, the amount of ammonia used in the AFEX pretreatment reaches an optimum at 1:1. Using 0.7:1 ammonia loading gives the highest degree of delignification. However, at the 1:1 biomass to ammonia condition there is some delignification and decrystallization (enough to improve hydrolysis) along with depolymerization of the corn stover and hydrolysis of hemicellulose as compared to the other ammonia loadings. According to the hydrolysis data the optimum ammonia loading is 1:1 where highest depolymerization is observed and this agrees with the previously stated optimum AFEX conditions [109]. The DRIFT changes caused by a change in ammonia loading are summarized in table 3.4.

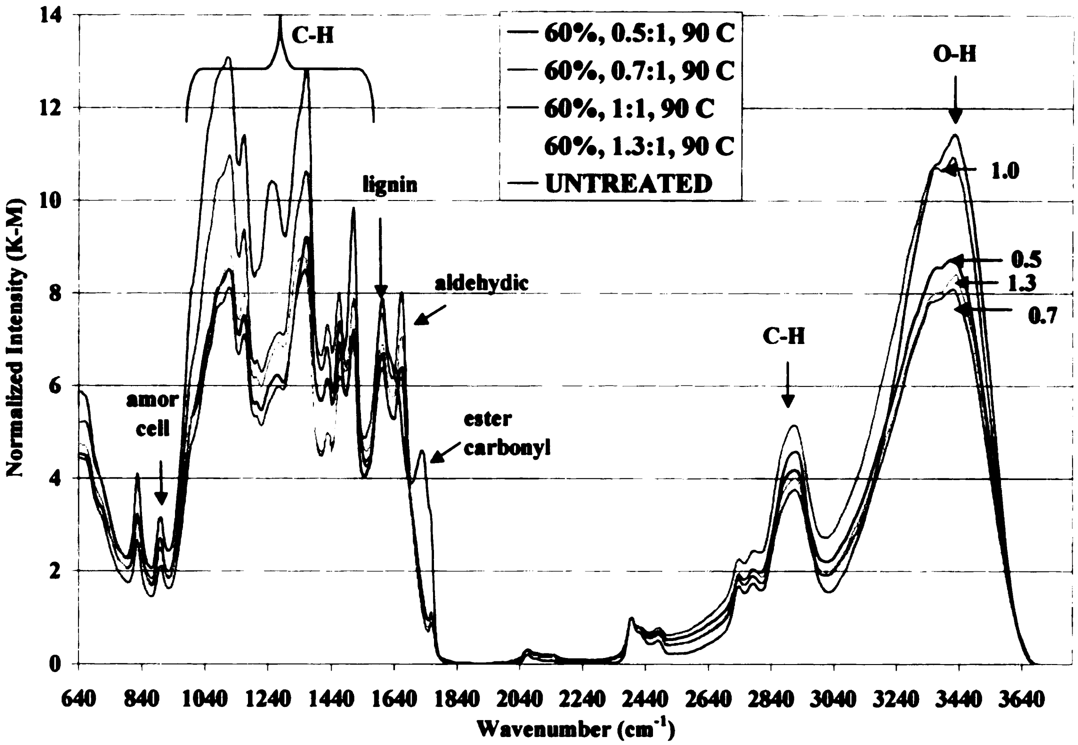

Figure 3.5: Effect of ammonia loading on DRIFT spectra of corn stover.

Table 3.4: Changes in DRIFT results from changes in ammonia loading

Predominant Peaks	0.5:1	0.7:1		1.0:1		1.3:1	
	Compared to untreated	Compared to untreated	Compared to 0.5:1	Compared to untreated	Compared to 0.7:1	Compared to untreated	Compared to 1.0:1
amorphous cellulose	-	-	-	-	+	-	-
lignin	0	0	0	0	0	-	-
aldehyde	+	+	0	+	+	+	-
ester carbonyl	-	-	0	-	-	-	+
C-H	-	-	0	-	+	-	-
O-H	-	-	-	-	+	-	-

Legend: + : increase
- : decrease
0 : no change

The effect of moisture content on the DRIFT spectra of corn stover is presented in figure 3.6. Pretreating corn stover with 20% moisture decreases the amorphous cellulose, lignin, ester carbonyl C-H and O-H peaks as compared to the untreated sample, while increasing the aldehyde peak. Thus, there is some delignification and hydrolysis of hemicellulose.

When the pretreated corn stover with 40 % moisture is analyzed by DRIFT, a decrease in amorphous cellulose and O-H peaks is observed as compared to 20% moisture pretreated corn stover. An increase in moisture causes an increase in hydrolysis of hemicellulose, and has little effect on the depolymerization, delignification and decrystallization.

An increase in corn stover moisture content to 60% causes a decrease in O-H and no effect in the C-H, ester carbonyl, aldehyde, lignin and amorphous cellulose peaks, as compared to 40 % moisture. This indicates that the presence of more water in the system has negligible effect on the chemical structure of biomass. The hydrolysis data indicate that the moisture content that gives the highest conversion is 60%. Apparently, other factors, perhaps surface area or pore size distribution are affected enough by the 60% moisture as compared to 40% moisture to more than compensate for the less favorable trends in these peak intensities. The changes in DRIFT as a result of a change in corn stover moisture content are summarized in table 3.5.

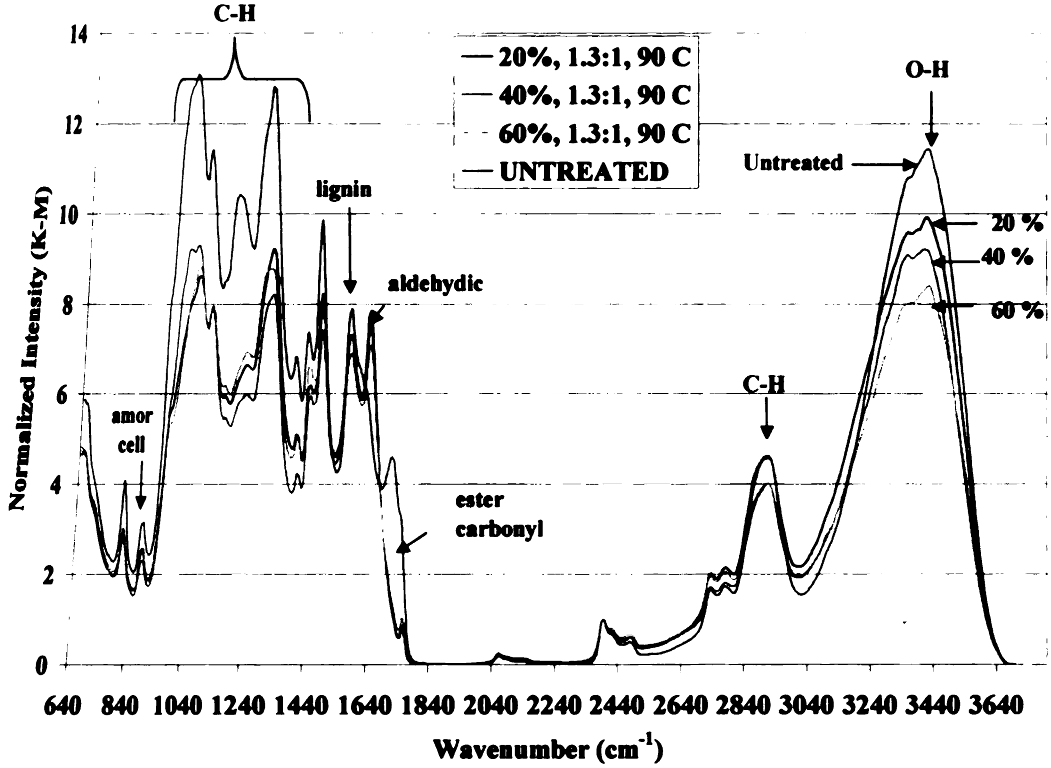

Figure 3.6: Effect of moisture content of corn stover on the DRIFT spectra.

Table 3.5: Changes in DRIFT results from corn stover moisture content

Predominant Peaks	20%	40%		60%	
	Compared to untreated	Compared to untreated	Compared to 20%	Compared to untreated	Compared to 40%
amorphous cellulose	-	-	-	-	0
lignin	-	-	0	-	0
aldehyde	+	+	0	+	0
ester carbonyl	-	-	0	-	0
C-H	-	-	0	-	0
O-H	-	-	-	-	-

Legend: + : increase
- : decrease
0 : no change

The effect of AFEX pretreatment time on the DRIFT spectra of corn stover is presented in figure 3.7. The corn stover was heated to the target temperature and held at that temperature for various times. When comparing the treatment for five (5) minutes with the untreated sample it is found that there is a decrease in amorphous cellulose, lignin, ester carbonyl, C-H and O-H peaks. On the other hand there is an increase in the aldehyde peak. This implies delignification of the biomass and hydrolysis of the hemicellulose. The increase of the pretreatment time to 10 minutes has negligible effect on the lignin, ester carbonyl and C-H peaks and increases the amorphous cellulose and O-H peaks. This result agrees with the hydrolysis data that an increase in pretreatment time beyond 5 minutes has little effect on the biomass conversion.

When the pretreatment time is increased to 15 minutes there is a decrease in amorphous cellulose, lignin, C-H and O-H as compared to 10 minutes indicating increase in delignification while also apparently hindering the breakage of the polymer into smaller molecules and biomass decrystallization. Table 3.6 shows the changes in the DRIFT as a result of a change in the AFEX pretreatment time.

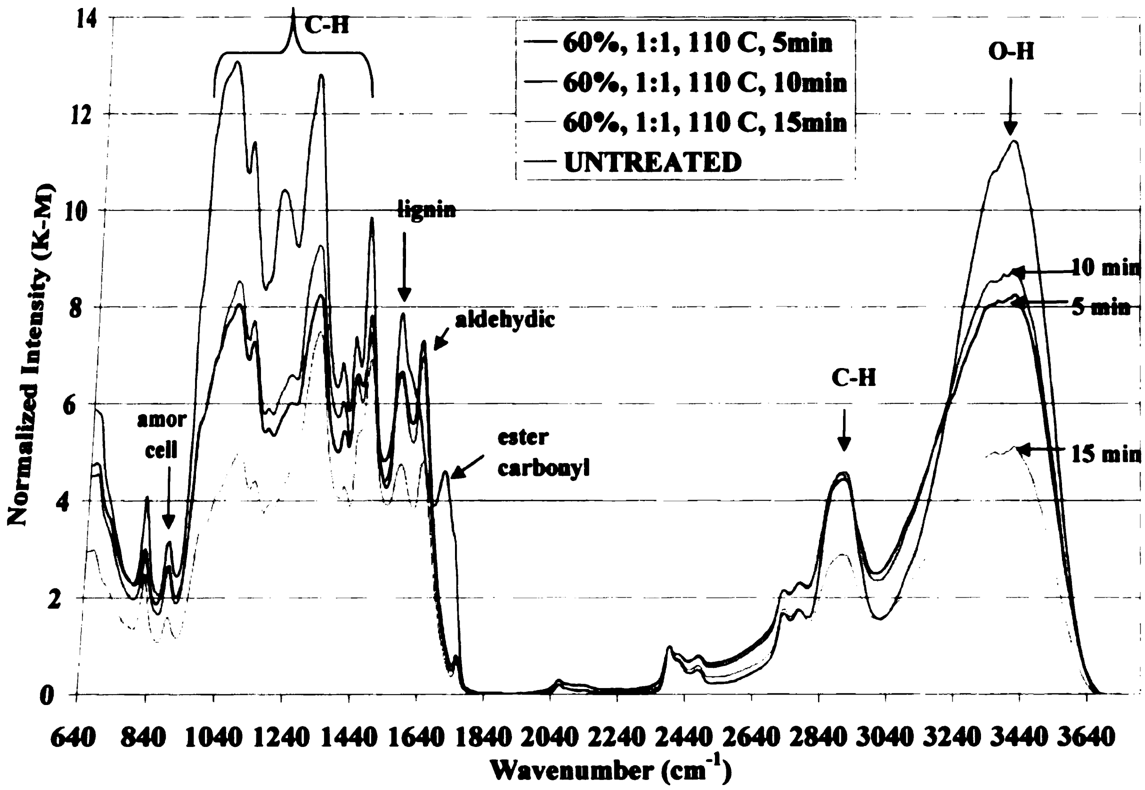

Figure 3.7: Effect of pretreatment time on the DRIFT spectra of corn stover

Table 3.6: Changes in DRIFT results from AFEX pretreatment time

Predominant Peaks	5 min	10 min		15 min	
	Compared to untreated	Compared to untreated	Compared to 5 min	Compared to untreated	Compared to 10 min
amorphous cellulose	-	-	+	-	-
lignin	-	-	0	-	-
aldehyde	+	+	+	-	+
ester carbonyl	-	-	0	-	0
C-H	-	-	0	-	-
O-H	-	-	+	-	-

Legend: + : increase
- : decrease
0 : no change

Figure 3.8 shows the DRIFT results of ammonia recycle percolation pretreated corn stover. When comparing the material pretreated for 10 minutes with the untreated sample a decrease in O-H, ester carbonyl and lignin peaks is observed while there is an increase in amorphous cellulose. As the pretreatment time increases from 10 to 20 minutes an increase in O-H, C-H, aldehyde and amorphous cellulose is observed, along with a decrease in the lignin peak. A further increase in pretreatment time from 20 to 30 minutes causes a decrease in the O-H and C-H, and an increase in the amorphous ellulose and lignin. This indicates that ARP is effective in delignifying the biomass, /drolyzing hemicellulose and provides some decrystallization. According to these ults the optimum pretreatment time is 20 minutes. However, the hydrolysis data icates that at these conditions a highest initial rate and the highest glucan conversion btained for this set of samples at 10 minutes.

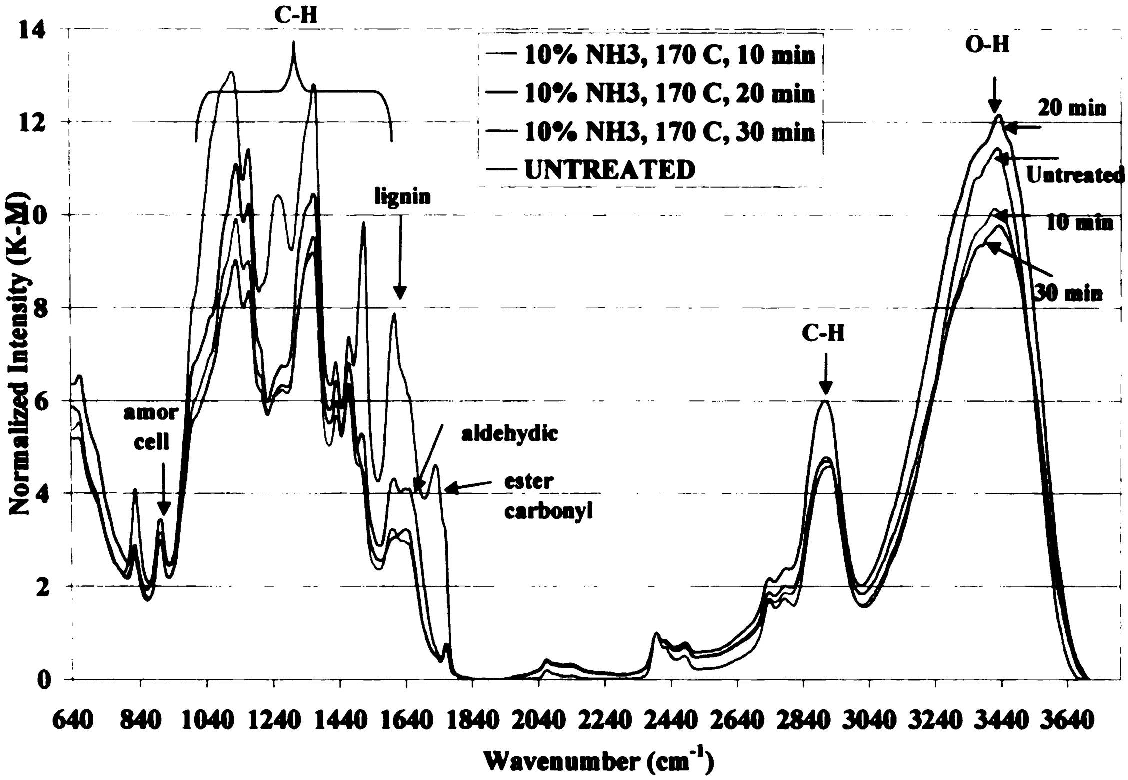

Figure3.8: Effect of ARP in biomass as determined by DRIFT

In figure 3.9 the effect of dilute acid pretreatment on the DRIFT spectra is observed. The spectra show a decrease in the amorphous cellulose, ester carbonyl and aldehyde peaks for all pretreatment conditions. An increase in C-H and O-H peaks is observed for all the conditions. These results indicate that dilute acid pretreatment is effective in depolymerization and delignification of the biomass and hydrolysis of the hemicellulose. It appears that the pretreatment conditions of time and temperature are interchangeable, in other words it seems that an increase in temperature and decrease in time is equivalent to a decrease in temperature and an increase in pretreatment time. This tradeoff (the basis of the severity factor) [124] has been independently proved by the DRIFT results presented here.

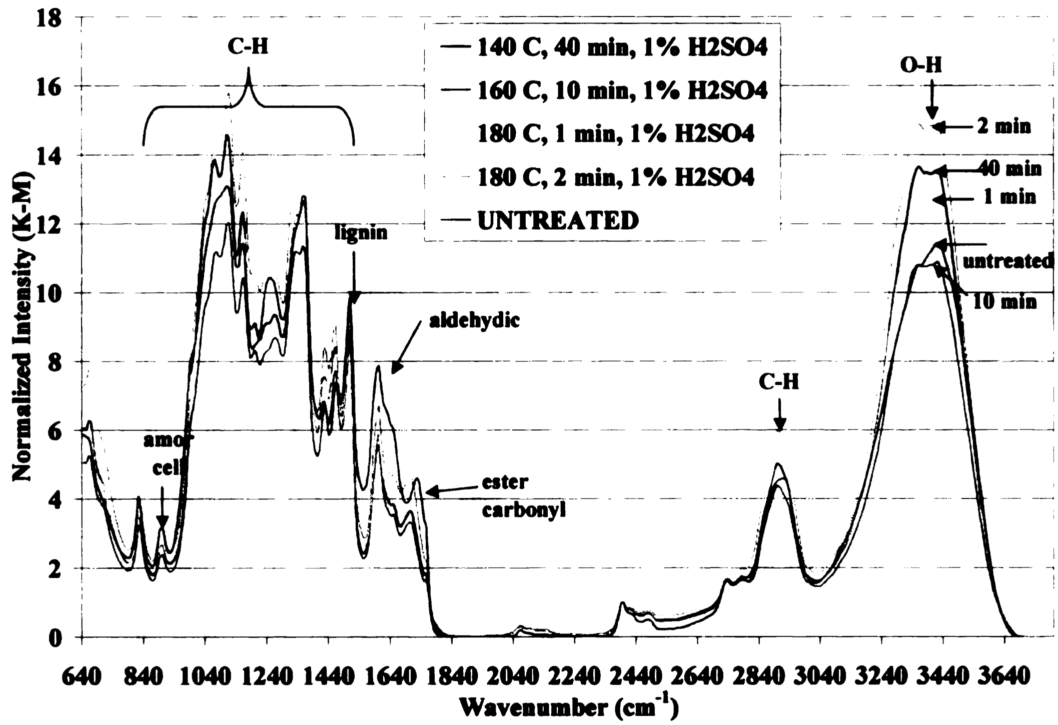

Figure 3.9: Effect of dilute acid pretreatment on DRIFT results.

Figure 3.10 shows the DRIFT results for the controlled pH pretreatment. A pretreatment at 160°C and 5 min and 200°C and 20 min both show an increase in the O-H, C-H, amorphous cellulose and lignin peaks as compared to the untreated sample, indicating breakage into smaller molecules, decrystallization and some delignification. However, based on the enzymatic hydrolysis data, the conditions of 190°C and 15 min of pretreatment are optimal, indicating that other factors not measured by DRIFT also influenced the results. At these conditions a decrease in ester carbonyl and lignin peaks are observed as compared to the untreated sample. These results agree with previous knowledge about the pretreatment. For controlled pH pretreatment, the main effect on the biomass to improve hydrolysis is the hemicellulose hydrolysis [123].

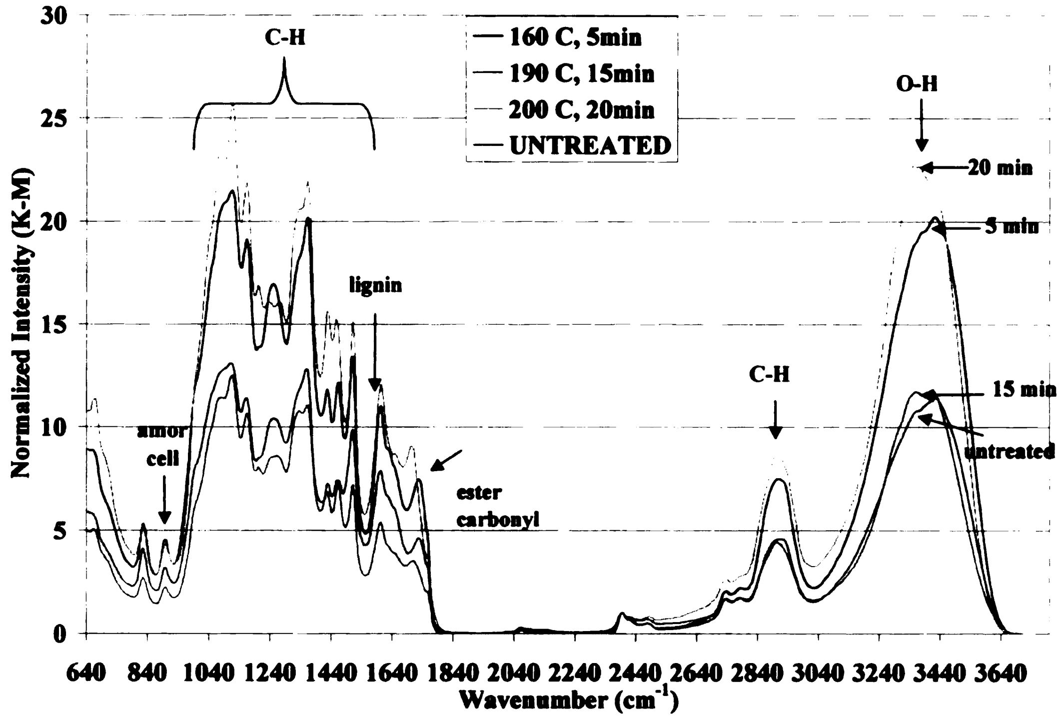

Figure 3.10: Effect of controlled pH pretreatment on the DRIFT results.

Figure 3.11 shows the DRIFT results of the different pretreatments as a way to compare them. All the pretreatments show a decrease in the ester carbonyl peak indicating that they are all effective in the hydrolysis of hemicellulose. Dilute acid and controlled pH show an increase in the O-H peaks while AFEX, ARP and Lime pretreatment show a decrease, as compared to the untreated corn stover. Dilute acid pretreatment shows an increase in the C-H peak while the other pretreatment show negligible effect. Thus, all the pretreatments show certain degree of depolymerization. It is interesting to note that all the basic pretreatments show decrease in the O-H peak as compared to the acidic pretreatments. All the pretreatments show a decrease in the ester carbonyl peak as compared to the untreated sample, indicating different degrees of hemicellulose hydrolysis. All the basic pretreatments in addition show a decrease in the lignin peak while the acidic pretreatments show either negligible or apparent increase in lignin. This indicates that the basic treatments affect the bonds present in the lignin molecules more effectively while the acids are more effective in the breakage of bonds present in the hemicellulose. The changes observed in the DRIFT are summarized in table 3.7.

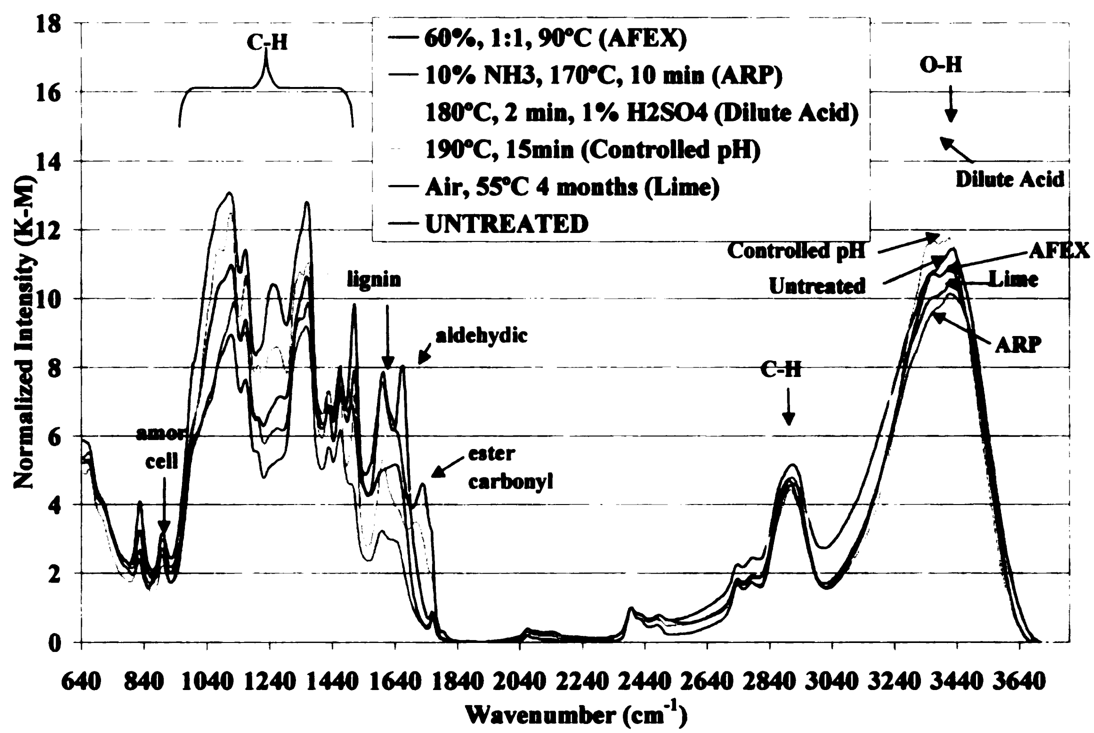

Figure 3.11: Effect of various pretreatments on corn stover as determined by DRIFT

In general, DRIFT results tend to support previous understanding of these pretreatments' effects on biomass. Previous literature has related the changes in biomass to the respective peaks in the DRIFT spectra [2,5,6,17,38,45] and these results confirm it.

Table 3.7: Changes in DRIFT results from the different pretreatments

Predominant Peaks	Pretreatments compared to untreated				
	AFEX	ARP	Dilute Acid	Controlled pH	Lime
amorphous cellulose	0	+	0	-	-
lignin	-	-	+	0	-
aldehyde	+	0	0	0	0
ester carbonyl	-	-	-	-	-
C-H	0	0	+	0	0
O-H	-	-	+	+	-

Legend: + : increase
- : decrease
0 : no change

3.4 Conclusions

From the results presented here it can be concluded that each parameter (i.e., temperature, moisture content, time, etc) of the AFEX pretreatment affects the DRIFT spectra. An increase in temperature causes a decrease in lignin and ester carbonyl; this agrees with the hydrolysis data and previous knowledge that an increase in temperature causes some dissolution of the lignin.

An increase in ammonia to biomass ratio caused an increase in C-H and O-H peaks. Ammonia in the AFEX pretreatment breaks ester bonds and generates smaller molecules. There is a relation between the amount of ammonia and the bonds breakage. As the amount of ammonia increases more bonds are broken until an optimum amount is obtained and a further increase in ammonia causes no additional effect. An increase in moisture causes a decrease in lignin and ester carbonyl peaks. The moisture in the biomass allows formation of ammonium hydroxide that alters the hemicellulose and lignin linkages. An increase in pretreatment time has little effect on the DRIFT spectra as is observed in the hydrolysis data.

According to the DRIFT spectra ARP is effective in delignifying the biomass, hydrolyzing hemicellulose and provides some decrystallization. Dilute acid pretreatment is effective in depolymerization of the biomass and hydrolysis of the hemicellulose. Lime pretreatment is effective in hydrolysis of hemicellulose and some delignification. Controlled pH pretreatment's main effect on the biomass is the hydrolysis of the hemicellulose. All these observations agree with previous knowledge of the pretreatments [25,47,58,70,79, 111, 123-125].

In conclusion, DRIFT spectra can be used as a powerful tool to identify the effects of the pretreatments on biomass. DRIFT also can be used to monitor how the pretreatment parameters (i.e., temperature, time) influence/affect the biomass and how these effects are related to the hydrolysis data. In addition, these results confirm that a change in one parameter (i.e temperature, pretreatment time) affects the entire spectrum indicating an interrelation between the different components of the cell wall.

Chapter 4
Statistical correlation of spectroscopic analysis and enzymatic hydrolysis of corn stover

4.1 Background

It is in the best interests of the biomass processing industry to understand biomass structure and the effects of pretreatments on structure in order to minimize the cost of both enzyme and pretreatment. The creation of an appropriate model may provide an easy, fast and inexpensive way to predict ethanol/sugar yield based on structural changes in biomass (corn stover) as a result of pretreatment. In addition, modeling will broaden the knowledge of biomass structures and properties and the effects that pretreatment has on these properties. This knowledge may help identify parameters that can be tailored in order to obtain an optimum sugar conversion.

Modification of the structural features of the substrate, in this case corn stover, enhance the hydrolysis rate [44]. The most generally cited factors affecting enzymatic hydrolysis are: 1) cellulose crystallinity [1,7,10,30]. The degree of crystallinity of cellulose is expressed in terms of the crystallinity index (CrI) as defined by Segal *et al.* [30], this is determined by the ratio of the crystalline peak to valley (amorphous region) in the diffractogram based on a monoclinic structure of cellulose. 2) cellulose protection by lignin [31,32,34,39]. Lignin is covalently bonded to polysaccharides in the intact plant cell wall, thus reducing accessible surface area of cellulose. The mechanisms that explain the protective effect of lignin against polysaccharides hydrolysis remain uncertain although a number of factors; such as the degree and type of cross-linkage to polysaccharide, the diversity of structures found in the lignin component and the distribution of phenolic polymers through the cell wall are important. 3) hemicellulose sheathing and degree of hemicellulose acetylation [12, 45, 46]. The bonds between lignin and carbohydrates are predominantly ester-linked to arabinose side chains of arabinoxylans. Xylans are extensively acetylated.

Many previous publications have attributed the limitation of enzyme hydrolysis to be due mainly to one aspect (single variable correlation). Some investigators studied lignin as the limiting component [4, 15, 31, 32, 44, 88, 100, 104, 108, 114, 120] while others focused on the crystalline structure of cellulose as the main barrier for enzymatic hydrolysis [1, 12, 30, 38, 51, 64, 79, 96, 97, 101, 102]. In addition, some investigators considered the surface area or pore size [27, 45, 47, 75, 111] of the biomass the limiting factor. It is important to note that the cell wall is a complete system and not a complex of isolated fractions. Hence, an analysis that studies and relates the change in biomass composition to sugar yield taking into account all of the cell wall structures may be more effective than single variable correlations.

Most of the procedures used nowadays for biomass analysis, such as enzymatic hydrolysis and acid hydrolysis and Kjehdahl method are empirical in nature and make determinations of the glucose conversion, lignin content, ethanol yield, etc difficult. Also these analyses are time consuming and expensive, and therefore impractical for an industrial setting. What is needed is a fast, inexpensive and easy to use analysis that can provide detailed qualitative and quantitative information.

The analytical methods used in this study are easy to use, fast and inexpensive as compared to enzyme hydrolysis. Diffuse reflectance Fourier transform infrared (DRIFT) has been identified as a reliable method for monitoring structural changes in biomass [7]. Sample preparation is faster and sensitivity is often higher than is found with normal

Fourier transform infrared (FT-IR). Quantitative precision is good, so that the composition of the sample can be determined in less time than is currently required for standard analytical techniques. X-ray diffraction has also been used in the field for decades to determine the biomass crystallinity. The determination of total lignin is performed using fluorescence spectroscopy. When combined with increased knowledge of cell wall composition and construction, autofluorescence is likely to make an increasing contribution to cell wall analysis [118].

A statistical analysis will mathematically correlate these spectroscopic data to experimental data (e.g. hydrolysis initial rate and yield). Multivariate analysis is widely used in spectral analyses because it can be used to identify variable interactions and reveal variables that strongly influence a process, thus providing a framework for optimizing the process or function [22]. Multivariate analysis also allows the scientist to relate and model different variables simultaneously.

Multivariate calibrations are useful in spectral analyses and can greatly improve the precision and applicability of quantitative spectral analysis [18]. With multivariate calibrations, empirical models are developed that relate the spectral data for multiple samples to the known concentration of the samples. These empirical relationships can then be used in multivariate prediction analyses of spectra of unknown samples to predict their concentrations. Good pattern recognition and detection of relationships can help generalize rules for predicting future values and outcomes based upon current known patterns and relationships in the data.

The multivariate methods are many and various, nearly all of them are used in order to simplify and reduce the complexity of a problem. Several models could be developed based on the final use of the model and the precision desired, however, in this study two models are made using two different multivariate techniques; multiple linear regression (MLR) and principal component regression (PCR). The best model will be chosen based on accuracy and variance analysis. In other words, the best model would be the one that predicts a sugar yield closest to the one determined by wet chemistry (within the desired degree of precision).

The multiple linear regression (MLR) model assumes that the best way to estimate the enzymatic hydrolysis yield of sugars in the sample is by finding a linear combination of the variables that minimizes the errors in reproducing the concentration. This model takes into account all the information available without discerning the importance of each item of information. In other words, MLR is incapable to discern between data in the spectra or noise. MLR is a general technique through which one can analyze the relationship between a dependent variable and a set of independent or predictor variables. The most important uses of the technique are: (1) to find the best linear prediction equation and evaluate its accuracy; (2) to control for other confounding variations in order to evaluate the contribution of a specific variable or set of variables; (3) to find relations between variables and provide explanations for them; and (4) to estimate population parameters and test hypotheses about the population.

Principal components are uncorrelated linear functions of the original variables. They are not only not correlated but in fact independent. The pattern of vectors reveals the nature of the relationship among the variables. The first principal component is the normalized linear combination with maximum variance, also known as an eigenvector. When all variations cannot be accounted for using one eigenvector, a second eigenvector can be found that is perpendicular to the first and describes the maximum amount of residual variation and so on. The principal components turn out to be the characteristic vectors of the covariance matrix and give a new set of linearly combined measurements. A detailed mathematical explanation of both models is presented elsewhere in chapter 2.

The Unscrambler® software helps in the statistical analysis with visual capabilities. It presents a way to change the multivariate relationship from a complicated set of equations into graphical presentation. Unscrambler® provides exploratory analysis, multivariate regression analysis, prediction and validation.

4.2 Materials and Methods

4.2.1 Materials

The description of the materials used is presented in section 3.2.1.

4.2.2 Experimental Equipment and Procedures

AFEX, ARP, Uncatalyzed Explosion/Dilute Acid, Controlled pH and Lime pretreatments are explained in detail in section 3.2.2

4.2.3 Analytical Methods

In order to perform the analytical procedures both the untreated and treated samples must be prepared. The samples treated with ARP, controlled pH and dilute acid were washed before we received them. The wet samples received were dried at 45°C overnight. Once the samples were dry, they were ground using a mortar and pestle and sieved through a 140 –mesh screen with 106μm openings. The fine powder obtained is analyzed by the following techniques.

4.2.3.1 Fluorescence

Fluorescence spectra are recorded using a SPEX-3 Fluorolog. Auto emission spectra were obtained at an excitation wavelength of 350 nm with an interval of 0.5 nm. The excitation and emission slits were set at 3 and 5 nm, respectively. The solid sample holder is filled with powdered sample and is held in place with a quartz cover slip. Sample was placed 45 ° from the incident beam. The mode of detection was front face.

4.2.3.2 Diffuse Reflectance FT-IR (DRIFT)

A detailed explanation is presented in section 3.2.3.1.

4.2.3.3 X-Ray Diffraction

Each spectrum is collected using θ-2θ method in a Rigaku Rotaflex 200B diffractometer at 45 kV and 100mA with slits size 0.5°,0.5°, 0.3° and 0.45°, respectively. Double-sided tape is put on a quartz slide, the powdered sample is loaded by pressing and is smoothed over with another slide. The slide sample is placed vertically in the holder and analyzed using the horizontal goneometer.

4.2.3.4 Enzymatic Hydrolysis

A detailed explanation is presented in section 3.2.3.2.

4.2.3.5 Simultaneous Saccharification and Fermentation (SSF)

A detailed explanation is presented in section 3.2.3.3.

4.2.3.6 Acid Hydrolysis

A detailed explanation is presented in section 3.2.3.4.

4.2.4 Statistical Analysis

The statistical analysis was performed using the software Unscrambler v8.0. (CAMO Process, New Jersey) Spectroscopic data were entered along with their respective hydrolysis data at 3 and 72 hrs in order to obtain both MLR and the principal components regression coefficients. A model is created and from this a prediction for the unknown concentration was obtained.

The steps to follow in multivariate modeling are to first study the raw data, then decide if reprocessing is needed. Principal component analysis (PCA), can help identify possible outliers and the quality of the spectral data along with its useful areas (peaks of interest), and to examine the distribution of the samples (whether or not the samples can be explained with a model). The next step is to calibrate the model. The different calibration models used are MLR and PCR. Once the model is calibrated the outliers can be identified. If any outlier is found and eliminated from the model, then a refinement of such model is needed. The model is then validated using different methods available including leverage correction, cross validation or test set method. After the validation, regressions using the developed models are performed and the final model interpreted. The statistics of the models are analyzed. Part of these statistics is analysis of variance (ANOVA), which includes the standard deviation and degrees of freedom. The root mean square error of prediction (RMSEP), bias and square error of prediction (SEP) are the error to be expected in future predictions, the mean difference between the reference and the data and the measure of the distribution of residuals, respectively. If the statistics show a satisfactory value (bias, RMSEP and SEP ~ 0) the models are used to predict values of the samples with unknown sugar yields.

The predictions of the unknown values were compared to the measured values. The percentage of difference between them was calculated using the following equation:

$$\%difference = \left| \frac{predicted - measured}{\frac{predicted + measured}{2}} \right| \times 100 \qquad (4.1)$$

In order to evaluate the effectiveness of the prediction a hypothesis was made and tested statistically. The Student's t test or t test was used in order to test the hypothesis. The hypothesis to be tested was whether the average predicted conversion value was equal to the average measured conversion value. The two-sided hypotheses are:

$$H_o: \mu=\mu_o \qquad \text{vs.} \qquad H_1: \mu\neq\mu_o$$

The null hypothesis (H_o) is rejected if the predicted average conversion value (μ) is too far away from the measured average conversion value (μ_o) in either direction; that is if the t is too large or too small. This is done with certain level of confidence (α). In this case the selected confidence level was 95%. The rejection region is then defined as:

$$R: |t| \geq t_{\alpha/2}$$

Here $t_{\alpha/2}$ is obtained from the t distribution table [126] with a degree of freedom equal to N-1. The t value is defined as:

$$t = \frac{(\mu - \mu_o)}{s/\sqrt{N}} \qquad (4.2)$$

where:

μ predicted average conversion value

μ_o measured average conversion value

s standard deviation; $s = \sqrt{\frac{\sum_{i=1}^{N}(X_i - \bar{X})^2}{N}}$

$\overline{X}$ predicted/measured glucan conversion mean

N number of samples

4.3 Results and Discussion

In order to characterize the samples several analytical methods were used that have been proven to measure important characteristics of the biomass. These methods are crystallinity, lignin content and changes in selected bonds present in biomass. The results of these spectroscopic techniques are presented below. In chapter 3 a detailed explanation of the DRIFT technique along with the resulting spectra were presented. The data obtained from these spectra were processed by the Unscrambler® software as part of the model.

The sample crystallinity was determined using X-Ray Diffraction (XRD) by the Segal et al. method presented earlier in chapter 2. Table 4.1 shows AFEX crystallinity index (CrI) results. A complete list of AFEX results at different conditions is presented in Appendix 4.

In general, AFEX treated samples show decrease in crystallinity as compared to untreated corn stover. However, it is important to notice that the optimal AFEX condition (highest sugar yield in enzymatic hydrolysis) shows the highest crystallinity index among the treated samples. This implies that the crystallinity is not the only factor affecting hydrolysis. It is also possible that ammonia-treated cellulose is assuming a different crystalline form that is more enzyme accessible than native cellulose.

Table 4.1: AFEX Crystallinity Index

Treatment Conditions	Crystallinity Index (%)
60%, 1.3:1, 60°C	**25.95**
60%, 1.3:1, 70°C	**29.82**
60%, 1.3:1, 80°C	**26.50**
60%, 1.3:1, 90°C	**26.98**
60%, 1:1, 60°C	**27.00**
60%, 1:1, 70°C	**23.15**
60%, 1:1, 80°C	**22.96**
60%, 1:1, 90°C	**36.29**
60%, 0.7:1, 60°C	**20.09**
60%, 0.7:1, 70°C	**24.00**
60%, 0.7:1, 80°C	**22.81**
60%, 0.7:1, 90°C	**31.94**
40%, 1.3:1, 60°C	**12.40**
40%, 1.3:1, 70°C	**19.25**
40%, 1.3:1,80°C	**19.25**
40%, 1.3:1, 90°C	**22.30**
40%, 1:1, 60°C	**23.45**
40%, 1:1, 70°C	**25.09**
40%, 1:1, 80°C	**13.71**
40%, 1:1, 90°C	**23.48**
20%, 0.7:1, 60°C	**20.21**
20%, 0.7:1, 70°C	**23.07**
20%, 0.7:1, 80°C	**23.61**
20%, 0.7:1, 90°C	**16.77**
Untreated	**50.30**
a-cellulose	**66.53**

Table 4.2 shows the CrI results for different pretreatments at their optimal conditions. A complete list of the samples analyzed is in appendix 4. AFEX and ARP are effective in decrystallizing cellulose. Controlled pH pretreatment also shows a decreased CrI. Lime and dilute acid give an apparent increase in CrI as compared to the untreated corn stover. These indices were also included in the models for the different conditions and pretreatments.

Table 4.2: Crystallinity Index of Different Pretreatments

Treatments and Conditions	**Crystallinity Index (%)**
Dilute Acid (180°C, 2 min, 1% H_2SO_4)	52.51
Controlled pH (190°C, 15 min)	44.52
Lime (Air, 55°C, 4 months)	56.17
AFEX (60%, 1:1, 90°C)	36.29
ARP (10% NH_3, 170°C, 10 min)	25.98
Untreated	***50.30***
a-cellulose	***66.53***

Fluorescence spectra show a direct relationship between the lignin content and the area under the curve at 425nm. Figure 4.1 shows the fluorescence spectra for different pretreatments. When the powdered sample is excited at 350nm, a peak at 425nm related to lignin will appear. All the pretreatments except ARP show a decrease in this peak as compared to that for untreated corn stover. However, it is well known that ARP is a delignification process so this result for ARP may not be particularly noteworthy. It is believed that since ARP extracts lignin some lignin might be re-deposited on the surface. Fluorescence, a surface analysis method, might thereby show a higher lignin content. The fluorescence spectra of all the samples were included in the models.

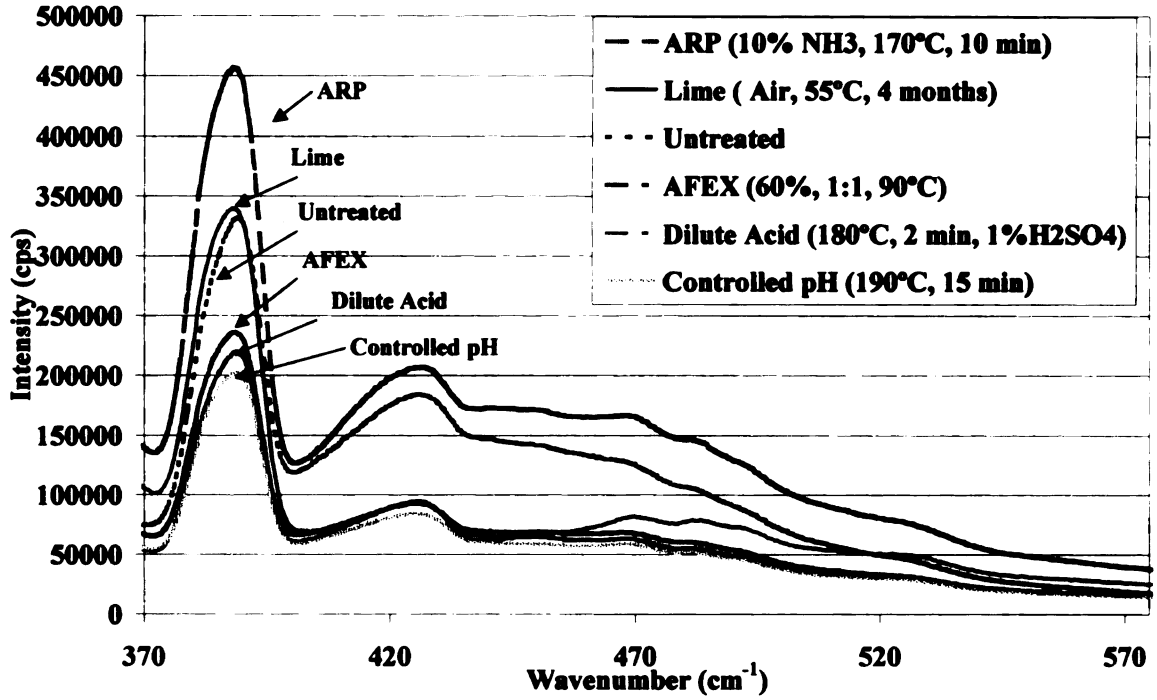

Figure 4.1: Fluorescence results for the different pretreatments

The data obtained from DRIFT, Fluorescence and XRD were input into the statistical analysis software Unscrambler ® in order to obtain a model using multiple linear regression. Because of the limitation that more samples than variables are needed to create a MLR model, the intensity of selected peaks (presented in table 3.1) were used from the DRIFT spectra along with the intensity of the fluorescence peak related to lignin and the crystallinity index. These intensities were determined using a baseline correction. In other words a new baseline was used for every peak in order to determine its intensity. The results for both initial rate and conversion at 72 hrs are presented below. Figure 4.2 shows the MLR model for initial rate using only DRIFT data and using DRIFT, Fluorescence and XRD data. The model using only the DRIFT data (a) gives a correlation of R^2 = 0.666 while the model using all the data gives a correlation of R^2 = 0.807. It is evident that an increase in the amount of data in the model gives a better fit of the data. When analyzing the coefficients of the models it is seen that the model using the DRIFT data is more affected by the ester carbonyl content, related to the degree of hemicellulose hydrolysis. A decrease in the ester carbonyl bonds will increase the initial rate. The model using all the data is more affected by the aldehyde. A decrease in the aldehyde bonds will cause an increase in the initial rate.

The model for the conversion at 72 hrs is presented in figure 4.3 using only the DRIFT data and also using all the data. The model with only DRIFT data gives a correlation of R^2 = 0.700. Analyzing the coefficients, it is found that the parameter that most influences the model using only DRIFT data is the lignin content. The model using all the data gives a correlation of R^2 = 0.757. In this case an increase in the amount of data has little effect on the data fit. When using all the data the parameter that influences most the model is the C-H bond, a result of hydrolysis of hemicellulose. An increase in this parameter will increase the glucan conversion at 72 hrs. The coefficients (B) for the initial rate and 72 hrs conversion MLR model using all the spectroscopic data are presented in the appendix 4; Table A4.3.

The differences observed between the initial rate model and the 72 hrs model may be due to the fact that some parameters that have not been taken into account in this model, (i.e. surface area, pore size) are more influential at the beginning of the hydrolysis than at 72 hrs.

a)

b)


Predicted Glucan Conversion (%)
Predicted Glucan Conversion (%)

Fig

a)

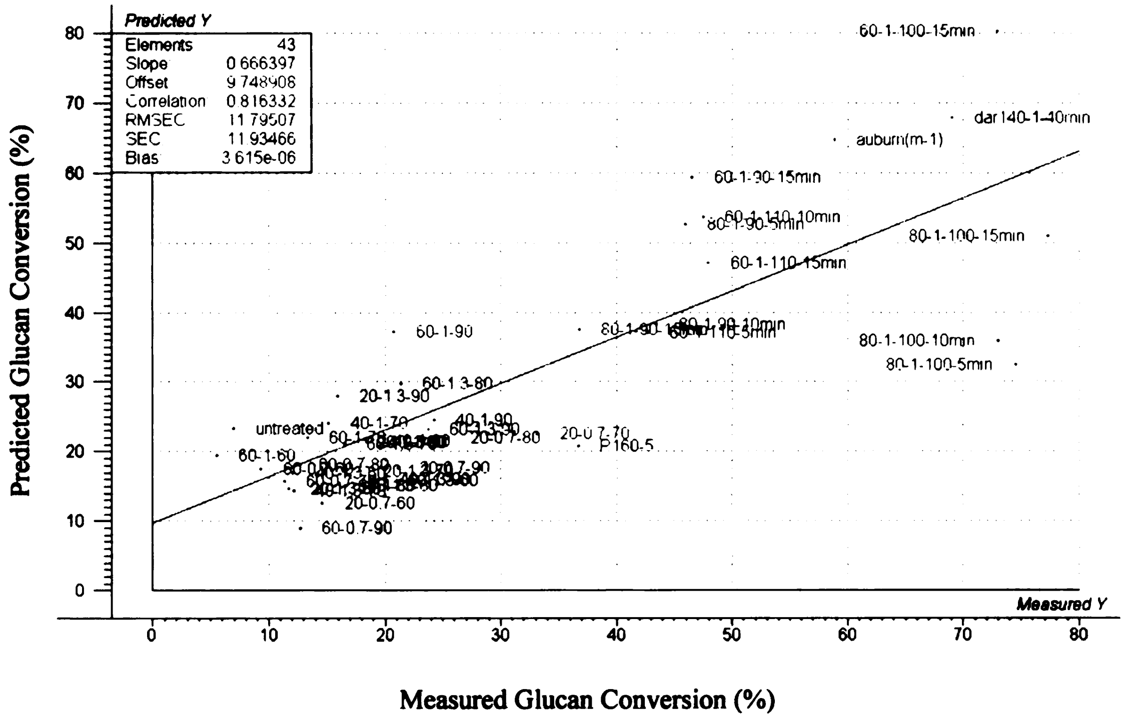

b)

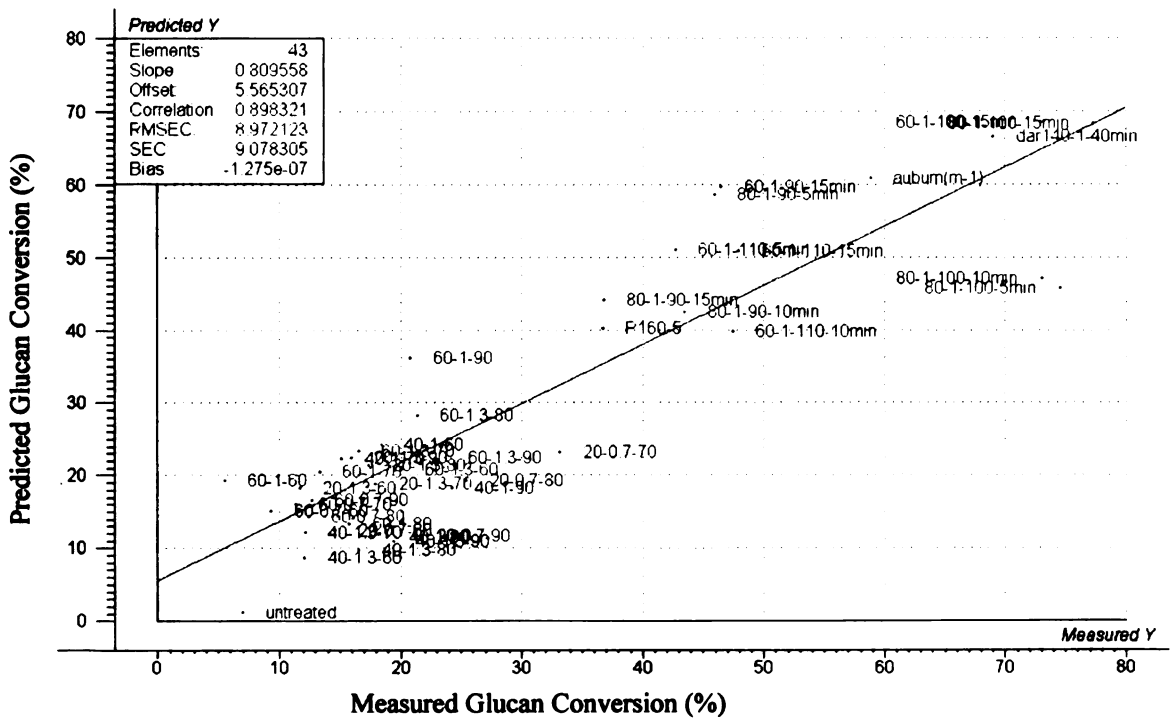

Figure 4.2: Initial Rate MLR Model using a) DRIFT data only and; b) all the data.

a)

Predicted Glucan Conversion (%)

b)

Predicted Glucan Conversion (%)

Figure

a)

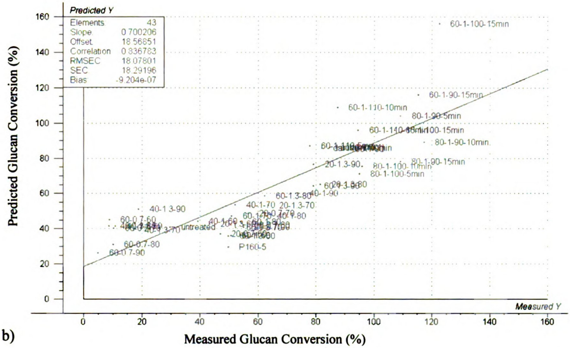

b)

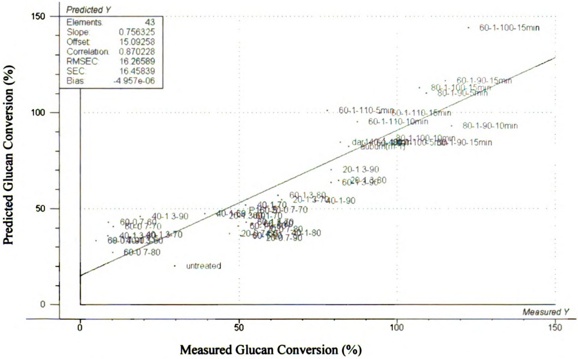

Figure 4.3: MLR model for the 72 hrs glucan conversion using a) DRIFT data only and; b) all the data.

conver

differe

72 hr

convers

size, w

to pred

differe

approx

This m

better t

conside

initial

influen

result

surface

pretrea

influen

Table 4.3 shows the predicted values for both the initial rate and the 72 hr glucan conversion using the MLR model. When using the MLR model the initial rate differences between measured and predicted values for AFEX are 16-73 %, while for the 72 hr data the differences are 10-26%. Thus, the model has a better fit to the 72 hr conversion. Once again, the model does not include factors such as surface area and pore size, which may have greater effect on the initial rate.

As can be seen by the results presented in the table this model could also be used to predict the glucan conversion obtained using pretreatments other than AFEX. For the different pretreatments the differences between measured and predicted values vary by approximately 2-40% for the initial rate and 7-57% for the glucan conversion at 72 hrs. This model predicts the initial rate obtained from the different pretreatments slightly better than the conversion at 72 hrs. Apparently the parameters that are not taken into consideration in this model have more influence at the 72 hrs conversion than on the initial rate in ARP, dilute acid and controlled pH pretreatments.

It appears that for the AFEX process the initial rate of glucan conversion is also influenced somewhat by the parameters not included in the model like surface area. This result agrees with previous knowledge that AFEX creates more enzyme accessible surface area in order to obtain higher yields [58]. For ARP, dilute acid and controlled pH pretreatment it seems that the other parameters (i.e. surface area, pore size) have more influence at the 72 hrs conversions.

Table 4.3: Prediction using MLR model for corn store

Sample	Initial Rate Predicted (%)	Initial Rate Measured (%)	% difference	Glucan Conversion Predicted at 72 hrs (%)	Glucan Conversion Measured at 72 hrs (%)	% difference
AFEX 20%-1.3:1-80C	21.42	17.39	20.76	64.87	81.48	22.70
AFEX 20%-1.3:1-90C	22.47	15.91	34.19	70.38	79.09	11.64
AFEX 60%-1:1-80C	13.32	15.76	16.80	42.15	54.09	24.81
AFEX 60%-1:1-110C-5min	50.90	42.67	17.58	101.20	77.87	26.06
AFEX 80%-1:1-100C-10min	47.15	72.97	42.99	86.58	95.87	10.18
ARP 10% NH3, 170C, 30 min	90.03	60.08	39.90	149.75	83.41	56.90
ARP 10% NH3, 170C, 20 min	49.67	56.10	12.17	66.69	84.00	22.97
Diltue Acid 180 C, 1% H2SO4, 1min	40.77	40.00	1.91	69.85	47.00	39.11
Dilute Acid 180C, 1% H2SO4, 2min	58.84	70.00	17.32	84.82	76.00	10.96
Controlled pH 190C, 15min	56.24	55.16	1.94	67.61	76.32	12.10
Controlled pH 200C, 20min	38.59	40.83	5.64	44.56	41.47	7.18

Here t

When

than 2

level.

measu

spectra

model

the co

for the

alone

inform

only

repres

Apper

Table 4.4 shows the results of the hypothesis testing with a 95% confidence level. Here the rejection region for both initial rate and 72 hrs conversion would be $|t| \geq 2.306$. When observing the calculated $|t|$ for both initial rate and 72 hrs conversion is smaller than 2.306, hence the null hypothesis (H_o: $\mu=\mu_o$) is not rejected with a 95% confidence level. In other words, there is no statistical difference between the predicted and the measured conversions.

Table 4.4: Corn stover MLR data for hypothesis testing

MLR	t	$t_{\alpha/2}$
initial rate	-0.0741	2.306
72 hr	-0.4219	2.306

Table 4.5 shows the correlation (R) obtained using PCR regression and different spectral inputs. In PCR every single data point from every spectrum was input into the model. In table 4.4 we see that including all the analytical techniques actually decreases the correlation for the initial rate, indicating that the model is over specified. However, for the 72 hr conversion the same correlation is obtained using either the DRIFT data alone or all the spectroscopic data available. Therefore DRIFT contains all the information necessary to make an adequate predictive model. Hence, the model using only DRIFT data will be used to make subsequent predictions. A graphical representation of the models using the various spectroscopic techniques is presented in Appendix 4.

D

data.

initial

hemic

param

breaka

coeffi

only a

the da

bonds

the P

believ

Table 4.5: Correlation using various spectroscopic techniques

Analytical Technique (s)	Initial Rate	72 hrs Glucan Conversion
DRIFT	R = 0.860	R = 0.903
Fluorescence	R = 0.664	R = 0.906
XRD	R = 0.691	R = 0.530
DRIFT + Fluorescence	R = 0.374	R = 0.033
DRIFT + XRD	R = 0.691	R = 0.529
Fluorescence + XRD	R = 0.374	R = 0.033
DRIFT + XRD +Fluorescence	R = 0.697	R = 0.903

Figure 4.4 shows the PCR model for predicting initial rate using only DRIFT data. When analyzing the coefficients it is found that the parameter that most affects the initial rate is the aldehyde content, representing the bonds between the lignin and hemicellulose.

Figure 4.5 shows the 72 hrs glucan conversion model using the DRIFT data. The parameter that affects the 72 hr glucan conversion is the C-H content reflecting the breakage of structural carbohydrate into smaller molecules. The most influential coefficients for the initial rate and 72-hrs conversion PCR models using the DRIFT data only are presented in appendix 4, table A4.4. It is very important to realize that given all the data points input into the model, PCR is able to identify the wave number of those bonds that have previously been identified as influential in the biomass hydrolysis. Thus the PCR method has independently verified the importance of those bonds already believed to most influence biomass hydrolysis.

Predicted Glucan Conversion (%)

Predicted Glucan Conversion (%)

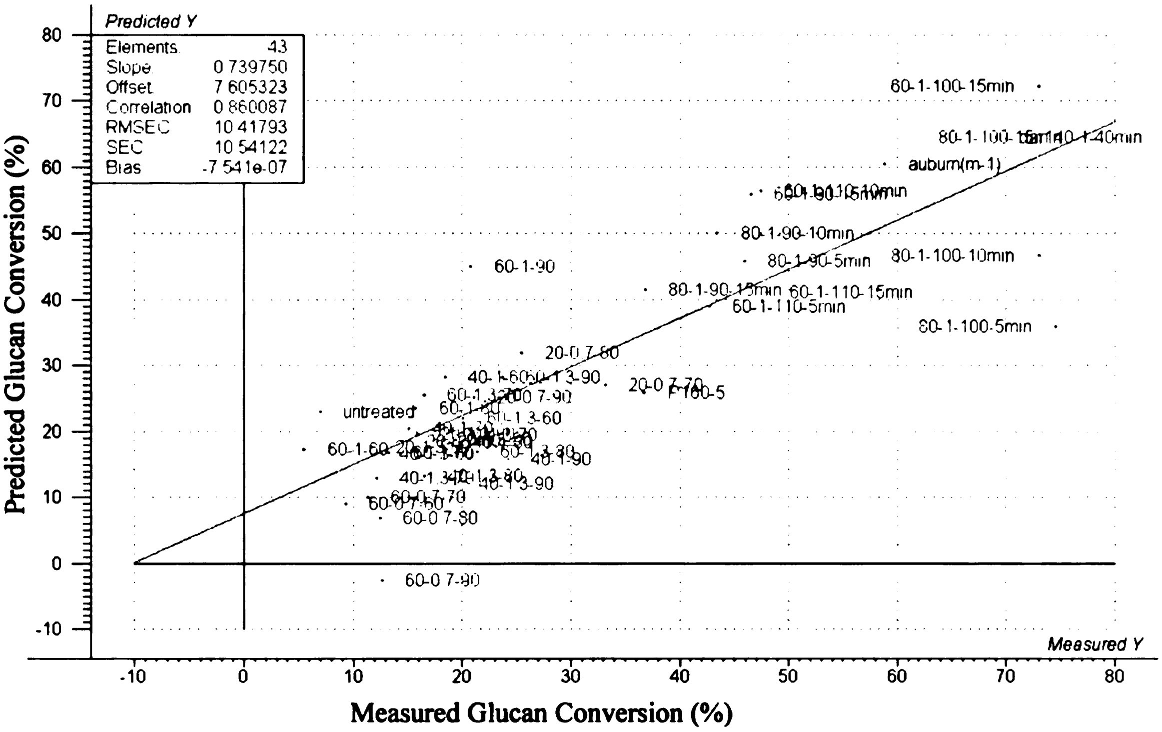

Figure 4.4: PCR model for initial rate using only DRIFT data.

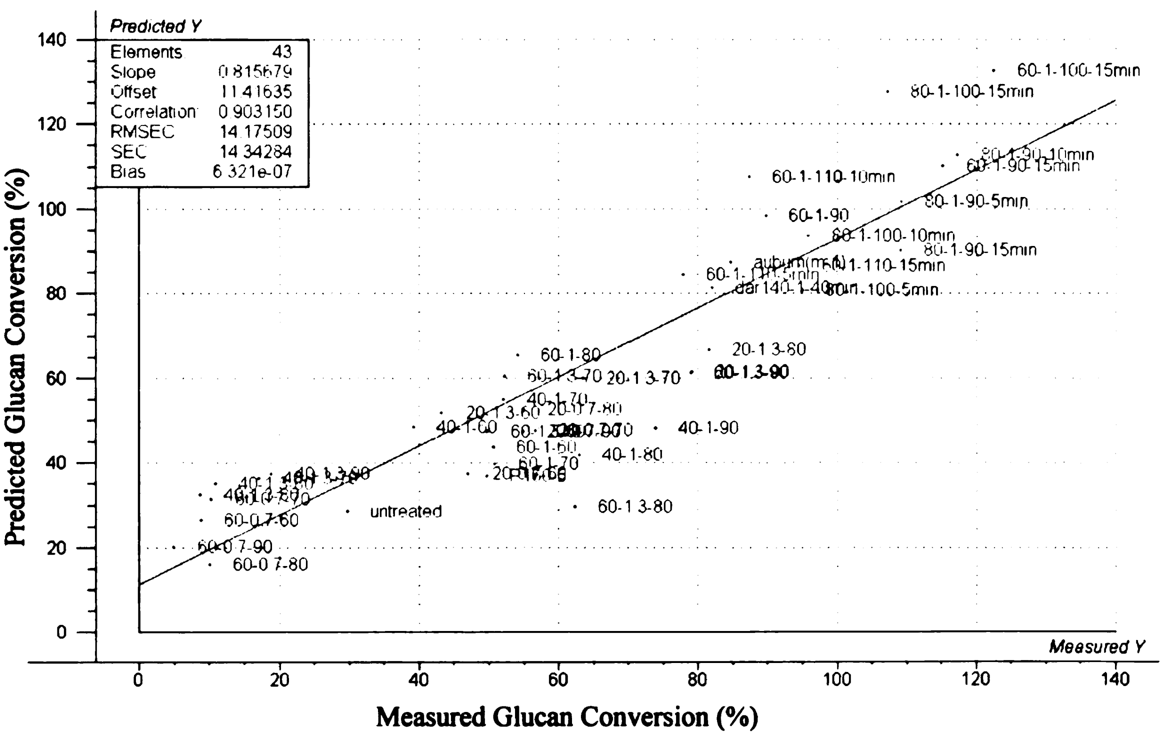

Figure 4.5: PCR model for glucan conversion at 72 hrs using only DRIFT data

AFEX

rate, r

Both t

and pr

used

differe

from a

hrs. H

the ini

the PC

acid a

better

The prediction obtained using the PCR model is presented in table 4.6. For the AFEX pretreatment, the difference between predicted and measured values of the initial rate, ranges from 3-74%. The difference for the 72 hr conversion is between 8-71%. Both the initial rate and 72 hr conversion therefore show a wide range between measured and predicted values.

As can be seen by the results presented in the table, the PCR model can also be used to predict the glucan conversion obtained using other pretreatments. For the different pretreatments the difference between predicted and measured values, ranges from approximately 7-77 % for the initial rate and 4-75% for the glucan conversion at 72 hrs. However, following closer examination we see that the model fails to predict either the initial rate or the 72 hr conversion of the ARP pretreated material. On the other hand, the PCR model seems to predict the initial rate and 72 hr conversion of both the dilute acid and controlled pH pretreatments. According to these results the MLR model gives a better prediction for the AFEX, ARP, dilute acid and controlled pH pretreatments.

Table 4.6: Prediction using PCR model for corn stover

Sample	Initial Rate Predicted (%)	Initial Rate Measured (%)	% difference	Glucan Conversion Predicted at 72 hrs (%)	Glucan Conversion Measured at 72 hrs (%)	% difference
AFEX 20%-1.3:1-80C	40.83	18.79	73.96	72.17	66.73	7.83
AFEX 20%-1.3:1-90C	36.55	19.70	59.92	73.59	61.54	17.83
AFEX 60%-1:1-110C-15 min	41.16	47.95	15.24	86.63	94.52	8.71
AFEX 60%-1.3:1-60C	22.57	21.97	2.72	22.72	47.50	70.59
AFEX 60%-1.3:1-70C	24.22	25.53	5.27	51.26	60.53	16.57
ARP 10% NH3, 170C, 30 min	134.87	60.08	76.73	184.50	83.41	75.47
ARP 10% NH3, 170C, 20 min	83.52	56.10	39.28	123.97	84.00	38.44
Dilute Acid 160C-1% H2SO4-10min	37.80	45.00	17.40	78.53	64.00	20.39
Diltue Acid 180 C, 1% H2SO4, 1min	32.27	40.00	21.39	58.85	47.00	22.39
Dilute Acid 180C, 1% H2SO4, 2min	51.74	70.00	29.99	79.28	76.00	4.22
Controlled pH 190C, 15min	59.22	55.26	6.91	84.30	76.32	9.94
Controlled pH 200C, 20min	26.14	40.83	43.87	44.74	41.47	7.60

Here t

When

than 2

level.

measu

4.4 Co

techni

increa

inform

impor

model

than v

glucar

necess

in the

Table 4.7 shows the results of the hypothesis testing with a 95% confidence level. Here the rejection region for both initial rate and 72 hrs conversion would be $|t| \geq 2.62$. When observing the calculated $|t|$ for both initial rate and 72 hrs conversion is smaller than 2.262, hence the null hypothesis (H_o: $\mu=\mu_o$) is not rejected with a 95% confidence level. In other words, there is no statistical difference between the predicted and the measured conversions.

Table 4.7: Corn stover PCR data for hypothesis testing

PCR	t	$t_{\alpha/2}$
initial rate	0.03711	2.262
72 hr	0.4255	2.262

4.4 Conclusion

Changes in plant cell wall components can be monitored by spectroscopic techniques and analyzed by statistical methods including MLR and PCR. In MLR an increase in the amount of data used improves the correlation between spectral information and enzymatic hydrolysis, both initial rate and 72 hr conversion. It is important to notice that for the MLR modeling only certain peaks were selected for the model due to the restriction that in order to create the model there must be more samples than variables. A model can be developed using spectroscopic data only to predict the glucan conversion. For the PCR model the DRIFT data seems to have all the information necessary for the modeling since increasing the amount of data actually causes a decrease in the correlation rate of

the li

indica

main

predic

PCR

invest

Both models (MLR and PCR) indicate that the factor that affects most the initial rate of hydrolysis is the aldehyde content, which is directly related to the bonds between the lignin and hemicellulose. However, for the 72-hr conversion the MLR model indicates that lignin is the main factor affecting hydrolysis, while PCR indicates that the main factor is C-H bond content, representing breakage into smaller molecules.

It was found that, in general, the MLR model gives better correlation, and better prediction for initial rate and 72-hr conversion for the AFEX samples. In addition, the PCR approach independently verified that the peaks thought to be important by previous investigation were in fact the crucial ones affecting enzymatic hydrolysis.

Sta

5.1Ba

by en

enzym

these

sampl

of bio

a bio

Popla

struct

spectr

chara

scatte

spectr

group

comp

enoug

the sa

the m

Chapter 5
Statistical correlation of spectroscopic analysis and hydrolysis of poplar samples

5.1Background

Pretreatment of lignocellulosic biomass is necessary to obtain high sugar yields by enzyme catalysis. However, the fundamental characteristics of biomass that limit its enzymatic conversion are not clearly understood. A better fundamental understanding of these factors would help improve pretreatment/hydrolysis systems.

In an effort to better understand these factors a series of hybrid poplar (*Populus*) samples was prepared varying the characteristics that are thought to affect the hydrolysis of biomass; e.g acetyl content, lignin content and crystallinity. Poplar has been studied as a biomass feedstock in order to improve hydrolysis and tailor pretreatment conditions. Poplar has been studied for effect of pore size [45], lignin content [24, 66], chemical structure [7, 94] and crystallinity [24]

In addition to the spectroscopic techniques discussed previously, Raman spectroscopy has been suggested [2] as a complementary technique in the characterization of biomass. In Raman spectroscopy less polar bonds give greater scattering. Hence, bonds that cannot be observed in DRIFT will be present in the Raman spectra. Stewart et al. believe that there are enough differences between the kinds of groups that are infrared active and those that are Raman active to make the techniques complementary to each other [2]. However, these same differences might give a specific enough Raman spectrum for the biomass samples that could be related to the changes in the sample characteristics (e.g. lignin content, cellulose crystallinity, etc.)

An important advantage of Raman is that water does not cause interference and the magnitude of the Raman shifts is independent of the wavelengths of excitation [8].

The a

meas

conve

relati

hydro

dimer

keepi

functi

that v

relatio

not ir

crysta

used i

analys

based

ability

and ar

simul

mathe

measu

The analysis presented here attempts to relate the changes in the biomass structure as measured by Raman, DRIFT, XRD and Fluorescence spectroscopy to the glucan conversion by enzymatic hydrolysis using statistical analysis.

A previous statistical analysis was performed by Texas A&M University [24] relating the crystallinity, acetylation and lignin content of the poplar samples to extent of hydrolysis by a model. They used Table Curve3D ™ software that only fits three-dimensional data (two x-variables related to one y-variable) and created a model by keeping the acetyl content as a constant. From this model they obtained an empirical function that was inserted into Sigma Plot software and created a polynomial equation that was then substituted in the four dimensional equation and obtained the acetyl content relationship to the other biomass parameters. This model was complicated since it did not involve a model that directly relates all the properties measured (e.g lignin, content, crystallinity and acetyl content) to the glucan conversion but the ratio of variables was used instead.

In the analysis presented here two models were developed based on multivariate analysis. The Unscrambler ® software finds the relationship between the parameters based on the variance of the parameters measured. An advantage of the software is the ability to correlate multiple variables at the same time. The entire spectrum can be used and analyzed for patterns recognition and correlation with hydrolysis data.

Multivariate analysis allows the scientist to relate and model different variables simultaneously. In other words, multivariate statistics is a collection of powerful mathematical tools that can be applied to chemical analysis when more than one measurement is acquired for each sample [10]. Multivariate calibrations are useful in spect

spect

that

samp

analy

desir

gluca

varia

into a

of inf

projec

reduc

small

mathe

capab

into g

predic

spectral analyses and can greatly improve the precision and applicability of quantitative spectral analysis [68]. With multivariate calibrations, empirical models are developed that relate the spectral data for multiple samples to the known concentration of the samples. These empirical relationships can then be used in multivariate prediction analyses of spectra of unknown samples to predict their glucan conversions.

The selection of the model is based on the final use intended and the precision desired. The multiple linear regression models assume that the best way to estimate the glucan conversion (hydrolysis) of the sample is finding a linear combination of the variables that minimizes the errors in reproducing the concentration. This model takes into account all the information available without discerning the importance of each item of information.

The principal component model uses the data and projects it into planes. These projections enable study of the deviations in the data. Principal component regression reduces the number of variables to be analyzed, discards the linear combinations with small variances and studies only those combinations with large variances. A detailed mathematical explanation of the models is presented elsewhere [40, 68, 110].

The Unscrambler® software helps in the statistical analysis with visual capabilities. Unscrambler® provides the meanings to translate multivariate relationships into graphical displays and permits exploratory analysis, multivariate regression analysis, prediction and validation.

5.2 M

5.2.1

were

perfo

Decr

way

A mo

5.2.2

5.2.2

5.2.2

5.2.2

5.2.2

Syst

The

samp

5.2.2

5.2 Materials and Methods

5.2.1 Materials

Hybrid poplar samples were obtained from Texas A&M University. The samples were selectively delignified, deacetylated and decrystallized. Delignification was performed using peracetic acid. Deacetylation was achieved using dilute KOH. Decrystallization was obtained with ball milling. The samples were prepared in such a way as to obtain a broad spectrum of crystallinities, acetyl contents and lignin contents. A more detailed explanation of sample preparation is presented elsewhere [24].

5.2.2 Analytical Methods

5.2.2.1 Fluorescence

A detailed explanation is presented in section 4.2.3.1

5.2.2.2 Diffuse Reflectance FT-IR (DRIFT)

A detailed explanation is presented in section 3.2.3.1

5.2.2.3 X-Ray Diffraction

A detailed explanation is presented in section 4.2.3.3

5.2.2.4 Raman Spectroscopy

The Raman analysis is performed in a Hololab Series 1000 from Kaiser Optical Systems, Inc. The sample is analyzed without removing it from the clear plastic bag. The laser probe (Model HFPH-632.8nm) is placed in close contact to the sample and the sample exposed to the laser 10 times for 5 seconds each time and the spectra collected.

5.2.2.5 Enzymatic Hydrolysis

A detailed explanation is presented in section 3.2.3.2

5.2.3

5.3 R

recei

crysta

vary

into c

5.1 s

Obvi

indic

chan

and t

5.2.3 Statistical Analysis

A detailed explanation is presented in section 4.2.4

5.3 Results and Discussion

Poplar samples with a range in crystallinity, acetyl and lignin content were received from Texas A & M University dry and ground for 0, 3 or 6 days according to the crystallinity desired. Presumably these samples were prepared in such a way as to only vary one of these three characteristics at the time [24]. The spectra were analyzed taking into consideration the variation obtained from the reproducibility of the spectrum. Figure 5.1 shows the DRIFT results for samples with constant lignin content and crystallinity. Obviously, a change in acetyl content causes changes in the whole DRIFT spectrum indicating that all the characteristics in the biomass are correlated. There is a marked change in the 1500-1800 cm^{-1} area. This area is related to the hydrolysis of hemicellulose and the peaks related to the acetyl links are also prominent in this region.

Intensity (K-M)

const

chan

area

Acco

1595

visib

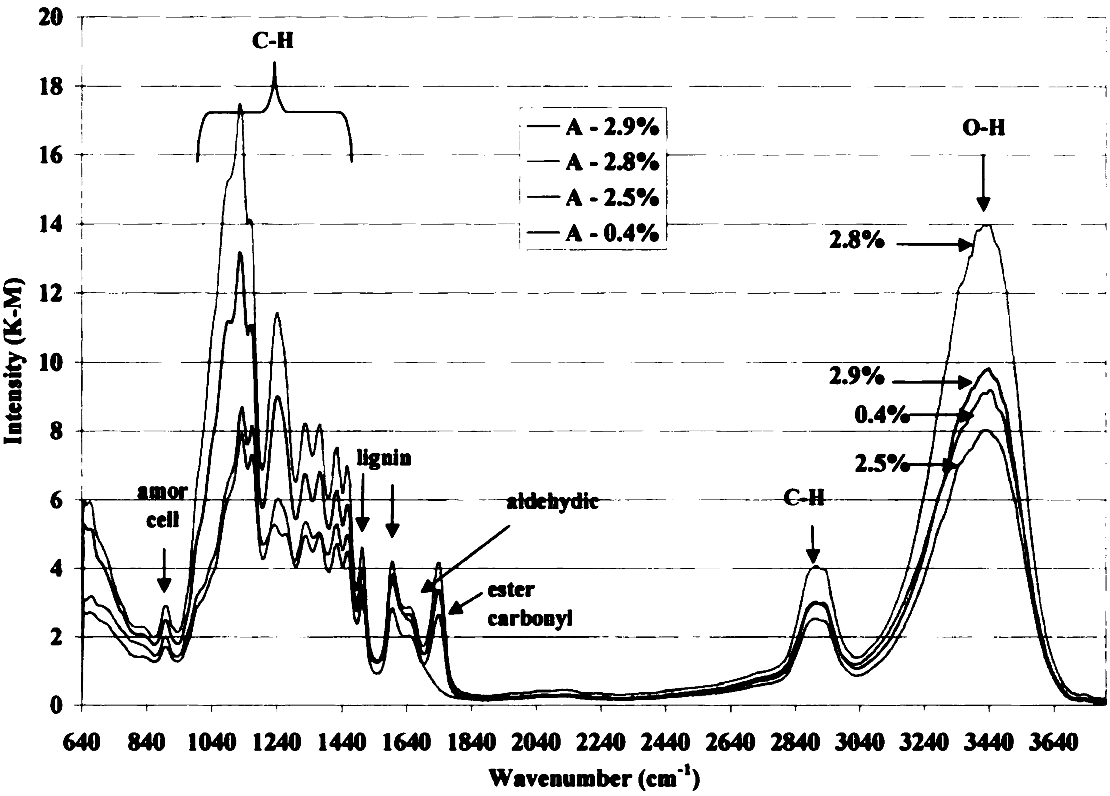

Figure 5.1: Effect of acetyl content on DRIFT spectra

Figure 5.2 shows the DRIFT spectra of samples with constant acetyl content and constant crystallinity but varying lignin. Once again, the graph shows that a supposed change in lignin content only, affects the whole spectrum. More drastic changes in the area around 1500-1620 cm^{-1} are noted as compared to the rest of the spectrum. According to Stewart et al. the peaks related to lignin in DRIFT are the ones at 1510 and 1595 cm^{-1}, which are in this area. Noticeable changes in the C-H and O-H peak are also visible.

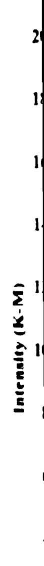
Intensity (K-M)

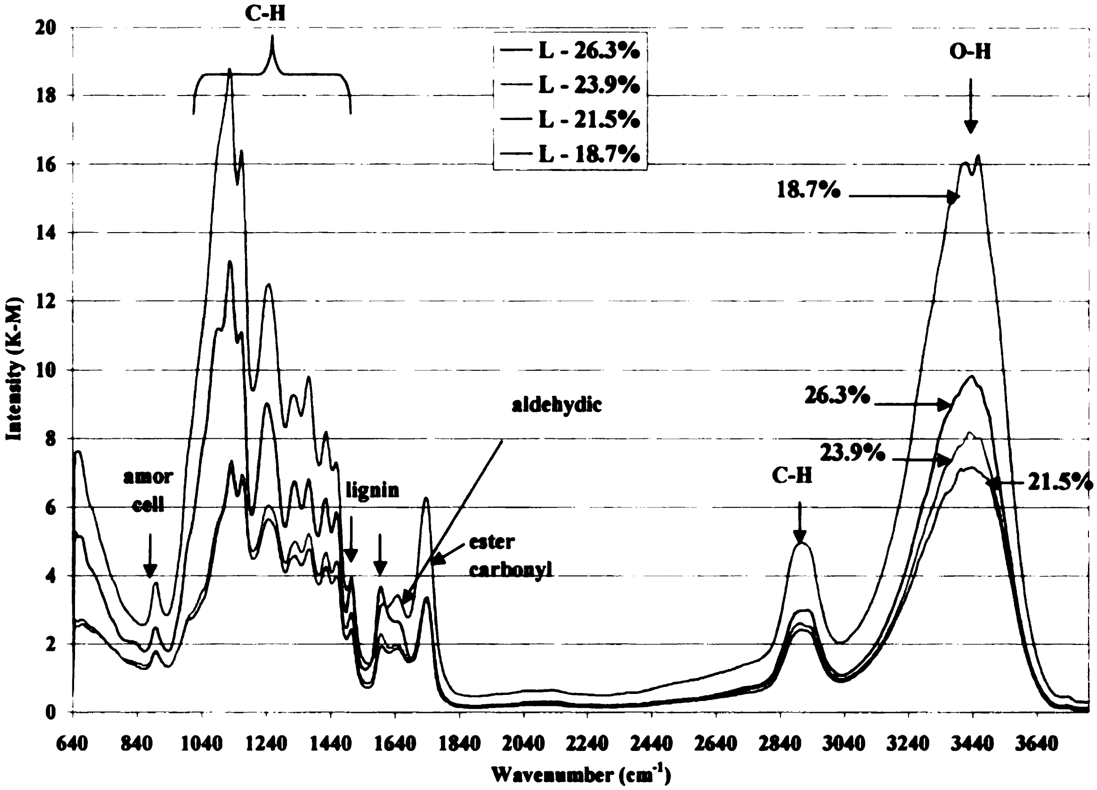

Figure 5.2: Effect of lignin content on the DRIFT spectra of poplar.

befor

chang

cellu

obser

that a

Figure 5.3 shows the effect of crystallinity index on the DRIFT spectrum. As before, a change in this one parameter affects the whole spectrum. The most notable change is observed in the C-H and O-H peaks, indicating that decrystallization of the cellulose is accompanied by breakage into smaller molecules. Some changes can also be observed in the 1540-1640 cm^{-1} area. This area is noted for aromatic C-O stretch bonds that are related to lignin.

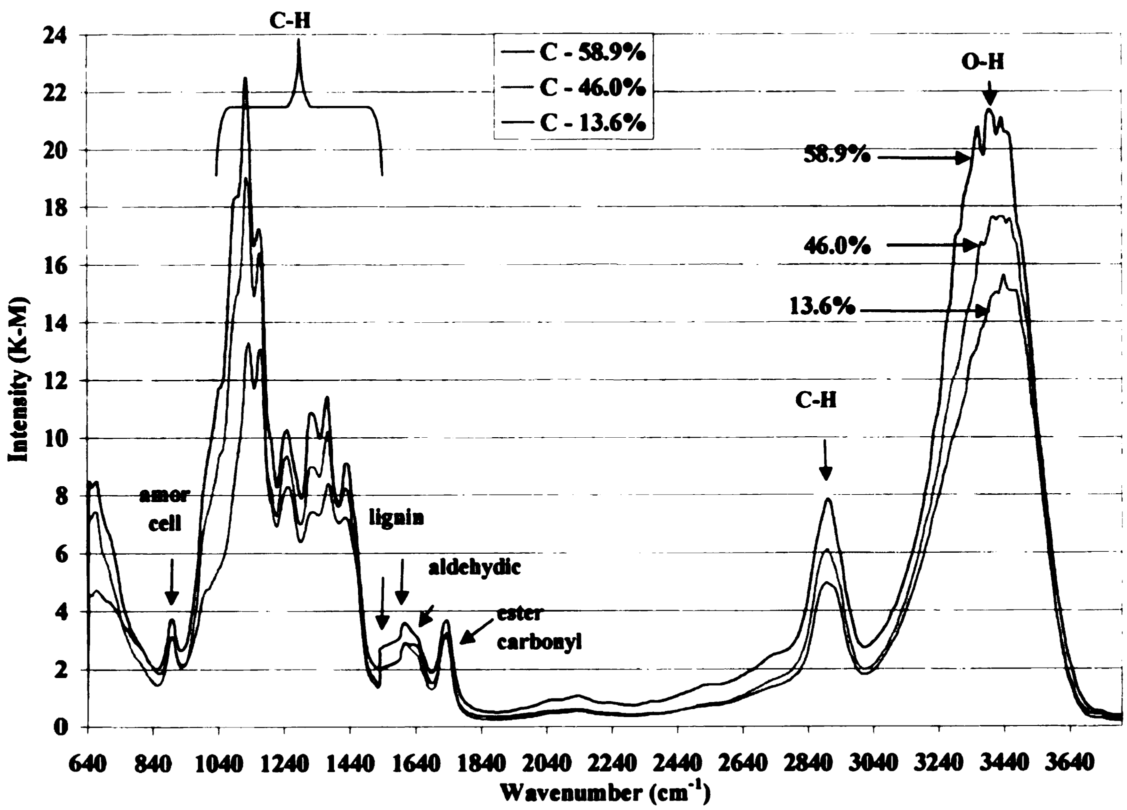

Figure 5.3: Effect of crystallinity on the DRIFT spectra

Michigan State University (MSU) also analyzed the samples for crystallinity in order to corroborate the Texas A & M University (TAMU) results. Table 5.1 shows the crystallinity index for some of the samples. A complete list of the crystallinity results determined by MSU is in Appendix 5. These samples are supposed to have a constant crystallinity index. The results show some variation from sample to sample but in general the CrI measured at MSU are in the same range as those CrI values provided by TAMU and the trend of decreasing CrI with increased milling time is also corroborated.

Table 5.1: Poplar crystallinity index

Sample	CrI (%) Measured by MSU			CrI (%) Measured by TAMU		
	0 days	3 days	6 days	0 days	3 days	6 days
DL01-DA000	47.7	24.5	15.6	53.9	34.8	24.8
DL01-DA015	55.7	26.8	18.1	52.2	36.2	21.2
DL01-DA035	52.7	22.5	18.0	55.3	37.0	20.0
DL01-DA055	50.2	20.7	23.2	56.6	35.9	26.9
DL01-DA150	55.5	21.2	15.1	62.6	37.2	21.4

In figure 5.4 the effect of acetyl content on the fluorescence results is presented. These samples had constant lignin content and crystallinity. The peak at 425 cm^{-1} is directly related to lignin content. As can be seen, a change in acetyl content causes little change in this peak. There is, in addition, little change in the rest of the spectra.

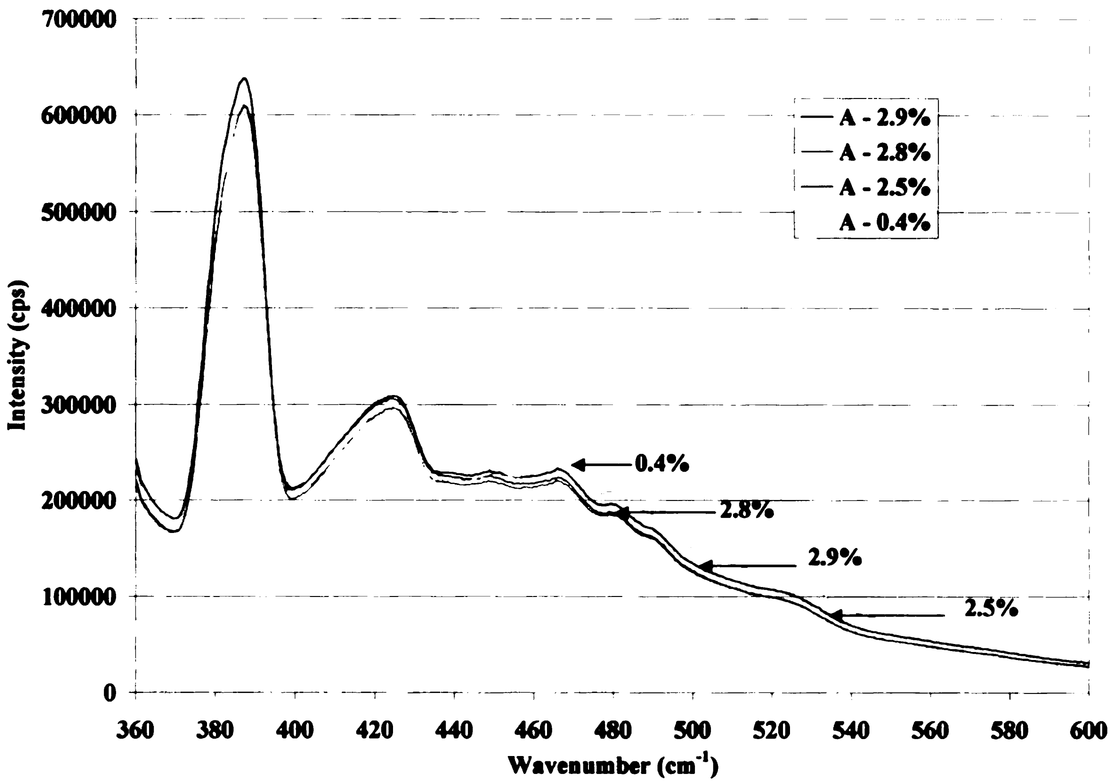

Figure 5.4: Effect of acetyl content on fluorescence results

Figure 5.5 shows the effect of lignin content on the fluorescence. There are notable differences between the samples at the 425 cm^{-1} peak. In addition there are more differences between the samples in the rest of the spectra.

Figure 5.6 shows the effect of crystallinity on the fluorescence spectra. At the smaller CrI, the spectra do not change. However, an increase in crystallinity causes decreased absorbance up to 450 cm^{-1} and then an increase after 450 cm^{-1}.

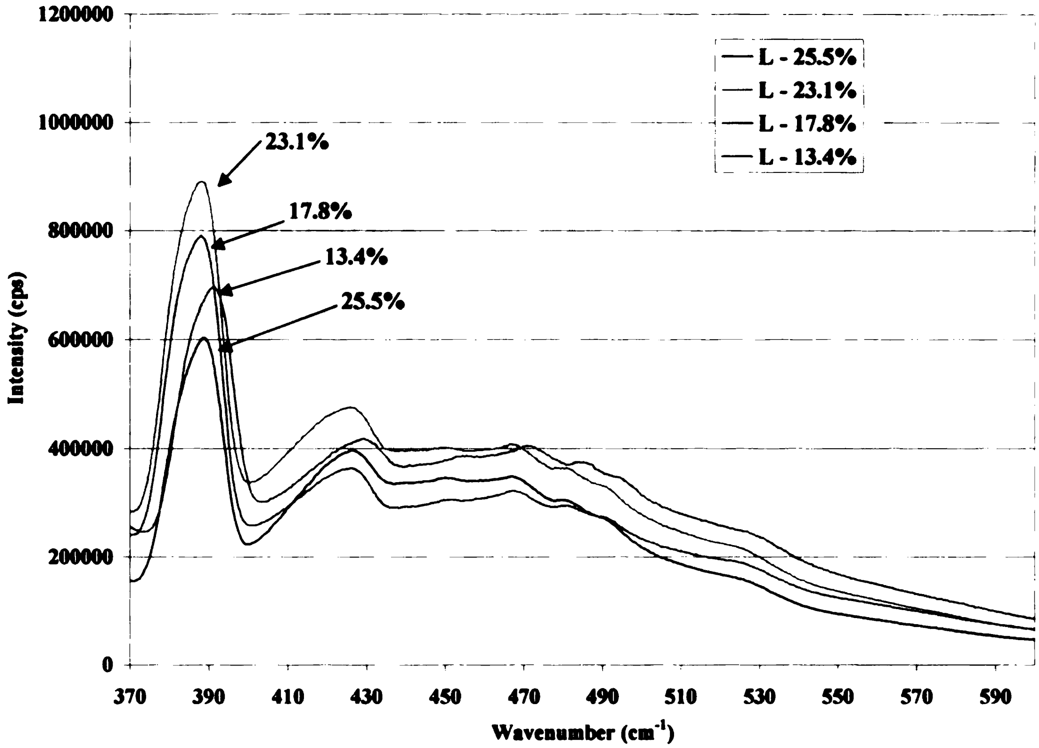

Figure 5.5: Effect of lignin content on fluorescence results.

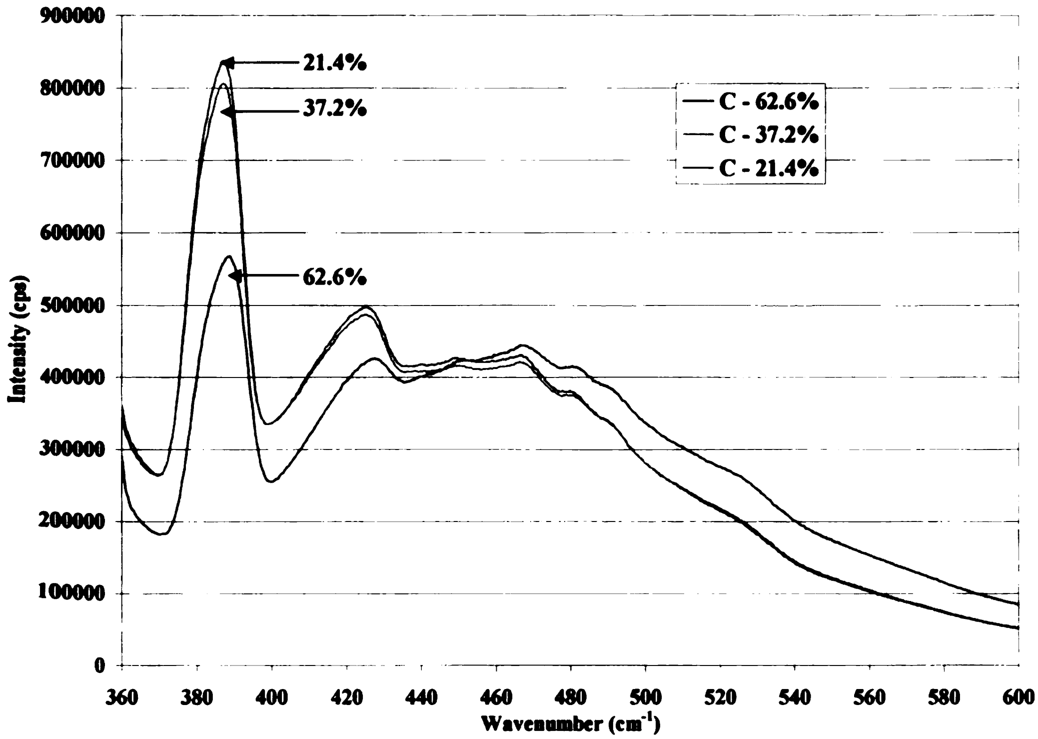

Figure 5.6: Effect of crystallinity on the fluorescent results

It is believed that Raman spectroscopy might be used as a complement to the DRIFT results [2]. The effect of acetyl content on Raman results is presented in figure 5.7. The peaks around 1400 cm^{-1} are directly related to crystalline cellulose. The peaks at 2900 cm^{-1} are related to C-H bonds in the biomass. The spectra are presented here to demonstrate the information that can be obtained from the different analytical methods.

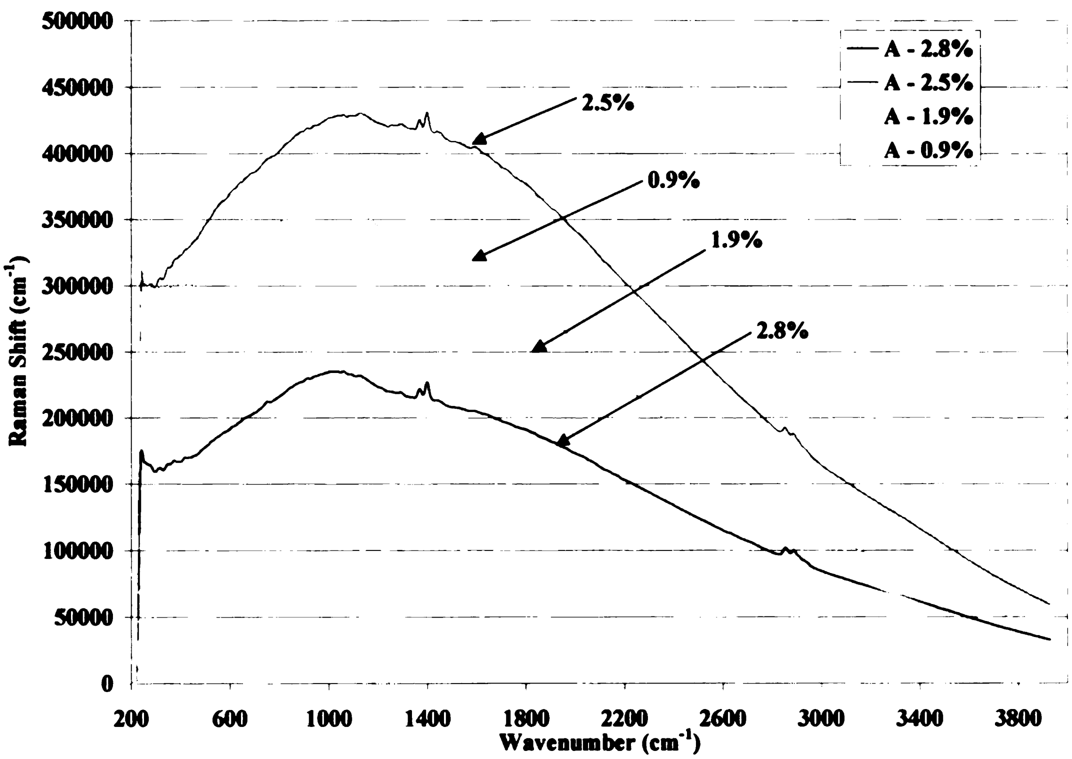

Figure 5.7: Effect of acetyl content on the Raman spectra

Figure 5.8 shows the effect of lignin content on the Raman spectra. It can be seen that a change in lignin content causes only a slight difference in the spectra. However, the difference is not as pronounced as the one observed in figure 5.7.

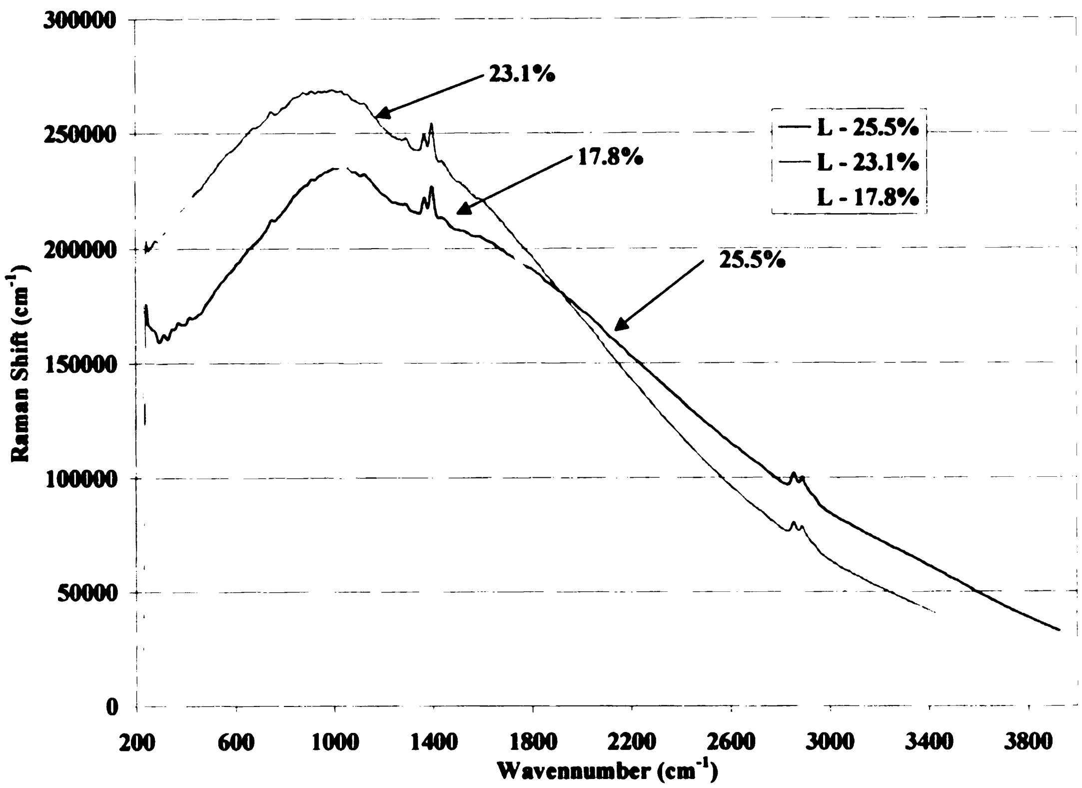

Figure 5.8: Effect of lignin on the Raman spectra.

Figure 5.9 shows the effect of crystallinity on the Raman spectra. The features are not easily distinguished, but a change in the crystallinity does change the intensity of the spectra.

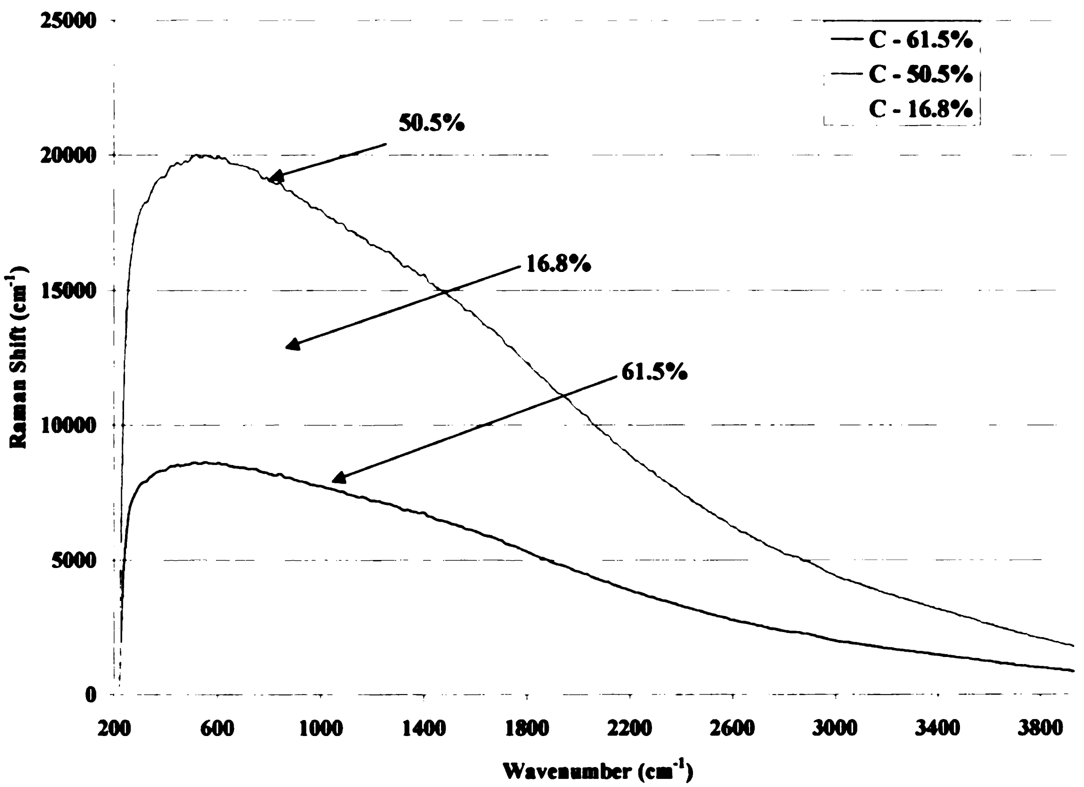

Figure 5.9: Effect of crystallinity on the Raman spectra.

The analyses of variance (ANOVA) correlations for the models of the initial rate using multi linear regression are presented in table 5.2. The initial rate is considered as the glucan conversion obtained at 1 hr by enzymatic hydrolysis using 5 FPU/g glucan. Different spectral information was used to create various models in order to obtain the best model with the least effort in terms of sample analysis. Because of the limitation that more samples than variables are needed to create a MLR model, the intensity of selected peaks (presented in table 3.1) was used from the DRIFT spectra along with the intensity of the fluorescence peak related to lignin, crystallinity index and selected peaks of the Raman spectra. These intensities were determined using a baseline correction. In other words a new baseline was used for every peak in order to determine its intensity.

The ANOVA correlations for the 72-hr hydrolysis MLR model are presented in table 5.2. The 72-hr hydrolysis was taken as the glucan conversion in enzymatic hydrolysis at 72 hrs using 5 FPU/g glucan.

Table 5.2: ANOVA correlations obtained using various techniques

Analytical Technique (s)	Initial Rate	72 hr Glucan Conversion
DRIFT	$R^2 = 0.746$	$R^2 = 0.733$
Raman	$R^2 = 0.365$	$R^2 = 0.697$
DRIFT + Raman	$R^2 = 0.778$	$R^2 = 0.847$
DRIFT + XRD	$R^2 = 0.775$	$R^2 = 0.740$
DRIFT + Fluorescence	$R^2 = 0.747$	$R^2 = 0.736$
Raman + XRD	$R^2 = 0.659$	$R^2 = 0.702$
Raman + Fluorescence	$R^2 = 0.397$	$R^2 = 0.698$
DRIFT + Raman +XRD	$R^2 = 0.806$	$R^2 = 0.849$
DRIFT + Raman + Fluorescence	$R^2 = 0.778$	$R^2 = 0.847$
Raman + Fluorescence + XRD	$R^2 = 0.659$	$R^2 = 0.704$
DRIFT + Raman + Fluorescence + XRD	$R^2 = 0.806$	$R^2 = 0.842$

The best correlation is obtained using the data obtained from DRIFT, Raman and XRD techniques. Addition of the fluorescence data has little effect on the model for the initial rate and decreases the correlation for the 72 hr conversion model. According to these results, adding the fluorescence data seems to over fit the 72 hr model. In addition, this result indicates that Raman can be used as a complement to the DRIFT spectra to improve the model predictions, as previously surmised.

The MLR model for initial rate using DRIFT, Raman and XRD techniques is presented in figure 5.10. When evaluating the regression coefficients it is found that the factor that affects most the initial rate is the aldehyde bonds, which are the bonds between lignin and hemicellulose.

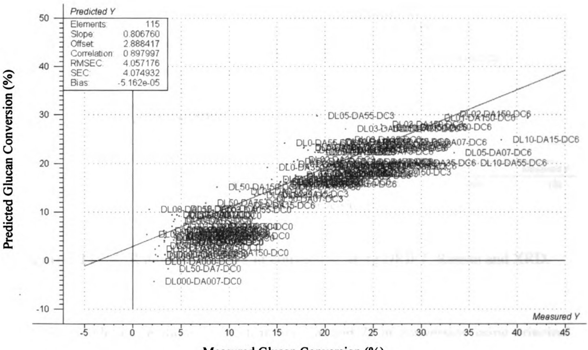

Figure 5.10: MLR model for the initial rate using DRIFT, Raman and XRD.

The MLR model for the 72hr glucan conversion using DRIFT, Raman and XRD is given in figure 5.11. The coefficients analysis indicate that the parameter that has the most influence on the 72 hr conversion is the aldehyde bonds, representing the bonds between lignin and hemicellulose. The coefficients (B) for the initial rate and 72 hrs conversion MLR model using all the spectroscopic data are presented in the appendix 5; Table A5.2.

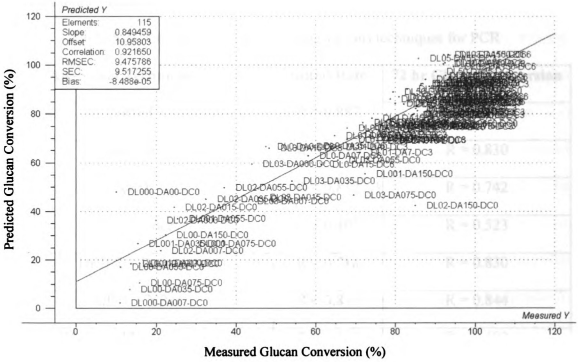

Figure 5.11: MLR model for the 72 hr conversion using DRIFT, Raman and XRD.

The model correlations for both initial rate and 72 hr conversion using principal component regression (PCR) are presented in table 5.3. As with the MLR models different spectroscopic data were used to relate the changes in the cell wall structure (changes in bonds) to the enzymatic hydrolysis yield. However, in this case every single data point from every spectrum was input into the model. The initial rate used here is defined as the glucan conversion at 1 hr of the enzymatic hydrolysis using 5 FPU/g glucan. The 72-hr hydrolysis was taken as the glucan conversion in enzymatic hydrolysis at 72 hrs using 5 FPU/g glucan. It is important to note that the correlation analyzed here is not the relation between the data and the initial rate but the relationship between the variables in the model.

Table 5.3: Correlations obtained using various techniques for PCR

Analytical Technique (s)	**Initial Rate**	**72 hr Glucan Conversion**
DRIFT	R = 0.887	R = 0.914
Raman	R = 0.518	R = 0.830
XRD	R = 0.812	R = 0.742
Fluorescence	R = 0.403	R = 0.523
DRIFT + Raman	R = 0.518	R = 0.830
DRIFT + XRD	R = 0.813	R = 0.844
DRIFT + Fluorescence	R = 0.424	R = 0.692
Raman + XRD	R = 0.740	R = 0.853
Raman + Fluorescence	R = 0.648	R = 0.866
Fluorescence + XRD	R = 0.812	R = 0.480
DRIFT + Raman +XRD	R = 0.591	R = 0.853
DRIFT + Raman + Fluorescence	R = 0.648	R = 0.834
Raman + Fluorescence + XRD	R = 0.648	R = 0.834
DRIFT + XRD + Fluorescence	R = 0.403	R = 0.692
DRIFT + Raman + Fluorescence + XRD	R = 0.648	R = 0.872

The data presented above indicate that the model with only the DRIFT data gives the best correlation for both initial rate and 72 hr hydrolysis. This is a useful finding because it decreases the amount of analysis necessary in order to obtain a good prediction.

The PCR model for the initial rate using DRIFT data only is presented in figure 5.12. When analyzing the coefficients of the PCR models, it is found that the factor that most affects both the initial rate and the 72 hr conversion is the O-H bonds content. It is important to mention that from all the data points (over 6000 points) input into the model PCR recognizes the wavenumber of the O-H bond as influential to the model. The content of O-H bonds is directly related to the breakage into smaller molecules. The model for the 72 hr conversion is presented in figure 5.13. The coefficients for the initial rate and 72 hrs conversion PCR model using DRIFT data are provided in the appendix 5; Table A5.3.

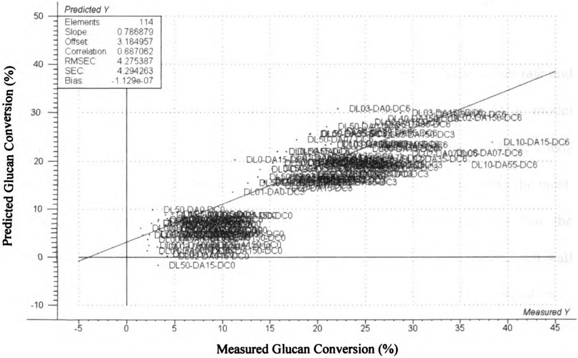

Figure 5.12: PCR model for initial rate using DRIFT data

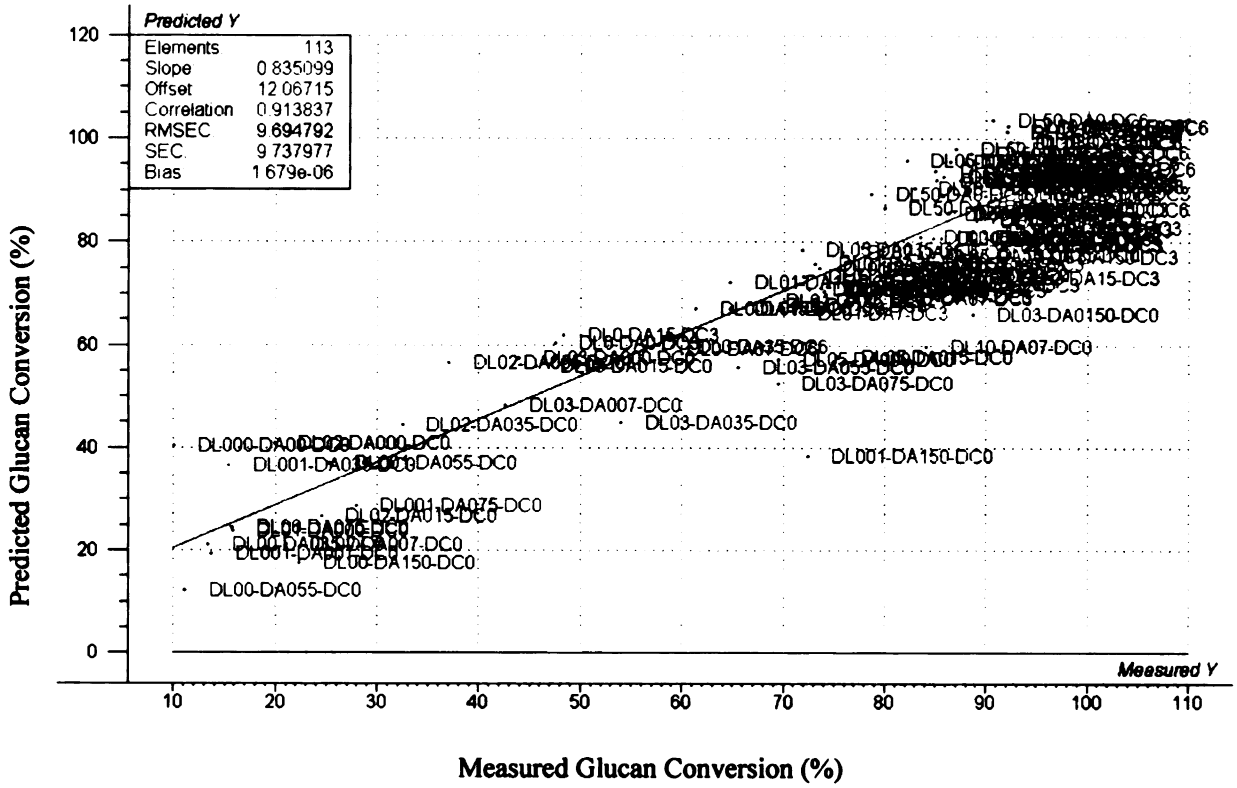

Figure 5.13: PCR model for the 72 hr conversion using DRIFT data only.

There are clear differences in the factors that most affect both the initial rate and 72 hr conversion according to the different models (MLR, PCR). The MLR model indicates that both initial and 72 hr conversion are more affected by the aldehyde bonds and the PCR models indicate that is O-H the factor that affects both conversions the most. However, both agree that it is through depolymerization of the biomass that the hydrolysis can be improved. Finding a way to break the bonds between various cell wall components (lignin, cellulose and hemicellulose) will facilitate the enzymatic digestion.

The predictions using all the models are presented below. The predictions for the MLR initial rate and 72 hr conversion using DRIFT, Raman and XRD data are presented in table 5.4. The results show that the models vary in their predictive capacity, they predict well some samples, but do not predict others. For the initial rate a difference from 5 – 68% in the predicted vs. measured value is found. On the other hand the predictions for the 72 hr conversion show differences between 3 – 22%. In this case, as with the AFEX treated sample model, it is observed that the model predicts better the conversion at 72 hr than it does the initial rate. Once again, this model does not include parameters that probably affect the initial rate, including surface area, pore size, etc. The predicted 72-hr conversion is over 100% indicating that the model must be modified in some way so as to constrain prediction between the established limits (0-100%). Another possible reason for observed discrepancies is that the MLR model may include some noise from the spectra that is assumed to be meaningful data.

Table 5.4: Predictions using MLR model for poplar

Sample	Initial Rate Predicted (%)	Initial Rate Measured (%)	% difference	Glucan Conversion Predicted at 72 hrs (%)	Glucan Conversion Measured at 72 hrs (%)	% difference
DL02-DA075-DC0	9.46	6.68	34.46	63.11	53.21	17.02
DL05-DA007-DC0	6.97	3.78	59.41	72.65	59.51	19.89
DL10-DA075-DC0	9.94	4.9	67.95	91.90	83.14	10.01
DL10-DA150-DC0	16.15	15.32	5.27	89.43	90.97	1.71
DL00-DA007-DC3	17.43	12.78	30.78	61.56	49.72	21.27
DL02-DA000-DC3	17.68	15.93	10.39	73.96	79.06	6.67
DL05-DA150-DC3	31.15	24.12	25.45	111.48	92.97	18.11
DL50-DA015-DC3	11.51	10.36	10.48	83.15	75.44	9.72
DL01-DA000-DC6	18.88	25.09	28.26	69.24	73.73	6.28
DL03-DA007-DC6	20.80	19.87	4.57	78.35	90.98	14.92
DL05-DA075-DC6	24.08	28.42	16.52	95.22	92.05	3.38

The PCR prediction for the initial rate and 72 hr conversion using the DRIFT data only models is presented in table 5.5. The same pattern is found here in that the models predict very well some samples (< 5 % difference) but do not well predict others. The initial rate informstion shows differences between measured and predicted values of approximately 5 – 33%, while the prediction for the 72 hr hydrolysis differs from the measured values by approximately 4 – 18%. The PCR model predicts the 72 hr hydrolysis conversion better than the initial rate (based on correlation and prediction values) confirming that there are some parameters that affect the initial rate that are not included in this model.

Table 5.5: Comparison between initial rate predicted by the PCR models and measured by enzymatic hydrolysis

Sample	Initial Rate Predicted (%)	Initial Rate Measured (%)	% difference	Glucan Conversion Predicted at 72 hrs (%)	Glucan Conversion Measured at 72 hrs (%)	% difference
DL02-DA75-DC0	7.91	6.68	8.41	39.72	53.21	14.52
DL05-DA07-DC0	7.54	3.78	33.23	49.21	59.51	9.47
DL10-DA75-DC0	7.40	4.90	20.34	58.11	83.14	17.72
DL10-DA150-DC0	10.08	15.32	20.63	67.56	90.97	14.77
DL00-DA07-DC3	18.88	12.78	19.26	71.32	49.72	17.85
DL02-DA00-DC3	14.52	15.93	4.61	75.85	79.06	2.08
DL05-DA150-DC3	28.78	24.14	8.77	79.25	92.97	7.97
DL50-DA15-DC3	16.16	10.36	21.87	83.80	75.44	5.25
DL01-DA00-DC6	19.34	25.09	12.94	84.28	73.73	6.68
DL03-DA07-DC6	23.41	19.87	8.18	98.51	90.98	3.97
DL05-DA75-DC6	24.83	28.42	6.74	107.09	92.05	7.55

c

a

w

fo

co

72

re

in

st

In general, PCR shows higher correlation for both the initial rate and 72hrs conversion compared to MLR. This higher correlation could be due to the fact that the PCR model does not take into consideration the spectral noise while MLR does not discern between important data and spectral noise. In addition, the predicted values show a smaller percent difference as compared to those measured by enzymatic hydrolysis when predicted by PCR than by MLR.

Table 5.6 shows the results of the hypothesis testing with a 95% confidence level for both MLR and PCR models. Here the rejection region for both initial rate and 72 hrs conversion would be $|t| \geq 2.62$. When observing the calculated $|t|$ for both initial rate and 72 hrs conversion is smaller than 2.262, hence the null hypothesis (H_o: $\mu=\mu_o$) is not rejected with a 95% confidence level.

The same results are observed for both MLR and PCR model. The $|t|$ for both initial rate and 72 hrs conversion is smaller than 2.262. In other words, there is no statistical difference between the predicted and the measured conversions.

Table 5.6: Poplar MLR and PCR data for hypothesis testing

MLR	t	$t_{\alpha/2}$	PCR	t	$t_{\alpha/2}$
initial rate	0.55619	2.262	initial rate	0.33395	2.262
72 hr	0.8218	2.262	72 hr	-0.1859	2.262

5.4 Conclusion

Statistical models predicting hydrolysis of poplar samples with a wide range of crystallinity values, lignin content and acetyl content were developed. Different spectroscopic techniques (DRIFT, XRD, Fluorescence and Raman), were used to track structural changes in the cell wall as reflected in bond intensities. The spectroscopic data were related to both the initial rate and 72-hr conversion obtained by enzymatic hydrolysis.

Different spectroscopic data were selected to develop the models in order to determine a simple (i.e., data from only one spectroscopic method) way to predict conversion and determine the factor that most affects hydrolysis. Then, correlations for each model containing different sets of spectroscopic data (DRIFT, XRD, DRIFT+XRD, etc) were determined and predictions using the models were made in order to examine the model accuracy.

This study has shown that it is possible to predict with some accuracy the enzymatic hydrolysis conversion using only spectroscopic data. In general, the PCR model gives not only better correlation, but also better predictions for initial rate and 72-hr conversion. In addition, using DRIFT data only gives accurate enough results so as to provide a reasonable predictive model. The MLR models overestimate the 72-hr conversion, which might be due to the fact that MLR uses all the data available without discerning whether it is relevant data for the model or just spectral noise.

When comparing the models for initial rate to the 72-hr conversion it is observed in both MLR and PCR that the models for 72-hr conversion give better correlations and predictions than the initial rate models. This may be due to the fact that only some of the factors that are known to affect hydrolysis have been studied here. Effects of variations in sample characteristics such as particle size, or surface area were not studied and are also likely to be most pronounced at early stages of the hydrolysis. Further study is needed to test this idea.

Chapter 6
Conclusion and Recommendations

AFEX has been widely studied using different feedstocks and ample literature is available [32-34, 56, 58-59, 86, 109]. AFEX is the basis for the model because of our expertise in this process. It has been shown that the changes produced by AFEX in chemical bonds can be easily identified by DRIFT. Each parameter (i.e., temperature, moisture content, time, etc) of the AFEX pretreatment affects the DRIFT spectra. It has also been proven that for native lignocellulosics, altering one structural feature results in substantial changes on other features.

DRIFT can be used to compare various pretreatments and their effect on the biomass. According to the DRIFT spectra ARP is effective in delignifying the biomass, hydrolyzing hemicellulose and provides some decrystallization. Lime is effective in hydrolysis of hemicellulose (breaking ester carbonyl bonds). Dilute acid pretreatment is effective in depolymerization and delignification of the biomass and hydrolysis of the hemicellulose. DRIFT thereby independently proved validity of the severity factor which indicates that time and temperature are interchangeable in acid pretreatment. Controlled pH pretreatments main effect on the biomass is hydrolysis of the hemicellulose. According to the DRIFT results AFEX is effective in hydrolysis of the hemicellulose. AFEX also shows (based on DRIFT spectra) some delignification, depolymerization and decrystallization.

Changes in the cell wall components can be monitored by spectroscopic techniques. Models were developed using spectroscopic data only to predict the glucan conversion. In this research the techniques, analysis and data handling have been widely studied before in various biomass areas. However, this is the first time that all of these factors were combined for corn stover. This combination of factors allowed us to obtain the most information from each analytical method and hydrolysis result.

Multivariate analysis was used to create models that relate the spectroscopic data to enzymatic hydrolysis results. The pretreated corn stover models (MLR and PCR) indicate that the factor that most affects the initial rate is the aldehyde content, i.e., the bonds between the lignin and hemicellulose. However, for the 72 hr conversion the MLR model indicates that lignin is the primary factor affecting hydrolysis, while PCR indicates that C-H bonds, representing breaking into smaller molecules are what affect hydrolysis the most. It is important to notice that the models based on AFEX pretreated materials are able to predict with some degree of certainty the glucan conversion of other pretreatments like dilute acid and controlled pH, indicating that these are broadly applicable phenomena that we are studying here.

This study has shown that it is possible to predict with some degree of accuracy the hydrolysis conversion with only spectroscopic data. It was found that, in general, the PCR model gives not only better correlation, but also better predictions for initial rate and 72-hr conversion for poplar samples. In addition, the PCR method has independently verified the importance of those bonds (amorphous cellulose, lignin, aldehyde, ester carbonyl, C-H and O-H) already believed to most influence biomass hydrolysis. On the other hand, MLR gives a better correlation and prediction for the AFEX pretreated corn stover. This difference in model applicability may be partly due to the nature of the samples. Corn stover includes different parts of the plant (leaves, stalks, etc) while for the poplar samples only the trunk of the tree is considered. In addition, poplar does not contain the protein that is present in corn stover. This result indicates that for these models to be more generally applied, more closely related biomass substrates may be required. However, according to hypothesis testing the predicted value is not statistically different from the measured value for both poplar and corn stover; MLR and PCR models and initial rate and 72 hr conversion.

Comparing the initial rate to 72-hr conversion within the model it is observed in both MLR and PCR that the models for 72-hr conversion give a better correlation and prediction than the initial rate models. This is probably due to the fact that factors other than lignin, biomass crystallinity and acetyl content affect enzymatic hydrolysis. Such factors might include degree of polymerization, particle and pore size and surface area. Hence a model including these parameters is probably necessary to provide greater accuracy in prediction.

APPENDICES

APPENDIX 1

Ammonia MSDS

Ingredients

===

Cas: 7664-41-7
RTECS #: BO0875000
Name: AMMONIA; (ANHYDROUS AMMONIA)
% low Wt: 99.5
% high Wt: 100.
OSHA PEL: 35 MG/M3;50 PPM
ACGIH TLV: 17 MG/M3;25 PPM
ACGIH STEL: 24 MG/M3;35 PPM
EPA Rpt Qty: 100 LBS
DOT Rpt Qty: 100 LBS

===

Health Hazards Data

===

Route Of Entry Inds - Inhalation: YES
Skin: YES
Ingestion: YES
Carcinogenicity Inds - NTP: NO
IARC: NO
OSHA: NO
Effects of Exposure: ACUTE: EYES: CONTACT MAY CAUSE CORROSION, PAIN, REDNESS AND ULCERATION OF THE CORNEA, LENS AND CONJUNCTIVA.
SKIN: CONTACT CAN CAUSE FROSTBITE, FREEZE BURNS AND/OR CHEMICAL BURNS, RESULTING IN SEVERE DERMAL DAMAGE.
INHALATION: GAS IS EXTREMELY IRRITATING TO MUCOUS MEMBRANES AND LUNG TISSUE. COUGHING, CHEST PAIN, AND DIFFICULTY IN BREATING MAY RESULT. PROLONGED EXPOSURE MAY RESULT IN BRONCHITIS, PUL MONARY EDEMA, AND CHEMICAL PNEUMONITIS. BREATHING HIGH CONCENTRATIONS MAY RESULT IN DEATH.
INGESTION: EXTREMELY IRRITATING TO MUCOUS MEMBRANES CAUSING VOMITING, NAUSEA AND BURNS.
CHRONIC: NO CHRONIC HEALTH EFFECTS HAVE (EFTS OF OVEREXP)

Signs And Symptoms Of Overexposure: HLTH HAZ: BEEN FOUND TO DATE.
Medical Cond Aggravated By Exposure: ADDITIONAL MEDICAL AND TOXICOLOGICAL
INFORMATION: MAY AGGRAVATE PREXISTING PULMONARY, LUNG, OR EYE CONDITIONS.

First Aid:

EYES: IMMED FLUSH W/LRG AMTS OF H*2O FOR AT LEAST 15 MIN, INCLUDING UNDER EYE LIDS. SEEK MED ATTN IMMED, PREFERABLY AN OPHTHALMOLOGIST. SPEED & THOROUGHNESS IN RINSING EYES ARE IMPORTANT TO AVOID PERM INJURY.
SKIN: IMMED FLUSH W/LRG AMTS OF TEPID WATER WHILE REMOVING CLOTHING. THAW FROZEN CLOTHING BEFORE REMOVAL. IF A FREEZE BURN HAS OCCURED, GET MED ATTN.
INHAL: REMOVE PROMPTLY TO FRESH AIR. IF BR EATHING HAS STOPPED, APPLY ARTF RESP. APPLY OXYGEN AS SOON AS POSSIBLE. SEEK MED ATTN IMMED. INGEST: DO NOT INDUCE VOMIT. RINSE MOUTH OUT W/WATER. DRINK LARGE AMTS OF WATER/MILK. SEEK MED ATTN IMMED.

Handling and Disposal

===

Spill Release Procedures: REMOVE SOURCES OF HEAT OR IGNITION, INCLUDING INTERNAL COMBUSTION ENGINES AND POWER TOOLS. KEEP PEOPLE AWAY. STAY UPWIND AND WARN PEOPLE DOWNWIND OF POSSIBLE EXPOSURE. WEAR NIOSH APPROVED SELF-CONTAIN ED BREATHING APPARATUS IF CONDITION WARRANTS. CONSULT DOT "EMERGENCY RESPONSE GUIDEBOOK"-GUIDE 15.
Waste Disposal Methods: ANHYDROUS AMMONIA WILL NOT LEAVE RESIDUE WHEN SPILLED; NO CHEMICAL CLEAN-UP WILL BE REQUIRED. VEGETATION, INSECTS, REPTILES, FISH AND SMALL MAMMALS CONTACTED BY LIQUID AMMONIA AND/OR THE VAPOR CLOUD WILL LIKELY DIE; POST-SPILL CONSERVATION MEASURES MAY BE REQUIRED.
Handling And Storage Precautions: STORE CYLINDERS & TANKS IN A WELL VENTILATED AREA, AWAY FROM INCOMPATIBLE MATERIALS (I.E. CHLORINE), SOURCES OF HEAT & IGNITION. EMPTY CONTAINERS MAY CONTAIN RESIDUAL GAS AND CAN BE DANGEROUS. GROUND/ BOND ALL LINES & EQUIPMENT USED FOR THE TRANSFER & STORAGE OF AMMONIA GAS TO PREVENT STATIC SPARKS.
Other Precautions: DO NOT PRESS, CUT, WELD, BRAZE, SOLDER, DRILL, GRIND/EXPOSE SUCH CONTRS TO HEAT, FLAMES, SPKS/OTHER SOURCES OF IGNIT; THEY MAY EXPLODE & CAUSE INJURY/DEATH. CONSULT COMPRESSED GAS ASSOC PUBLICATIONS: (G-2) "ANHYDROUS AMMONIA"; (G-2.1) "AMERICAN NATIONAL STD SFTY REQS FOR STOR & HNDLG OF ANHYDROUS AM MONIA. ANSI K61.1".

Fire and Explosion Hazard Information

===

Autoignition Temp: =651.1C, 1204.F
Lower Limits: 16.0%
Upper Limits: 25.0%
Extinguishing Media: WATER FOG IS BEST. (AMMONIA WILL REACT WITH CARBON DIOXIDE TO FORM A DENSE WHITE CLOUD).

Fire Fighting Procedures: USE NIOSH APPROVED SCBA & FULL PROTECTIVE EQUIPMENT (FPN). USE WATER SPRAY OR FOG TO KEEP FIRE-EXPLOSION CONTAINERS COOL. DO NOT COMPLETELY EXTINGUISH FLAME UNLESS GAS FLOW IS SHUT OFF! AMMONIA BURNS TO FORM OXIDES OF NITROGEN.
Unusual Fire/Explosion Hazard: FLASH POINT: NOT FLAMMABLE UNDER CONDITIONS TYPICALLY ENCOUNTERED. ALTHOUGH CLASSIFIED NONFLAMMABLE, AMMONIA DOES HAVE AN EXPLOSIVE RANGE. AMMONIA CAN BE A DANGEROUS FIRE AND EXPLOSION HAZARD WHEN MIXED WITH AIR. NFPA CODE: H - 3; F - 1; R - 0.

==

Control Measures

==

Respiratory Protection: USE NIOSH APPROVED FULL FACE RESPIRATORY PROTECTIVE EQUIPMENT WHEN CONCENTRATIONS OF GASEOUS AMMONIA ARE GREATER THAN STEL. SCBA IS REQUIRED TO CONTAIN A LIQUID LEAK, UPON ENTRY ITO BUILDINGS AND ENTR Y INTO DESIGNATED CONFINED SPACE AREAS, OR IN ANY SITUATIONS WHERE AIRBORNE CONENTRATIONS MAY EXCEED OCCUPATIONAL EXPOSURE LIMITS.
Ventilation: PROVIDE ADEQ GEN & LOC EXHST VENT TO ATTAIN OCCUP EXPOS LIMITS, TO PVNT FORMATION OF EXPLOSIVE ATM; & TO PVNT FORMATION OF AN OXYGEN DEFICIENT ATM, (SUPDAT)
Protective Gloves: NONPOROUS GLOVES.
Eye Protection: ANSI APPRVD CHEM WORK GOGGS & FULL LENGTH FACESHLD (FP N). AMMONIA IS (SUPDAT)
Other Protective Equipment: EYE WASH & DELUGE SHWR MTG ANSI DESIGN CRIT (FP N). AMMONIA IS SEVERELY CORROSIVE TO EPIDERMAL TISSUE. WEARING NONPOROUS CLOTHING: PANTS, SLEEVES & FOOTWEAR IS RECOMMENDED PROTECTION AGAINST SKIN CONT.
Supplemental Safety and Health: VENT: PATICULARLY IN CONFINED SPACE AREA. EYE PROT: EXTREMELY CORROSIVE TO MUCOSAL MEMBRANES (EYES, NOSE, THROAT). REMOVE CONTACT LENSES AND WEAR CHEMICAL GOGGLES. A FACE SHIELD IS ALSO ADVISED FOR ADDITIONAL SKIN PROTECTION WHERE CONTACT WITH LIQUID OR VAPOR MAY OCCUR.

Physical/Chemical Properties

==

Boiling Point: =-33.3C, -28.F
B.P. Text: @ 1 ATMOSPHERE
Vapor Pres: 124 @ 68F
Vapor Density: 0.6(AIR=1)
Solubility in Water: 5 LG/100G @ 68F
Appearance and Odor: COLORLESS LIQUEFIED GAS; PUNGENT AND EXTREMELY IRRITATING ODOR.
Percent Volatiles by Volume: 100%

Reactivity Data

===

Stability Indicator: YES
Materials To Avoid: ACIDS, STRONG OXIDIZING AGENTS, CHLORINE, BROMINE, PENTAFLUORIDE, NITROGEN TRIFLUORIDE, MERCURY, SILVER OXIDE, CALCIUM, AND CHLORIDES OF IRON. DO NOT USE COPPER, BRASS, BRONZE, OR GALVANIZED STEEL IN AMMONIA SERVICE.
Hazardous Decomposition Products: AMMONIA AND OXIDES OF NITROGEN (NITROGEN DIOXIDE, NITRIC OXIDE).
Hazardous Polymerization Indicator: NO
Conditions To Avoid Polymerization: WILL NOT OCCUR.

Toxicological Information

===

Ecological Information

===

MSDS Transport Information

===

Transport Information: DOT HAZARD CLASS: 2.2.

Regulatory Information

===

Sara Title III Information: ANHYDROUS AMMONIA: EPA SARA TITLE III INFORMATION: SECTION 311/312 HAZARD CATEGORIZATION: ACUTE, FIRE, PRESSURE. SARA HAZARDOUS SUBSTANCES: INGREDIENT: ANHYDROUS AMONIA. CAS NO: 7664-41-7, % WT: 99.5- 100, SEC 313, SEC 302, RQ LB: 100 TPQ LB: 500. SEC 313 = TOXIC CHEMICAL, SECTION 313. SEC 302 = EXTREMELY HAZARDOUS SUBSTANCES (EHS), SECTION 302. RQ: REPORTABLE QUANTITY OF EHS. TPQ = THRESHOLD PLANN ING QUANTITY OF EHS.

Other Information

===

Other Information: CHEMICAL FORMULA: NH*3. ANHYDROUS AMMONIA: NFPA CODE: 3: HEALTH HAZARD (BLUE): CAN CAUSE INJURY DESPITE MEDICAL TREATMENT. 1: FLAMMABLILITY HAZARD (RED): IGNITES AFTER CONSIDERABLE PREHEATING. 0: REACTIVITY HAZARD (YELLOW): NORMALLY STABLE. NOT REACTIVE WITH WATER. NONE: SPECIAL NOTICE (WHITE): NONE LISTED.

HAZCOM Label

===

Product ID: ANHYDROUS AMMONIA, STCC# 4904210, UN 1005
Cage: 1F8L6
Company Name: COASTAL ST HELENS CHEMICAL
Street: 63149 COLUMBIA RIVER HWY
City: ST HELENS OR
Zipcode: 97051
Health Emergency Phone: 800-424-9300 (CHEMTREC)
Label Required IND: Y
Date Of Label Review: 09/28/1999
Status Code: A
Origination Code: F
Eye Protection IND: YES
Skin Protection IND: YES
Signal Word: DANGER
Respiratory Protection IND: YES
Health Hazard: Severe
Contact Hazard: Severe
Fire Hazard: Slight
Reactivity Hazard: None
Hazard And Precautions: CORROSIVE. ACUTE:
EYES: CONTACT MAY CAUSE CORROSION, PAIN, REDNESS AND ULCERATION OF CORNEA, LENS AND CONJUNCTIVA.
SKIN: CONTACT CAN CAUSE FROSTBITE, FREEZE BURNS AND/OR CHEMICAL BURNS, RESULTING IN SEVERE DERMAL DAMAGE.
INHALATION: GAS IS EXTREMELY IRRITATING TO MUCOUS MEMBRANES AND LUNG TISSUE. COUGHING, CHEST PAIN, AND DIFFICULTY IN BREATHING MAY RESULT. PROLONGED EXPOSURE MAY RESULT IN BRONCHITIS, PULMONARY EDEMA, AND CHEMICAL PNEUMONITIS. BREATHING HIGH CONCENTRATIONS MAY RESULT IN DEATH.
INGESTION: EXTREMELY IRRITATING TO MUCOUS MEMBRANES CAUSING VOMITING, NAUSEA AND BURNS. CHRONIC: NO CHRONIC HEALTH EFFECTS HAVE BEEN FOUND TO DATE.

APPENDIX 2

Safety Requirements and Equipment

Safety requirements are continuously reviewed. Major areas of concern are the location of safety equipment, toxicity of the chemicals, high temperature, electrical and mechanical equipment.

The characterization techniques in this research include high temperatures or electrical apparatus. When working with the electrical equipment it is important to avoid water near the plugs and connections and to not touch any hot surface. Whenever needed, we use tweezers to work with hot objects. Work in the hood at all times is necessary as well as protective gloves when handling these chemicals. One always wears protective glasses, lab coat and gloves at all times when working in the lab. These are to maintain safety and to avoid contact of chemicals with skin and eyes.

The laboratory is equipped with chemical hoods, fire extinguishers, chemical safety showers, chemical spill kit and several eye wash stations. Other available equipment include gloves, organic vapor masks, dust masks, face shields, protective clothing and eye protection. Material safety data sheets (MSDS) have been obtained for all chemicals used in the laboratory are placed at the entrance to a rapid access in case of emergency. A list of people to contact and the protective equipment needed in the area also are posted at the entrance to the laboratory. Specific emergency procedures are placed near all the equipment to ease the shut down in case of emergency.

APPENDIX 3
DRIFT Results (Raw Data)

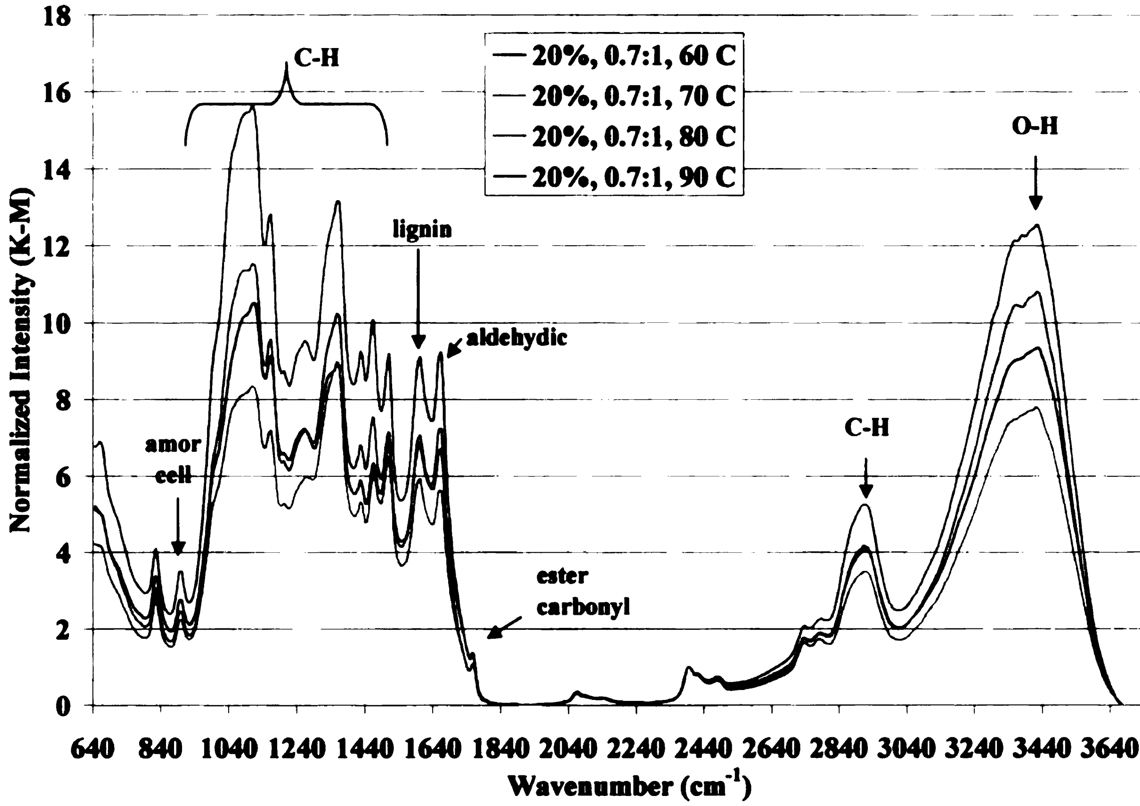

Figure A3.1: AFEX DRIFT results (20%, 0.7:1, 60-90C)

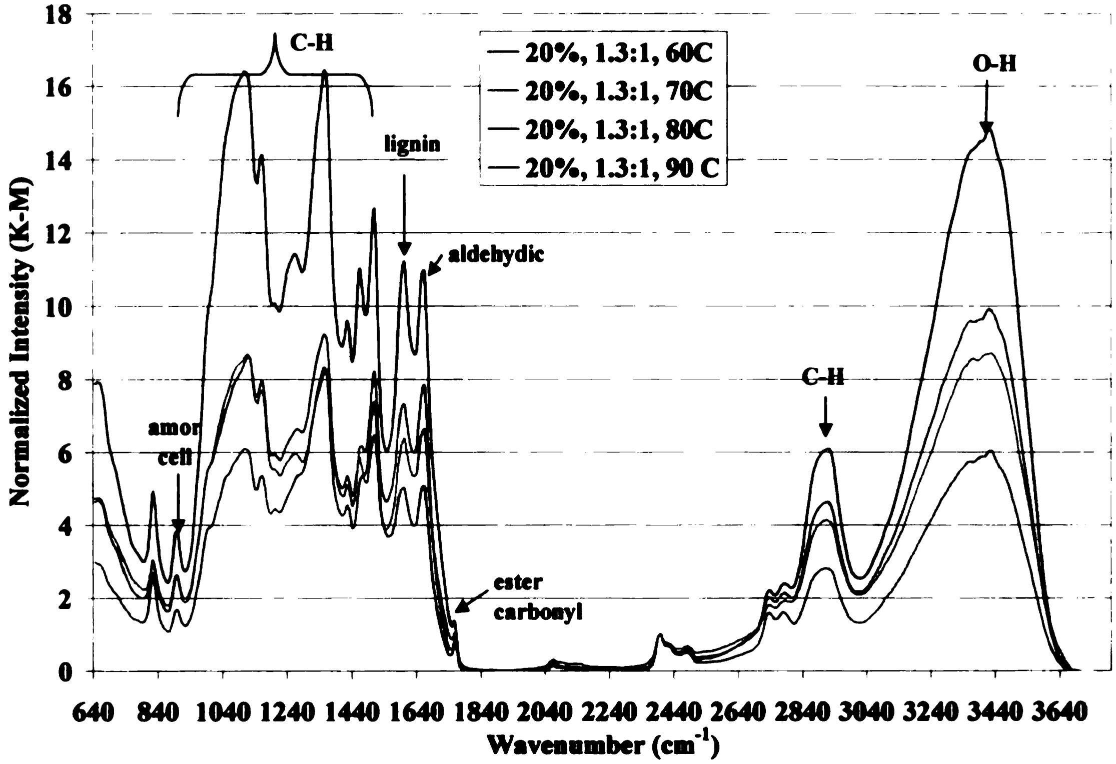

Figure A3.2: AFEX DRIFT results (20%, 1.3:1, 60-90C)

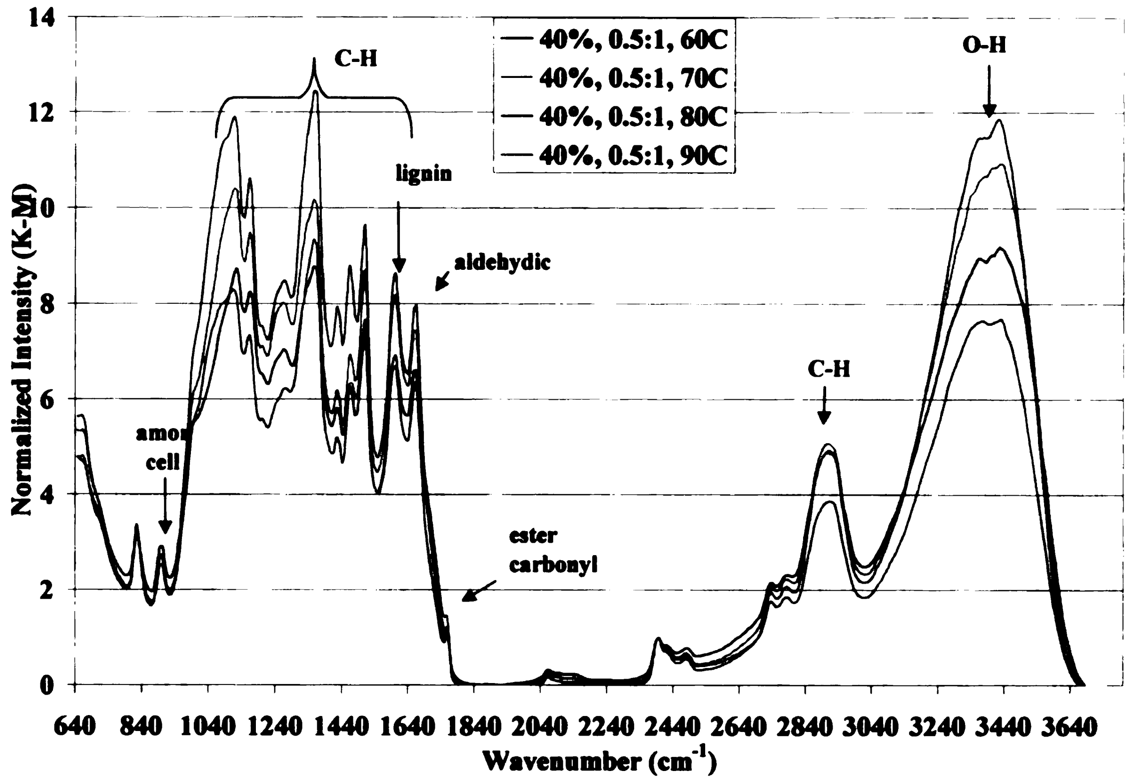

Figure A3.3: AFEX DRIFT results (40%, 0.5:1, 60-90C)

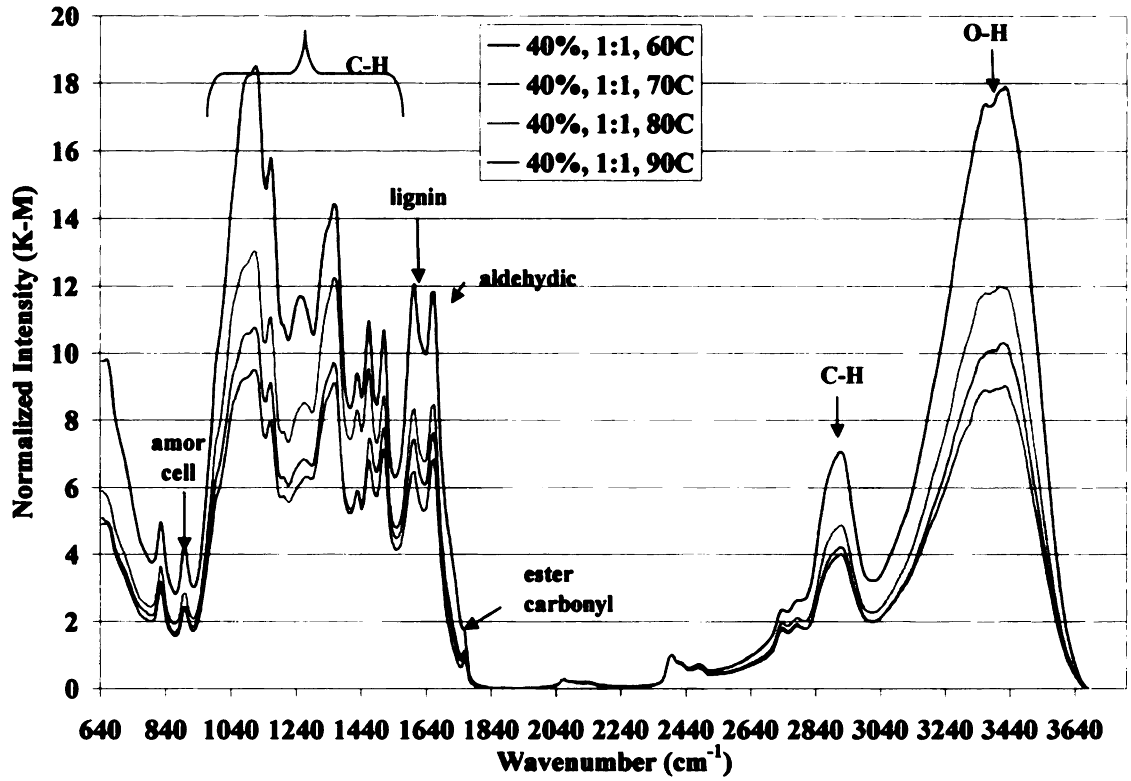

Figure A3.4: AFEX DRIFT results (40%, 1:1, 60-90C)

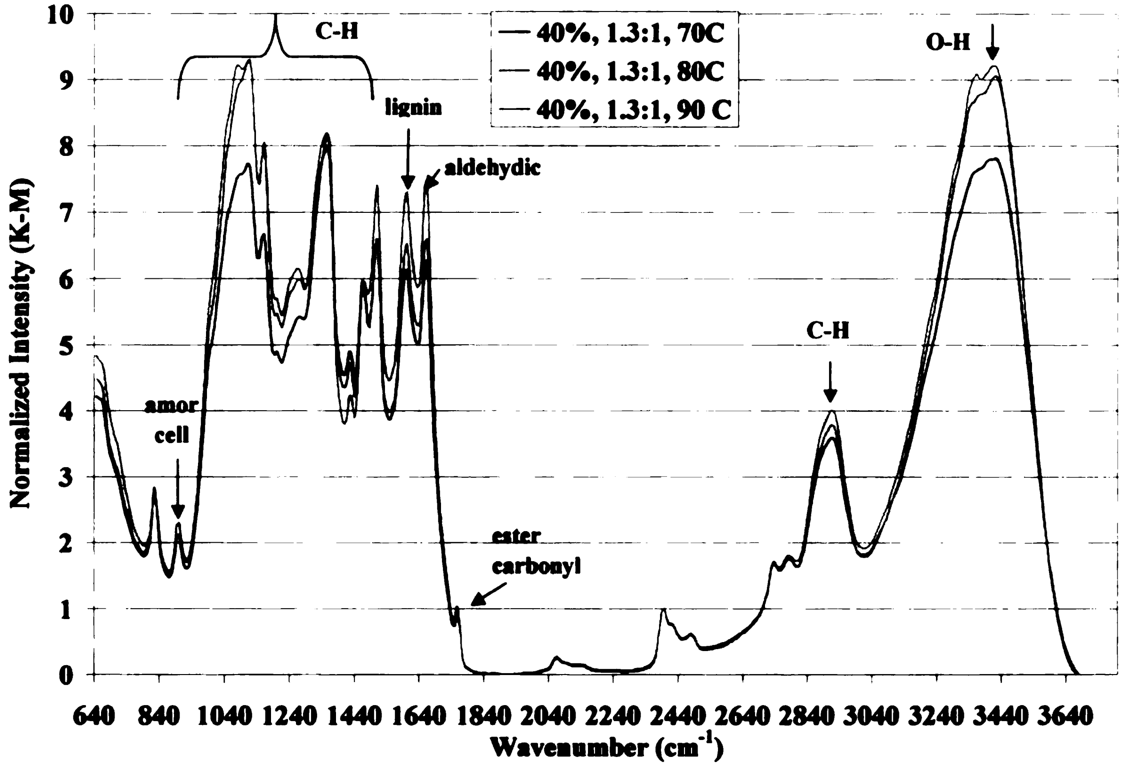

Figure A3.5: AFEX DRIFT results (40%, 1.3:1, 70-90C)

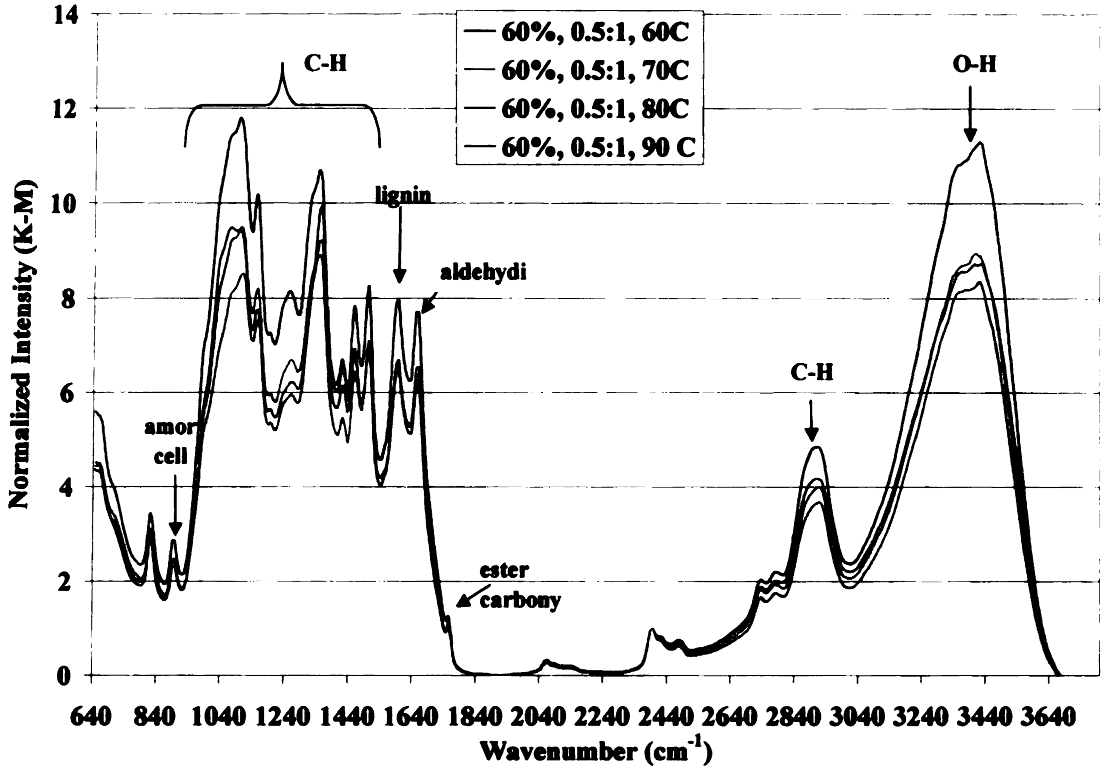

Figure A3.6: AFEX DRIFT results (60%, 0.5:1, 60-90C)

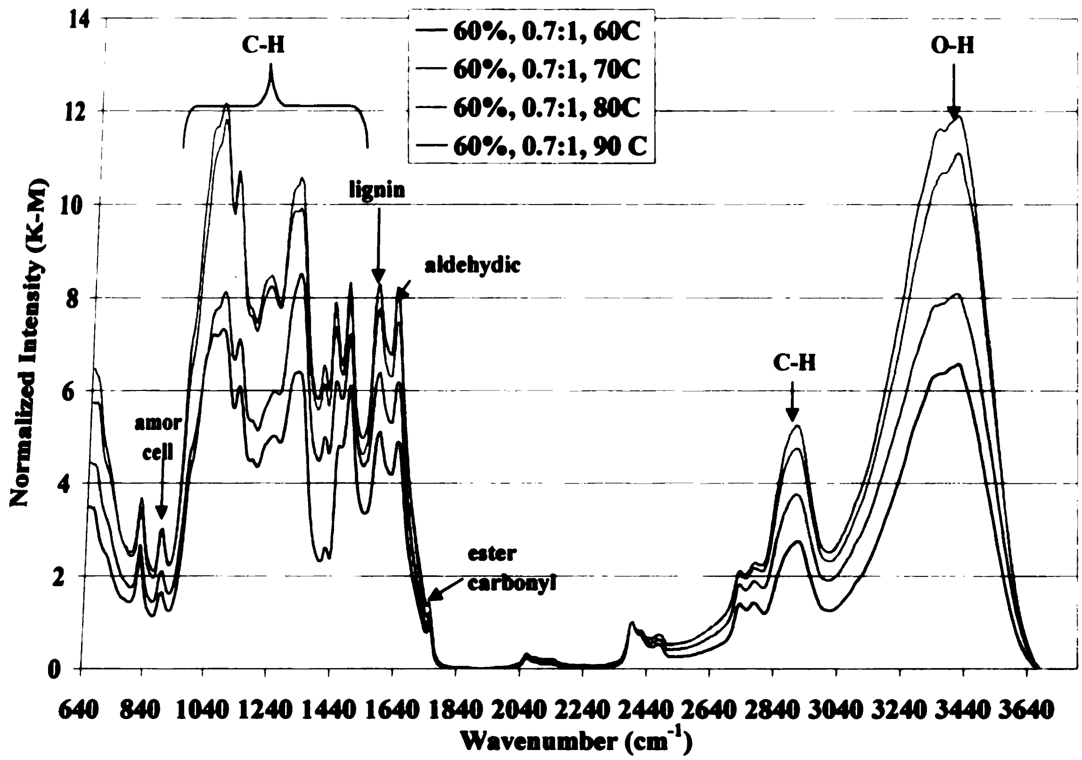

Figure A3.7: AFEX DRIFT results (60%, 0.7:1, 60-90C)

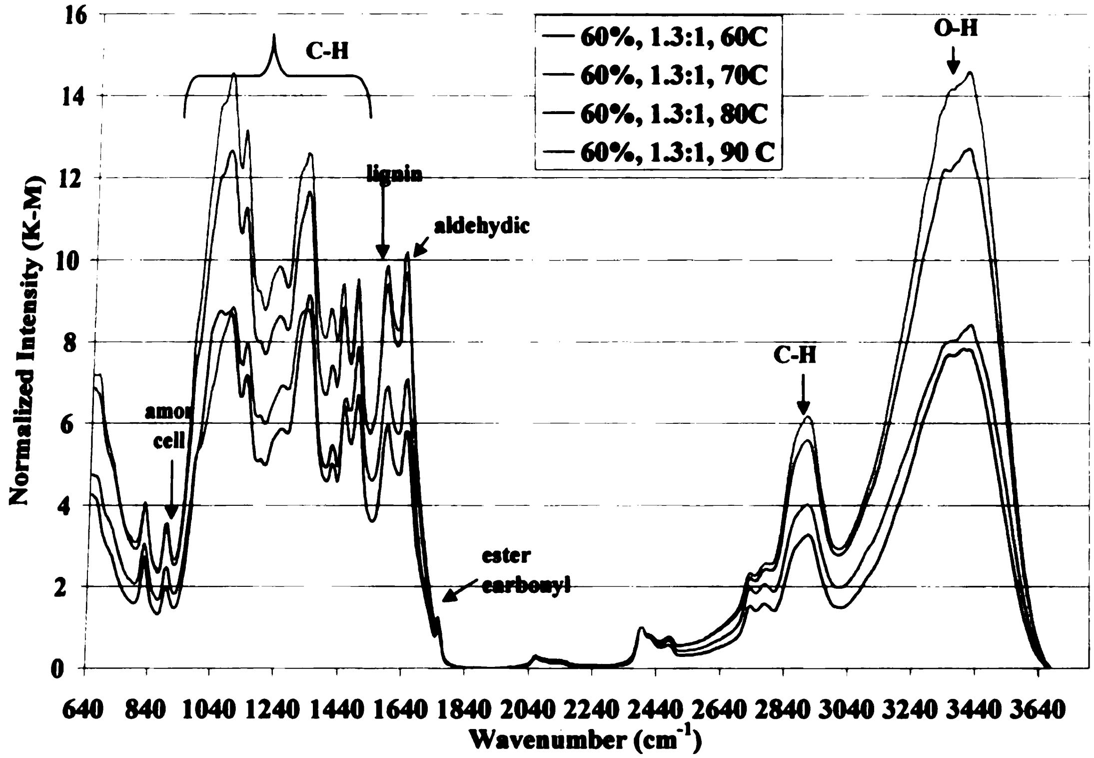

Figure A3.8: AFEX DRIFT results (60%, 1.3:1, 60-90C)

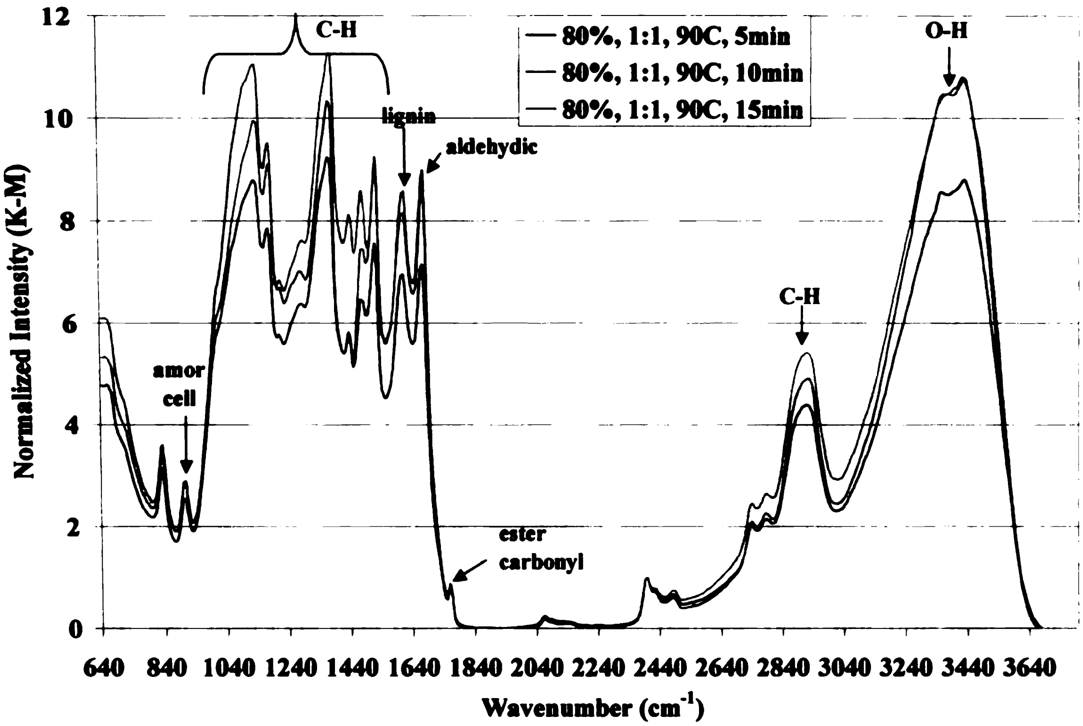

Figure A3.9: AFEX DRIFT results (80%, 1:1, 90C, 5-15 min)

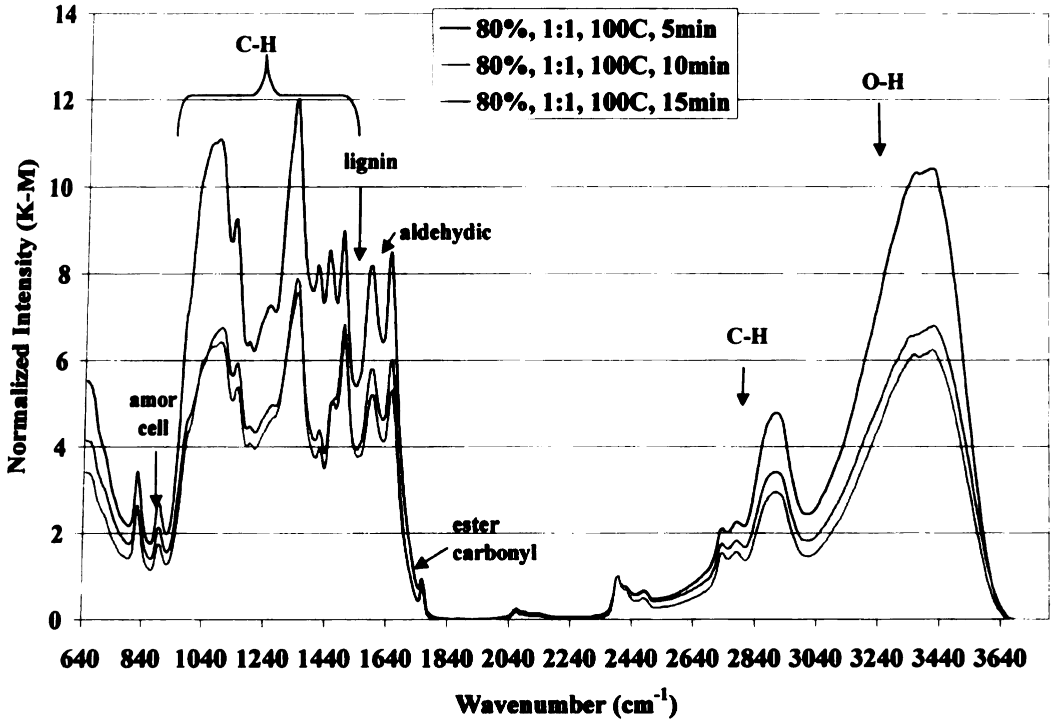

Figure A3.10: AFEX DRIFT results (80%, 1:1, 100C, 5-15 min)

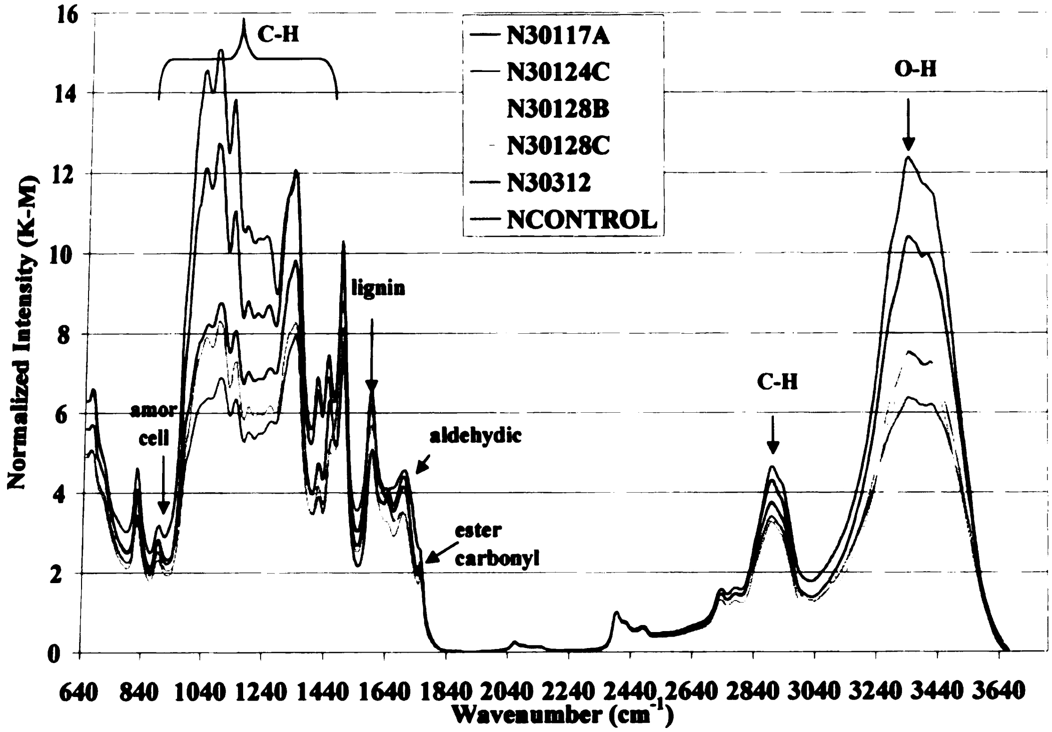

Figure A3.11: NREL samples DRIFT results

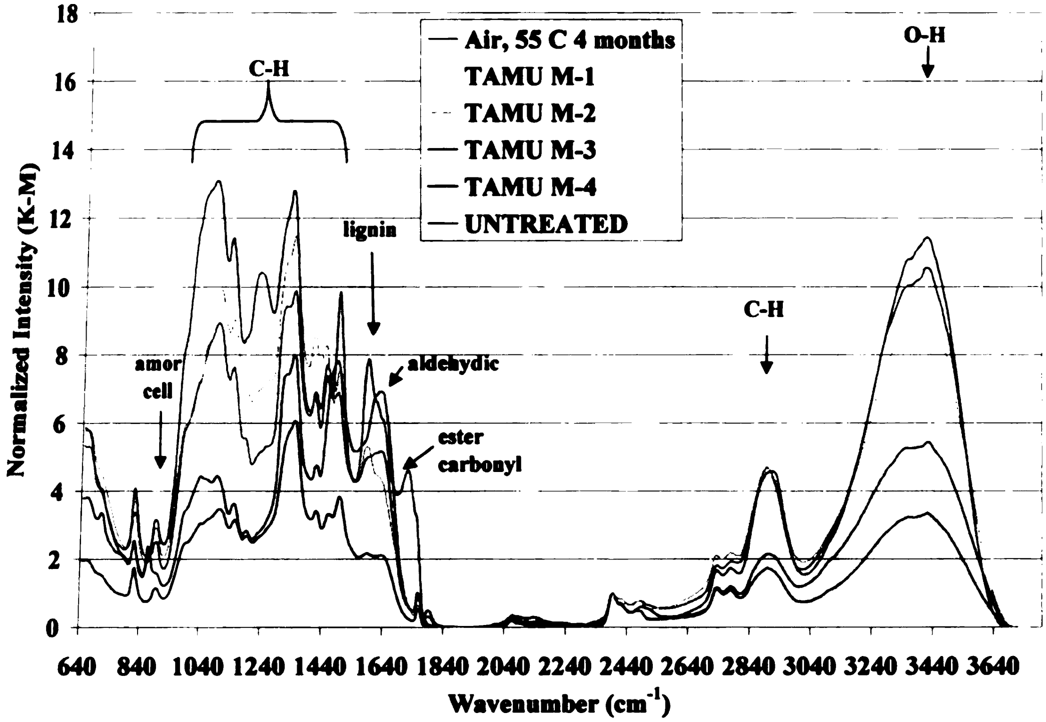

Figure A3.12: Lime treated samples DRIFT results

APPENDIX 4
Corn Stover Characterization Raw Data

Table A4.1: Crystallinity Index for AFEX pretreated corn stover

Samples Treatment and conditions	Crystallinity index (%)
20%, 0.7:1, 60°C	20.21
20%, 0.7:1, 70°C	23.07
20%, 0.7:1, 80°C	23.61
20%, 0.7:1, 90°C	16.77
20%,1.3:1, 60°C	34.83
20%, 1.3:1, 70°C	33.59
20%, 1.3:1,80°C	35.86
20%, 1.3:1, 90°C	36.16
40%,0.5:1, 60°C	36.25
40%, 0.5:1, 70°C	32.72
40%, 0.5:1, 80°C	42.29
40%, 0.5:1, 90°C	35.89
40%, 1:1, 60°C	23.45
40%, 1:1, 70°C	25.09
40%, 1:1, 80°C	13.71
40%, 1:1, 90°C	23.48
40%, 1.3:1, 60°C	12.40
40%, 1.3:1, 70°C	19.25
40%, 1.3:1,80°C	19.25
40%, 1.3:1, 90°C	22.30
60%, 0.5:1, 60°C	48.83
60%, 0.5:1, 70°C	60.43
60%, 0.5:1, 80°C	55.63
60%, 0.5:1, 90°C	52.04
60%, 0.7:1, 60°C	20.09
60%, 0.7:1, 70°C	24.00
60%, 0.7:1, 80°C	22.81
60%, 0.7:1, 90°C	31.94

Table A4.1 (cont'd)

Samples Treatment and conditions	Crystallinity index (%)
60%, 1:1, 60°C	27.00
60%, 1:1, 70°C	23.15
60%, 1:1, 80°C	22.96
60%, 1:1, 90°C	36.29
60%, 1.3:1, 60°C	25.95
60%, 1.3:1, 70°C	29.82
60%, 1.3:1, 80°C	26.50
60%, 1.3:1, 90°C	26.98
60%, 1:1, 90°C, 15min	63.66
60%, 1:1, 110°C, 5min	68.68
60%, 1:1, 110°C, 10min	48.93
60%, 1:1, 110°C, 15min	61.30
60%, 1:1, 100°C, 15min	50.67
80%, 1:1, 90°C, 5min	55.89
80%, 1:1, 90°C, 10min	47.84
80%, 1:1, 90°C, 15min	50.07
80%, 1:1, 100°C, 5min	57.18
80%, 1:1, 100°C, 10min	50.78
80%, 1:1, 100°C, 15min	69.73
Untreated	50.3

Table A4.2: Crystallinity Index for pretreated corn stover

Samples Treatment and conditions	Crystallinity index (%)
ARP #1(3D)7-25-03	56.17
ARP #2(5D)7-25-03	48.40
ARP 10%NH3,170°C, 10 min	25.98
ARP 10%NH3,170°C, 20 min	42.07
ARP 10%NH3,170°C, 30 min	37.27
Dilute Acid, 140°C, 40 min, 1% H2SO4	39.94
Dilute Acid 160°C, 10 min, 1% H2SO4	45.79
Dilute Acid, 180°C, 1 min, 1% H2SO4	48.00
Dilute Acid, 180°C, 2 min, 1% H2SO4	52.51
Dilute Acid 190°C, 20ml/min, 0.05% H2SO4	64.09
Dilute Acid, 200°C, 20ml/min, H_2O	51.33
Controlled pH, 160°C, 5min	53.84
Controlled pH, 190°C,15 min	44.52
Controlled pH, 200°C, 20min	54.12
NREL-P030312	44.84
NREL-030117A	48.88
NREL-030124C	41.86
NREL-030128B	51.73
NREL-030128C	49.44
NREL-CONTROL1&2	48.25
Lime (M-1)	43.09
Lime (M-2)	38.99
Lime (M-3)	54.41
Lime (M-4)	44.90
Lime-02	56.17
Lime-03	51.76
Untreated	50.3
α-cellulose	66.53

Table A4.3: MLR model coefficients for corn stover using all spectroscopic data

	Initial Rate B-coefficients	72-hr Conversion B-coefficients
Intercept	5.077	37.823
CrI	0.648	0.645
Amorphous Cell (902.537)	5.431	-4.232
Ligning (1511.94)	3.085	26.34
Lignin (1604.51)	6.501	-22.37
Aldehyde (1658.51)	-12.995	2.94
Ester Carbonyl (1712.51)	-7.038	-14.372
C-H (2915.89)	12.638	35.478
O-H (3417.3)	-2.655	-11.032
Fluorescence (425.5)	-5.79E-06	-5.64E-06

Table A4.4: PCR model coefficients for corn stover using DRIFT data

	Initial Rate						
	Amorphous Cell (902.54)	Lignin 1511.94	Lignin 1604.51	Aldehyde 1658.51	Ester Carbonyl 1712.51	C-H 2915.89	O-H 3417.3
PC_01 (X-Vars + Interactions)	0.015	0.016	0.020	0.018	0.009	0.019	0.033
PC_02 (X-Vars + Interactions)	0.030	0.049	0.094	0.087	-0.030	0.079	-0.004
PC_03 (X-Vars + Interactions)	0.045	0.049	0.096	0.088	-0.016	0.073	-0.042
PC_04 (X-Vars + Interactions)	0.166	-0.032	-0.354	-0.314	0.001	0.215	0.028
PC_05 (X-Vars + Interactions)	0.149	0.107	-0.267	-0.291	0.131	0.229	0.042
PC_06 (X-Vars + Interactions)	0.029	0.140	-0.380	-0.514	0.227	0.325	0.135
PC_07 (X-Vars + Interactions)	0.045	-0.290	-0.570	-0.874	-0.603	0.565	-0.275
PC_08 (X-Vars + Interactions)	0.031	-0.258	-0.552	-0.877	-0.649	0.557	-0.237
PC_09 (X-Vars + Interactions)	0.031	-0.116	-0.681	-1.259	-1.012	0.781	-0.133
PC_10 (X-Vars + Interactions)	0.029	-0.001	-0.580	-1.316	-1.013	0.859	-0.224
PC_11 (X-Vars + Interactions)	0.101	-0.003	-0.575	-1.354	-1.093	0.913	-0.103
PC_12 (X-Vars + Interactions)	0.165	-0.936	-0.158	-1.347	-1.052	0.624	-0.383
PC_13 (X-Vars + Interactions)	0.191	-0.953	-0.170	-1.314	-1.078	0.579	-0.363
PC_14 (X-Vars + Interactions)	0.204	-0.936	-0.165	-1.320	-1.103	0.581	-0.417
PC_15 (X-Vars + Interactions)	0.180	-0.932	-0.172	-1.320	-1.094	0.551	-0.477
PC_16 (X-Vars + Interactions)	0.762	-0.550	-1.112	-1.831	-0.918	0.800	-2.166
PC_17 (X-Vars + Interactions)	0.858	-0.569	-1.132	-1.897	-0.929	0.746	-2.395
PC_18 (X-Vars + Interactions)	0.676	0.282	-2.082	-2.000	-0.924	1.282	-2.418
PC_19 (X-Vars + Interactions)	0.711	0.286	-2.118	-2.008	-0.937	1.283	-2.366
PC_20 (X-Vars + Interactions)	0.697	0.026	-1.465	-1.910	-0.894	1.597	-2.505
	72 hr conversion						
	Amorphous Cell (902.54)	Lignin 1511.94	Lignin 1604.51	Aldehyde 1658.51	Ester Carbonyl 1712.51	C-H 2915.89	O-H 3417.3
PC_01 (X-Vars + Interactions)	0.020	0.021	0.027	0.025	0.012	0.025	0.044
PC_02 (X-Vars + Interactions)	0.066	0.124	0.282	0.292	-0.111	0.214	-0.072
PC_03 (X-Vars + Interactions)	0.058	0.124	0.281	0.294	-0.119	0.217	-0.052
PC_04 (X-Vars + Interactions)	0.222	0.014	-0.294	-0.407	-0.095	0.410	0.043
PC_05 (X-Vars + Interactions)	0.185	0.315	-0.108	-0.354	0.187	0.439	0.073
PC_06 (X-Vars + Interactions)	0.118	0.333	-0.170	-0.511	0.240	0.493	0.125
PC_07 (X-Vars + Interactions)	0.144	-0.406	-0.327	-1.037	-1.187	0.906	-0.580
PC_08 (X-Vars + Interactions)	0.036	-0.147	-0.129	-0.852	-1.547	0.846	-0.279
PC_09 (X-Vars + Interactions)	0.036	-0.204	-0.097	-0.670	-1.402	0.756	-0.320
PC_10 (X-Vars + Interactions)	0.032	0.055	0.124	-0.829	-1.405	0.933	-0.525
PC_11 (X-Vars + Interactions)	0.197	0.049	0.083	-0.989	-1.589	1.055	-0.246
PC_12 (X-Vars + Interactions)	0.110	1.307	-0.611	-0.735	-1.644	1.444	0.131
PC_13 (X-Vars + Interactions)	-0.069	1.426	-0.569	-1.012	-1.462	1.763	-0.007
PC_14 (X-Vars + Interactions)	0.015	1.528	-0.572	-1.022	-1.612	1.775	-0.338
PC_15 (X-Vars + Interactions)	0.327	1.467	-0.535	-0.880	-1.719	2.165	0.444
PC_16 (X-Vars + Interactions)	0.630	1.666	-0.846	-1.098	-1.627	2.294	-0.434
PC_17 (X-Vars + Interactions)	0.403	1.710	-0.695	-1.165	-1.601	2.421	0.106
PC_18 (X-Vars + Interactions)	0.212	2.604	-1.541	-1.021	-1.596	2.984	0.083
PC_19 (X-Vars + Interactions)	-0.385	2.528	-1.574	-0.940	-1.379	2.971	-0.811
PC_20 (X-Vars + Interactions)	-0.388	2.458	-1.297	-1.086	-1.367	3.055	-0.848

Table A4.5: MLR Raw data for AFEX treated corn stover Unscrambler Modeling

AFEX Conditions	Initial Conversion	72 hr Conversion	CrI	Amorphous Cellulose	Lignin	Lignin	Aldehyde	Ester Carbonyl	C-H	O-H	Fluorescence
20-0.7-60	14.582122	47.00513	20.2138	2.2658451	2.93079	4.3175	4.65591	1.87229	3.03679	7.10034	1.74E+05
20-0.7-70	33.126671	56.58599	23.0699	3.4506159	4.01417	5.7517	6.027483	2.581855	4.57958	9.79861	1.19E+05
20-0.7-80	25.445362	54.94281	23.6107	5.051744	6.20674	9.0665	9.436663	3.977695	6.38625	13.5359	1.32E+05
20-0.7-90	21.086733	54.8974	16.7683	2.916136	3.74261	5.5083	5.934785	2.179224	4.03377	9.54688	1.09E+05
20-1.3-60	11.683777	43.19607	34.8297	1.431939	2.53624	3.3974	3.745461	1.332364	2.24579	6.30807	1.04E+05
20-1.3-70	17.91564	63.40086	33.5856	1.375549	2.59712	3.5547	4.03247	1.242687	2.55593	6.54226	7.38E+04
20-1.3-80	17.388397	81.47572	35.8584	1.55826	2.8041	3.7548	4.420683	1.150971	2.8374	6.89432	7.38E+04
20-1.3-90	15.91172	79.0871	36.1607	2.3586521	4.18245	5.4158	6.222168	1.764136	4.32729	10.4928	8.88E+04
40-0.5-60	m	15.51636	36.2491	1.887974	3.55736	4.5403	4.528491	1.813123	3.31089	8.71527	9.75E+04
40-0.5-70	m	15.41342	32.7249	1.757002	3.33203	4.3656	4.450801	1.967598	3.21083	8.42273	1.32E+05
40-0.5-80	m	14.21958	42.2892	1.584417	2.8802	3.8374	4.054025	1.523967	2.66417	6.88091	1.49E+05
40-0.5-90	m	22.00139	35.8913	2.021435	3.60647	4.8204	5.109474	1.860871	3.5486	9.44428	1.21E+05
40-1-60	18.405565	39.18448	23.4486	3.81321	4.39733	6.1697	6.19516	3.179807	4.59913	9.22244	2.00E+05
40-1-70	15.125252	52.1017	25.0927	3.1541641	3.79291	5.1422	5.366601	2.391274	3.69382	7.72074	1.51E+05
40-1-80	18.83864	62.92634	13.7069	2.6958101	3.33414	4.9192	5.270827	1.88684	3.51647	7.97909	1.36E+05
40-1-90	24.230513	73.87222	23.4755	2.6025441	3.19674	4.2868	4.77509	1.662512	3.03787	6.64144	1.57E+05
40-1.3-60	12.071383	10.84921	12.4041	2.503684	3.31315	4.5856	4.873533	2.030616	3.28505	7.92866	1.50E+05
40-1.3-70	12.145831	17.06903	19.245	3.0821011	3.79087	5.6071	6.218038	2.178183	4.2089	10.0236	1.40E+05
40-1.3-80	16.553133	8.678007	19.2458	1.507985	2.22815	3.4115	3.804906	1.119988	2.3075	6.00884	1.55E+05
40-1.3-90	19.374275	18.80384	22.3003	2.0357831	2.98521	4.0513	4.619017	1.557951	2.64697	6.33175	1.51E+05
60-0.5-60	m	15.41443	48.8292	3.763391	4.52083	6.1745	6.382354	3.026507	4.89144	9.61027	1.12E+05
60-0.5-70	m	19.38564	60.4291	5.7020431	7.07757	9.8659	9.826607	4.728756	7.3452	13.861	1.20E+05
60-0.5-80	m	17.43585	55.6256	4.4436698	5.30183	7.4482	7.315739	3.571665	5.88884	11.1434	1.13E+05
60-0.5-90	m	17.26768	52.0409	5.0191932	5.79123	7.6157	7.849838	3.900492	6.03569	12.0298	1.11E+05
60-0.7-60	9.2901602	8.766775	20.0911	2.137181	2.70186	3.8234	4.049492	1.721558	2.6471	5.8362	1.80E+05
60-0.7-70	11.342645	10.31331	23.9958	2.179749	2.78636	3.9806	4.249293	1.732426	2.75594	6.5335	1.60E+05
60-0.7-80	12.421634	10.05193	22.8063	2.676317	3.36465	5.0199	5.166181	2.023615	3.29783	8.37356	1.94E+05
60-0.7-90	12.65335	4.874799	31.9423	4.4497809	5.74406	8.1001	8.653449	3.7234	5.62681	13.3266	1.46E+05
60-1-60	5.4927187	50.57309	27.001	2.5393159	3.28002	5.164	5.270546	2.031191	3.53181	8.15014	1.75E+05
60-1-70	13.307735	50.83123	23.1546	1.825696	2.12525	3.1521	3.306175	1.234235	2.45901	5.67974	1.54E+05
60-1-80	15.763963	54.08817	22.9628	0.3677371	0.94378	1.5698	1.774695	0.379584	1.04779	3.14785	1.56E+05
60-1-90	20.790194	89.73552	36.2858	3.904192	5.00832	6.7902	7.295038	2.778517	5.57527	10.8115	1.15E+05
60-1-90-15min	46.519829	115.1998	63.6594	5.1673241	6.09841	8.2859	8.565197	3.39686	7.17253	12.3832	1.74E+06
60-1-100-15mi	72.960358	122.4265	50.6732	6.52811	8.28626	11.274	11.71844	4.304543	9.72407	16.5127	4.03E+04
60-1-110-5min	42.672844	77.86687	68.6754	2.3673639	3.01771	4.141	4.532546	1.453167	3.58483	6.40021	1.20E+06
60-1-110-10mi	47.429924	87.31892	48.9339	3.6313729	4.67816	6.4911	6.82345	2.271889	5.69845	10.2574	2.34E+06
60-1-110-15mi	47.950237	94.52048	61.2992	3.3744509	4.07211	5.3512	5.674253	2.002612	4.63488	8.70196	1.26E+06
60-1.3-60	20.084051	49.75323	25.9468	3.444277	4.13033	5.8907	6.152644	2.784384	4.48941	10.1888	1.75E+05
60-1.3-70	16.509945	52.19736	29.817	3.7347341	4.55295	6.7135	6.986624	2.858991	4.83853	10.7316	1.38E+05
60-1.3-80	21.381002	62.30127	26.5018	4.3410592	5.18761	7.5187	7.901489	3.123646	6.1008	12.871	1.27E+05
60-1.3-90	23.682922	78.9688	26.9776	3.1078329	4.06281	5.3766	5.967174	2.320657	4.31855	9.23333	1.20E+05
80-1-90-5min	45.923897	109.1964	55.8939	4.8832259	5.93628	7.9672	8.230081	3.368195	6.53693	11.6453	7.26E+04
80-1-90-10min	43.437111	117.1937	47.8409	4.1162901	5.33559	7.0567	7.571356	2.980752	5.41611	10.1421	8.80E+04
80-1-90-15min	36.777916	109.0775	50.0729	3.841012	4.77474	6.5254	6.841831	2.694047	4.90846	9.44807	8.49E+04
80-1-100-5min	74.531647	94.97057	57.1772	2.342391	3.21754	4.4953	4.693123	1.725395	3.43866	6.80248	8.59E+04
80-1-100-10mi	72.971161	95.87077	50.7768	4.1628089	4.92708	6.8669	7.260736	2.871164	5.61197	10.9943	7.79E+04
80-1-100-15mi	77.267792	107.1232	69.7343	5.3936749	6.16658	8.3967	8.808738	3.42447	7.2015	13.9098	6.68E+04
untreated	6.9943924	29.70606	25.102	2.9457941	3.67382	4.497	3.944827	3.069079	3.4408	7.20473	4.88E+06

Table A4.6: MLR Raw data for pretreated corn stover Unscrambler modeling

Pretreatment Conditions	Initial Conversion	72 hr Conversion	CrI	Amorphous Cellulose	Lignin	Lignin	Aldehyde	Ester Carbonyl	C-H	O-H	Fluorescence
ARP #1(3d)	m	m	56.17173	7.0009971	6.00535	7.51139	7.39592	3.781651	8.11501	15.3116	6.11E+06
ARP #2(5d)	m	m	48.40425	3.844847	3.5116	4.64896	4.62644	1.945199	5.11984	11.9974	8.27E+06
ARP (m-1)	58.8408775	84.658684	25.97577	5.1601272	3.65596	4.4876	4.34035	1.960869	6.06766	13.14	1.95E+05
ARP (m-2)	60.0839996	83.410561	61.88677	7.3573952	4.80892	5.8415	5.81705	2.781693	10.0802	17.7046	5.72E+06
ARP (m-3)	56.0999985	84	39.62355	5.1537371	4.29205	5.46584	5.0577	2.43774	6.67422	14.7409	3.49E+06
Diute Acid 140-1-40min	69	82	39.94452	6.035809	7.98318	8.16018	6.6114	5.84257	7.90263	17.8077	9.13E+04
Diute Acid 160-1-10min	45	64	45.79125	46.138039	27.3827	28.5212	36.5596	39.60081	28.4676	10.6897	9.12E+04
Diute Acid 180-1-1min	40	47	47.99651	1.169782	2.05102	2.05284	1.71872	1.535233	2.08943	5.31434	1.02E+05
Diute Acid 180-1-2min	70	76	52.50553	4.2079029	5.6761	5.73124	4.80067	4.353647	5.2678	11.625	9.80E+04
Diute Acid 190-0.5-20min	m	m	64.08518	1.989834	1.9674	2.0267	1.67541	1.369273	2.74561	6.67788	7.32E+04
Diute Acid H2O,200-20min	m	m	51.3285	5.487751	5.95861	6.30871	5.60039	4.594391	7.42092	14.5882	8.50E+04
N30117A	m	m	48.87965	1.643373	4.30022	3.63442	2.51756	2.626048	2.77521	7.89448	5.88E+04
N30124C	m	m	41.85971	1.399238	3.45387	3.0504	2.09402	1.854255	2.31294	6.49896	4.89E+04
N30128B	m	m	51.72516	1.585817	4.11981	3.41617	2.29342	2.437111	2.82617	8.26123	4.90E+04
N30128C	m	m	49.43994	1.480437	4.06083	3.4031	2.26229	2.40852	2.57882	7.78656	4.69E+04
N30312	m	m	44.84406	1.101234	2.17822	1.87406	1.67883	1.878799	1.86435	6.54081	1.78E+05
NCONTROL	m	m	48.25349	1.2276011	3.2375	2.69974	1.85649	1.958468	2.04736	6.26117	3.12E+04
Controlled pH 160-5 min	36.7099991	49.650002	53.8385	1.218468	2.17878	2.53287	1.90791	1.741462	1.98009	6.24789	1.54E+05
Controlled pH 190-15 min	55.1599998	76.32	44.51891	4.857059	6.16566	7.04042	5.83835	5.22491	6.40656	13.7855	9.97E+04
Controlled pH 200-20 min	40.8300018	41.470001	54.12198	1.216235	2.99358	2.95039	2.23267	2.31867	2.7203	9.55115	4.61E+04
Lime -02	m	m	56.17324	5.0347061	5.31745	6.70671	7.03433	2.768158	6.92222	15.3137	1.17E+05
Lime (M-1)	m	m	43.08876	2.989944	3.47016	5.49145	7.07131	1.2576	4.30297	14.6075	1.83E+05
Lime (M-2)	m	m	38.9861	1.7200789	2.64397	2.88241	2.25607	0.748511	3.13487	8.86534	3.19E+05
Lime (M-3)	m	m	54.40832	1.6146311	3.52561	4.70055	5.6501	0.973273	2.46976	9.68316	4.95E+05
Lime (M-4)	m	m	44.9021	3.1843729	4.27766	5.37503	5.05547	1.006298	5.34805	14.9419	1.62E+05

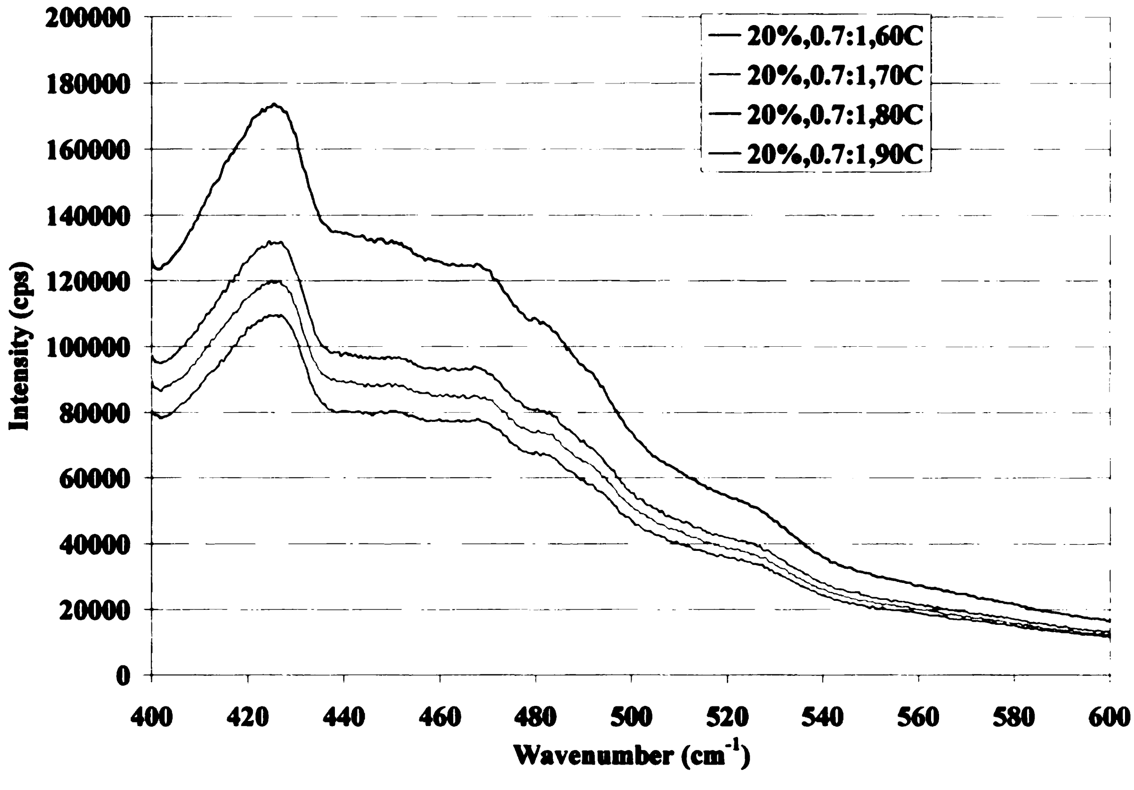

Figure A4.1: AFEX fluorescence results (20%, 0.7:1, 60-90C)

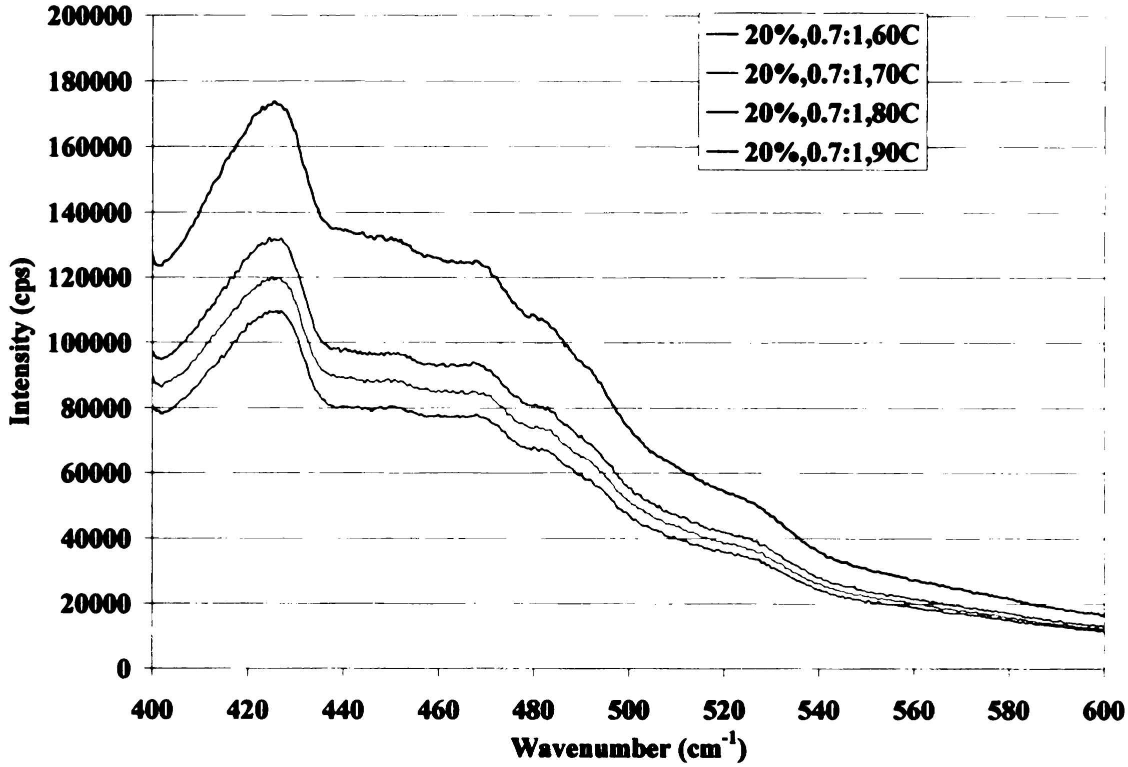

Figure A4.1: AFEX fluorescence results (20%, 0.7:1, 60-90C)

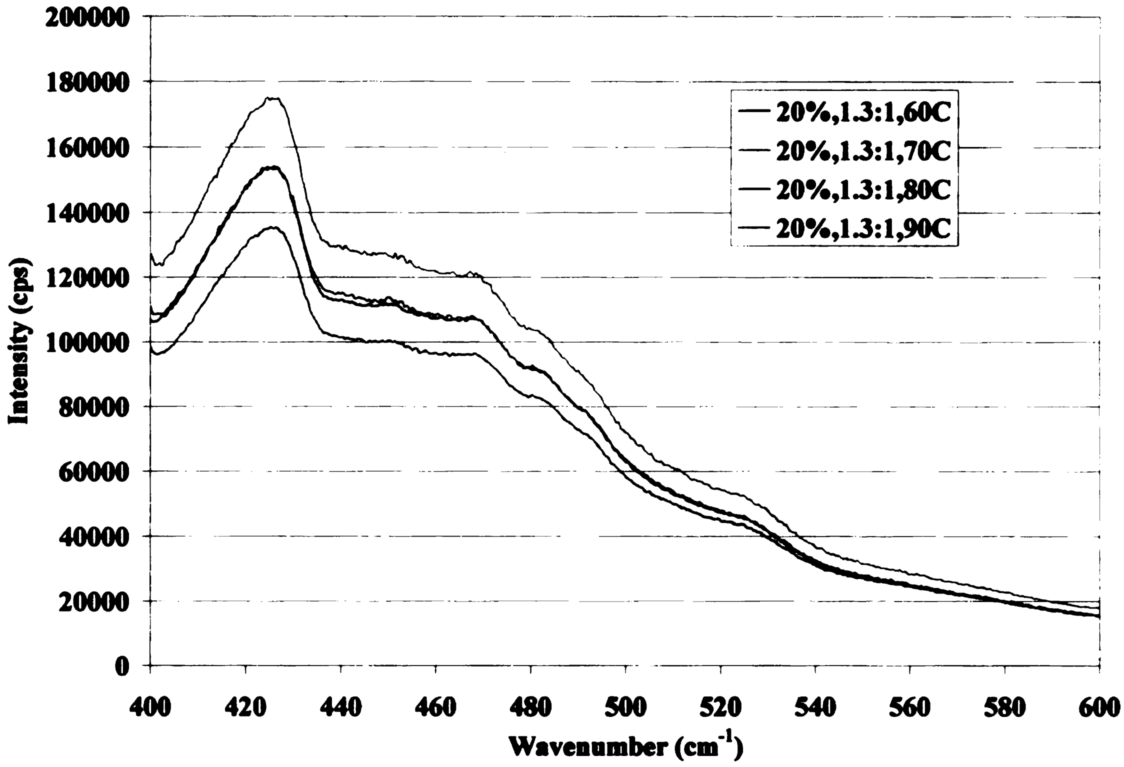

Figure A4.2: AFEX fluorescence results (20%, 1.3:1, 60-90C)

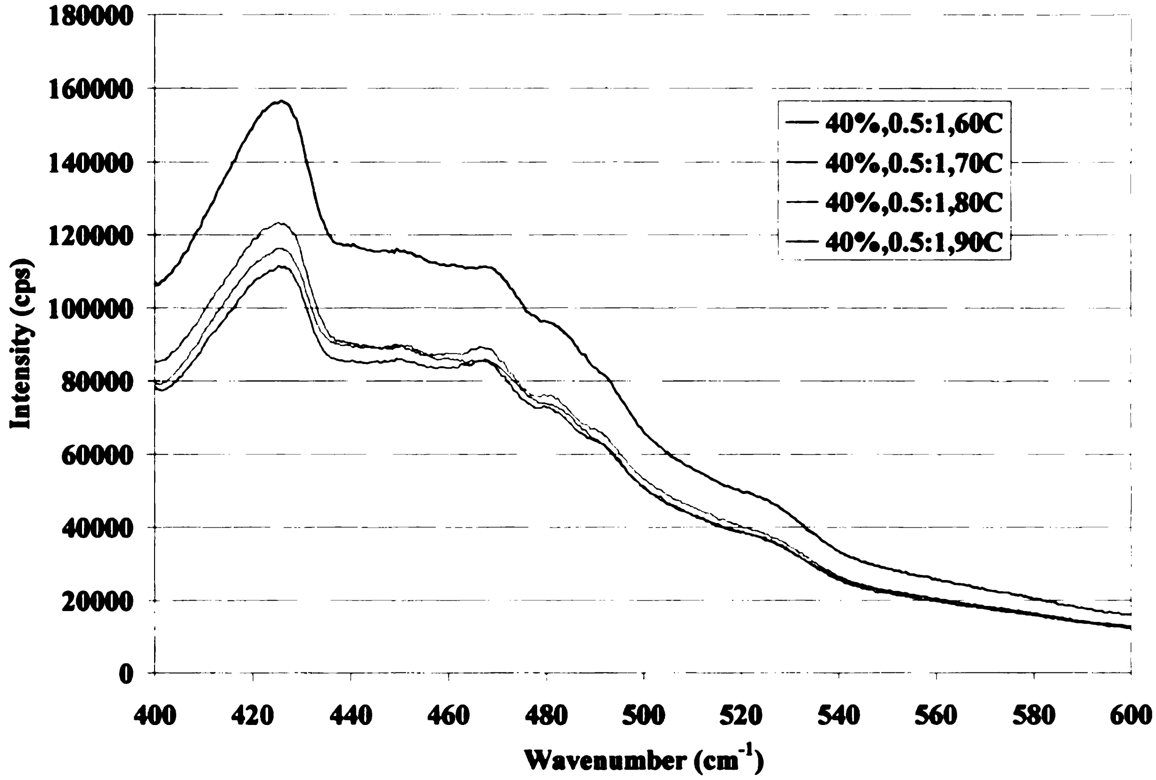

Figure A4.3: AFEX fluorescence results (40%, 0.5:1, 60-90C)

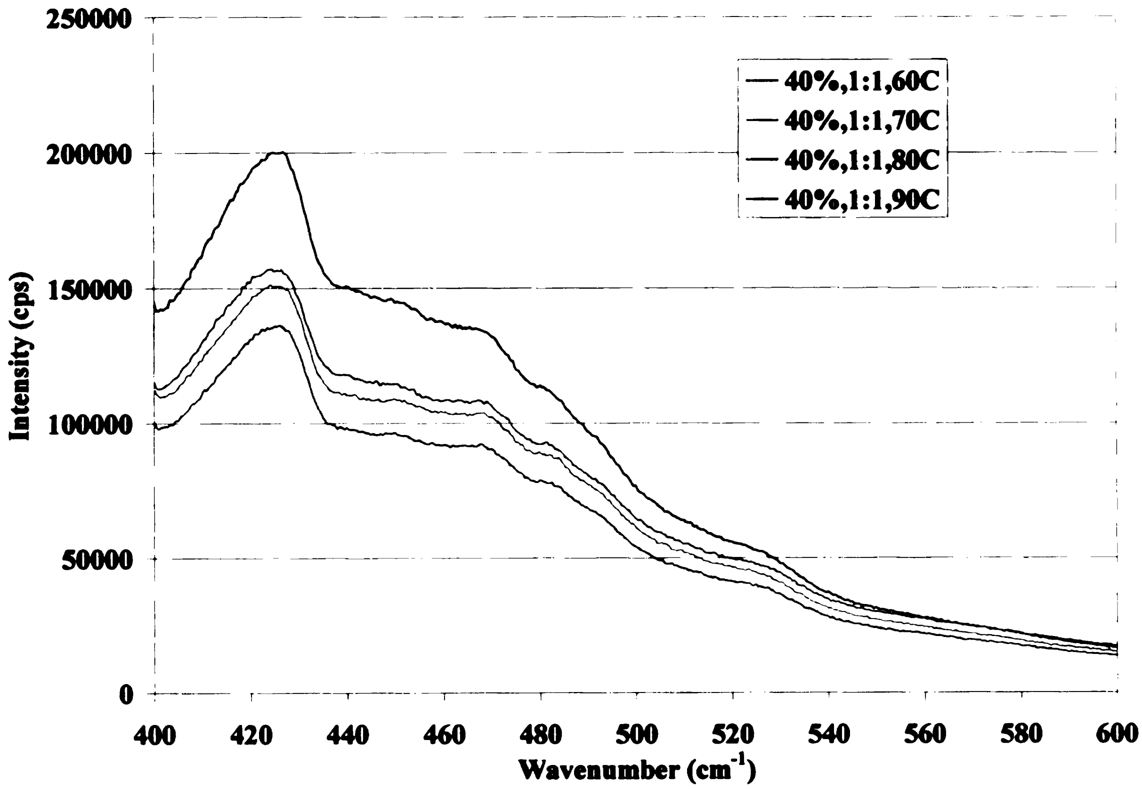

Figure A4.4: AFEX fluorescence results (40%, 1:1, 60-90C)

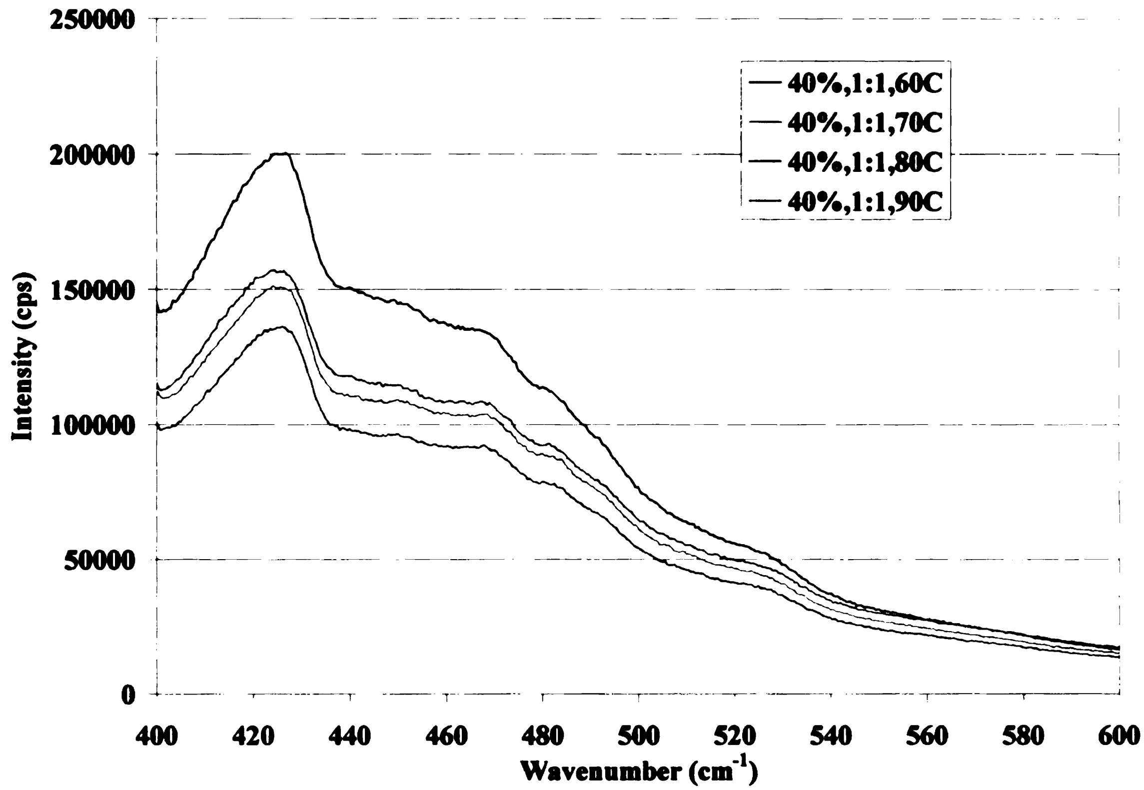

Figure A4.4: AFEX fluorescence results (40%, 1:1, 60-90C)

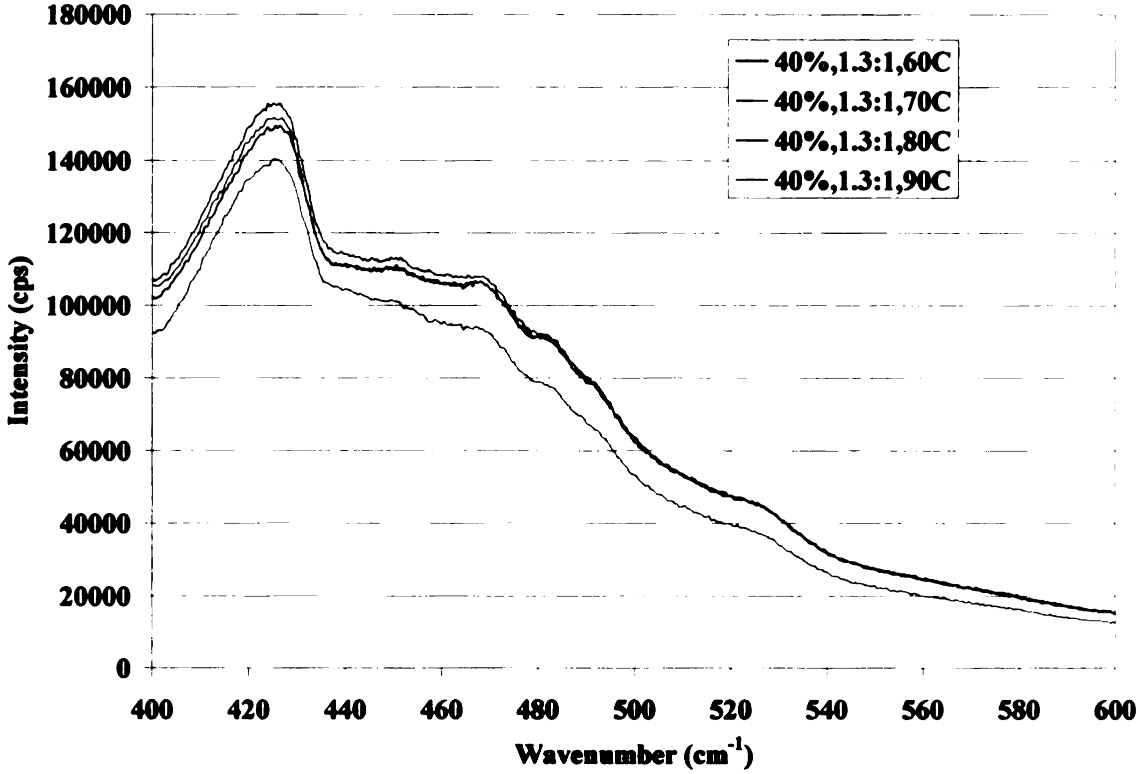

Figure A4.5: AFEX fluorescence results (40%, 1.3:1, 60-90C)

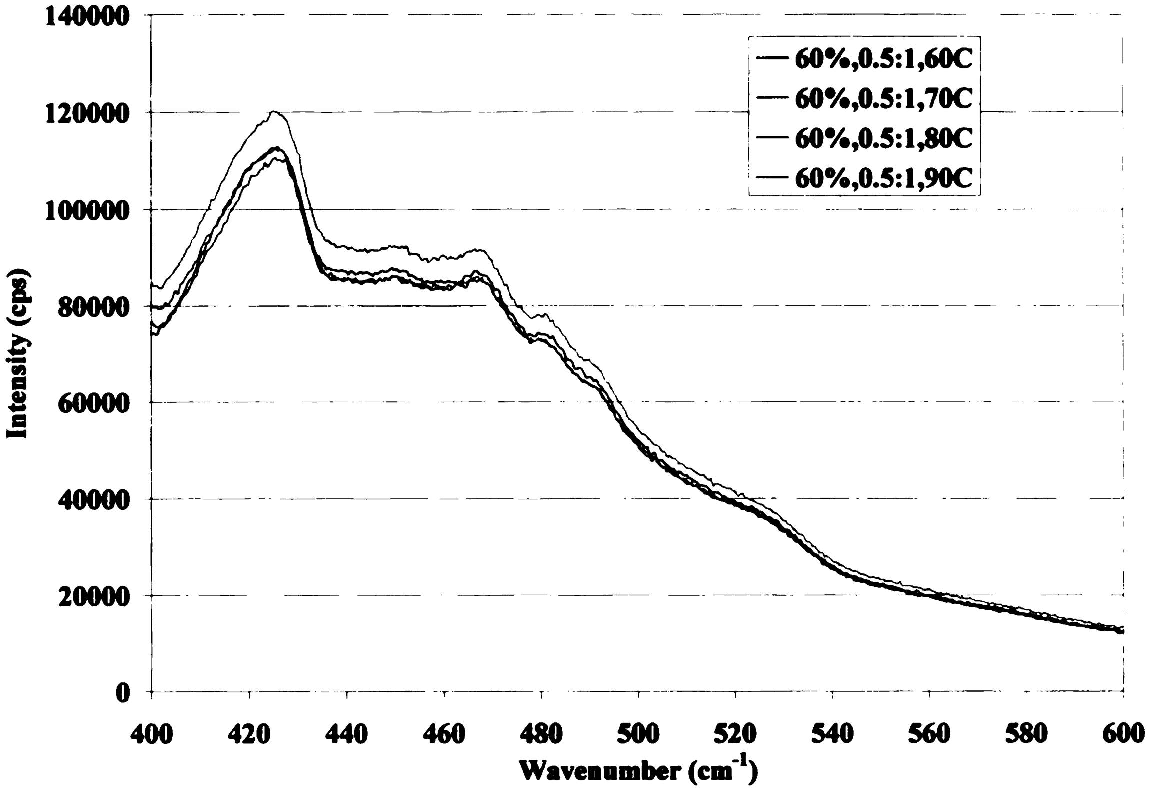

Figure A4.6: AFEX fluorescence results (60%, 0.5:1, 60-90C)

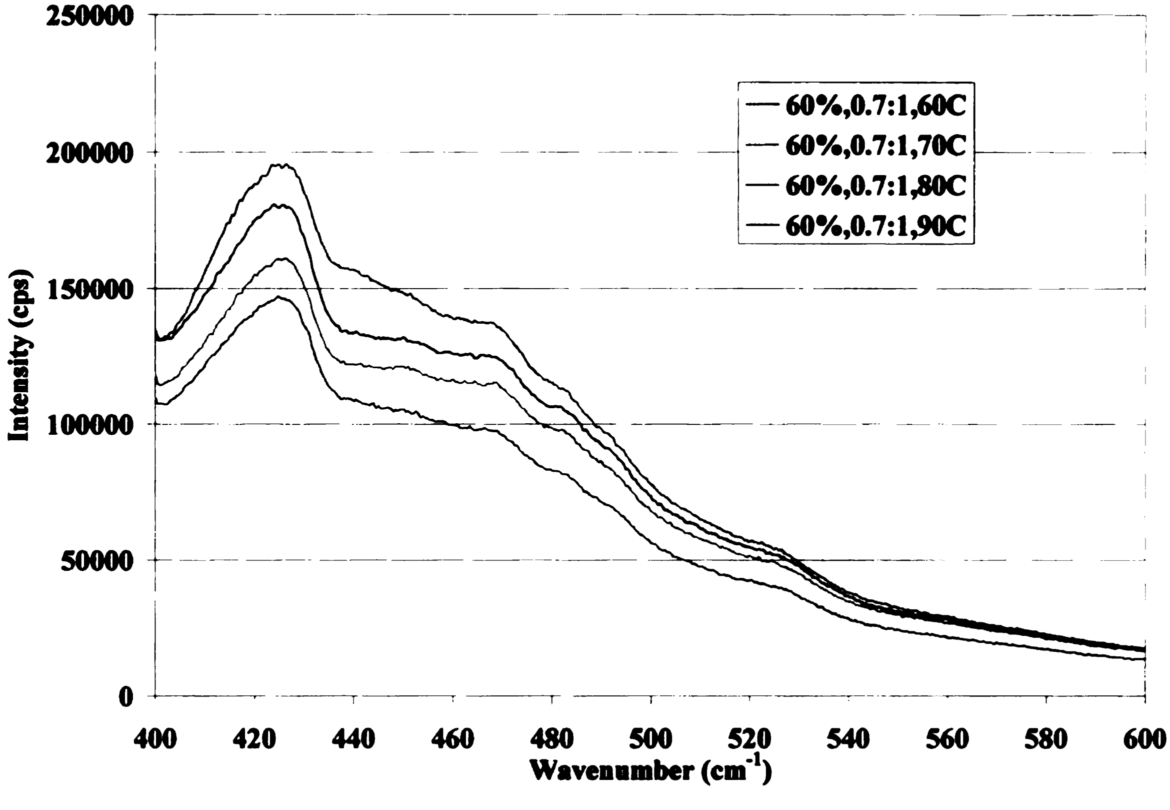

Figure A4.7: AFEX fluorescence results (60%, 0.7:1, 60-90C)

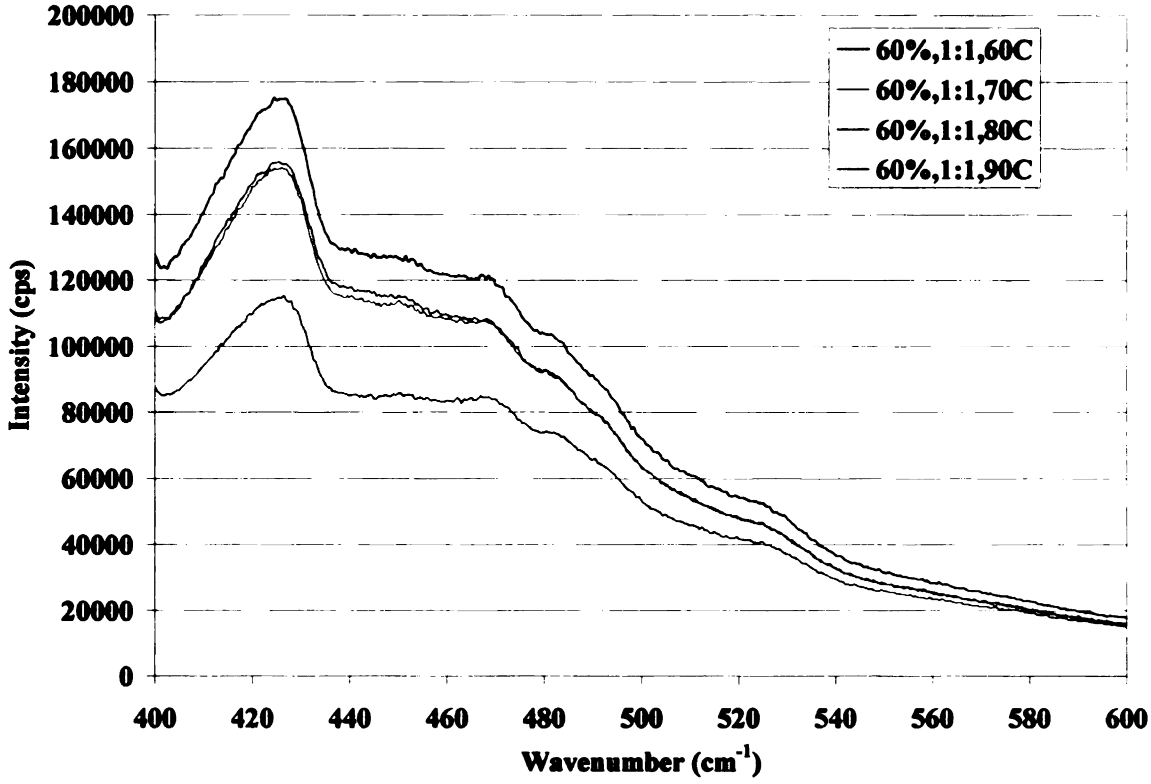

Figure A4.8: AFEX fluorescence results (60%, 1:1, 60-90C)

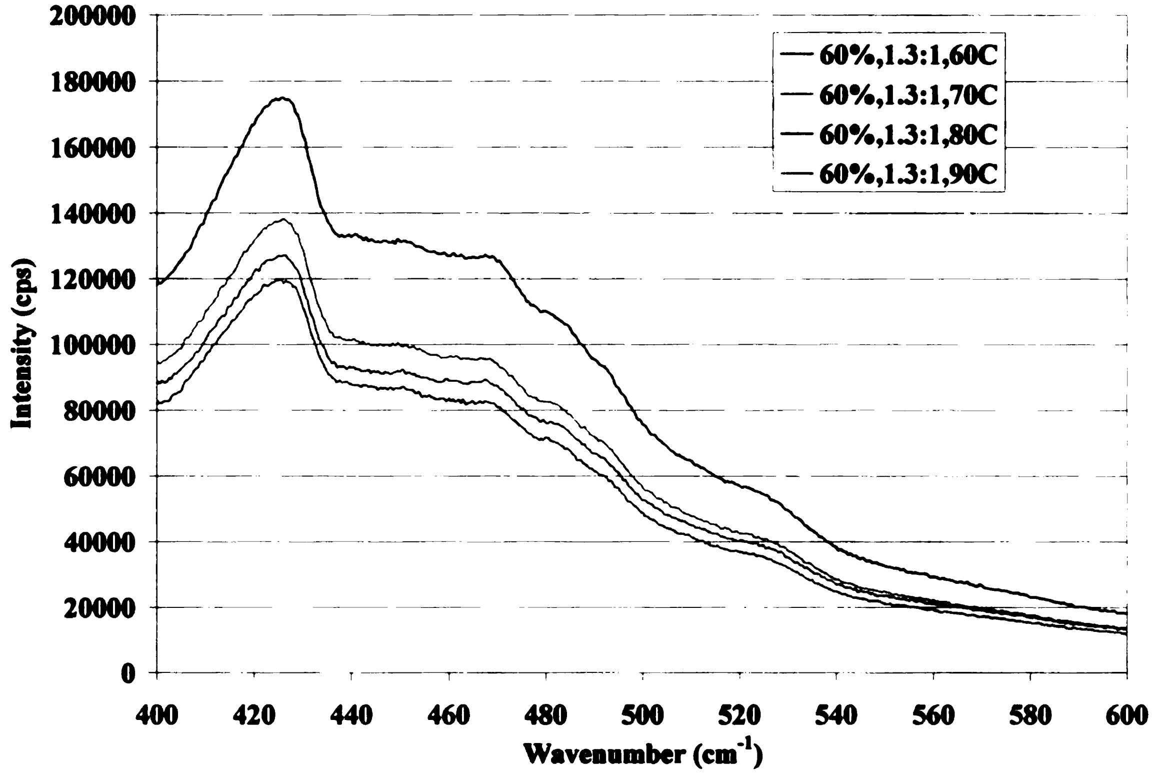

Figure A4.9: AFEX fluorescence results (60%, 1.3:1, 60-90C)

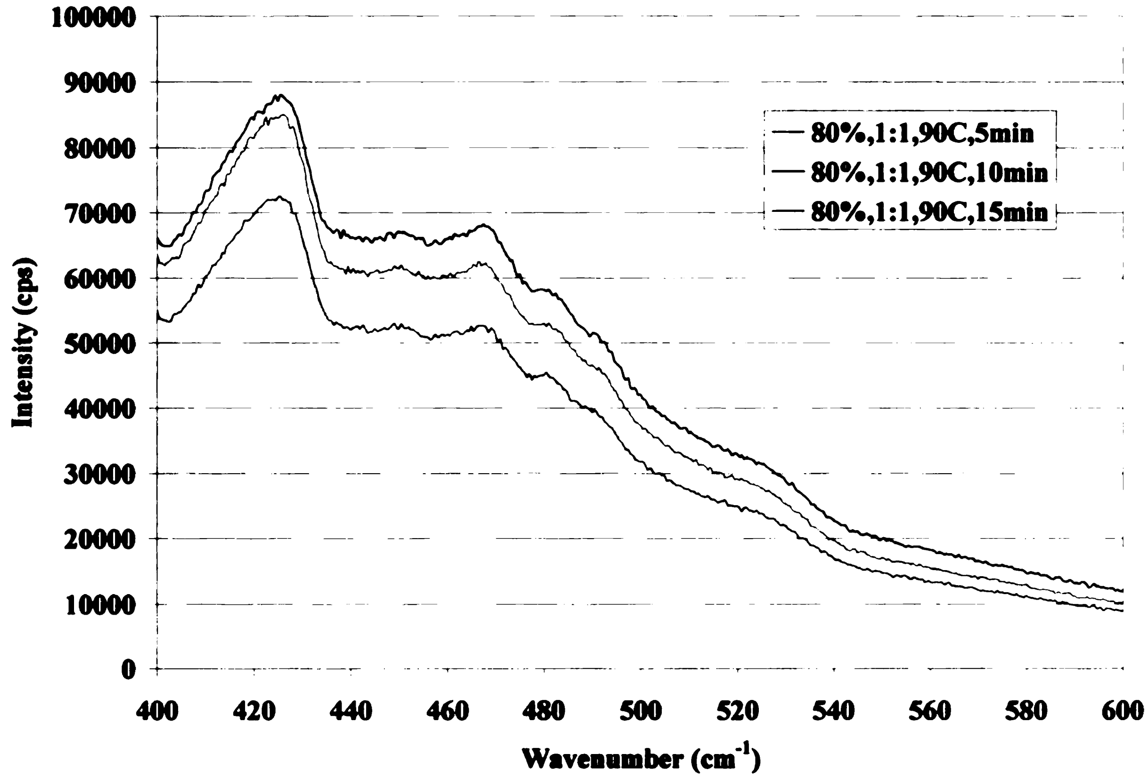

Figure A4.10: AFEX fluorescence results (80%, 1:1, 90C, 5-15min)

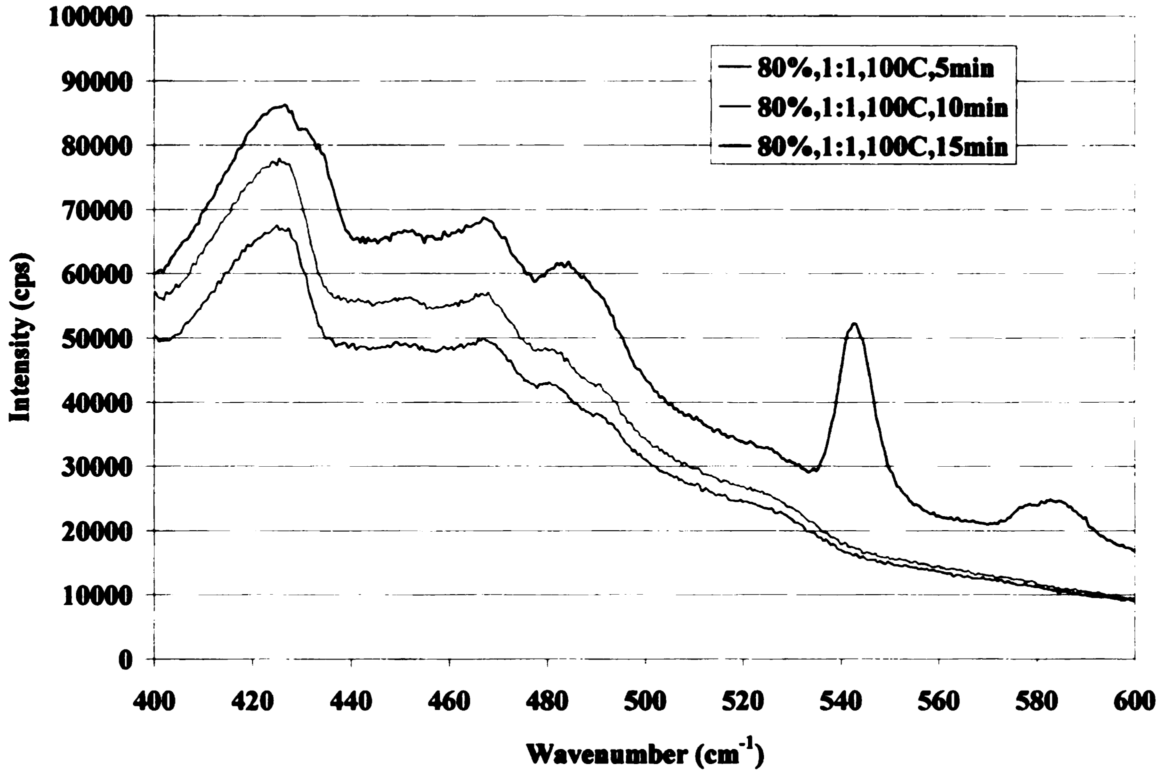

Figure A4.11: AFEX fluorescence results (80%, 1:1, 100C, 5-15min)

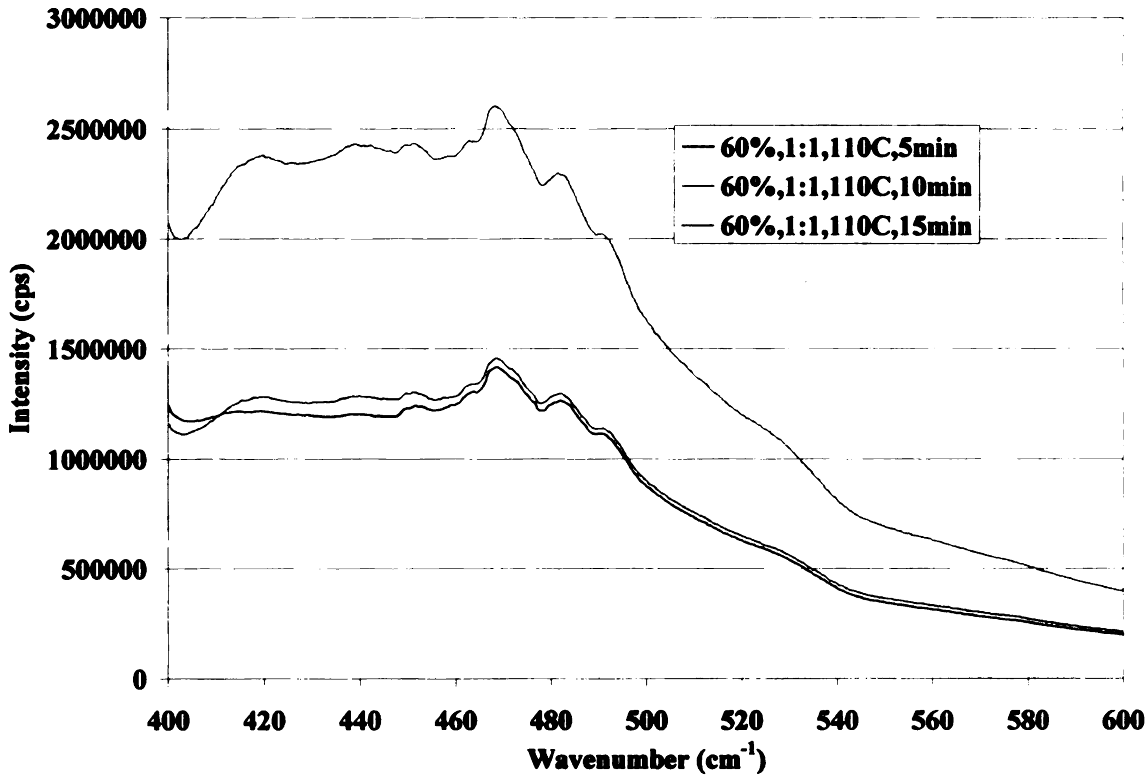

Figure A4.12: AFEX fluorescence results (60%, 1:1, 110C, 5-15min)

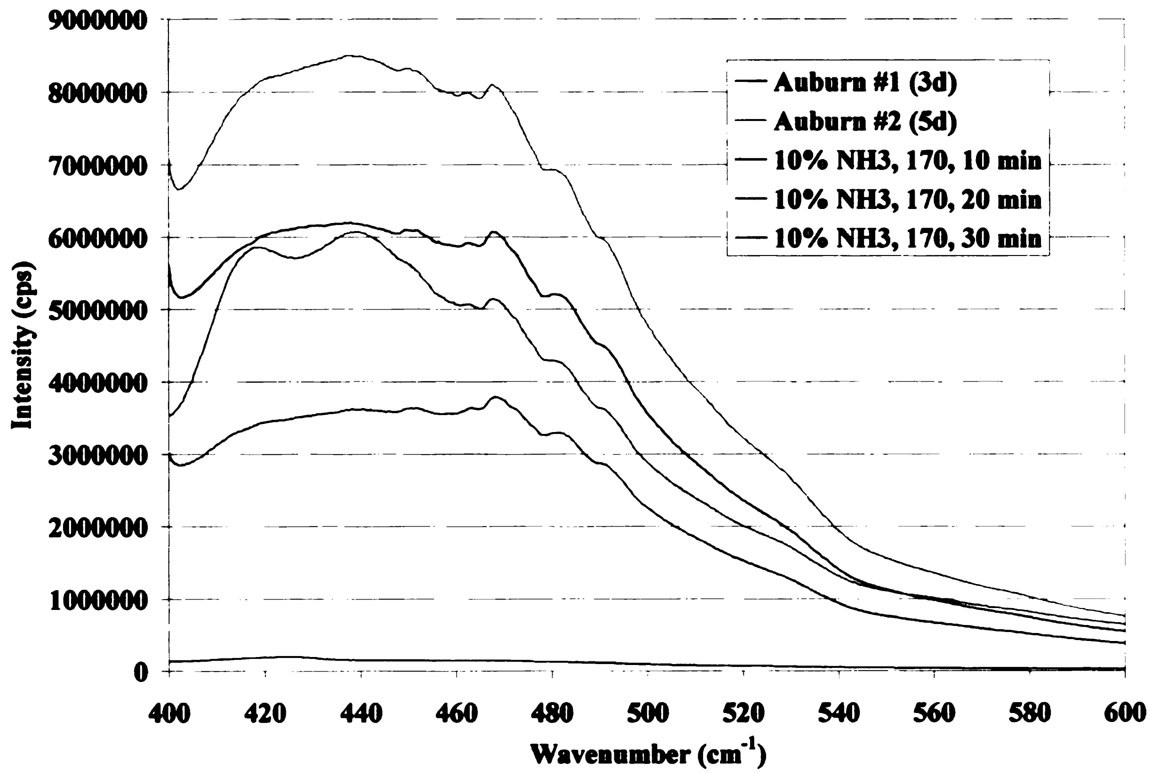

Figure A4.13: ARP fluorescence results

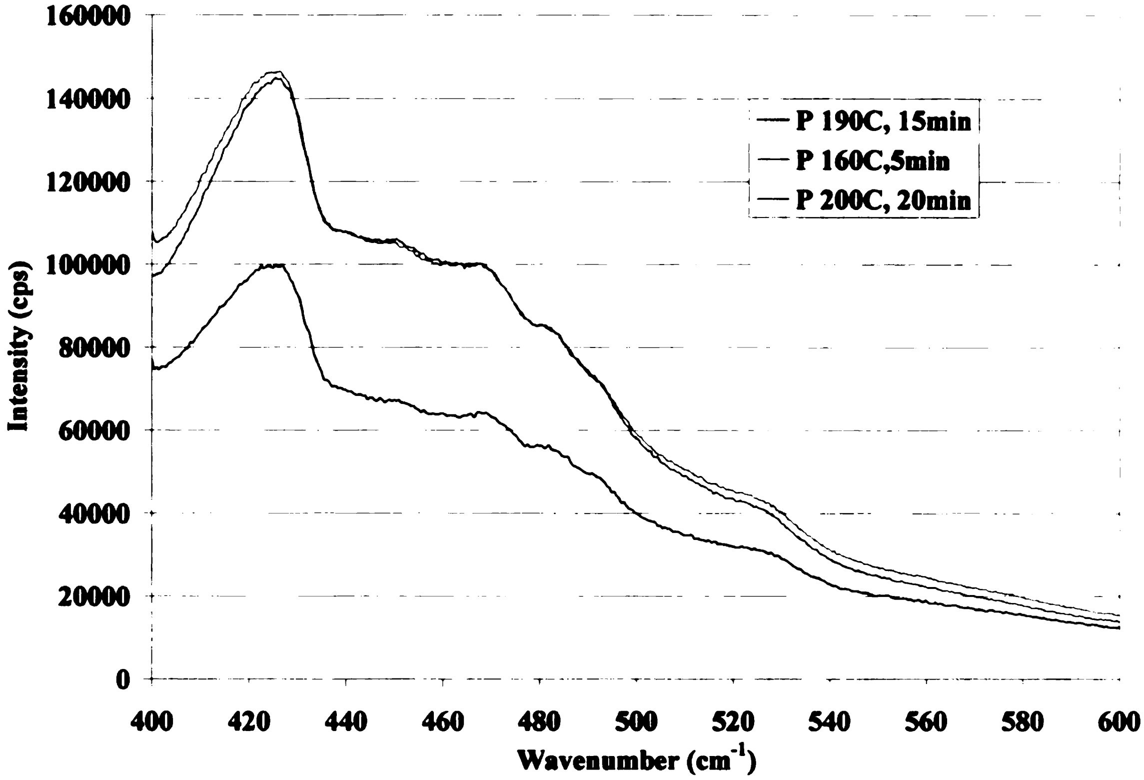

Figure A4.14: Controlled pH fluorescence results

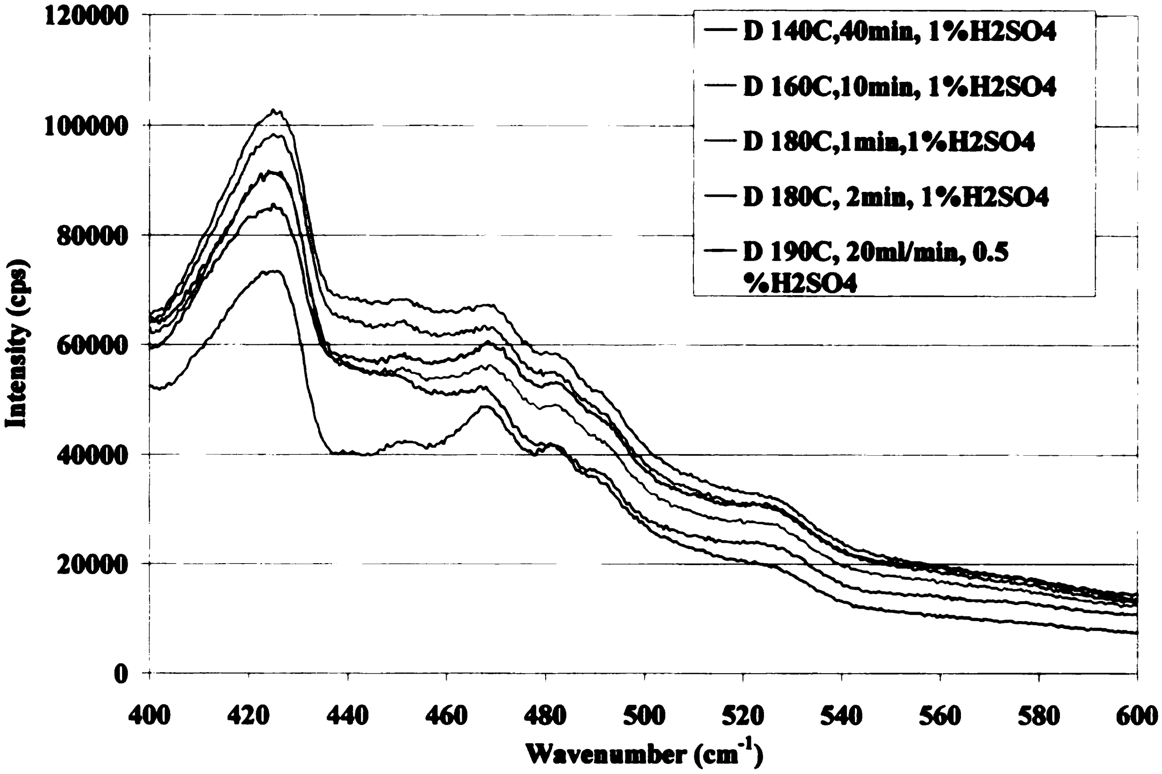

Figure A4.15: Dilute acid fluorescence results

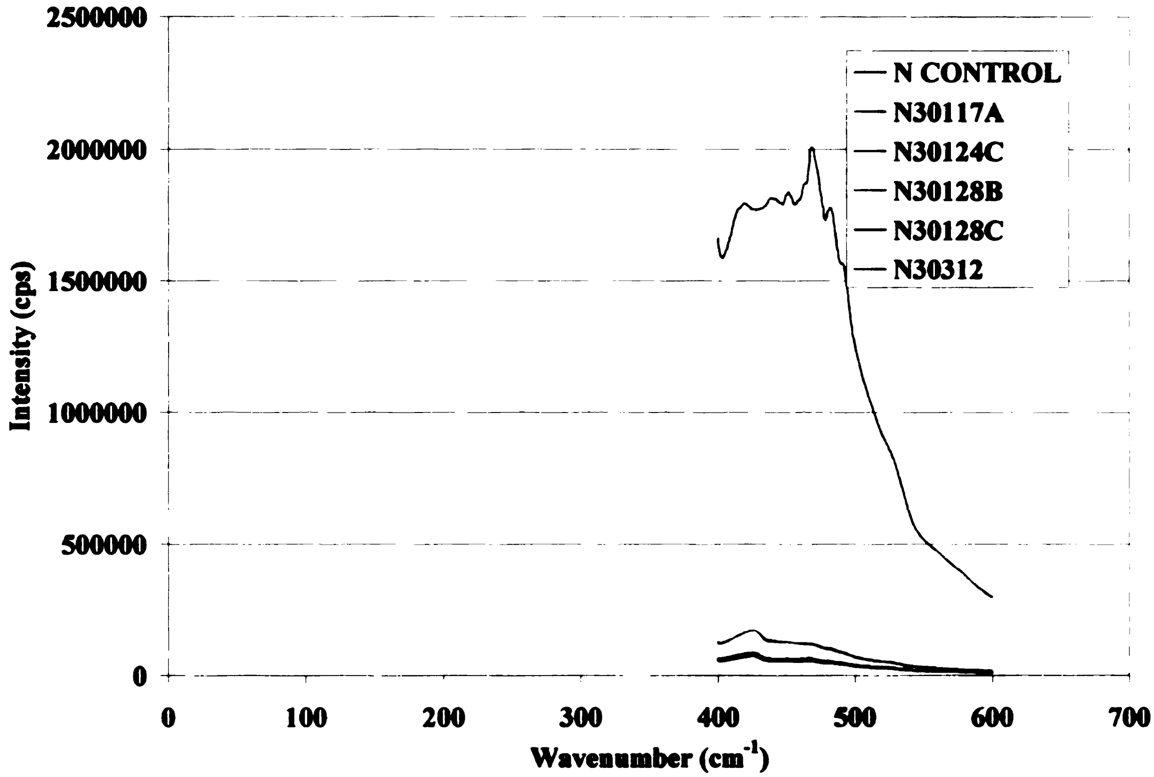

Figure A4.16: NREL samples fluorescence results

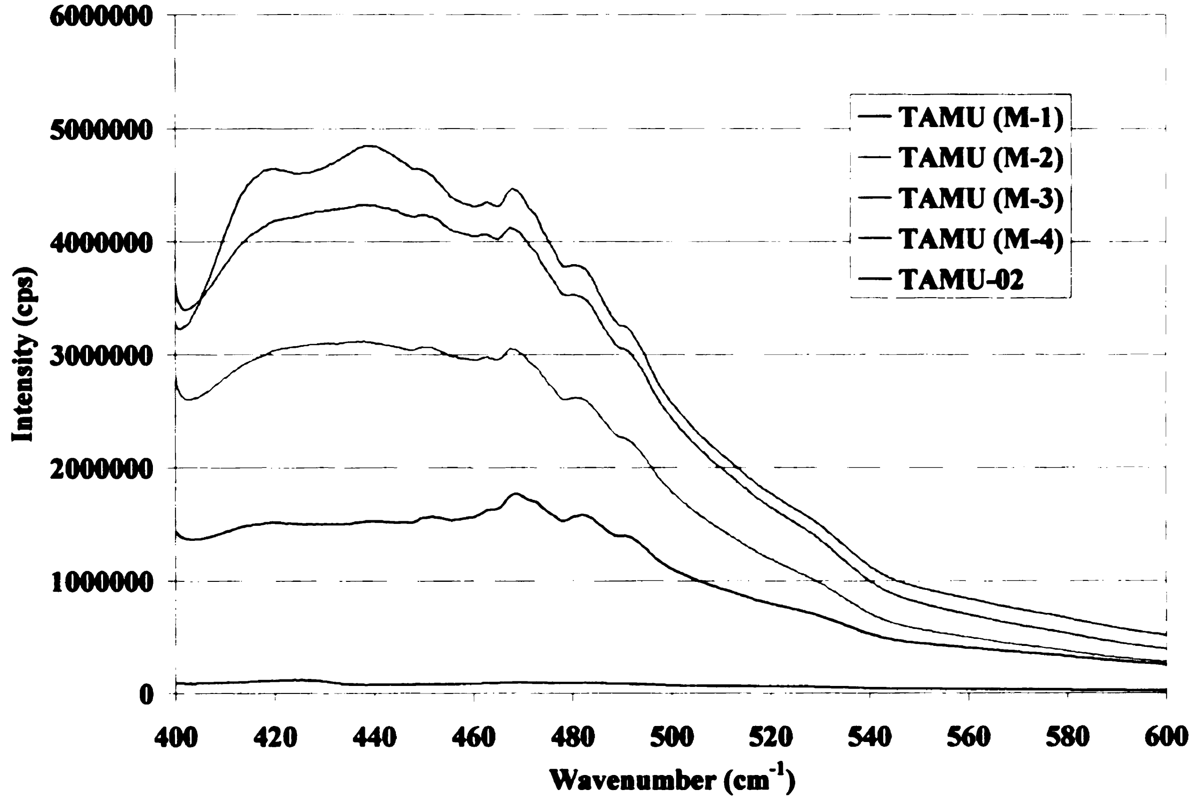

Figure A4.17: Lime treated samples fluorescence results

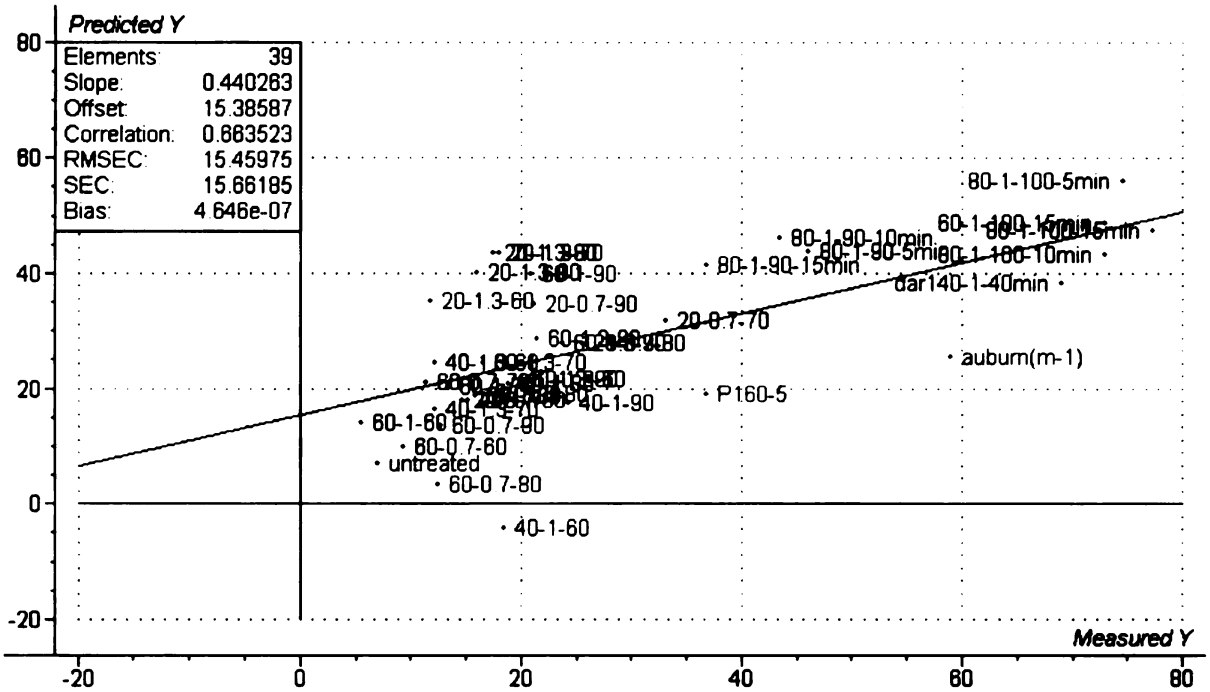

Figure A4.18: PCR initial rate model using fluorescence data.

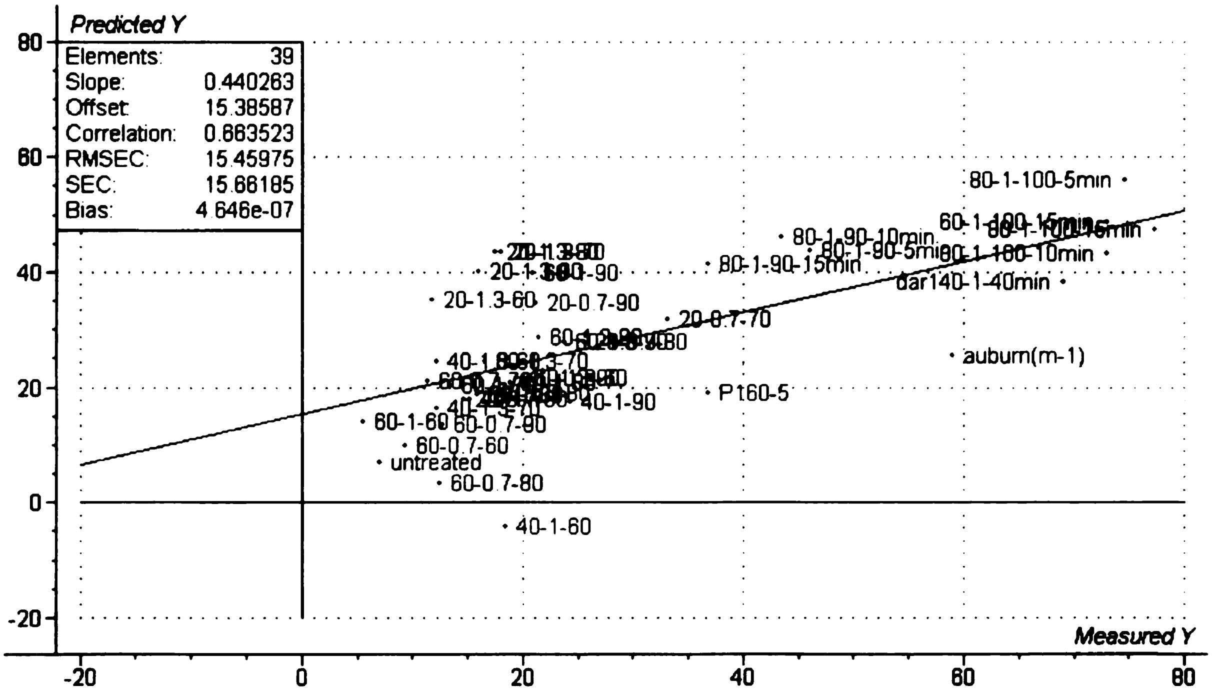

Figure A4.19: PCR 72-hr model using fluorescence data.

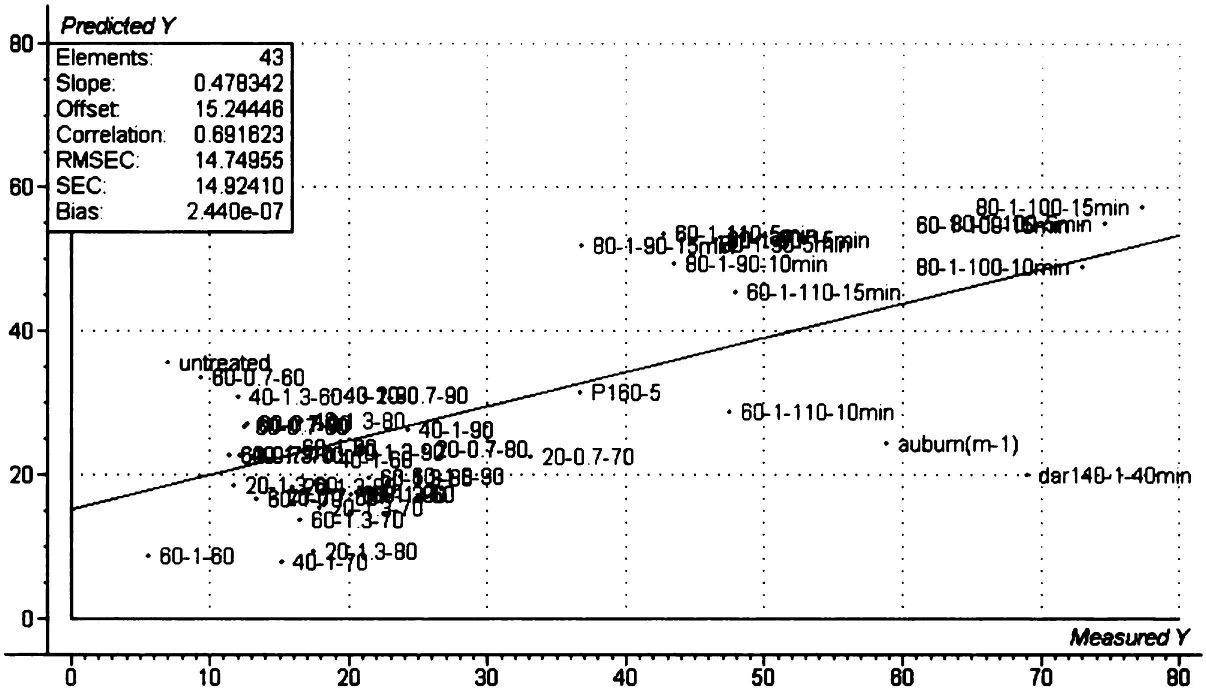

Figure A4.20: PCR initial rate model using XRD data

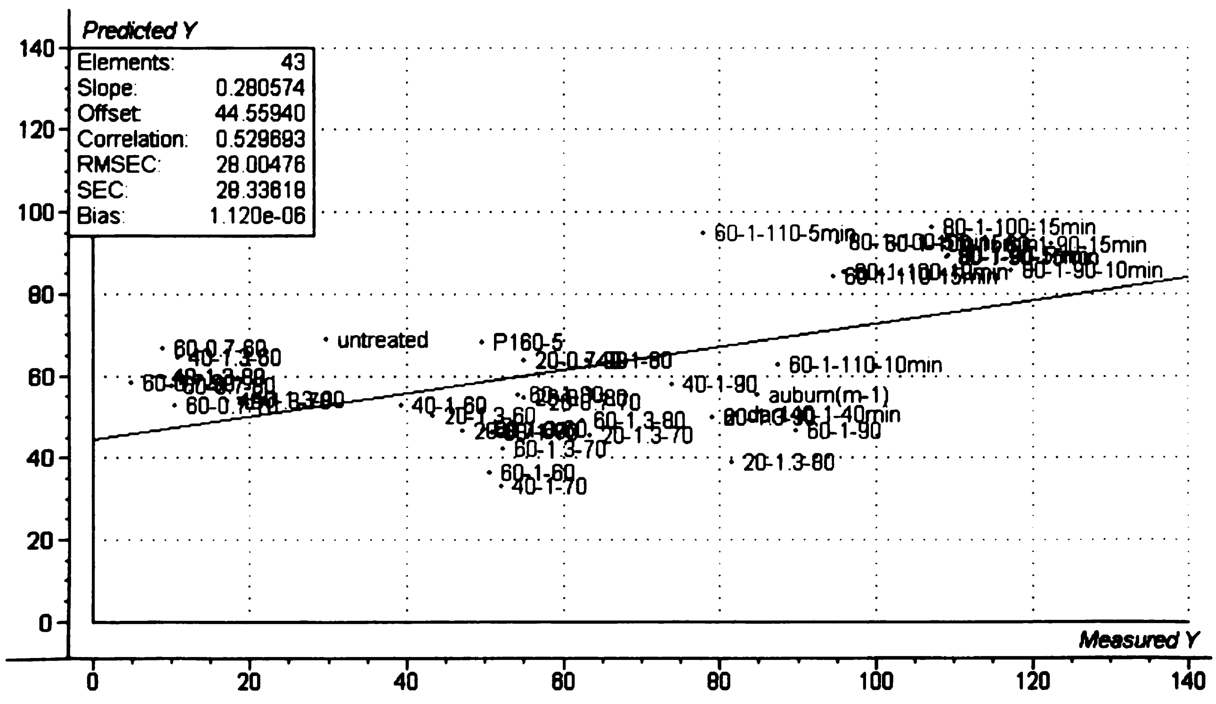

Figure A4.21: PCR 72-hr model using XRD data

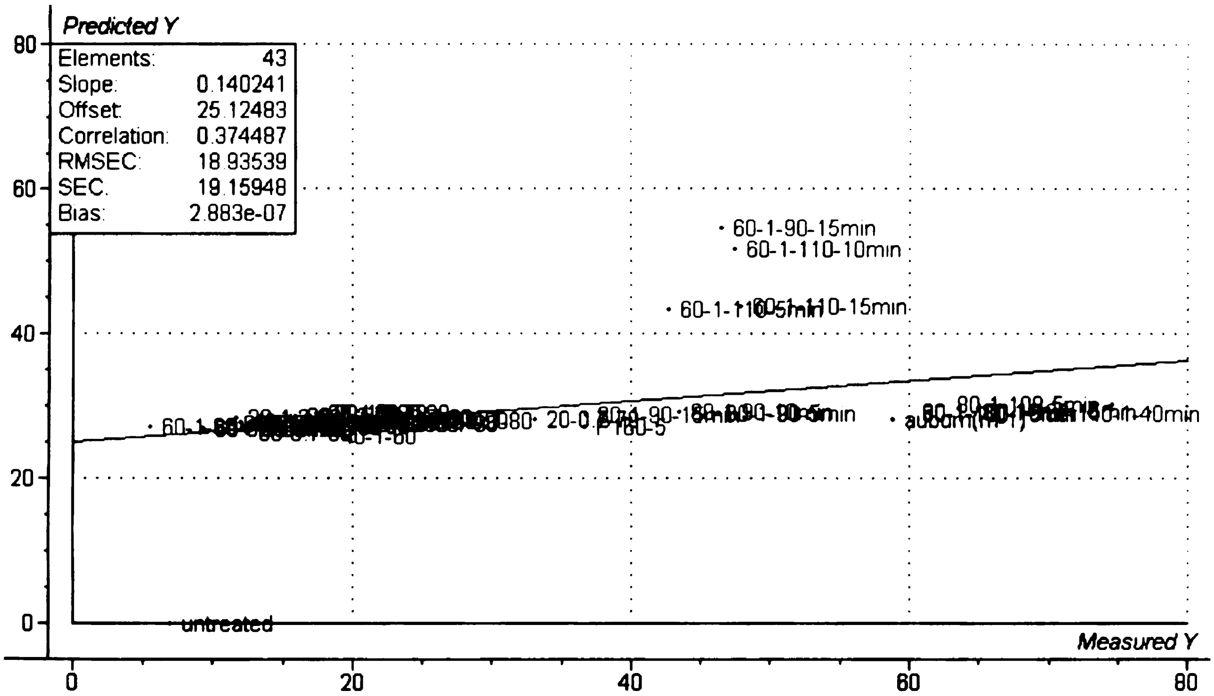

Figure A4.22: PCR initial rate model using DRIFT and fluorescence data

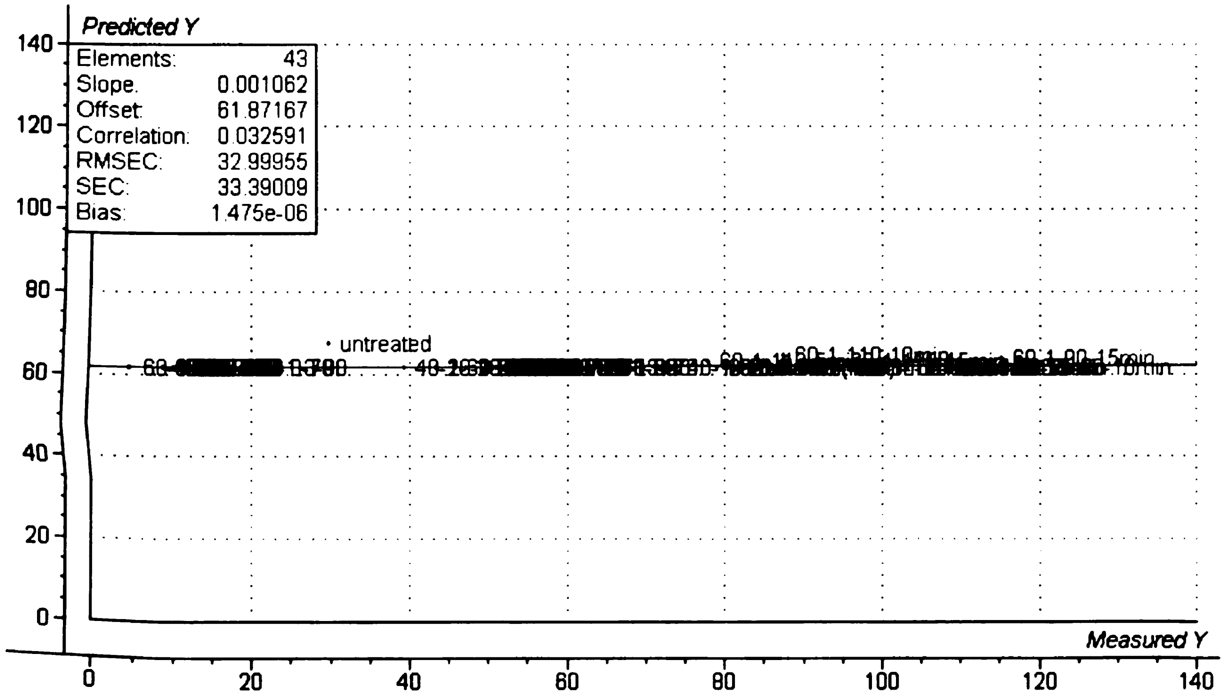

Figure A4.23: PCR 72-hr model using DRIFT and fluorescence data

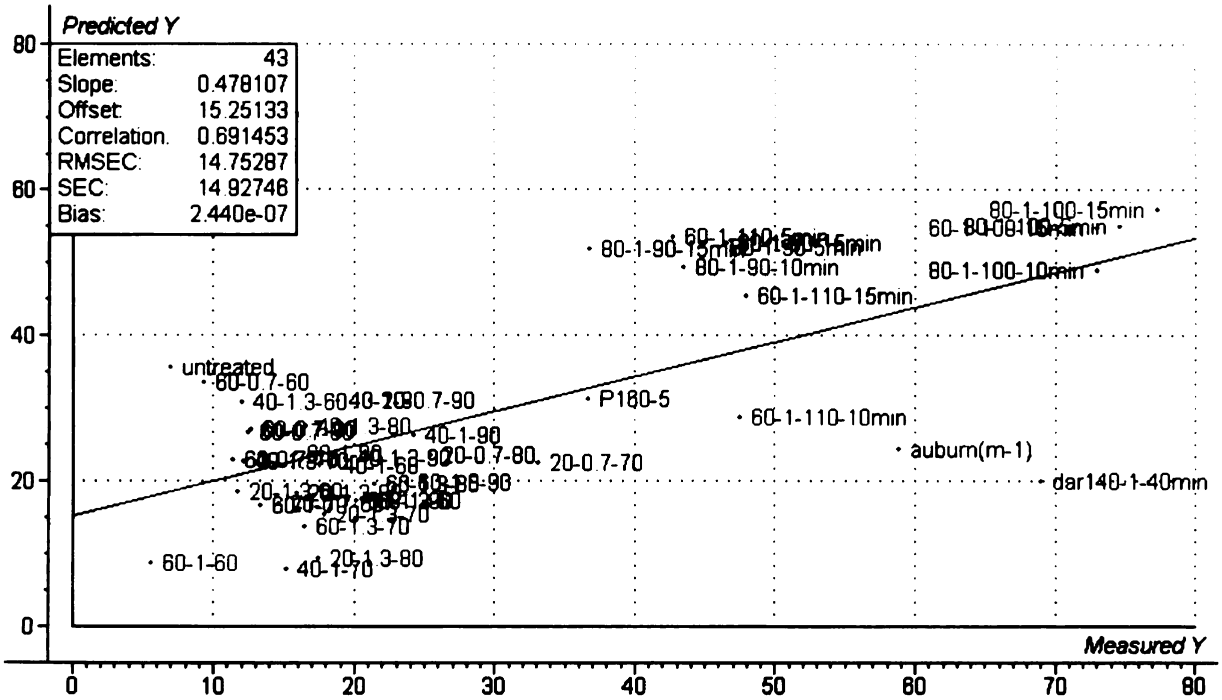

Figure A4.24: PCR initial rate model using DRIFT and XRD data

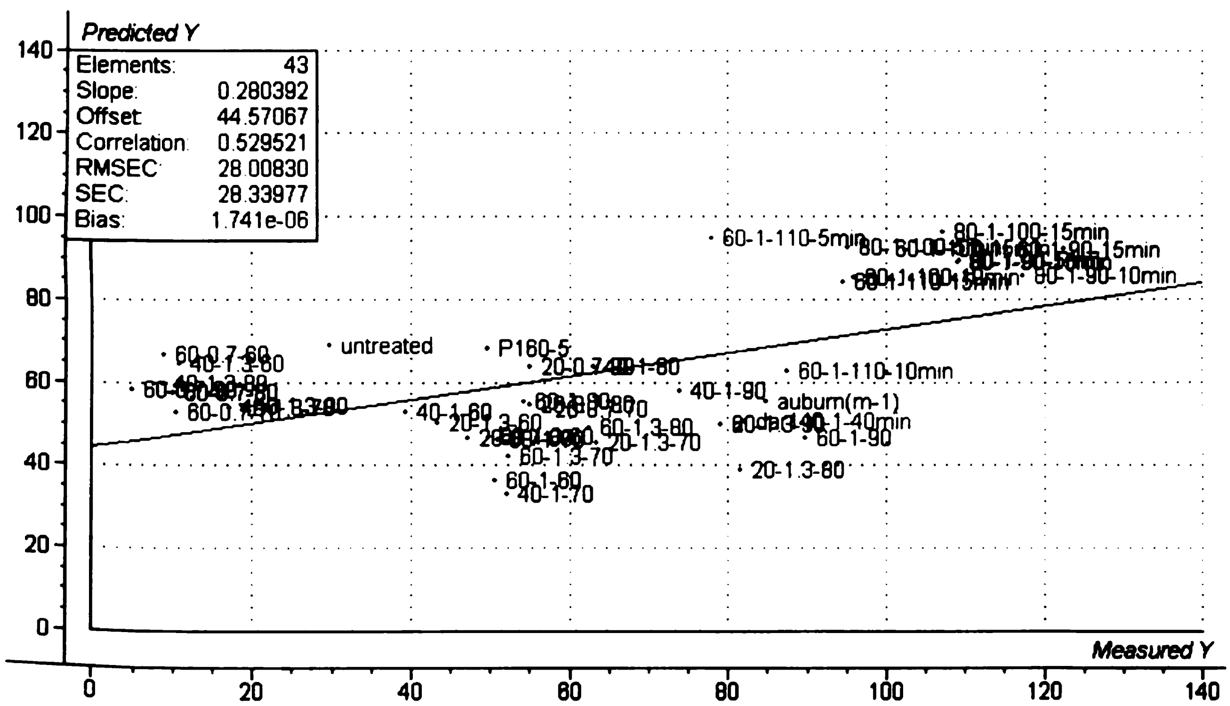

Figure A4.25: PCR 72-hr model using DRIFT and XRD data

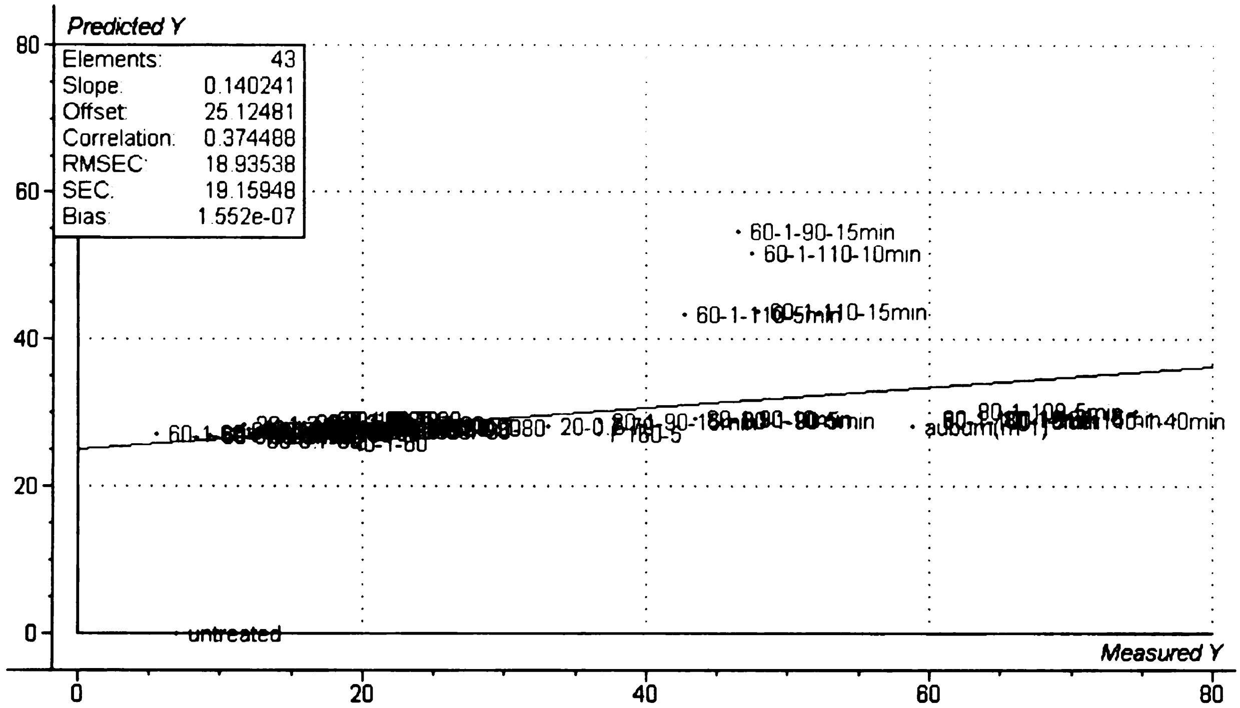

Figure A4.26: PCR initial rate model using fluorescence and XRD data

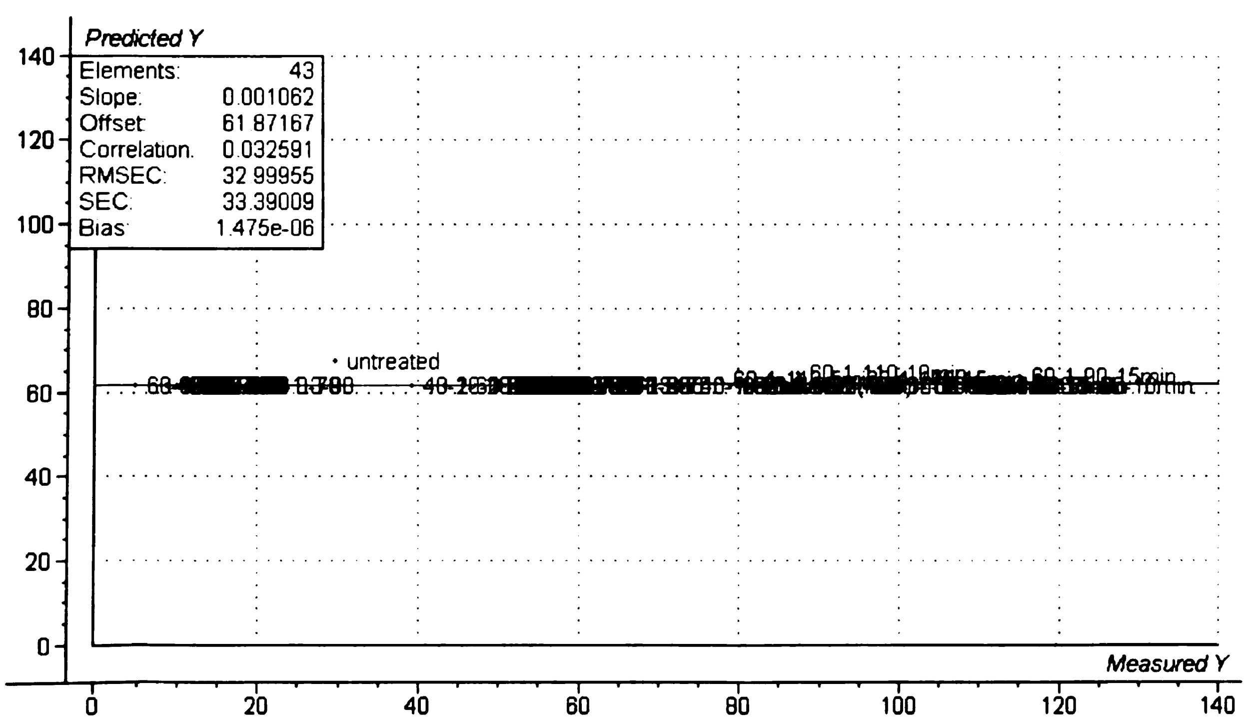

Figure A4.27: PCR 72-hr model using fluorescence and XRD data

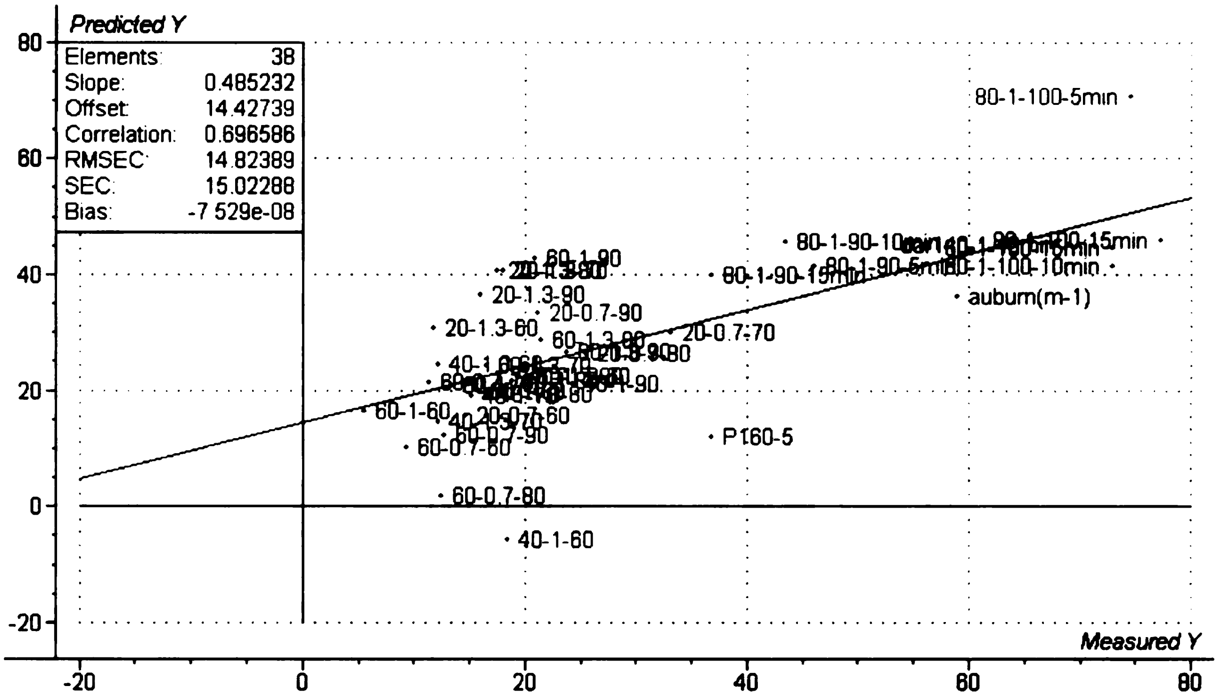

Figure A4.28: PCR initial rate model using DRIFT, fluorescence and XRD data

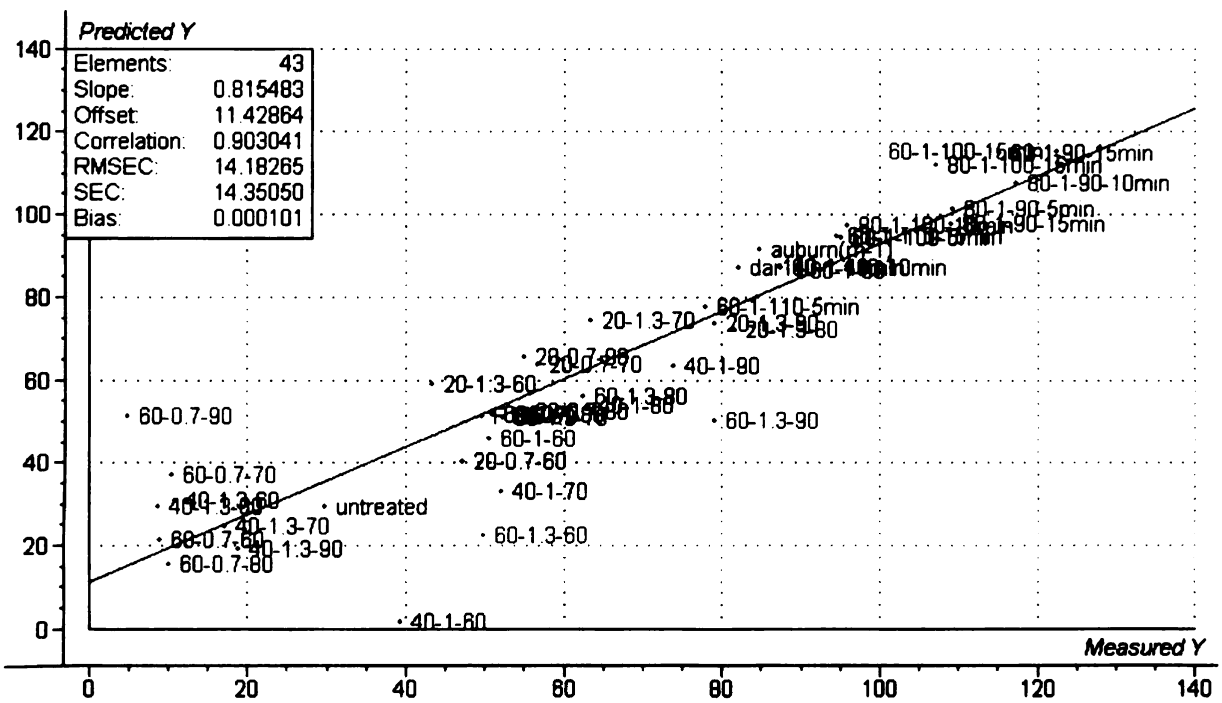

Figure A4.29: PCR 72-hr model using DRIFT, fluorescence and XRD data

Appendix 5

Table A5.1: Crystallinity Index for TAMU poplar samples

Sample	**Crystallinity Index (%)**
DL0-DA00-DC0	35.91
DL0-DA007-DC0	48.12
DL0-DA15-DC0	50.55
DL0-DA35-DC0	44.12
DL0-DA55-DC0	12.82
DL0-DA75-DC0	52.05
DL0-DA150-DC0	59.17
DL01-DA00-DC0	47.70
DL01-DA07-DC0	39.58
DL01-DA15-DC0	55.72
DLO1-DA35-DC0	52.73
DL01-DA55-DC0	50.24
DL01-DA75-DC0	36.08
DL01-DA150-DC0	55.47
DL02-DA0-DC0	37.81
DL02-DA07-DC0	26.25
DL02-DA15-DC0	54.73
DL02-DA35-DC0	50.39
DL02-DA55-DC0	56.05
DL02-DA75-DC0	52.33
DL02-DA150-DC0	58.76
DL03-DA0-DC0	53.85
DL03-DA07-DC0	42.17
DL03-DA15-DC0	47.26
DL03-DA35-DC0	48.01
DL03-DA55-DC0	39.78
DL03-DA75-DC0	56.92
DL03-DA150-DC0	58.80

Table A5.1 (cont'd)

Sample	Crystallinity Index (%)
DL5-DA0-DC0	31.66
DL05-DA007-DC0	41.78
DL5-DA15-DC0	46.51
DL05-DA035-DC0	44.31
DL5-DA55-DC0	45.85
DL05-DA075-DC0	38.90
DL5-DA150-DC0	60.10
DL10-DA0-DC0	29.88
DL10-DA7-DC-0	45.45
DL10-DA15-DC0	35.92
DL10-DA55-DC0	39.31
DL10-DA75-DC0	34.33
DL10-DA150-DC0	48.69
DL50-DA0-DC0	50.60
DL50-DA07-DC0	50.59
DL50-DA15-DC0	54.32
DL50-DA35-DC0	55.00
DL50-DA55-DC0	52.98
DL50-DA75-DC0	51.21
DL50-DA150-DC0	55.56
DL0-DA0-DC3	22.95
DL0-DA7-DC3	24.62
DL0-DA15-DC3	21.22
DL0-DA150-DC3	22.15

Table A5.1 (cont'd)

Sample	Crystallinity Index (%)
DL1-DA0-DC3	24.48
DL1-DA7-DC3	25.67
DL1-DA15-DC3	26.75
DL1-DA35-DC3	22.51
DL1-DA55-DC3	20.68
DL1-DA75-DC3	16.03
DL1-DA150-DC3	21.16
DL2-DA0-DC3	11.07
DL2-DA7-DC3	22.39
DL2-DA15-DC3	23.34
DL2-DA35-DC3	23.53
DL2-DA55-DC3	22.17
DL2-DA75-DC3	21.76
DL2-DA150-DC3	23.52
DL3-DA0-DC3	18.30
DL3-DA7-DC3	24.96
DL3-DA15-DC3	24.77
DL3-DA35-DC3	24.80
DL3-DA55-DC3	24.73
DL3-DA75-DC3	28.99
DL3-DA150-DC3	20.10
DL5-DA0-DC3	19.47
DL5-DA07-DC3	26.14
DL5-DA15-DC3	21.61
DL5-DA35-DC3	23.13
DL5-DA55-DC3	16.99
DL5-DA75-DC3	24.85
DL5-DA150-DC3	17.62

Table A5.1 (cont'd)

Sample	Crystallinity Index (%)
DL10-DA0-DC3	19.85
DL10-DA07-DC3	16.75
DL10-DA15-DC3	17.13
DL10-DA35-DC3	26.67
DL10-DA55-DC3	23.75
DL10-DA75-DC3	14.76
DL10-DA150-DC3	19.26
DL50-DA0-DC3	25.77
DL50-DA7-DC3	37.04
DL50-DA15-DC3	41.24
DL50-DA35-DC3	35.87
DL50-DA55-DC3	37.13
DL50-DA75-DC3	31.26
DL0-DA7-DC6	19.39
DL0-DA15-DC6	67.83
DL0-DA35-DC6	21.46
DL0-DA55-DC6	14.57
DL0-DA75-DC6	14.53
DL0-DA150-DC6	20.12
DL1-DA0-DC6	15.63
DL1-DA15-DC6	18.10
DL1-DA35-DC6	18.05
DL1-DA55-DC6	23.16
DL1-DA150-DC6	15.07

Table A5.1 (cont'd)

Sample	Crystallinity Index (%)
DL2-DA7-DC6	12.06
DL2-DA35-DC6	24.68
DL2-DA75-DC6	23.33
DL2-DA150-DC6	10.62
DL3-DA0-DC6	17.11
DL3-DA07-DC6	23.36
DL3-DA15-DC6	13.71
DL3-DA35-DC6	14.12
DL3-DA55-DC6	18.45
DL3-DA75-DC6	15.22
DL3-DA150-DC6	26.00
DL5-DA0-DC6	8.47
DL5-DA7-DC6	22.32
DL5-DA15-DC6	13.89
DL5-DA35-DC6	17.89
DL5-DA75-DC6	15.08
DL10-DA0-DC6	18.23
DL10-DA15-DC6	13.01
DL10-DA55-DC6	21.68
DL10-DA150-DC6	15.25
DL50-DA0-DC6	10.37
DL50-DA07-DC6	13.35
DL50-DA35-DC6	11.84
DL50-DA75-DC6	17.58
DL50-DA150-DC6	32.13

Table A5.2: MLR model coefficients for poplar usingRaman, DRIFT and XRD data

	Initial Rate B-coefficients	72 hr Conversion B-coefficients
Intercept	16.9030	81.2270
CrI	-0.1930	-0.1360
Raman (1038.9)	-0.0005	-0.0016
Raman (1293.3)	0.0039	0.0094
Raman (1369.5)	-0.0097	-0.0161
Raman (1399.5)	0.0055	0.0068
Raman (1445.1)	0.0009	0.0018
Raman (2888.7)	-0.0022	-0.0038
Raman (2919.6)	0.0020	0.0032
Amorphous cellulose (902.54)	0.0000	0.0000
Lignin 1(1504.23)	2.8130	7.9840
Lignign 2(1596.8)	-0.9670	-13.7100
Aldehyde (1650.79)	-2.3570	0.7890
Ester carbonyl (1735.65)	7.1900	14.0580
C-H (2900.46)	-2.0340	-2.8540
O-H (3394.16)	-6.0690	-5.4140

Table A5.3: PCR model coefficients for poplar using DRIFT data

	Initial Rate						
	Amorphous Cell (902.54)	Lignin 1511.94	Lignin 1604.51	Aldehyde 1658.51	Ester Carbonyl 1712.51	C-H 2915.89	O-H 3417.3
PC_01 (X-Vars + Interactions)	0.0009	0.0004	0.0005	0.0008	0.0013	0.0017	0.0043
PC_02 (X-Vars + Interactions)	-0.0247	-0.0453	-0.0400	-0.0324	-0.0233	-0.0643	0.0276
PC_03 (X-Vars + Interactions)	-0.0275	-0.0575	-0.0462	-0.0357	-0.0372	-0.0596	0.0384
PC_04 (X-Vars + Interactions)	-0.0253	-0.0170	0.0178	-0.0128	-0.1190	-0.0628	0.0309
PC_05 (X-Vars + Interactions)	-0.0008	0.1290	0.1280	0.0456	-0.0605	-0.1480	-0.0004
PC_06 (X-Vars + Interactions)	0.0339	0.0361	0.0283	0.0105	-0.1560	-0.1640	-0.1050
PC_07 (X-Vars + Interactions)	0.0990	-0.0612	-0.0330	0.0376	-0.0824	-0.2160	-0.1690
PC_08 (X-Vars + Interactions)	0.1110	-0.0554	-0.0414	0.0272	-0.0993	-0.2230	-0.1590
PC_09 (X-Vars + Interactions)	0.1260	-0.1710	-0.0137	0.0662	-0.0684	-0.2160	-0.2950
PC_10 (X-Vars + Interactions)	0.1270	-0.1880	0.0011	0.0847	-0.0267	-0.2330	-0.2160
PC_11 (X-Vars + Interactions)	0.1280	-0.1900	0.0019	0.0854	-0.0254	-0.2340	-0.2140
PC_12 (X-Vars + Interactions)	0.1250	-0.1720	0.0059	0.0918	-0.0231	-0.2430	-0.2570
PC_13 (X-Vars + Interactions)	0.1240	-0.2120	0.0489	0.1750	0.0132	-0.2580	-0.1490
PC_14 (X-Vars + Interactions)	0.1210	-0.2020	0.0175	0.1960	0.0357	-0.2830	-0.1630
PC_15 (X-Vars + Interactions)	0.1300	-0.1190	-0.0349	0.1790	0.0307	-0.2800	-0.1300
PC_16 (X-Vars + Interactions)	0.1260	-0.1100	-0.0180	0.1800	0.0310	-0.2940	-0.1440
PC_17 (X-Vars + Interactions)	0.1480	-0.0949	-0.0892	0.1060	0.0285	-0.3220	-0.0875
PC_18 (X-Vars + Interactions)	0.1410	-0.3590	-0.1630	0.3110	-0.2580	-0.4450	0.1290
PC_19 (X-Vars + Interactions)	0.1580	-0.3900	-0.1530	0.3310	-0.2140	-0.4070	0.2140
PC_20 (X-Vars + Interactions)	0.1140	-0.3850	-0.2200	0.2710	-0.3840	-0.5290	0.2920
	72 hr conversion						
	Amorphous Cell (902.54)	Lignin 1511.94	Lignin 1604.51	Aldehyde 1658.51	Ester Carbonyl 1712.51	C-H 2915.89	O-H 3417.3
PC_01 (X-Vars + Interactions)	0.0048	0.0021	0.0028	0.0040	0.0057	0.0087	0.0241
PC_02 (X-Vars + Interactions)	-0.0362	-0.0697	-0.0614	-0.0492	-0.0403	-0.0975	0.0983
PC_03 (X-Vars + Interactions)	-0.0612	-0.1730	-0.1130	-0.0775	-0.1240	-0.0632	0.2080
PC_04 (X-Vars + Interactions)	-0.0657	-0.2480	-0.2310	-0.1200	-0.0157	-0.0579	0.2160
PC_05 (X-Vars + Interactions)	-0.0516	-0.1610	-0.1670	-0.0864	0.0077	-0.1050	0.2180
PC_06 (X-Vars + Interactions)	0.0413	-0.4100	-0.4380	-0.1850	-0.1580	-0.1460	0.0130
PC_07 (X-Vars + Interactions)	0.2880	-0.7700	-0.6790	-0.0934	0.1370	-0.3520	-0.0806
PC_08 (X-Vars + Interactions)	0.3840	-0.7250	-0.7460	-0.1750	0.0523	-0.4050	-0.0029
PC_09 (X-Vars + Interactions)	0.4550	-1.3040	-0.5410	0.0974	0.1810	-0.5250	0.0271
PC_10 (X-Vars + Interactions)	0.6430	-2.7840	-0.3450	0.3550	0.1640	-0.5400	0.3020
PC_11 (X-Vars + Interactions)	0.6860	-2.8640	-0.5780	0.1550	0.0088	-0.1480	-0.0100
PC_12 (X-Vars + Interactions)	0.6620	-2.8480	-0.4200	0.5660	0.3210	-0.3080	-0.2350
PC_13 (X-Vars + Interactions)	0.6660	-2.8800	-0.3650	0.5420	0.2770	-0.2870	-0.4740
PC_14 (X-Vars + Interactions)	0.6660	-2.8790	-0.3660	0.5420	0.2780	-0.2860	-0.4750
PC_15 (X-Vars + Interactions)	0.7110	-2.9870	-0.5350	0.5300	0.2860	-0.1500	-0.5050
PC_16 (X-Vars + Interactions)	0.6590	-3.0190	-0.3660	0.7030	0.2960	-0.1330	0.2450
PC_17 (X-Vars + Interactions)	0.6210	-4.5210	-0.7970	1.8630	-0.3850	-0.5920	-1.6050
PC_18 (X-Vars + Interactions)	0.6810	-4.6240	-0.7500	1.9350	-0.3490	-0.4230	-1.2980
PC_19 (X-Vars + Interactions)	0.6470	-4.6340	-0.8020	1.9050	-0.3490	-0.4860	-0.9610
PC_20 (X-Vars + Interactions)	0.6960	-4.5340	-0.7960	1.7500	-0.5910	-0.5610	-1.0650

Table A5.4: MLR Raw Data for poplar Unscrambler Modeling

Samples	Initial rate Conversion	72 hrs Conversion	CrI	Raman (1038.9)	Raman (1293.3)	Raman (1369.5)	Raman (1399.5)	Raman (1445.1)	Raman (2888.7)	Raman (2919.6)
DL000-DA00-DC0	1.4821248	10.04119	35.90664	1.31E+04	1.26E+04	1.25E+04	1.25E+04	1.22E+04	6.30E+03	6.17E+03
DL000-DA007-DC0	2.1774251	10.92	48.11784	2.35E+05	2.19E+05	2.22E+05	2.27E+05	2.13E+05	1.00E+05	9.35E+04
DL00-DA015-DC0	1.3160888	9.520001	50.5508	4.29E+05	4.22E+05	4.25E+05	4.31E+05	4.16E+05	1.88E+05	1.79E+05
DL00-DA035-DC0	2.3507454	13.36963	44.11765	3.68E+05	3.15E+05	3.09E+05	3.12E+05	2.95E+05	1.08E+05	1.00E+05
DL00-DA055-DC0	1.7086589	11.09052	12.82051	3.22E+05	2.91E+05	2.90E+05	2.94E+05	2.77E+05	1.03E+05	9.54E+04
DL00-DA075-DC0	3.3196602	15.78108	52.05183	3.60E+05	3.40E+05	3.42E+05	3.47E+05	3.30E+05	1.34E+05	1.27E+05
DL00-DA150-DC0	3.2563374	22.32638	59.1716	6.52E+05	6.50E+05	6.52E+05	6.56E+05	6.38E+05	2.47E+05	2.35E+05
DL01-DA000-DC0	2.1500621	15.79749	47.70318	3.56E+05	3.28E+05	3.26E+05	3.29E+05	3.11E+05	9.29E+04	8.61E+04
DL001-DA007-DC0	2.2849016	13.72189	39.58333	2.68E+05	2.48E+05	2.50E+05	2.55E+05	2.37E+05	7.87E+04	7.25E+04
DL001-DA015-DC0	2.7889709	16.81503	55.72139	2.40E+05	2.22E+05	2.24E+05	2.29E+05	2.12E+05	7.30E+04	6.70E+04
DL001-DA035-DC0	2.6065848	15.40983	52.72727	3.37E+05	3.19E+05	3.19E+05	3.24E+05	3.06E+05	1.05E+05	9.75E+04
DL001-DA055-DC0	4.0460176	25.38489	50.23697	4.29E+05	4.12E+05	4.12E+05	4.16E+05	3.99E+05	1.50E+05	1.42E+05
DL001-DA075-DC0	5.0786853	27.93634	36.07595	2.58E+05	2.45E+05	2.47E+05	2.53E+05	2.37E+05	9.06E+04	8.31E+04
DL001-DA150-DC0	5.6063766	72.39646	55.47368	5.97E+05	5.63E+05	5.57E+05	5.58E+05	5.38E+05	1.78E+05	1.69E+05
DL02-DA000-DC0	3.3391209	19.89745	37.80761	2.84E+05	2.72E+05	2.73E+05	2.78E+05	2.62E+05	8.84E+04	8.01E+04
DL02-DA007-DC0	3.1987064	21.07347	26.25	8.89E+04	8.81E+04	9.46E+04	1.01E+05	8.65E+04	4.03E+04	3.53E+04
DL02-DA015-DC0	4.1924396	24.52341	54.72603	1.72E+05	1.64E+05	1.65E+05	1.68E+05	1.58E+05	5.63E+04	5.13E+04
DL02-DA035-DC0	4.567791	32.47076	50.39164	2.40E+05	2.24E+05	2.24E+05	2.28E+05	2.14E+05	7.26E+04	6.60E+04
DL02-DA055-DC0	5.6471677	37.03661	56.04992	3.38E+05	3.26E+05	3.25E+05	3.29E+05	3.13E+05	1.10E+05	1.02E+05
DL02-DA075-DC0	6.6840892	53.20943	52.33236	3.27E+05	3.14E+05	3.12E+05	3.15E+05	3.03E+05	1.05E+05	9.68E+04
DL02-DA150-DC0	7.5956335	85.02252	58.75764	2.25E+05	2.15E+05	2.17E+05	2.22E+05	2.07E+05	7.25E+04	6.60E+04

Table A5.4 (cont'd)

Samples	Fluorescence (427)	amorphous cell (902.537)	Lignin 1 (1504.23)	Lignin 2 (1596.8)	Aldehyde (1650.79)	Ester carbonyl (1735.65)	C-H (2900.46)	O-H (3394.16)
DL000-DA00-DC0	2.79E+05	4.2227302	6.98734	6.55706	4.868528	6.2255759	6.890016	14.16935
DL000-DA007-DC0	3.96E+05	2.5400419	4.65821	4.19596	2.967827	3.846971	4.413594	9.091128
DL00-DA015-DC0	4.04E+05	1.542118	3.16584	3.17081	2.101163	2.570838	3.451869	7.928103
DL00-DA035-DC0	3.49E+05	2.868207	5.13052	4.54635	3.274433	3.6689191	4.782938	10.13521
DL00-DA055-DC0	3.88E+05	3.072412	5.71285	5.35706	3.91477	2.9803319	5.521928	13.60627
DL00-DA075-DC0	2.80E+05	2.561137	4.84022	4.9271	3.467766	1.946705	5.033156	11.88173
DL00-DA150-DC0	2.94E+05	3.439086	5.84701	6.12734	4.075962	0.851706	6.179063	13.66099
DL01-DA000-DC0	4.44E+05	3.0154581	5.37608	4.32178	3.58965	6.3256488	5.69631	12.61379
DL001-DA007-DC0	4.74E+05	2.6601641	4.55383	3.8852	3.241175	5.301002	5.215036	11.41908
DL001-DA015-DC0	4.23E+05	1.8501379	3.09134	2.86119	2.210562	3.533411	3.627455	8.282207
DL001-DA035-DC0	4.15E+05	2.0179951	3.51884	3.49545	2.553265	3.8342459	4.236115	9.383376
DL001-DA055-DC0	4.41E+05	2.131501	3.63639	3.78009	2.681975	3.165776	4.474175	10.3575
DL001-DA075-DC0	4.20E+05	3.690763	5.76517	6.02421	4.495999	4.064321	6.633593	13.61843
DL001-DA150-DC0	4.26E+05	3.8256669	5.46572	6.28268	4.570681	1.463679	7.315939	12.15671
DL02-DA000-DC0	3.47E+05	2.048749	2.96494	2.42343	2.28914	4.118176	3.923536	8.926623
DL02-DA007-DC0	3.15E+05	2.6527619	3.86006	3.316	3.047892	5.3633661	5.191731	12.73055
DL02-DA015-DC0	3.45E+05	2.856257	4.45718	4.00132	3.229393	5.6240201	5.257272	12.69776
DL02-DA035-DC0	3.10E+05	1.936483	3.02804	3.03863	2.282228	3.8126609	4.033142	8.211503
DL02-DA055-DC0	3.62E+05	0.901357	1.72636	1.74965	1.254186	1.939211	2.289018	4.425431
DL02-DA075-DC0	4.79E+05	1.481146	2.35362	2.60388	1.896522	2.2183321	3.374407	6.672039
DL02-DA150-DC0	3.08E+05	3.356432	4.46307	5.27706	3.539952	1.418816	7.00622	13.25974

Table A5.4 (cont'd)

Samples	Initial rate Conversion	72 hrs Conversion	CrI	Raman (1038.9)	Raman (1293.3)	Raman (1369.5)	Raman (1399.5)	Raman (1445.1)	Raman (2888.7)	Raman (2919.6)
DL03-DA000-DC0	4.3203936	43.94729	53.85487	3.32E+05	3.15E+05	3.12E+05	3.13E+05	3.00E+05	9.38E+04	8.69E+04
DL03-DA007-DC0	5.3941746	42.58196	42.17172	2.35E+05	2.29E+05	2.31E+05	2.36E+05	2.22E+05	7.71E+04	6.97E+04
DL03-DA015-DC0	4.6397848	45.65708	47.25739	3.73E+05	3.49E+05	3.45E+05	3.48E+05	3.30E+05	1.07E+05	9.87E+04
DL03-DA035-DC0	6.4419146	54.0009	48.00693	2.73E+05	2.68E+05	2.69E+05	2.74E+05	2.60E+05	8.82E+04	8.13E+04
DL03-DA055-DC0	7.8567634	65.5275	39.78102	3.66E+05	3.52E+05	3.50E+05	3.53E+05	3.36E+05	1.13E+05	1.06E+05
DL03-DA075-DC0	4.9360976	69.4529	56.91882	2.33E+05	2.31E+05	2.35E+05	2.40E+05	2.27E+05	8.49E+04	7.78E+04
DL03-DA0150-DC0	7.5100002	88.68085	58.79828	4.54E+05	4.33E+05	4.28E+05	4.30E+05	4.13E+05	1.31E+05	1.22E+05
DL05-DA000-DC0	4.0244265	69.52886	31.65736	1.13E+04	1.07E+04	1.06E+04	1.05E+04	1.02E+04	3.95E+03	3.87E+03
DL05-DA007-DC0	3.7807186	59.51271	41.78082	1.64E+04	1.57E+04	1.55E+04	1.56E+04	1.51E+04	5.99E+03	5.78E+03
DL05-DA015-DC0	4.2237029	75.26768	46.50838	1.04E+04	9.93E+03	9.77E+03	9.75E+03	9.51E+03	3.75E+03	3.66E+03
DL05-DA035-DC0	4.3904452	71.83848	44.30622	1.22E+04	1.18E+04	1.18E+04	1.18E+04	1.14E+04	4.73E+03	4.57E+03
DL05-DA055-DC0	4.9726262	77.74549	45.85492	5.55E+03	7.42E+03	8.14E+03	8.42E+03	8.75E+03	5.54E+03	5.27E+03
DL05-DA075-DC0	4.7530894	82.1423	38.89943	1.51E+04	1.48E+04	1.48E+04	1.48E+04	1.44E+04	6.30E+03	6.11E+03
DL05-DA150-DC0	7.6982327	85.53094	60.09756	8.09E+03	1.05E+04	1.14E+04	1.17E+04	1.22E+04	6.60E+03	6.30E+03
DL10-DA0-DC0	4.5796385	84.72303	29.87805	1.67E+04	1.54E+04	1.50E+04	1.49E+04	1.45E+04	4.81E+03	4.67E+03
DL10-DA07-DC0	4.4106493	84.10455	45.45454	9.27E+03	1.16E+04	1.25E+04	1.29E+04	1.33E+04	6.22E+03	5.91E+03
DL10-DA15-DC0	4.3541026	89.01374	35.92233	1.59E+04	1.48E+04	1.44E+04	1.43E+04	1.40E+04	4.77E+03	4.65E+03
DL10-DA55-DC0	4.8339505	89.87002	39.30636	1.14E+04	1.07E+04	1.05E+04	1.04E+04	1.02E+04	3.75E+03	3.66E+03
DL10-DA75-DC0	4.900938	83.13855	34.33476	1.12E+04	1.05E+04	1.03E+04	1.03E+04	1.00E+04	3.76E+03	3.66E+03
DL10-DA150-DC0	15.315553	90.9734	48.68755	8.25E+03	7.77E+03	7.64E+03	7.63E+03	7.38E+03	2.90E+03	2.82E+03
DL50-DA0-DC0	2.6810155	78.67026	50.60241	1.21E+04	1.09E+04	1.06E+04	1.05E+04	1.01E+04	3.15E+03	3.06E+03

Table A5.4 (cont'd)

Samples	Fluorescence (427)	amorphous cell (902.537)	Lignin 1 (1504.23)	Lignin 2 (1596.8)	Aldehyde (1650.79)	Ester carbonyl (1735.65)	C-H (2900.46)	O-H (3394.16)
DL03-DA000-DC0	3.88E+05	1.119419	1.62784	1.23887	1.303837	2.849371	2.799954	5.554885
DL03-DA007-DC0	3.62E+05	1.631848	2.21392	1.76447	1.764347	3.602097	3.474531	7.325074
DL03-DA015-DC0	3.31E+05	1.006677	1.67156	1.52667	1.418094	2.8705859	2.557081	5.188705
DL03-DA035-DC0	3.20E+05	2.3213489	3.15674	3.30068	2.711265	4.6733351	4.588122	9.542482
DL03-DA055-DC0	3.71E+05	2.033258	2.72906	3.01909	2.336611	3.9094629	4.352558	9.437632
DL03-DA075-DC0	3.33E+05	1.91916	2.50582	2.98459	2.239451	3.119849	4.092506	8.18627
DL03-DA0150-DC0	3.55E+05	3.300977	3.38976	4.47575	3.366891	1.649111	6.269724	10.39283
DL05-DA000-DC0	4.58E+05	1.310504	1.39682	1.24166	1.451161	3.5480311	3.340969	9.086257
DL05-DA007-DC0	8.29E+06	1.423785	1.56448	1.50359	1.723345	3.026644	2.798485	5.63348
DL05-DA015-DC0	4.12E+05	3.2158661	3.86061	4.58392	3.952961	6.784256	6.660973	15.30296
DL05-DA035-DC0	8.67E+06	1.914246	1.91226	2.36829	2.108117	2.67048	2.923295	4.547462
DL05-DA055-DC0	4.24E+05	3.5420721	3.59066	5.27478	3.92983	5.1190872	7.468124	16.37052
DL05-DA075-DC0	1.11E+07	2.446382	1.76397	2.67375	1.992674	1.275717	3.836524	7.027184
DL05-DA150-DC0	4.11E+05	5.0403318	3.42758	3.11676	4.359046	7.8031092	8.220604	17.06015
DL10-DA0-DC0	1.16E+07	1.918637	1.14119	1.06633	1.384489	2.847543	2.60161	4.516871
DL10-DA07-DC0	1.99E+07	4.3233371	3.08261	3.28443	4.113013	8.0145969	8.483309	18.88313
DL10-DA15-DC0	1.98E+07	3.1014559	2.13136	2.82076	2.80504	4.4352632	4.777718	9.10479
DL10-DA55-DC0	9.49E+06	4.6667218	3.61816	5.50904	4.993716	7.476851	8.864622	20.98018
DL10-DA75-DC0	1.98E+07	4.6157241	3.82046	5.7335	4.933512	6.295362	8.341424	17.79555
DL10-DA150-DC0	1.98E+07	2.8923011	1.84901	3.09125	2.30943	1.6303101	6.900988	21.23504
DL50-DA0-DC0	1.98E+07	7.0432892	3.83549	3.39394	5.508231	11.2811298	13.79653	30.55952

Table A5.4 (cont'd)

Samples	Initial rate Conversion	72 hrs Conversion	CrI	Raman (1038.9)	Raman (1293.3)	Raman (1369.5)	Raman (1399.5)	Raman (1445.1)	Raman (2888.7)	Raman (2919.6)
DL50-DA7-DC0	3.6357665	85.075	50.58731	1.08E+04	9.76E+03	9.45E+03	9.37E+03	9.07E+03	2.92E+03	2.84E+03
DL50-DA15-DC0	3.2427487	79.43701	54.32185	1.17E+04	1.06E+04	1.02E+04	1.01E+04	9.82E+03	3.15E+03	3.06E+03
DL50-DA35-DC0	5.9091005	87.07832	55	7.66E+03	6.99E+03	6.80E+03	6.77E+03	6.53E+03	2.25E+03	2.18E+03
DL50-DA55-DC0	4.2050276	79.96072	52.98471	7.39E+03	6.77E+03	6.60E+03	6.58E+03	6.35E+03	2.26E+03	2.19E+03
DL50-DA75-DC0	7.5442624	88.80865	51.20719	5.47E+03	5.06E+03	4.95E+03	4.95E+03	4.75E+03	1.84E+03	1.78E+03
DL50-DA150-DC0	8.7481699	80.86882	55.56492	2.80E+03	2.67E+03	2.66E+03	2.68E+03	2.55E+03	1.22E+03	1.18E+03
DL0-DA0-DC3	16.931301	47.49509	22.94543	3.32E+04	2.99E+04	2.91E+04	2.89E+04	2.83E+04	1.22E+04	1.19E+04
DL0-DA07-DC3	12.78	49.72	24.62428	2.80E+04	2.50E+04	2.43E+04	2.42E+04	2.36E+04	9.91E+03	9.67E+03
DL0-DA15-DC3	16.093796	48.36166	21.22241	1.93E+04	1.72E+04	1.67E+04	1.66E+04	1.62E+04	7.05E+03	6.90E+03
DL0-DA150-DC3	19.086815	67.88278	22.15299	3.44E+04	3.31E+04	3.27E+04	3.26E+04	3.21E+04	1.46E+04	1.43E+04
DL01-DA0-DC3	11.08	64.76	24.48103	2.13E+04	1.99E+04	1.95E+04	1.93E+04	1.89E+04	7.08E+03	6.88E+03
DL01-DA7-DC3	22.113394	71.04749	25.66845	1.10E+04	1.05E+04	1.04E+04	1.04E+04	1.02E+04	4.40E+03	4.30E+03
DL01-DA15-DC3	16.870001	64.77	26.75019	1.64E+04	1.54E+04	1.51E+04	1.50E+04	1.47E+04	5.82E+03	5.68E+03
DL01-DA35-DC3	15.912683	67.89529	22.51012	1.69E+04	1.58E+04	1.56E+04	1.55E+04	1.52E+04	6.18E+03	6.02E+03
DL01-DA55-DC3	14.39	73.54	20.67608	1.98E+04	1.86E+04	1.83E+04	1.82E+04	1.78E+04	7.28E+03	7.10E+03
DL01-DA75-DC3	18.236858	79.60728	16.03343	2.10E+04	1.98E+04	1.95E+04	1.94E+04	1.90E+04	7.78E+03	7.58E+03
DL01-DA150-DC3	24.540001	91.62	21.16183	2.20E+04	2.10E+04	2.06E+04	2.05E+04	2.02E+04	8.33E+03	8.12E+03
DL02-DA0-DC3	15.926565	79.06399	11.07121	2.29E+04	2.10E+04	2.05E+04	2.03E+04	1.98E+04	7.40E+03	7.20E+03
DL02-DA07-DC3	16.459999	78.23	22.39186	1.79E+04	1.70E+04	1.67E+04	1.66E+04	1.63E+04	6.49E+03	6.33E+03
DL02-DA15-DC3	14.346943	72.53054	23.33664	1.72E+04	1.64E+04	1.61E+04	1.60E+04	1.57E+04	6.36E+03	6.18E+03
DL02-DA35-DC3	17.1	82.94	23.52941	1.74E+04	1.66E+04	1.64E+04	1.63E+04	1.59E+04	6.60E+03	6.44E+03

Table A5.4 (cont'd)

Samples	Fluorescence (427)	amorphous cell (902.537)	Lignin 1 (1504.23)	Lignin 2 (1596.8)	Aldehyde (1650.79)	Ester carbonyl (1735.65)	C-H (2900.46)	O-H (3394.16)
DL50-DA7-DC0	1.85E+07	7.7030458	4.1722	3.9504	5.795308	12.70854	15.37669	33.56179
DL50-DA15-DC0	1.98E+07	6.4760561	3.62329	4.11125	5.300209	10.3408899	12.6462	29.15903
DL50-DA35-DC0	1.98E+07	4.924015	2.78819	4.12448	4.127255	7.1314111	11.44296	28.88517
DL50-DA55-DC0	1.98E+07	3.4553001	2.08803	3.15396	2.739657	4.1701012	7.357323	19.22116
DL50-DA75-DC0	1.90E+07	3.675879	2.27647	3.35071	2.964704	3.684773	7.846987	21.36133
DL50-DA150-DC0	1.98E+07	2.5147879	1.34619	2.24431	1.637762	0.678637	6.171241	19.76933
DL0-DA0-DC3	3.03E+05	2.454756	3.95401	3.68216	2.65438	3.3283379	2.964617	9.26338
DL0-DA07-DC3	2.90E+05	2.896831	4.61727	4.21752	2.868539	4.142962	4.054488	13.46382
DL0-DA15-DC3	3.00E+05	1.6866471	3.12258	2.83935	2.026667	2.6174669	2.521335	7.592674
DL0-DA150-DC3	2.88E+05	1.966365	3.49676	3.82084	2.482875	0.5274819	3.016202	8.665699
DL01-DA0-DC3	9.38E+05	1.7717431	2.90578	2.29061	1.971439	3.3609321	2.600497	7.750099
DL01-DA7-DC3	7.39E+05	3.9161119	5.1742	4.50522	3.573334	6.0403442	5.210744	16.01687
DL01-DA15-DC3	8.66E+05	4.2972679	5.25773	4.92868	3.943011	5.626698	4.796014	12.71258
DL01-DA35-DC3	8.57E+05	2.6102841	3.62596	3.58641	2.54978	3.888031	3.401772	10.33879
DL01-DA55-DC3	9.09E+05	2.9107671	4.13867	4.2565	3.070907	3.638221	3.962296	10.61683
DL01-DA75-DC3	1.89E+07	1.905432	2.75963	3.03847	2.103947	1.98982	2.847677	8.875924
DL01-DA150-DC3	4.82E+05	2.472698	3.69763	4.53186	3.192772	1.129717	4.774673	11.83553
DL02-DA0-DC3	1.53E+07	1.730648	2.42092	1.92082	1.863169	3.2397189	2.40639	7.026453
DL02-DA07-DC3	4.16E+05	2.217495	3.0125	2.5239	2.294947	4.4088821	3.606884	11.33373
DL02-DA15-DC3	1.74E+07	1.475178	2.03732	1.82	1.446288	3.022161	2.603094	8.325666
DL02-DA35-DC3	4.88E+05	2.978806	3.88368	4.10768	3.147573	4.971158	4.606628	16.2611

Table A5.4 (cont'd)

Samples	Initial rate Conversion	72 hrs Conversion	CrI	Raman (1038.9)	Raman (1293.3)	Raman (1369.5)	Raman (1399.5)	Raman (1445.1)	Raman (2888.7)	Raman (2919.6)
DL02-DA55-DC3	15.899638	80.47083	22.17492	1.36E+04	1.32E+04	1.31E+04	1.31E+04	1.28E+04	5.79E+03	5.65E+03
DL02-DA75-DC3	20.870001	90.07	21.75884	1.85E+04	1.77E+04	1.74E+04	1.74E+04	1.70E+04	7.07E+03	6.90E+03
DL02-DA150-DC3	24.074194	89.76148	23.51747	2.25E+04	2.15E+04	2.11E+04	2.10E+04	2.05E+04	8.28E+03	8.09E+03
DL03-DA0-DC3	20.959999	92.2	18.29837	2.34E+04	2.21E+04	2.17E+04	2.17E+04	2.12E+04	8.06E+03	7.86E+03
DL03-DA07-DC3	15.382006	81.67345	24.95873	1.94E+04	1.85E+04	1.82E+04	1.81E+04	1.77E+04	6.89E+03	6.72E+03
DL03-DA15-DC3	18.610001	90.78	24.76621	2.02E+04	1.93E+04	1.90E+04	1.89E+04	1.85E+04	7.22E+03	7.03E+03
DL03-DA35-DC3	17.894875	82.13904	24.79733	1.89E+04	1.80E+04	1.78E+04	1.77E+04	1.73E+04	6.89E+03	6.71E+03
DL03-DA55-DC3	21.08	93.01	24.73347	1.87E+04	1.80E+04	1.78E+04	1.78E+04	1.74E+04	7.28E+03	7.10E+03
DL03-DA75-DC3	19.925745	90.95091	28.99491	2.35E+04	2.26E+04	2.23E+04	2.22E+04	2.18E+04	9.03E+03	8.83E+03
DL03-DA150-DC3	25.82	91.98	20.09569	2.16E+04	2.06E+04	2.03E+04	2.02E+04	1.98E+04	8.01E+03	7.81E+03
DL05-DA0-DC3	19.547627	84.36663	19.47431	2.61E+04	2.46E+04	2.42E+04	2.41E+04	2.35E+04	8.72E+03	8.50E+03
DL05-DA07-DC3	19.81	90.59	26.14491	1.98E+04	1.88E+04	1.85E+04	1.84E+04	1.80E+04	6.87E+03	6.69E+03
DL05-DA15-DC3	18.89958	83.58689	21.60804	2.26E+04	2.14E+04	2.10E+04	2.09E+04	2.04E+04	7.67E+03	7.45E+03
DL05-DA35-DC3	20.219999	92.03	23.12849	2.25E+04	2.13E+04	2.09E+04	2.08E+04	2.04E+04	7.70E+03	7.52E+03
DL05-DA55-DC3	19.140776	85.80457	16.98861	2.26E+04	2.16E+04	2.13E+04	2.11E+04	2.07E+04	8.19E+03	7.98E+03
DL05-DA75-DC3	23.16	87.69	24.85272	2.26E+04	2.16E+04	2.13E+04	2.12E+04	2.08E+04	8.27E+03	8.07E+03
DL05-DA150-DC3	24.137411	92.97169	17.61557	2.28E+04	2.17E+04	2.13E+04	2.12E+04	2.07E+04	8.14E+03	7.92E+03
DL10-DA0-DC3	24.08	92.13	19.85397	3.42E+04	3.17E+04	3.09E+04	3.07E+04	3.00E+04	1.01E+04	9.85E+03
DL10-DA07-DC3	18.166258	91.69036	16.75423	2.44E+04	2.28E+04	2.23E+04	2.22E+04	2.16E+04	7.57E+03	7.37E+03
DL10-DA15-DC3	20.290001	91.28	17.13131	2.50E+04	2.34E+04	2.28E+04	2.27E+04	2.21E+04	7.70E+03	7.50E+03
DL10-DA35-DC3	19.668501	93.21772	26.67261	2.41E+04	2.25E+04	2.21E+04	2.19E+04	2.14E+04	7.59E+03	7.39E+03

Table A5.4 (cont'd)

Samples	Fluorescence (427)	amorphous cell (902.537)	Lignin 1 (1504.23)	Lignin 2 (1596.8)	Aldehyde (1650.79)	Ester carbonyl (1735.65)	C-H (2900.46)	O-H (3394.16)
DL02-DA55-DC3	1.80E+07	1.76481	2.34994	2.6695	1.84051	2.695111	3.039591	10.27918
DL02-DA75-DC3	4.41E+05	3.0932441	4.15249	4.89906	3.480111	3.96819	5.614354	16.10679
DL02-DA150-DC3	4.22E+05	2.451551	3.30967	4.22006	3.17224	1.434953	4.712458	12.10632
DL03-DA0-DC3	4.48E+05	3.7757211	3.91402	3.0895	3.421074	6.2787471	4.960033	15.55904
DL03-DA07-DC3	4.72E+05	2.6419771	3.03154	2.61735	2.706728	4.6951289	3.849485	10.56603
DL03-DA15-DC3	4.00E+05	3.092998	3.38117	3.13211	2.999056	5.8847508	4.939226	15.07329
DL03-DA35-DC3	6.08E+05	15.6458302	14.5878	12.7286	14.91818	9.5941772	10.32008	3.70711
DL03-DA55-DC3	4.64E+05	3.1815209	3.49227	4.2098	3.22888	4.880806	4.832267	14.37894
DL03-DA75-DC3	5.17E+05	2.053293	2.17883	2.93066	2.207487	2.9287519	3.624348	12.44493
DL03-DA150-DC3	5.27E+05	3.664758	3.38509	5.20615	3.694596	1.712049	6.625044	20.71171
DL05-DA0-DC3	5.45E+05	1.937306	1.8775	1.41911	1.91094	3.7613871	2.799562	8.644809
DL05-DA07-DC3	4.89E+05	3.2530091	2.81911	2.39311	2.880038	6.369987	5.047239	16.36178
DL05-DA15-DC3	4.48E+05	4.0040531	3.46031	3.18503	3.562036	6.8373442	5.416021	16.95552
DL05-DA35-DC3	5.20E+05	2.611866	2.36668	2.71678	2.451261	4.435514	3.656141	11.50262
DL05-DA55-DC3	5.66E+05	5.2629042	4.81142	6.37705	5.656536	7.6610398	7.526914	23.48846
DL05-DA75-DC3	5.44E+05	3.05353	2.67961	3.81231	2.982063	4.1819391	4.73587	14.7898
DL05-DA150-DC3	7.39E+05	4.7178192	3.51868	5.49649	4.368391	2.287168	7.54054	22.36814
DL10-DA0-DC3	8.74E+05	2.4712729	1.59171	1.23106	2.103042	4.4002419	3.651439	11.02942
DL10-DA07-DC3	8.76E+05	3.268832	2.10292	1.88692	2.917787	5.7562499	4.953444	15.22677
DL10-DA15-DC3	9.19E+05	2.613271	1.65708	1.63709	2.291538	5.2060599	4.665533	14.50802
DL10-DA35-DC3	8.45E+05	3.532443	2.42843	3.23136	3.48515	5.9619522	6.174494	18.28305

Table A5.4 (cont'd)

Samples	Initial rate Conversion	72 hrs Conversion	CrI	Raman (1038.9)	Raman (1293.3)	Raman (1369.5)	Raman (1399.5)	Raman (1445.1)	Raman (2888.7)	Raman (2919.6)
DL10-DA55-DC3	21.799999	90.98	23.75356	2.28E+04	2.14E+04	2.09E+04	2.08E+04	2.03E+04	7.32E+03	7.14E+03
DL10-DA75-DC3	20.86071	92.38311	14.75645	2.17E+04	2.04E+04	2.00E+04	1.99E+04	1.94E+04	7.17E+03	6.99E+03
DL10-DA150-DC3	22.48	92.74	19.26007	1.65E+04	1.55E+04	1.52E+04	1.52E+04	1.48E+04	5.62E+03	5.47E+03
DL50-DA0-DC3	16.713457	86.42483	25.76651	2.47E+04	2.27E+04	2.20E+04	2.18E+04	2.12E+04	6.84E+03	6.65E+03
DL50-DA07-DC3	13.76	85.46	37.04404	1.86E+04	1.70E+04	1.65E+04	1.63E+04	1.58E+04	5.09E+03	4.96E+03
DL50-DA15-DC3	10.361994	75.43884	41.24143	1.88E+04	1.71E+04	1.67E+04	1.65E+04	1.60E+04	5.11E+03	4.97E+03
DL50-DA35-DC3	12.69	82.94	35.86681	1.77E+04	1.62E+04	1.57E+04	1.56E+04	1.51E+04	4.96E+03	4.83E+03
DL50-DA55-DC3	15.3204	86.91856	37.12507	1.29E+04	1.19E+04	1.16E+04	1.15E+04	1.12E+04	3.90E+03	3.79E+03
DL50-DA75-DC3	15.19	88.52	31.25671	1.18E+04	1.09E+04	1.07E+04	1.07E+04	1.03E+04	3.67E+03	3.58E+03
DL0-DA07-DC6	19.207554	58.13152	19.39332	2.81E+04	2.52E+04	2.45E+04	2.44E+04	2.39E+04	1.00E+04	9.79E+03
DL0-DA15-DC6	11.33	61.38	67.8282	2.85E+04	2.64E+04	2.59E+04	2.58E+04	2.53E+04	1.11E+04	1.08E+04
DL0-DA35-DC6	13.97683	59.09062	21.45713	2.96E+04	2.60E+04	2.52E+04	2.51E+04	2.44E+04	1.01E+04	9.88E+03
DL0-DA55-DC6	15.79	72.01	14.56607	3.50E+04	3.30E+04	3.24E+04	3.23E+04	3.17E+04	1.39E+04	1.36E+04
DL0-DA75-DC6	20.295704	74.32294	14.52915	3.70E+04	3.52E+04	3.47E+04	3.46E+04	3.40E+04	1.49E+04	1.46E+04
DL0-DA150-DC6	17.76	74.05	20.11959	3.72E+04	3.56E+04	3.52E+04	3.52E+04	3.46E+04	1.59E+04	1.56E+04
DL01-DA0-DC6	25.092217	73.72573	15.63178	2.03E+04	1.94E+04	1.91E+04	1.90E+04	1.86E+04	7.21E+03	7.03E+03
DL01-DA15-DC6	18.310011	78.11327	18.09872	1.51E+04	1.42E+04	1.39E+04	1.38E+04	1.35E+04	5.28E+03	5.12E+03
DL01-DA35-DC6	16.040001	73.1	18.04842	2.00E+04	1.90E+04	1.87E+04	1.86E+04	1.82E+04	7.44E+03	7.25E+03
DL01-DA55-DC6	25.567278	73.69124	23.16335	1.72E+04	1.63E+04	1.60E+04	1.59E+04	1.56E+04	6.29E+03	6.11E+03
DL01-DA150-DC6	41.090939	86.33337	15.07118	2.57E+04	2.42E+04	2.38E+04	2.37E+04	2.31E+04	9.05E+03	8.84E+03
DL02-DA07-DC6	28.733097	83.50393	12.06485	1.96E+04	1.85E+04	1.83E+04	1.82E+04	1.79E+04	7.01E+03	6.83E+03
DL02-DA35-DC6	27.625748	75.84586	24.68487	1.59E+04	1.52E+04	1.50E+04	1.49E+04	1.46E+04	5.88E+03	5.73E+03

Table A5.4 (cont'd)

Samples	Fluorescence (427)	amorphous cell (902.537)	Lignin 1 (1504.23)	Lignin 2 (1596.8)	Aldehyde (1650.79)	Ester carbonyl (1735.65)	C-H (2900.46)	O-H (3394.16)
DL10-DA55-DC3	9.06E+05	2.7486401	1.96093	3.01371	2.728196	4.327949	4.830323	14.80537
DL10-DA75-DC3	9.23E+05	3.400773	2.26717	3.67291	3.354244	4.5369558	5.944187	18.24933
DL10-DA150-DC3	1.14E+06	1.763391	1.17748	1.89165	1.684885	0.9269139	3.435541	10.05956
DL50-DA0-DC3	5.45E+05	3.055985	1.40078	1.17516	2.205397	4.6773882	5.208658	16.20395
DL50-DA07-DC3	1.59E+06	2.1681869	1.08386	0.97117	1.641907	3.682996	3.981771	11.03963
DL50-DA15-DC3	2.07E+06	2.2989459	1.12418	1.21117	1.675266	3.7591181	4.045019	11.43861
DL50-DA35-DC3	1.93E+06	3.1972489	1.82951	2.45584	2.555441	4.23558	5.10286	12.82996
DL50-DA55-DC3	1.70E+06	3.3023701	1.94143	2.89862	2.760088	4.029686	5.734713	15.74029
DL50-DA75-DC3	1.72E+06	3.0878711	1.63991	2.62422	2.338724	3.2346749	6.092376	17.12019
DL0-DA07-DC6	3.93E+05	2.3010349	4.40509	4.09695	3.1294	4.080729	3.76207	10.76864
DL0-DA15-DC6	3.75E+05	3.935997	5.88555	5.46823	4.116149	4.9975219	4.664279	13.64479
DL0-DA35-DC6	3.26E+05	3.684849	5.24032	5.01252	3.523787	3.8477249	4.426139	12.67928
DL0-DA55-DC6	3.52E+05	3.942817	5.9436	5.96984	4.539651	3.4936719	5.049215	13.41196
DL0-DA75-DC6	4.06E+05	2.2195539	3.95371	4.12957	2.894296	1.544902	3.618458	11.92591
DL0-DA150-DC6	4.35E+06	2.8364949	4.26715	4.85553	3.10776	0.6507317	4.080534	12.13954
DL01-DA0-DC6	4.54E+06	2.6470211	3.47879	2.67281	2.297464	4.258183	3.359874	10.90356
DL01-DA15-DC6	5.76E+06	2.760653	3.73851	3.43085	2.600112	4.3496442	3.771295	12.01303
DL01-DA35-DC6	1.57E+07	2.443671	3.3487	3.67169	2.408541	3.0424211	4.026394	13.88187
DL01-DA55-DC6	1.47E+07	2.9547119	4.07084	4.10123	2.955459	4.6846719	4.505341	15.62782
DL01-DA150-DC6	1.98E+07	4.18156	4.96022	6.48917	4.253184	1.2816401	6.904037	21.0648
DL02-DA07-DC6	1.92E+07	5.2160792	5.96472	5.09014	4.845368	7.6129189	5.877203	16.29848
DL02-DA35-DC6	1.98E+07	4.3458238	5.09049	5.45502	4.277932	6.3200598	6.094211	18.13809

Table A5.4 (cont'd)

Samples	Initial rate Conversion	72 hrs Conversion	CrI	Raman (1038.9)	Raman (1293.3)	Raman (1369.5)	Raman (1399.5)	Raman (1445.1)	Raman (2888.7)	Raman (2919.6)
DL02-DA75-DC6	24.790251	88.09355	23.33462	2.18E+04	2.09E+04	2.06E+04	2.05E+04	2.01E+04	8.23E+03	8.02E+03
DL02-DA150-DC6	32.84	94.6	10.61947	2.45E+04	2.34E+04	2.30E+04	2.29E+04	2.24E+04	8.97E+03	8.74E+03
DL03-DA0-DC6	22.139099	89.3421	17.10611	1.95E+04	1.83E+04	1.80E+04	1.79E+04	1.74E+04	6.41E+03	6.24E+03
DL03-DA07-DC6	19.870001	90.98	23.36218	1.63E+04	1.54E+04	1.51E+04	1.51E+04	1.47E+04	5.57E+03	5.41E+03
DL03-DA15-DC6	21.425026	88.90923	13.70757	1.69E+04	1.60E+04	1.57E+04	1.56E+04	1.52E+04	5.79E+03	5.63E+03
DL03-DA35-DC6	21.860001	92.99	14.12184	1.46E+04	1.39E+04	1.36E+04	1.36E+04	1.33E+04	5.23E+03	5.11E+03
DL03-DA55-DC6	24.464684	90.20191	18.44609	1.98E+04	1.88E+04	1.85E+04	1.84E+04	1.80E+04	7.00E+03	6.82E+03
DL03-DA75-DC6	23.15	92.21	15.21739	1.97E+04	1.89E+04	1.85E+04	1.84E+04	1.81E+04	7.07E+03	6.90E+03
DL03-DA150-DC6	28.738356	93.28838	26	2.06E+04	1.97E+04	1.93E+04	1.92E+04	1.88E+04	7.25E+03	7.07E+03
DL05-DA0-DC6	25.549999	93.71	8.467202	2.63E+04	2.49E+04	2.44E+04	2.43E+04	2.37E+04	8.74E+03	8.55E+03
DL05-DA07-DC6	33.431095	88.87137	22.32317	1.61E+04	1.51E+04	1.49E+04	1.48E+04	1.44E+04	5.27E+03	5.13E+03
DL05-DA15-DC6	24.56	92.67	13.89307	2.45E+04	2.33E+04	2.29E+04	2.28E+04	2.23E+04	8.50E+03	8.29E+03
DL05-DA35-DC6	25.868912	93.65652	17.89234	2.38E+04	2.28E+04	2.25E+04	2.24E+04	2.19E+04	8.35E+03	8.12E+03
DL05-DA75-DC6	28.415638	92.05256	15.07582	2.01E+04	1.91E+04	1.87E+04	1.86E+04	1.81E+04	6.91E+03	6.73E+03
DL10-DA0-DC6	25.196377	91.41272	18.23129	2.31E+04	2.14E+04	2.08E+04	2.07E+04	2.01E+04	6.86E+03	6.68E+03
DL10-DA15-DC6	38.379597	92.54469	13.01146	1.67E+04	1.55E+04	1.51E+04	1.50E+04	1.46E+04	5.25E+03	5.11E+03
DL10-DA55-DC6	34.990936	90.89683	21.68088	1.91E+04	1.80E+04	1.76E+04	1.75E+04	1.71E+04	6.34E+03	6.20E+03
DL10-DA150-DC6	26.213427	92.15222	15.25169	1.24E+04	1.17E+04	1.14E+04	1.14E+04	1.11E+04	4.21E+03	4.10E+03
DL50-DA0-DC6	20.959999	90.7	10.36562	2.51E+04	2.30E+04	2.24E+04	2.22E+04	2.16E+04	7.17E+03	6.98E+03
DL50-DA07-DC6	17.789854	87.47612	13.34713	1.19E+04	1.10E+04	1.07E+04	1.06E+04	1.03E+04	3.71E+03	3.61E+03
DL50-DA35-DC6	19.234497	90.06944	11.84443	1.20E+04	1.10E+04	1.07E+04	1.07E+04	1.03E+04	3.62E+03	3.52E+03
DL50-DA150-DC6	18.85	92.64	32.13186	7.95E+03	7.48E+03	7.40E+03	7.40E+03	7.17E+03	2.89E+03	2.81E+03

Table A5.4 (cont'd)

Samples	Fluorescence (427)	amorphous cell (902.537)	Lignin 1 (1504.23)	Lignin 2 (1596.8)	Aldehyde (1650.79)	Ester carbonyl (1735.65)	C-H (2900.46)	O-H (3394.16)
DL02-DA75-DC6	1.94E+07	4.4543228	5.58393	6.60969	4.885926	5.3985581	7.113056	21.98882
DL02-DA150-DC6	1.01E+07	3.9126821	3.83991	5.2817	3.741366	1.456576	6.082461	18.51928
DL03-DA0-DC6	2.95E+05	5.2166352	5.39727	4.40019	5.085544	9.5951996	8.123602	26.12412
DL03-DA07-DC6	6.13E+05	2.995326	3.04553	2.53481	2.758462	5.65098	4.446926	15.34508
DL03-DA15-DC6	8.02E+05	2.4705939	2.52594	2.30422	2.372669	4.8636799	4.012446	14.75399
DL03-DA35-DC6	8.83E+05	3.3478251	3.55046	4.14361	3.507515	6.0209942	5.589786	19.67887
DL03-DA55-DC6	9.70E+06	3.249716	3.43636	4.36678	3.488366	5.150579	5.335299	17.75342
DL03-DA75-DC6	7.88E+06	2.900414	3.05016	4.00827	2.967632	3.9095991	4.728464	15.53754
DL03-DA150-DC6	8.95E+06	4.0965328	3.67261	5.42186	4.269397	1.903574	6.795607	19.37087
DL05-DA0-DC6	9.23E+06	3.0186269	2.57469	1.96265	2.749305	5.7881842	4.627803	15.22137
DL05-DA07-DC6	4.35E+05	3.9461629	3.44781	2.98302	3.721229	7.39992	6.016971	18.81545
DL05-DA15-DC6	4.36E+05	2.946384	2.46268	2.20171	2.545815	5.2782688	3.903486	13.88455
DL05-DA35-DC6	5.36E+05	4.3088999	3.76567	4.51931	4.38325	7.3468409	6.488944	21.68001
DL05-DA75-DC6	5.22E+05	3.018635	2.59244	3.92584	3.231593	4.2892051	5.383648	17.42386
DL10-DA0-DC6	5.17E+05	2.4163311	1.39917	1.08072	2.104796	4.7496471	4.475765	15.77646
DL10-DA15-DC6	4.84E+05	2.973531	1.68728	1.67124	2.524876	5.1506619	4.265479	14.38112
DL10-DA55-DC6	5.55E+05	2.2742031	1.48268	2.3706	2.268586	3.3964641	3.883294	12.11247
DL10-DA150-DC6	8.06E+05	2.7306719	1.48427	2.59996	2.417328	1.176005	5.186178	16.4042
DL50-DA0-DC6	8.97E+05	3.2404499	1.35213	1.02257	2.029989	4.529902	4.70901	15.26502
DL50-DA07-DC6	8.76E+05	2.7238979	1.13103	1.00266	1.917065	4.2365842	4.420378	14.65277
DL50-DA35-DC6	1.03E+06	2.8954051	1.27589	1.85186	2.169107	3.811281	4.793857	14.55476
DL50-DA150-DC6	2.00E+06	1.715067	1.07161	1.60383	1.388969	0.512742	3.435193	9.448717

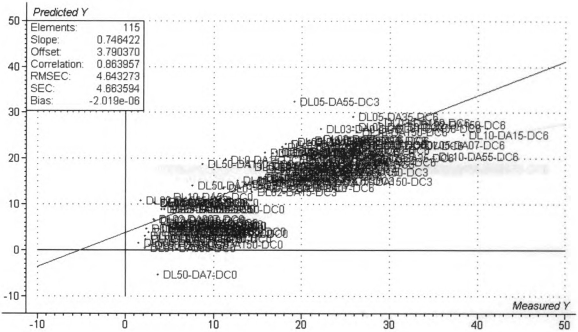

Figure A5.1: MLR initial rate model using DRIFT data

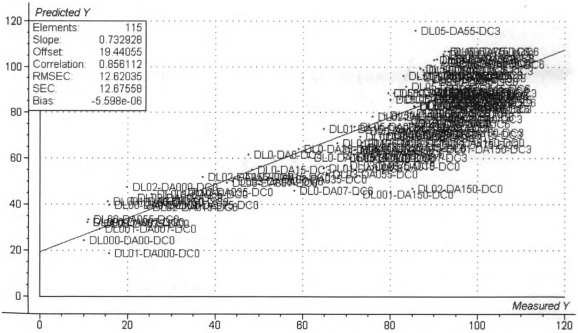

Figure A5.2: MLR 72-hr model using DRIFT data

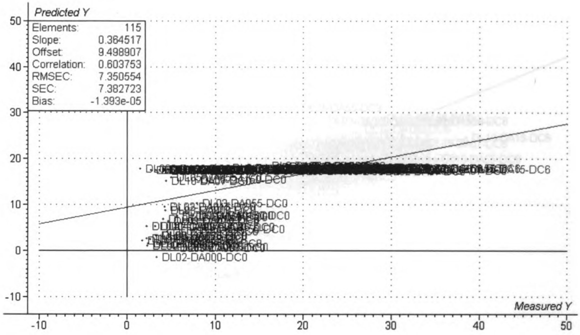

Figure A5.3: MLR initial rate model using Raman data

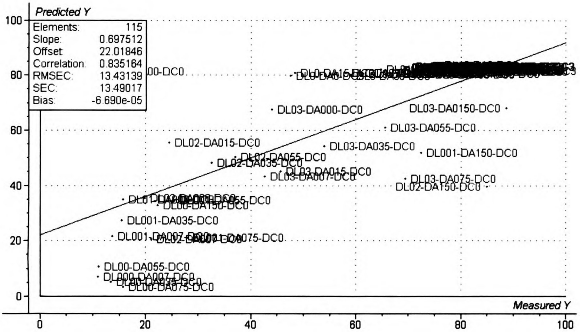

Figure A5.4: MLR 72-hr model using Raman data

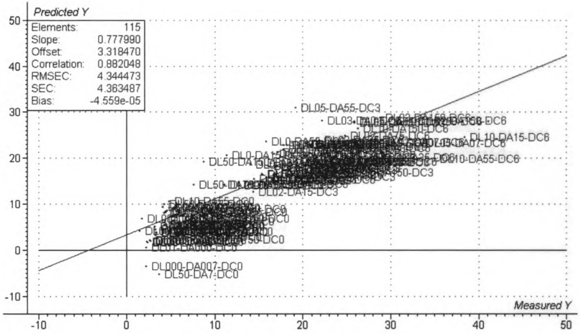

Figure A5.5: MLR initial rate model using DRIFT and Raman data

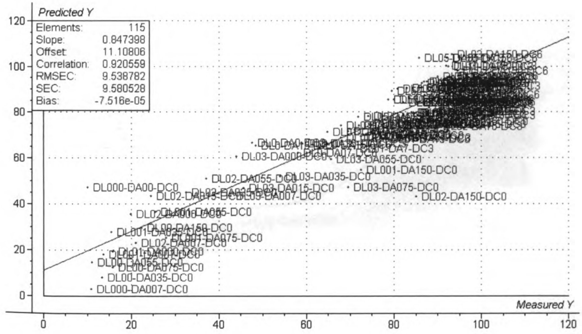

Figure A5.6: MLR 72-hr model using DRIFT and Raman data

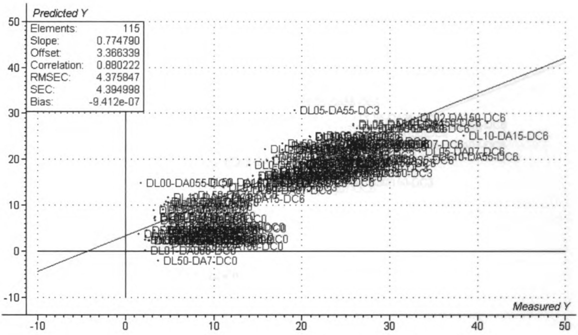

Figure A5.7: MLR initial rate model using DRIFT and XRD data

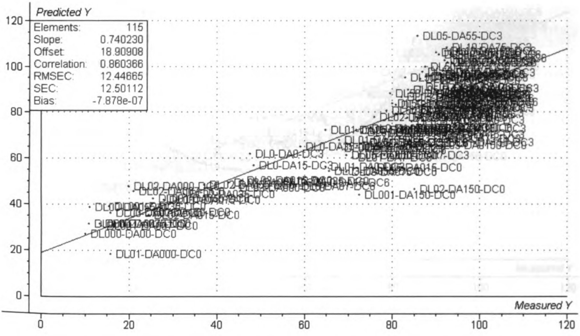

Figure A5.8: MLR 72-hr model using DRIFT and XRD data

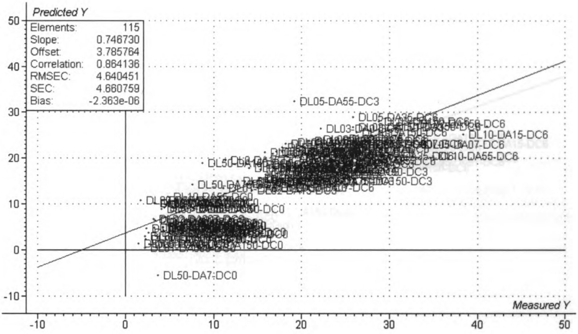

Figure A5.9: MLR initial rate model using DRIFT and fluorescence data

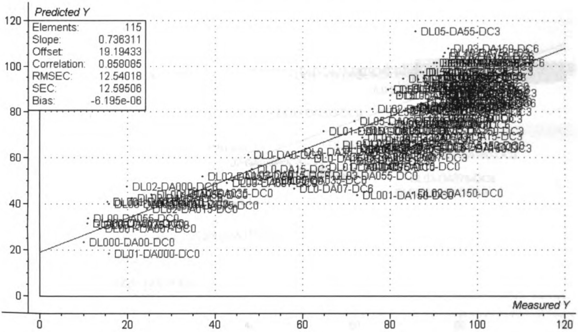

Figure A5.10: MLR 72-hr model using DRIFT and fluorescence data

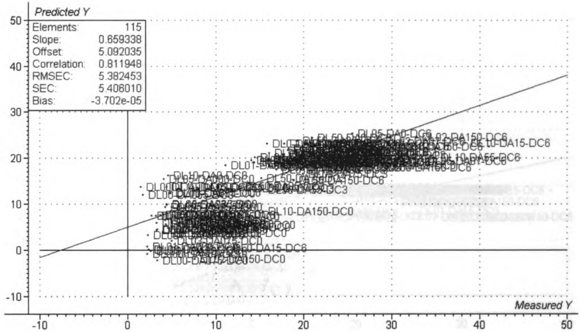

Figure A5.11: MLR initial rate model using Raman and XRD data

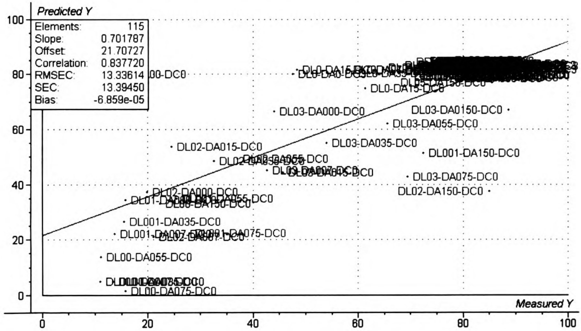

Figure A5.12: MLR 72-hr model using Raman and XRD data

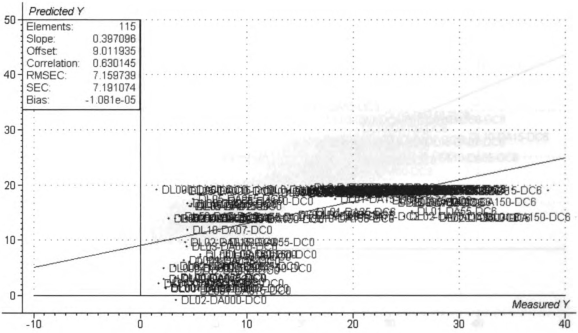

Figure A5.13: MLR initial rate model using Raman and fluorescence data

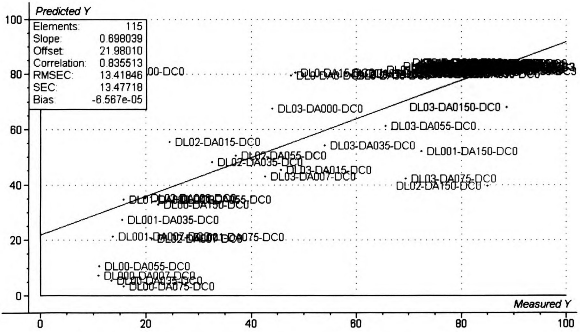

Figure A5.14: MLR 72-hr model using Raman and fluorescence data

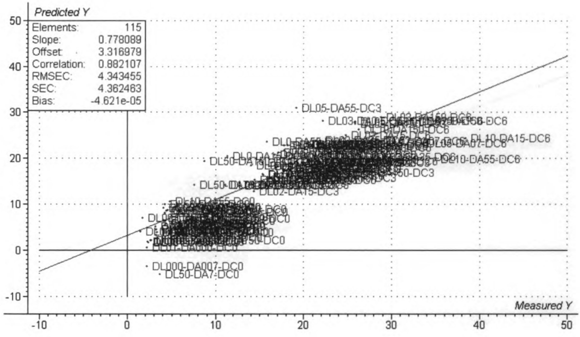

Figure A5.15: MLR initial rate model using DRIFT, Raman and fluorescence data

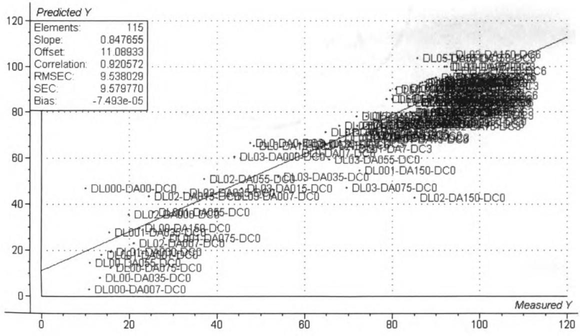

Figure A5.16: MLR 72-hr model using DRIFT, Raman and fluorescence data

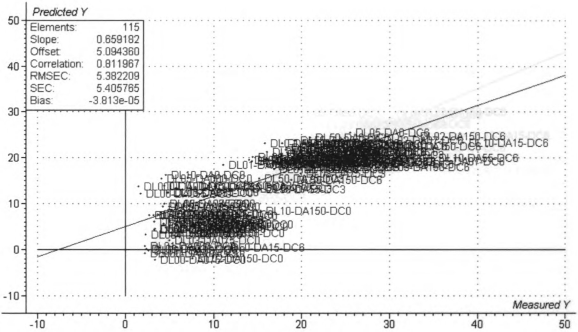

Figure A5.17: MLR initial rate model using XRD, Raman and fluorescence data

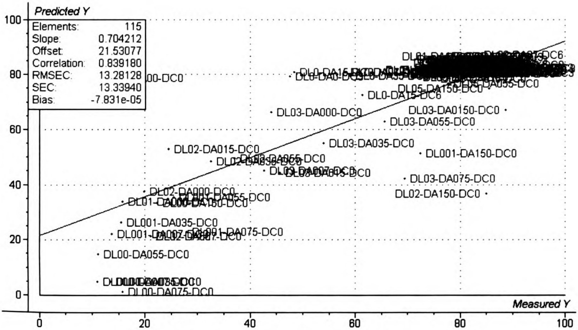

Figure A5.18: MLR 72-hr model using XRD, Raman and fluorescence data

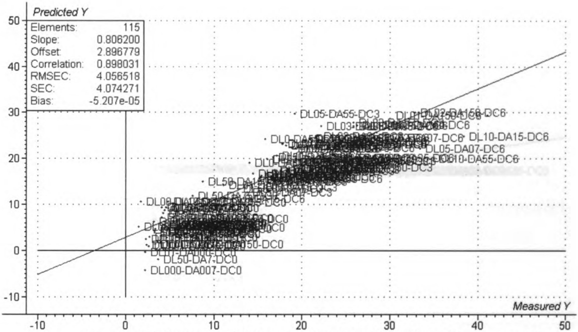

Figure A5.19: MLR initial rate model using DRIFT, XRD, Raman and fluorescence data

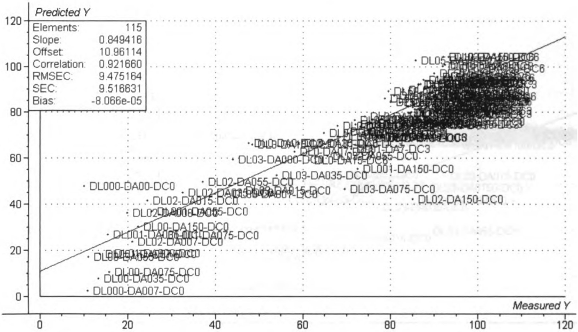

Figure A5.20: MLR 72-hr model using DRIFT, XRD, Raman and fluorescence data

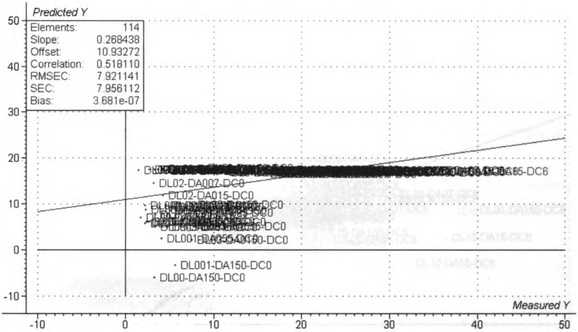

Figure A5.21: PCR initial rate model using Raman data

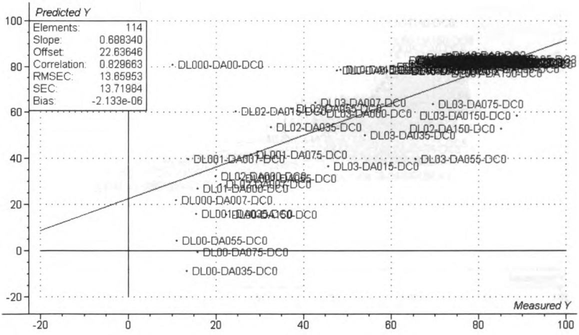

Figure A5.22: PCR 72-hr model using Raman data

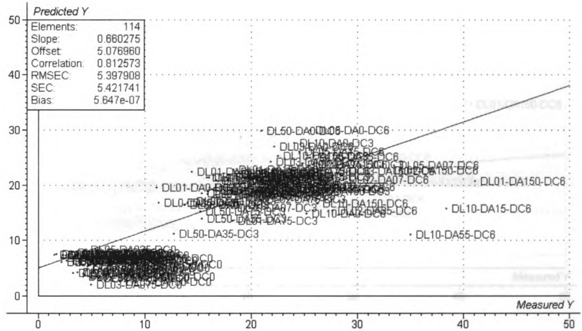

Figure A5.23: PCR initial rate model using XRD data

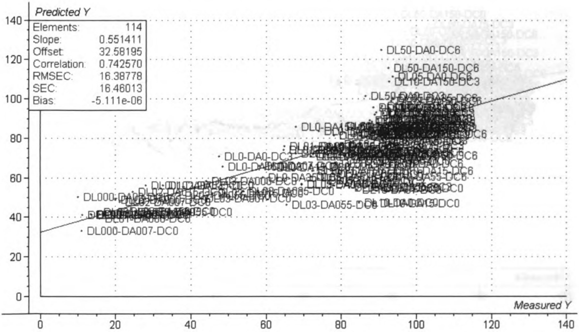

Figure A5.24: PCR 72-hr model using XRD data

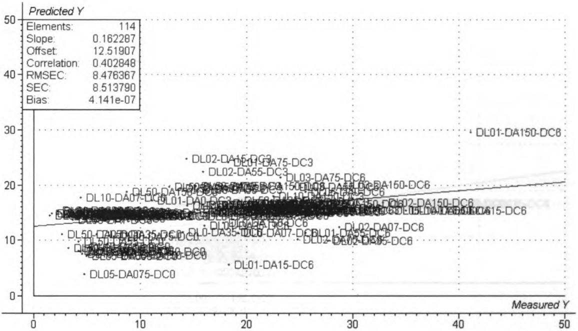

Figure A5.25: PCR initial rate model using fluorescence data

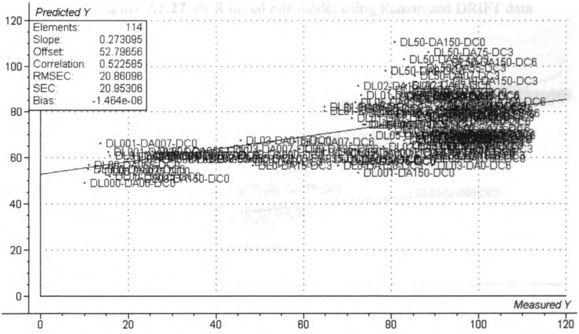

Figure A5.26: PCR 72-hr model using fluorescence data

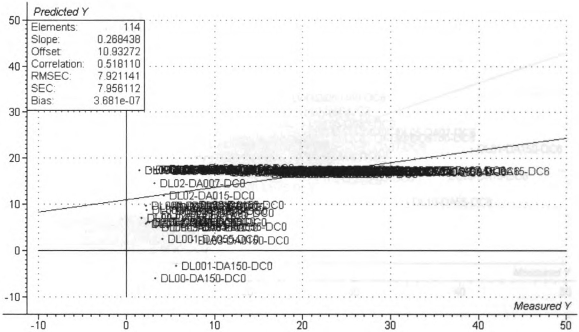

Figure A5.27: PCR initial rate model using Raman and DRIFT data

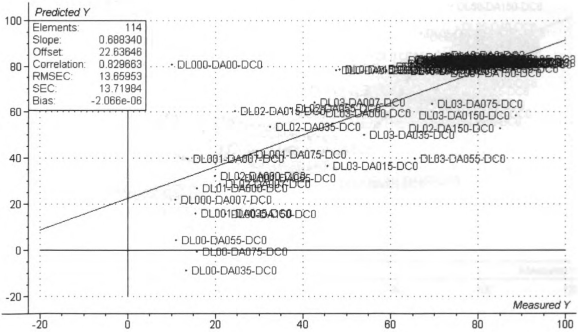

Figure A5.28: PCR 72-hr model using Raman and DRIFT data

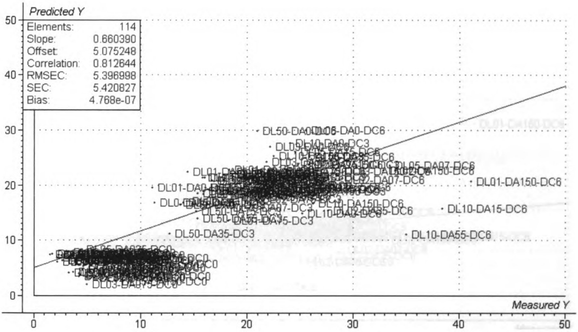

Figure A5.29: PCR initial rate model using XRD and DRIFT data

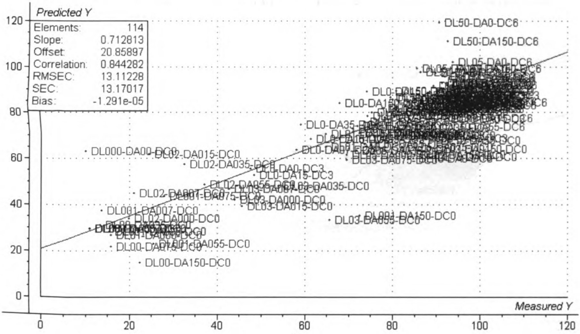

Figure A5.30: PCR 72-hr model using XRD and DRIFT data

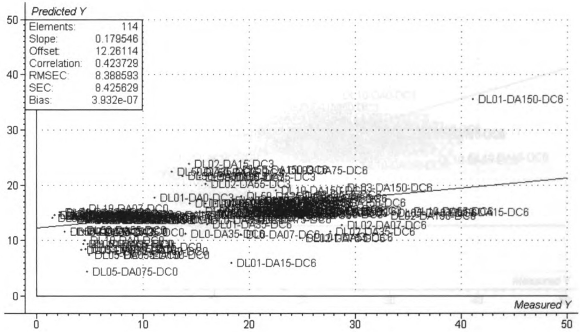

Figure A5.31: PCR initial rate model using DRIFT and fluorescence data

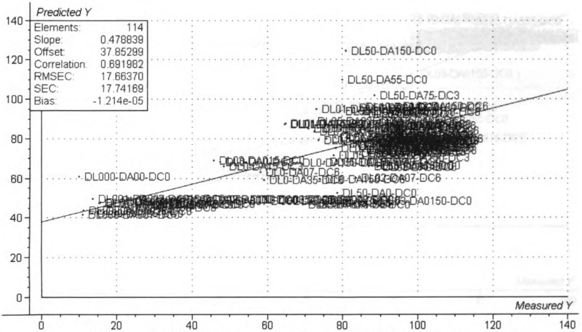

Figure A5.32: PCR 72-hr model using DRIFT and fluorescence data

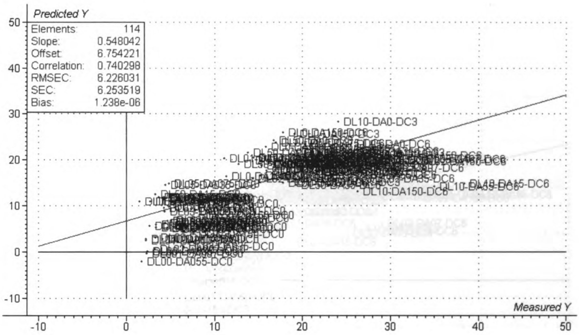

Figure A5.33: PCR initial rate model using Raman and XRD data

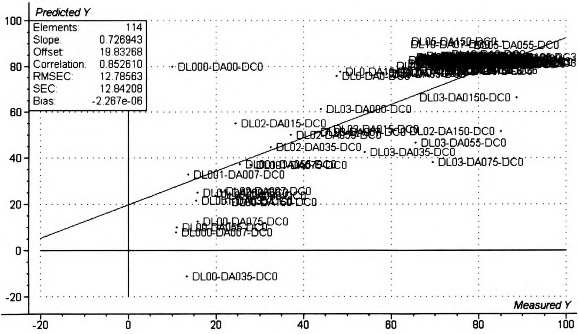

Figure A5.34: PCR 72-hr model using Raman and XRD data

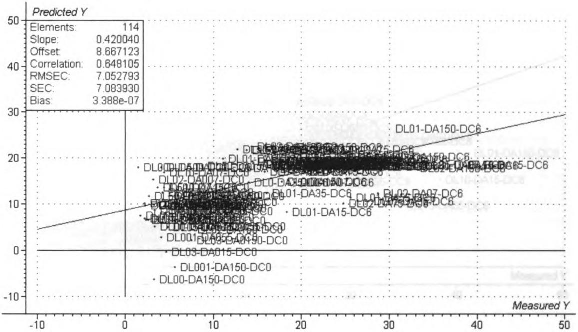

Figure A5.35: PCR initial rate model using Raman and fluorescence data

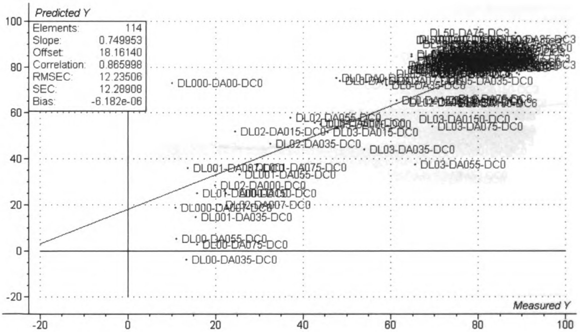

Figure A5.36: PCR 72-hr model using Raman and fluorescence data

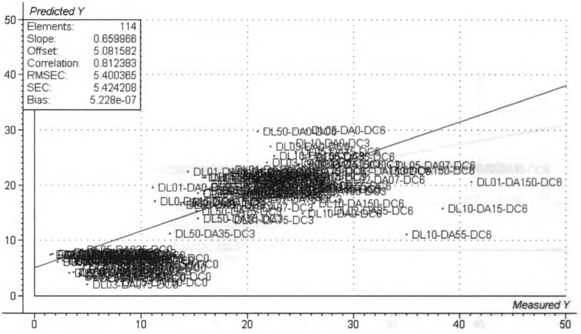

Figure A5.37: PCR initial rate model using XRD and fluorescence data

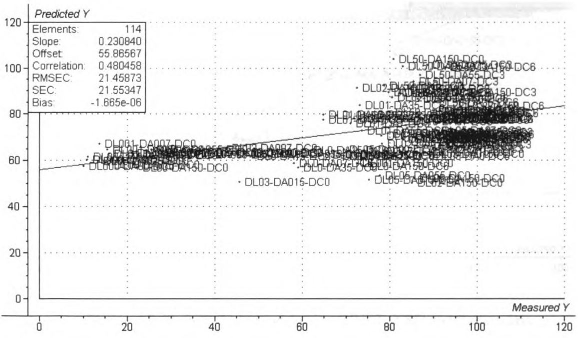

Figure A5.38: PCR 72-hr model using XRD and fluorescence data

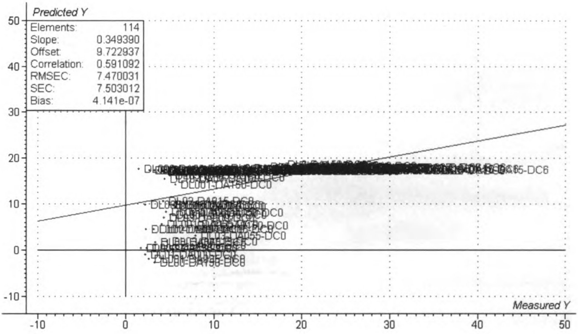

Figure A5.39: PCR initial rate model using DRIFT, XRD and Raman data

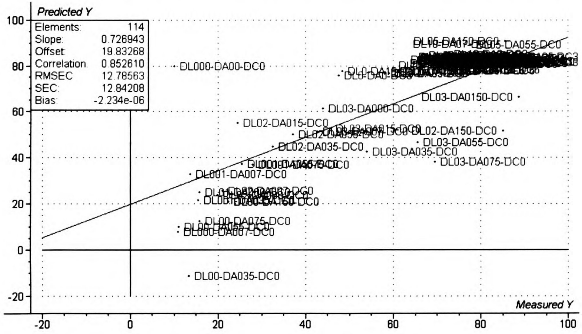

Figure A5.40: PCR 72-hr model using DRIFT, XRD and Raman data

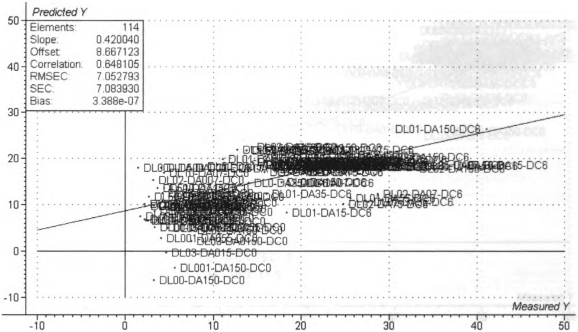

Figure A5.41: PCR initial model using DRIFT, fluorescence and Raman data

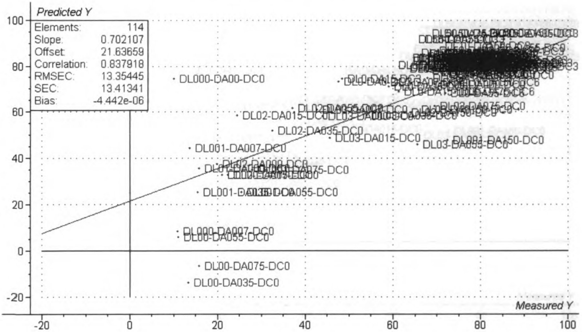

Figure A5.42: PCR 72-hr using DRIFT, fluorescence and Raman data

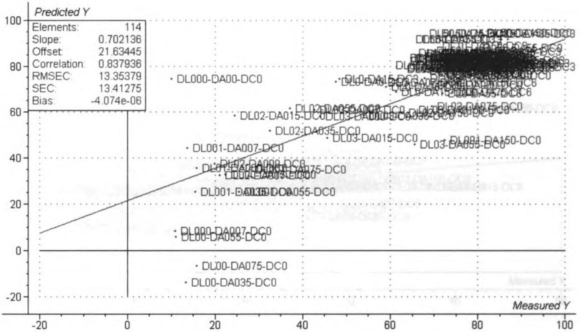

Figure A5.43: PCR initial rate using XRD, fluorescence and Raman data

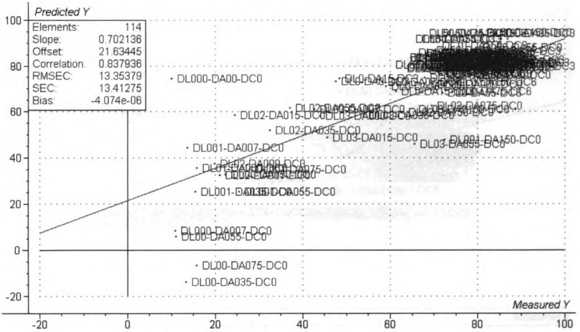

Figure A5.44: PCR 72-hr using XRD, fluorescence and Raman data

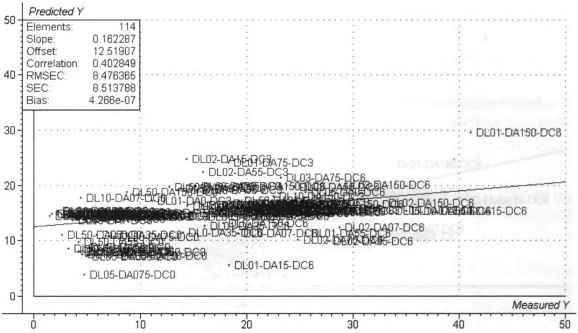

Figure A5.45: PCR initial rate model using DRIFT, XRD and fluorescence data

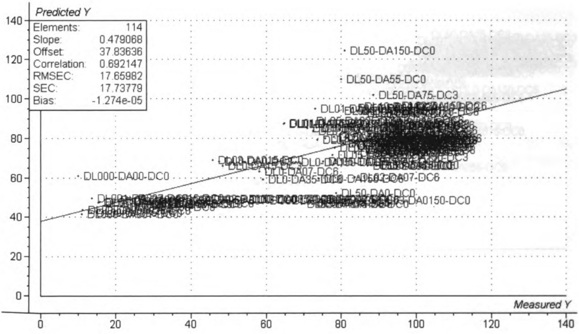

Figure A5.46: PCR 72-hr model using DRIFT, XRD and fluorescence data

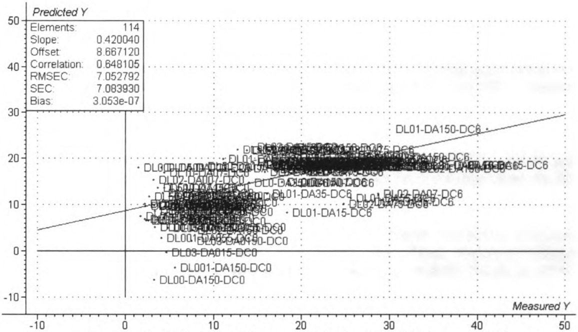

Figure A5.47: PCR initial rate model using DRIFT, Raman, XRD and fluorescence data

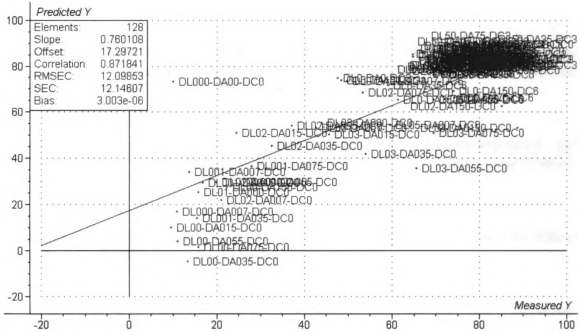

Figure A5.48: PCR 72-hr model using DRIFT, Raman, XRD and fluorescence data

BIBLIOGRAPHY

1. Abraham, Mariamma and G. Muraleedhara Kurup. (1997), "Pretreatment Studies of Cellulose Wastes for Optimization of Cellulase Enzyme Activity", *Applied Biochemistry and Biotechnology*, **Vol. 62**, 201-211.

2. Adar, Fran, Gwenaelle le Bourbon, John Reffner, and Andrew Whitley. "FT-IR and Raman Microscopy on a United Platform", *Spectroscopy* 18(2) February 2003, 34-40.

3. Akin, D.E., A. Sethuraman, W.H. Morrison III, S.A. Martin and K.E.L. Eriksson, (1993) "Microbial Delignification with White Rot Fungi Improves Forage Digestibility", *Applied and Environmental Microbiology*, **Vol.59, No.12**, p. 4274-4282.

4. Akin, D. E., L.L. Rigsby, Anand Sethuraman, W.H. Morrison III, G.R. Gamble and K.-E.L. Eriksson, (1995), "Alteration in Structure, Chemistry and Biodegradability of Grass Lignocellulose Treated with the White Rot Fungi", *Applied and Environmental Microbiology*, **Vol. 61, No. 4**, pp. 1591-1598.

5. Akin, D.E. and L.L Rigsby, (1992), "Scanning Electron Microscopy and Ultraviolet Absorption Microspectrophotometry of plant cell types of different Biodegradabilities", *Food Structure*, **Vol. 11**, pp. 259-271.

6. Akin, Danny E. and Roy D. Hartley, (1992) "Microspectrophotometry and Digestibility of Alkali-Treated Walls in Bermudagrass Cell Types", *Crop Science*, **Vol. 32,** 1116-1122.

7. Backa, Stefan and Anders Brolin " Determination of pulp characteristics by diffuse reflectance FTIR", *Tappi Journal*, **May 1991**, 218-226.

8. Ball, David W., "Theory of Raman Spectroscopy" *Spectroscopy* 16(11) November 2001, 32-34.

9. Ball, David W., "Raman Spectroscopy" *Spectroscopy* 17(2) February 2002, 50-52.

10. Beebe, Kenneth R. and Bruce R. Kowalski. (1987) "An Introduction to Multivariate Calibration and Analysis", *Analytical Chemistry*, **Vol. 59, No. 17**, September 1, 1987, 1007A-1017A.

11. Belkacemi, Khaled, Ginette Turcotte, Damien de Halleux and Phillipe Savoie. (1998) "Ethanol Production from AFEX-Treated Forages and Agricultural Residues", *Applied Biochem and Biotech*, **Vol. 70/72**, 441-462.

12. Bertran, Maria Silvia and Bruce E. Dale. (1985) "Enzymatic Hydrolysis and Recrystallization Behavior of initially Amorphous Cellulose", *Biotechnology and Bioengineering*, **Vol. XXVII**, Pp 177-181.

13. Beyer, M., D. Steger and K. Fischer ((1993) "The luminescence of lignin-containing pulps – A comparison with the fluorescence of model compounds in several media" *J. Photochem. Photobiol. A: Chem*, **76**, 217-224.

14. Billa, E., E. Koutsoula and E.G. Koukios (1999). "Fluorescence analysis of paper pulps", *Bioresource Technology*, **67**, 25-33.

15. Billa E. and B Monties. (1995) "Molecular Variability of lignin fractions isolated from wheat straw" *Res. Chem Intermed*, **Vol. 21, Nos. 3-5**, pp303-311.

16. Boudet, Alain-M.. "A new view of lignification", *Trend in Plant Science*, February 1998, **Vol. 3, No. 2**, 67-71.

17. Buchanan, Bob B.. Wilhelm Gruissem and Russell L. Jones. Biochemistry & Molecular Biology of Plants, 3rd edition Courier Companies, Inc., 2001, 1367p

18. Burns, Donald B and Emil W Ciurczak, Handbook of Near-Infrared Analysis 1992, Marcel Dekker Inc, New York, USA, 681p.

19. Castellan, Alain, Hasneen Choudhury, R Stephen Davidson and Stephane Grelier. (1994), " Comparative study of stone-ground wood pulp and native wood 2. Comparison of the fluorescence of stone-ground wood pulp and native wood." *J. Photochem. Photobiol. A.: Chem.*, **81**, Pp. 117-122.

20. Castellan, Alain and R. Stephen Davidson (1994) "Steady-state and dynamic fluorescence emission from Abies wood" *J. Photochem. Photobiol. A: Chem.*, **78**, Pp. 275-279.

21. Castellan , A., V. Trichet, J.-C. Pommier, A. Siohan and S. Armancq, (1995) "Photo and Thermal Stability of Totally Chlorine Free Softwood Pulps Studied by UV/VIS Diffuse Reflectance and Fluorescence Spectroscopy", *Journal of Pulp and Paper Science*, **Vol. 21, No. 9**, J291-J295.

22. Chan, Christina, Daehee Hwang, Gregory N. Stephanopoulos, Martin L. Yarmush and George Stephanopoulos, (2003), "Application of Multivariate Analysis to Function of Cultured Hepatocytes." *Biotechnol. Prog.*, **19**, p. 580-598.

23. Chang, Vincent S., Barry Burr and Mark T. Holtzapple. (1997) "Lime Pretreatment of Switchgrass", *Applied Biochemistry and Biotechnology*, **Vol. 63-65**, 3-19.

24. Chang, Vincent S., and Mark T. Holtzapple. (2000) "Fundamental Factors Affecting Biomass Enzymatic Reactivity", *Applied Biochemistry and Biotechnology*, **Vol. 84-86**, 5-35.

25. Chang, Vincent S., Murlidhar Nagwani and Mark T. Holtzapple. (1998) "Lime Pretreatment of Crop Residues Bagasse and Wheat Straw" *Applied Biochemistry and Biotechnology*, **Vol. 74**, 135-159.Charles, Nichola, Shawn D. Mansfield, Olga Mirochnik and Sheldon J.B. Duff, (2003) "Effect of Oxygen Delignification Operating Parameters on Downstream Enzymatic Hydrolysis of Softwood Substrates" *Biotechnology Progress*, **19**, 1606-1611.Chesson, Andrew, Peter T. Gardner and Timothy J. Wood, (1997) "Cell Wall Porosity and Available Surface Area of Wheat Straw and Wheat Grain Fractions", *J. Sci. Food Agric.*, **75**, p. 289-295.Choudhury, Hasneen, Stephen Collins and R. Stephen Davidson (1992), "The colour reversion of papers made from high yield pulp-a photochromic process?" *J. Photochem. Photobiol. A.: Chem.*, **69**, Pp. 109-119.Christy, Alfred A., Egil Nodland, Alan K. Burnham, Olav M. Kvalheim and Birger Dahl, (1994), "Determination of Kinetic Parameters for the Dehydration of Calcium Oxalate Monohydrate by Diffuse Reflectance FT-IR Spectroscopy", *Applied Spectroscopy*, **Vol. 48, No. 5**, p. 561-568.Cullitty, B.D and S. R. Stock. Elements of X-Ray Diffraction, 3rd ed., Upper Saddle River, NJ: Prentice Hall, c2001Dale, B.E., C.K. Leong, T.K. Pham, V.M. Esquivel, I. Rios and V.M. Latimer. (1996) "Hydrolysis of Lignocellulosics at Low Enzyme Levels: Application of the AFEX Process", *Bioresource Technology*, **56**, 11-116.

32. Dale, Bruce E., Justin Weaver and F. Michael Byers. (1999) "Extrusion processing for Ammonia Fiber Explosion (AFEX)", *Applied Biochemistry and Biotechnology*, **Vol. 77-79**, 35-45.

33. Dale, Bruce E, Lisa E. Gollapalli and Douglas M. Rivers. "Predicting Digestibility of Ammonia Fiber Explosion (AFEX) treated Rice Straw", *Applied Biochemistry and Biotechnology*, 2001

34. Dale, B.E. and M.J. Moreira, (1983), 1982. "A Freeze-Explosion Technique for Increasing Cellulose Hydrolysis." Biotech. and Bioengr. Symp. #12, "Biotechnology in Energy Production and Conversation," p. 13.

35. Davis, Mark W. (1998), " A rapid modified method for compositional carbohydrate analysis of lignocellulosics by high pH anion-exchange chromatography with pulsed amperometric detection (HPAEC/PAD)", *Journal of Wood Chemistry and Technology*, **18(2)**, pp. 235-252.

36. Davidson, R. Stephen and Linda A Dunn, (1991) "A study of the phhotobleaching and photoyellowing of paper containing lignin using fluorescence spectroscopy" *J. Photochem. Photobiol. A.: Chem.*, **58**, Pp. 349-359.

37. De La Rosa, Luis B., Sultan Reshamwala, Vivian Latimer, Bahha T. Shawky, Bruce E. Dale and Earnest D. Stuart, (1994), "Integrated Production of Ethanol Fuel and Protein from Coastal Bermudagrass", *Applied Biochemistry and Biotechnology*, **Vol. 45/46**, p.483-497.

38. Fan, L.T., Yong-Hyun Lee, and David H. Beardmore. (1980) "Mechanism of the Enzymatic Hydrolysis of Cellulose: Effects of Major Structural Features of Cellulose on Enzymatic Hydrolysis", *Biotechnology and Bioengineering*, **Vol. XXIII**, Pp 177-199.

39. Ferraz, André, Jaime Baeza, Jaime Rodriguez and Juanita Freer. (2000) "Estimating the chemical composition of biodegraded pine and eucalyptus wood by DRIFT spectroscopy and multivariate analysis", *Bioresource Technology*, **74**, 201-212.

40. Fuller, M.P., G.L. Ritter and C.S. Draper. "Partial least squares quantitative analysis of infrared spectroscopy data. Part I: Algorithm Implementation" *Applied Spectroscopy* submitted.

41. Fuller, Michael P., Issam M. Hamadeh, Peter Griffiths and Douglas E. Lowenhaupt, (1982), "Diffuse reflectance infrared spectrometry of powdered coals", *Fuel*, **Vol. 61**, 529-536.

42. Fuller, Michael P. and Peter R. Griffiths, (1978), "Diffuse Reflectance Measurements by Infrared Fourier Transform Spectrometry", *Analytical Chemistry*, **Vol. 50, No. 13**, pp. 1906-1910.

43. Gardner, Peter T., Timothy J. Wood, Andrew Chesson and Trevor Stuchbury, (1999), "Effect of degradation on the porosity and surface area of forage cell walls of differing lignin content", *Journal of the Science of Food and Agriculture*, **79**: 11-18.

44. Gharpuray, M.M., Young-Hyun Lee and L.T. Fan. (1983) "Structural Modification of Lignocellulosics by Pretreatment to Enhance Enzymatic Hydrolysis" *Biotechnology and Bioengineering*, **Vol. XXV**, Pp 157-172.

45. Grethlein, Hans. (1985) "The Effect of Pore Size Distribution on the Rate of Enzymatic Hydrolysis of Cellulosic Substrates", *Bio/Technology*, February 1985, 155-160.

46. Grethlein, Hans E. "Pretreatment of Biomass for Enzymatic Hydrolysis", 939-953.

47. Grethlein, Hans E. and Alvin O. Converse, "Common Aspects of Acid Prehydrolysis and Steam Explosion for Pretreating Wood." *Bioresource Technology* **36** (1991), 77-82.

48. Guettler, Michael V., (1984) "Bacteria and Cellulose", Manuscript

49. Guilardi Ruggiero, Silvana, Alain Castellan, Stephan Grelier, Aziz Nourmamode and Michel Cotrait, (1999) "Luminescence properties and spatial arrangement of lignin model in the solid II. Crystal structures of 2,2'-dibenzyloxy-5,5'-di(1-hydroxyethyl)-3.3'dimethoxybiphenyl and 2,2'-dibenzyloxy-5,5'-dihydroxymethyl-3,3'-dimethoxybiphenyl and their fluoescence emission." *Journal of Molecular Structure* **484**, 235-248.

50. Guilardi Ruggiero, Silvana, Alain Castellan, Michel Cotrait, Stephan Grelier, Mariza Guimaraes Drumond and Dorila Pilo Veloso, (1997) "Luminescence properties and spatial arrangement of lignin model in the solid. Part 1. Crystal structures of 5,5'-diacetyl-2, 2'-dibenzyloxy-3. 3' dimethoxybiphenyl and 2,2'-dibenzyloxy-5,5'-diformyl-3,3'-dimethoxybiphenyl and their phosphorescence emission." *Journal of Molecular Structure* **435**, 77-87.

51. Hall, D.O.; F. Rosillo-Calle; R.H. Williams; J. Woods. 1993 "Biomass for Energy: Supply Prospects" in <u>Renewable Energy-Sources for Fuels and Electricity</u>, L. Burham,ed.

52. Hames, Bonnie R., Steven R. Thomas, Amie D Sluiter, Christine J. Roth and David W. Templeton, "Rapid Biomass Analysis: New Tools for Compositional Analysis of Corn Stover Feedstocks and Process Intermediates from Ethanol Production" *Applied Biochemistry and Biotechnology*, 2002

53. Hattori, Tadashi, Kenji Shirai, Miki Niwa and Yuichi Murakami, (1981), "Performance of an Emisionless Infrared Diffuse Reflectance Spectrometer", *Anal. Chem.*, **53**, 1129-1130.

54. Hecht, Harry G., (1983), "A Comparison of the Kubelka-Munk, Rozenberg, and Pitss-Giovanelli Methods of Analysis of Diffuse Reflectance for Several Model Systems", *Applied Spectroscopy*, **Vol. 37, No. 4**, p. 348-354.

55. Henderson, D.O., E. Silberman, N. Chen and F. Snyder, (1993), "Adsorption Kinetics of EGDN on ZnO by Diffuse Reflectance Infrared Fourier Transform Spectroscopy" *Applied Spectroscopy*, **Vol. 47, No. 4**, p. 528-531.

56. Hespell, Robert. B, Patricia J. O'Bryan, Mohammed Moniruzzaman and Rodney J. Bothast. (1997) "Hydrolysis by Commercial Enzyme Mixtures of AFEX-Treated Corn Fiber and Isolated Xylans", *Applied Biochemistry and Biotechnology*, **Vol. 62,** 87-97.

57. Hogan, Charlene M. and Mary Mes-Hartree. (1990) " Recycle of cellulases and the use of lignocellulosic residue for enzyme production after hydrolysis of steam-pretreated aspenwood", *Journal of Industrial Microbiology*, **6**, 253-262.

58. Holtzapple, Mark T, Jae-Hoon Jun, Ganesh Ashok, Srinivas L. Patibandla, and Bruce E. Dale. (1991) "The Ammonia Freeze Explosion (AFEX) Process", *Applied Biochem and Biotech,* **Vol. 28/29,** 59-74.

59. Holtzapple, Mark T., Joseph E. Lundeen, Russell Sturgis, John E. Lewis, and Bruce E. Dale. (1992) "Pretreatment of Lignocellulosic municipal Solid Waste by Ammonia Fiber Explosion (AFEX)", *Applied Biochemistry and Biotechnology,* **Vol. 34/35,** 5-21.

60. Holtzapple, Mark T., and Robert Torget. (1997) "Thermal and Biological Processing", *Applied Biochemistry and Biotechnology,* **Vol. 63-65,** 1-2.

61. Itagaki, Hideyuki and Sanami Kato (1999), "Dynamic process of recrystallization of poly(ethylene terephthalate) solids revealed by fluorescence spectroscopy", *Polymer,* **40,** Pp. 3501-3504.

62. Iyer, Prashant V., Zhang-Wen Wu, Sung Bae Kim and Yoon Y. Lee. (1996) "Ammonia Recycled Percolation Process for Pretreatment of Herbaceous Biomass", *Applied Biochemistry and Biotechnology,* **Vol. 57/58,** 121-132.

63. Juang, Ring-Hwei and David E. Storey, (1998), "Quantitative Determination of the Extent of Neutralization of Carboxylic Acid Functionality in Carbopol® 974P NF by Diffuse Reflectance Fourier Transform Infrared Spectrometry Using Kubelka-Munk Function", *Pharmaceutical Research,* **Vol. 15, No. 11,** p. 1714-1720.

64. Jung, H.G. and M.S. Allen (1995), "Characteristics of Plant Cell Walls Affecting Intake and Digestibility of Forages by Ruminants", *Journal of Animal Science* **73:** 2774-2790.

65. Jung, Hans-Joachim G.. (1997) "Analysis of Forage Fiber and Cell Walls in Rumiant Nutrition" *Conference: New developments in Forage Science Contributing to Enhance Fiber Utilization by Rumiants,* 810S-813S.

66. Jung, H.G., D.R. Mertens and A.J. Payne. (1997) "Correlation of Acid Detergent Lignin and Klason Lignin with Digestibility of Forage Dry Matter and Neutral Detergent Fiber", *J. Dairy Science,* **Vol. 80,** 1622-1628.

67. Kabner, Petra and Manfred Baerns, (1996), "Comparative characterization of basicity and acidity of metal oxide catalysts for the oxidative coupling of methane by different methods", *Applied Catalysis A: General* **139**, pp107-129.

68. Kendall, Sir Maurice, Multivariate Analysis 2nd edition, 1980, Macmillan Publishing, Co., New York, USA, 210p

69. Kerley, M.S., G.C. Fahey, Jr., J.M.Gould and E.L. Iannotti (1988), "Effects of Lignfication, Cellulose Crystallinity and Enzyme Accessible Space on the Digestibility of Plant Cell Wall Carbohydrates by the Rumiant". *Food Microstructure*, **Vol. 7**, pp. 59-65.

70. Kim, Tae Hyun, Jun Seok Kim, Changshin Sunwoo and Y.Y. Lee, "Pretreatment of corn stover by aqueous ammonia" *Bioresource Technology* **90** (2003), 39-47

71. Klass, Donald L. "An Introduction to Biomass Energy:A renewable resource" from http://www.bera1.org/about.html

72. Klier, K. "Reflectance Spectroscopy as a Tool for investigating Dispersed Solids and Their Surfaces" *Catal. Rev.*, **1**, (1967), 207-232.

73. Klier, K. (1980) "Investigations of Adsorption Centers, Molecules, Surface Complexes, and Interactions Among Catalyst Components by Diffuse Reflectance Spectroscopy", Vibrational Spectroscopies for Adsorbed Species, ACS Symposium Series #137, p. 141-162.

74. Knappert, Diane, Hans Grethlein and Alvin Converse. (1980) "Partial Acid Hydrolysis of Cellulosic Materials as a Pretreatment for Enzymatic Hydrolysis", *Biotechnology and Bioengineering*, **Vol. XXII**, Pp. 1449-1463.

75. Kong, Fanran, Cady R. Engler and E(1992) "Effects of Cell-Wall Acetate, Xylan Backbone, and Lignin on Enzymatic Hydrolysis of Aspen Wood", *Applied Biochemistry and Biotechnology*, **Vol.** d J. Soltes. **34/35**, 23-35.

76. Košíková, B., L. Zákutná and D. Joniak. (1978) "Investigation of the Lignin-Saccharidic Complex by Electron Microscopy", *Holzforschung*, **Bd. 32**, 15-18.

77. Krishnan, K., S.L. Hill and R.H. Brown, (1980), "FTIR spectroscopy using diffuse reflectance and a diamond cell" *American Laboratory*, p.106-114.

78. Krivacsy, Z. and J. Hlavay, (1995), "Comparison of Calibration methods in Quantitative Diffuse Reflectance Infrared Spectroscopy", *Talanta*, **Vol. 42, No. 4**, pp. 613-620.

79. Ladisch, M.R., K.W. Lin, M. Voloch and G.T. Tsao, (1983) "Process considerations in the enzymatic hydrolysis of biomass", *Enzyme Microb. Technol.*, **Vol. 5**, 82-102.

80. Lakowicz, Joseph R. Principles of Fluorescence Spectroscopy, Plenum Press, New York.

81. Laureano-Perez, Lizbeth, Farzaneh Teymouri, Hasan Alizadeh and Bruce Dale (2004) "Understanding Factors that Limit Enzymatic Hydrolysis of Biomass: Characterization of Pretreated Corn Store", *Applied Biochemistry and Biotechnology* (In Press)

82. Lundquist, Knut, Björn Josefsson and Gunnar Nyquist.(1978) "Analysis of Lignin Products by Fluorescence Spectroscopy", *Holzforschung*, **Bd32**, 27-32.

83. Lynd, Lee R., Charles E. Wyman and Tillman U. Gerngross. (1999) "Biocommodity Engineering", *Biotechnol. Prog*, **15**, 777-793.

84. Mandels, Mary, (1982) "Cellulases" Annual Reports on Fermentation Processes, Vol.5, Pp. 35-77.

85. Molecular Fluorescence Spectrometry Sec 15.3

86. Moniruzzaman, M., B.E. Dale, R.B. Hespell and R.J. Bothast (1997) "Enzymatic Hydrolysis of High-Moisture Corn Fiber Pretreated by AFEX and Recovery and Recycling of the Enzyme Complex", *Applied Biochemistry and Biotechnology*, **Vol. 67**, 113-126.

87. Morrison, I.M. (1974) "Structural investigations on the lignin-carbohydrate complexes from *Lolium perenne*", *Biochem J.*, **139**:197-204.

88. Morrison, Ian M. and Derek Stewart, " Determination of Lignin in the Presence of Ester-Bound Substituted Cinnamic Acids by a Modified Acetyl Bromide Procedure" *J Sci Food Agric* 1995, **69**, 151-157.

89. Naummann, D. "Infrared and NIR Raman Spectroscopy in Medical Microbiology" *In press*

90. Noutary, C., P. Fornier de Violet, J. Vercauteren and A. Castellan (1995), "Photochemical studies of phenolic phenylcoumarone lignin model molecule in relation to the photodegradation of lignocellulosics materials. Part 2. Photophysical and photochemical studies", *Res. Chem. Intermed.* **Vol. 21, Nos. 3-5**, pp. 247-262.

91. Nunes Pereira, Eduardo J., Mario N. Berberan-Santos, Aleksandre Fedorov, Michel Vincent, Jacques Gallay and Jose M. G. Martinho, (1999), "Molecular radiative transport. III. Experimental intensity decays", *Journal of Chemical Physics*, **Vol. 110, No. 3**, pp. 1600-1610.

92. Olmstead, J.A. and D.G. Gray (1997) "Fluorescence Spectroscopy of Cellulose, Lignin and Mechanical Pulps: A Review", *Journal of Pulp and Paper Science*, **Vol. 23, No. 12** December 1997, J571-J579.

93. Orskov, E.R. and G.W. Reid, (1988) "Comparison of Chemical and Biological Methods for Predicting Feed Intakes and Animal Performance" *Animal Production*, 158-165.

94. Pandey, K.K. (1998), " A study of Chemical Structure of Soft and Hardwood and Wood Polymers by FTIR Spectroscopy", *Journal of Applied Polymer Science*, **Vol. 71**, 1969-1975.

95. Pandley, Krishna K. and Dwarika P. Khali, (1998), " Accelerated Weathering of Wood Surface Modified by Chromium Trioxide", *Holzforschung*, **Vol.52**, pp. 467-471.

96. Paralikar, K.M. and S. Aravindanath. (1988) "Crystallization of Cellulose", *Journal of Applied Polymer Science*, **Vol. 35**, 2085-2089.

97. Puri, Vinod P., (1984) "Effect of Crystallinity and Degree of Polymerization of Cellulose Enzymatic Saccharification", *Biotechnology and Bioengineering,* **Vol. XXVI**, Pp 1219-1222.

98. Reeves, James B. and Barry A. Francis (1997), "Pyrolysis-gas-chromatography-mass-spectrometry for the analysis of forages and by-products", *Journal of Analytical and Applied Pyrolysis*, **40-41**, Pp. 243-265.

99. Russell, J.D., I. Murray and A.R. Fraser "Near and Mid-Infrared studies of the cell wall structure of cereal straw in relation to its rumen degradability.

100. Samac, Deborah A., Lynn Litterer, Glena Temple, Hans-Joachim G. Jung and David A. Somers, "Expression of UDP-Glucose Dehydrogenase Reduces Cell-Wall Polysaccharide Concentration and Increases Xylose Content in Alfalfa Stems", *Applied Biochemistry and Biotechnology*, **Vol. 113-116**, p. 1167-1182.

101. Sasaki, Takashi, Takashi Tanaka, Noriko Nanbu, Yohko Sato and Keiji Kainuma. (1979) "Correlation between X-Ray Diffraction Measurements of Cellulose Crystalline Structure and the Susceptibility to Microbial Cellulase", *Biotechnology and Bioengineering*, **Vol. XXI**, Pp 1031-1042.

102. Segal, L., J.J. Creely, A.E. Martin, Jr., and C. M. Conrad (1959) "An Empirical Method for Estimating the Degree of Crystallinity of Native Cellulose Using the X-Ray Diffractometer", *Textile Res. J.* **29**, 786 –794.

103. Sewalt, Vincent J.H., Joseph P. Fontenot, Vivien G. Allen and Wolfgang G.Glasser. (1996) "Fiber Composition and *in vitro* Digestibility of Corn Stover Fractions in Response to Ammonia Treatment", *J.Agric. Food Chem.*, **44**, 3136-3142.

104. Sewalt, V.J.H., W.G. Glasser and K.A Beauchemin. (1997) "Lignin Impact on Fiber Degradation. 3. Reversal of Inhibition of Enzymatic Hydrolysis by Chemical Modification of Lignin and by Additives", *J. Agric. Food Chem.*, **Vol. 45**, 1823-1828.

105. Skoog, Douglas A and James J Leary, Principles of Instrumental Analysis 4th edition, 1992, Saunders College Publishing, Fort Worth, USA, 196-208

106. Smyrl, N.R., E.L. Fuller, Jr., and G.L. Powell, (1983), "Monitoring the Heterogeneous Reaction of LiH and LiOH with H_2O and CO_2 by Diffuse Reflectance Infrared Fourier Transform Spectroscopy", *Applied Spectroscopy*, **Vol. 37, No. 1**, p 38-44

107. Stewart, D., H.M. Wilson, P.J. Hendra and I.M Morrison (1995). "Fourier-Transform Infrared Spectroscopic Study of Biochemical and Chemical Treatments of Oak Wood (*Quercus rubra*) and Barley (*Hordeum vulgare*) Straw", *J. Agric Food Chem.*, **43**, 2219-2225.

108. Sugiyama, J., T. Okano, H. Yamamoto, F. Horii. (1990) "Macromolecules transformation of Valonia cellulose crystals by an alkaline hydrothermal treatment, **23**, 2461-2498

109. Teymouri, Farzaneh, Lizbeth Laureano-Perez, Hasan Alizadeh and Bruce E. Dale (2004) "Ammonia Fiber Explosion Treatment of Corn Stover" *Applied Biochemistry and Biotechnology*, **Vol. 113-116**, 951-963.

110. Thomas, Howard V. and David Haaland. (1990) "Comparison of Multivariate Calibration Methods for Quantitative Spectra Analysis", *Analytical Chemistry*, **Vol. 62, No. 10**, May 15, 1990, 1091-1099.

111. Thompson David N., Hsin-Chih Chen and Hans Grethlein. (1992) " Comparison of Pretreatment Methods on the Basis of Available Surface Area", *Bioresource Technology*, **39**, 155-163.

112. Van Every, Kenneth W. and Peter R. Griffiths, (1991), "Characterization of Diffuse Reflectance FT-IR Spectrometry for Heterogeneous Catalyst Studies", *Applied Spectroscopy*, **Vol. 45, No. 3**, 347-359.

113. Van Soest, P.J. and R.H. Wine (1968), "Determination of Lignin and Cellulose in Acid-Detergent Fiber with Permanganate", *Journal of the A.O.A.C.*, **Vol. 51, No. 4**, Pp. 780-785.

114. Wallace,G. A. Chesson, J.A. Lomax and M.C. Jarvis. (1991) "Lignin-carbohydrate complexes in graminaceous cell walls in relation to digestibility", *Animal Feed Science and Technology*, **32**, 193-199.

115. Wang, Lin, Bruce E. Dale, Lale Yuritas and I. Golwasser. (1998) "Cost estimates and Sensitivity Analyses for the Ammonia Fiber Explosion Process", *Applied Biochemistry and Biotechnology*, **Vol. 70-72**, 51-66.

116. Wei, Chia-Jenn and Chung-Yueh Cheng, (1985) "Effect of Hydrogen Peroxide Pretreatment on the Structural Features nad the Enzymatic Hydrolysis of Rice Straw". *Biotechnology and Bioengineering*, **Vol. XXVII**, Pp. 1418-1426.Windham, W.R., D.R. Mertens and F.E. Barton II. "Protocol for NIRS Calibration: Sample Selection and Equation Development and Validation" 96-103.

117. Wielage, B., Th. Lampke, G. Marx, K. Nestler and D. Starke, (1999), "Thermogravimetric and differential scanning calorimetric analysis of natural fibers and polypropylene", *Thermochimica Acta*, **337**, pp. 169-177.

118. Willemse, M.T.M., (1988)"Cell Wall Autofluorescence" Acta Botanical Neerlandica, p.50-57.

119. Willey, R.R., (1976), "Fourier Transform Infrared Spectrophotometer for Transmittance and Diffuse Reflectance Measurements", *Applied Spectroscopy*, **Vol. 30, No. 6**, p. 593-601.

120. Wilson, J.R. and D.R. Mertens (1995) "Cell Wall Accessibility and Cell Wall Structure Limitations to Microbial Digestion of Forage", *Crop Science*, **Vol. 35**, 251-259.

121. Windham, W.R., D.R. Mertens and F.E. Barton II. "Protocol for NIRS Calibration: Sample Selection and Equation Development and Validation" 96-103.

122. Wu, Zhangwen and Y.Y. Lee. (1997) "Ammonia Recycled Percolation as a Complementary Pretreatment to the Dilute-Acid Process", *Applied Biochemistry and Biotechnology*, **Vol. 63-65**, 21-34.

123. Wyman, Charles (editor). <u>Handbook on Bioethanol: Production and Utilization</u>, Taylor and Francis, Washington, DC, USA 1996, 424p

124. Wyman, Charles E. (1994) "Ethanol from Lignocellulosic Biomass: technology, Economics and Opportunities", *Bioresource Technology*, **50**, 3-16.

125. Yoon, H.H., Z.W. Wu and Y.Y. Lee. (1995) "Ammonia-Recycled Percolation Process for Pretreatment of Biomass Feedstock", *Applied Biochem and Biotech,* **Vol. 51/52,** 5-19.

126. Bhattacharyya, Gouri K. and Richard A. Johnson Statistical Concepts and Methods John Wiley and Sons Inc., New York, USA 1977, p.599